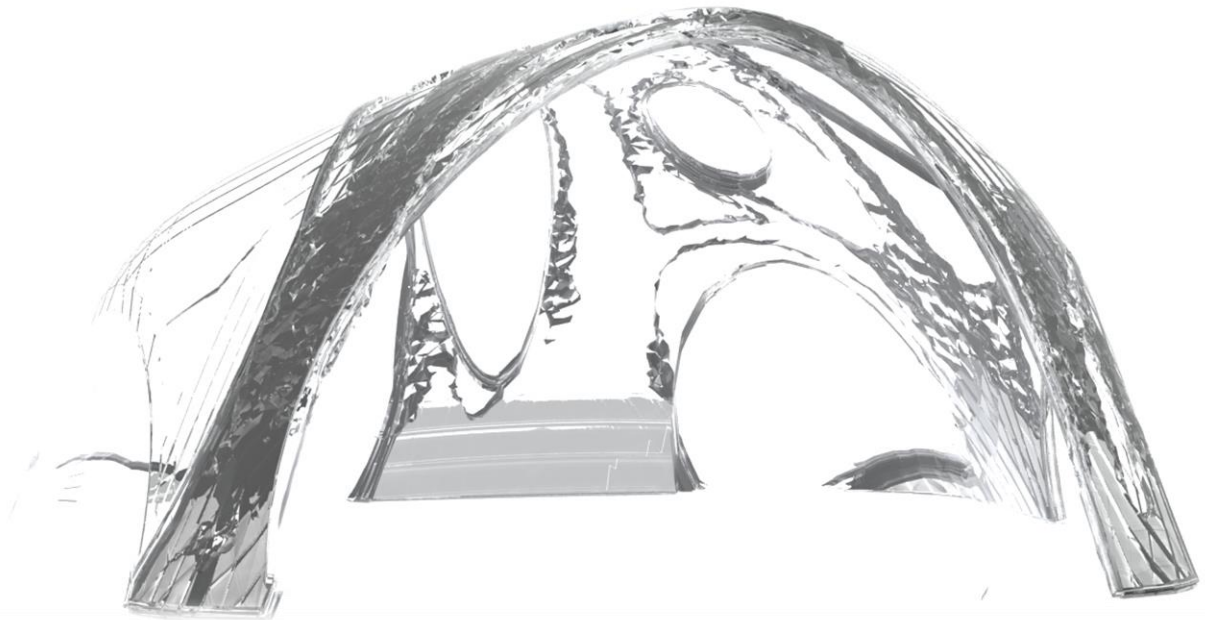


Daniella Naous

Topologically Optimised Cast Glass Shell

Topological optimisation and new fabrication methods for compressive free-form glass structures



Topologically Optimised Cast Glass Shell

Topological optimisation and new fabrication methods for
compressive free-form glass structures

By

Daniella Naous

4290038

in partial fulfilment of the requirements for the degree of

Master of Science

in Building Technology

at the Delft University of Technology,

to be defended publicly on Monday July 6, 2020 at 02:30 PM.

1st Supervisor:

Dr. ir. Faidra Oikonomopoulou

2nd Supervisor

Dr. ing. Marcel Bilow

This thesis is confidential and cannot be made public until July 7, 2020.

An electronic version of this thesis is available at <http://repository.tudelft.nl/>.

Abstract

Glass is a material which can be seen as a double-edged sword. Its monolithic, smooth, and transparent look transmits a sense of elegance and simplicity. However, due to its brittle mechanical property, it can create complex engineering challenges when intended for a structural load-bearing application. Many forget glass has a comparable compression strength to steel and excels when compared to the mechanical properties of unreinforced concrete. (Oikonomopoulou, 2019; Ashby, 2006) Until now, there have been 4 primary discovered manufacturing techniques for glass. Float glass has a 25mm thickness limitation. (AGC, 2019) Extruded and float glass cannot form complex 3D geometries. (Roeder, 1971) 3D printed glass is not structurally validated. (Klein, 2015) Cast glass can offer a solution to all of these limitations. (Oikonomopoulou, 2019)

This thesis answers the following question: To what extent can topological optimisation and new fabrication methods be employed to create compressive free-form glass structures? To answer this this thesis will delve into glass, topology optimisation and shell structures. Throughout the thesis it will notice how topology optimisation and shell structures offer solutions to glass related challenges.

Compression Shells are ideal for Glass. Why? Because glass is brittle. This means that it fractures without warning when tension is applied to a crack. Glass has a low tensile strength but a very high compressive strength. That is why shell structures are ideal for glass as they experience compression only loads. (Adriaenssens et al., 2014) Shells best utilize the strengths of glass and avoid testing its weakest limitations.

Annealing time is one of the most challenging aspects of cast glass. As the volume/mass ratio increases the annealing time increases exponentially. (Oikonomopoulou, 2019) This means careful consideration should be attributed to decreasing this time. This thesis used topology optimisation as a tool to decrease the thickness and thus the annealing time. This thesis explains structural optimisation and evaluates different topological optimisation approaches and software. At the end a 43% mass reduction was achieved.

The goal in this thesis was to design an 6x6m booth from cast glass for the martial district exhibition. After the shell was topologically optimised and structurally validated by means of finite element analyses, the booth was designed for manufacturing, transportation and assembly. The booth was subdivided to fit in trucks and be assembled using spider cranes. The manufacturing procedure was developed using additively manufactured sand mould designs. Demountable and reusable connections, and foundation designs were also developed for the shell.

Table of Contents

Chapter 1: Introduction	12
1.1 Case study (context selection and design).....	12
1.1.1 Bounding dimensions of the booth	13
1.2 Problem statement	14
1.2.1 Research question:	14
1.2.2 Sub-questions	15
1.3 Outline of thesis	15
1.3.2 Research Methodology Scheme	16
Chapter 2: About Glass	18
2.1 The potential of glass in structures	18
2.2 Physical, structural, mechanical optical properties of glass	19
2.2.1 Homogeneous material.....	19
2.2.2 Isotropic material.....	19
2.2.3 Compressive strength vs tensile strength	19
2.2.4 Strength vs toughness	19
2.2.5 Fracture toughness mechanics	20
2.2.6 The fracture toughness–Young’s modulus chart	21
2.2.7 The fracture toughness–Yield strength chart	22
2.2.8 Conclusion on glass mechanical and structural properties.....	22
2.3 Glass types and compositions.....	24
2.3.1 Soda-lime glass composition.....	24
2.3.2 Lead-oxide silicate glass composition.....	24
2.3.3 Aluminosilicate glass composition	24
2.3.4 Fused quartz/ 99.5% silica composition and 96% silica glass composition.....	24
2.3.5 Sodium borosilicate glass composition	25
2.3.6 Conclusion regarding glass compositions	26
2.4 Glass manufacturing methods.....	27
2.4.1 Float glass.....	27
2.4.2 Extruded glass	29
2.4.3 Additive Manufacturing of glass (3D Printed)	32
2.4.4 Cast glass.....	33
2.5 Annealing of glass.....	36
2.5.1 Design principals for strong cast glass and annealing	37
2.5.2 What affects annealing?.....	37
2.6 Mass optimisation of the glass giants: lessons learned from the cast glass blanks of the giant ground telescopes.	38
2.6.1 Hooker telescope.....	39

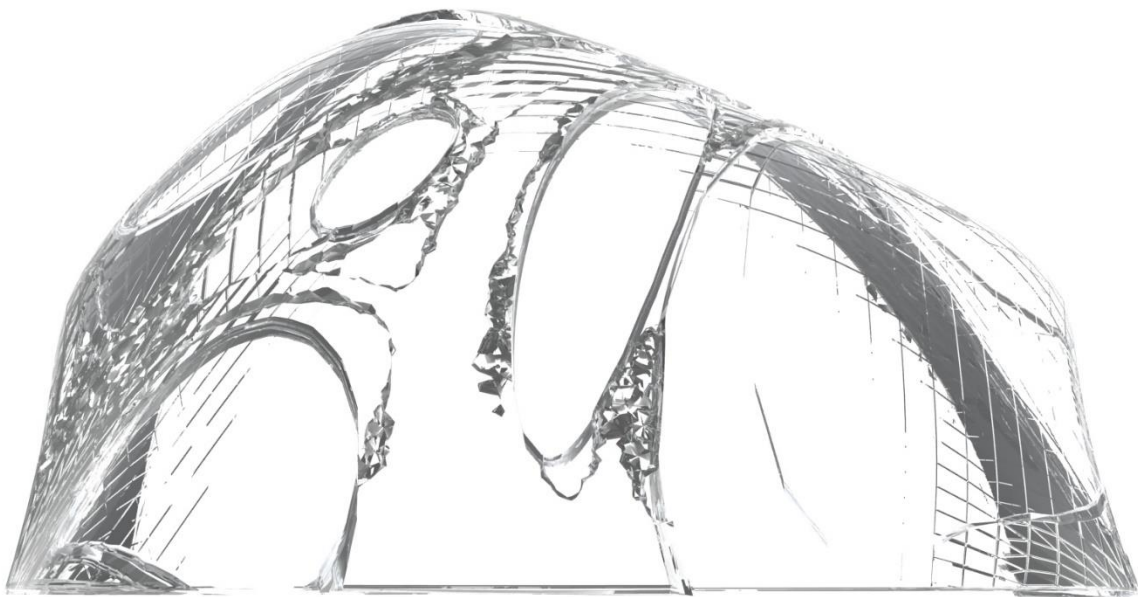
2.6.2 Hale Telescope mirror in Mt. Palomar	39
2.6.3 Giant Magellan Telescope mirror	39
2.6.4 Conclusions regarding the annealing of cast glass	39
2.7 Mould types.....	41
2.7.1 Disposable moulds.....	41
2.7.2 Permanent moulds	41
2.7.3 Additive Manufacturing (3D-Printing)	42
2.8 Conclusions and decisions regarding glass	44
Chapter 3 About Topological Optimisations (TO)	46
3.1 Structural optimisation theory	46
3.1.1 Size optimisation:	47
3.1.1 Shape optimisation:.....	47
3.1.3 Topological optimisation	47
3.2 Topological optimisation approaches	49
3.2.1 Level set method	50
3.2.2 Generalized Shape Optimisation (GSO) using Isotropic-Solid or Empty elements (ISE) - TO for isotropic materials	50
3.2.3 SIMP (Solid Isotropic Microstructure with Penalty for intermediate densities)	50
3.2.4 Sequential Element Rejections and Admissions (SARA) (also known as “Hard-Kill” Methods).....	51
3.2.5 Homogenisation method (TO for Anisotropic Materials).....	52
3.3 Examples of TO productions.....	53
3.3.1 ETH Zurich concrete slabs	53
3.3.2 The light rider.....	54
3.3.3 The Glass Swing	54
3.3.4 Kolumba museum cast glass column.....	55
3.3.5 The shell node.....	58
3.4 Challenges and limitations to TO of glass and other brittle materials	59
3.4.1 What is minimum compliance (compliance based TO)?	59
3.4.2 What is von Mises stress (stress-based optimisation)?.....	59
3.4.3 What is Drucker-Prager?	60
3.4.4 Dilemma: Should this research opt for a compliance-based or a stress-based topological optimisation?	60
3.4.5 Conclusion on TO for glass	61
3.5 Different software packages.....	62
3.5.1 ANSYS	62
3.5.2 Ameba	62
3.5.3 Millipede	62
3.5.4 Autodesk Fusion 360	62
3.5.5 Autodesk Generative Design.....	62

3.5.6 Karamba3D.....	62
3.5.7 Optistruct (Altair Hyper Works)	62
3.6 Conclusions and decisions regarding TO.....	64
Chapter 4: About free form shell structures	66
4.1 What is a shell?.....	66
4.2 Why building a shell structure is ideal for Glass?	66
4.3 Hooke’s Law and Antoni Gaudi.....	66
4.4 Structural mechanics of shells	68
4.5 Eccentricity, deformation and bending in shell structures	70
4.6 Buckling.....	70
4.7 Shell geometries	71
4.8 Form finding methods of shell structures.....	71
4.8.1 Particle-spring method: Rhino grasshopper meshing, Weaverbird tessellation, and Kangaroo dynamic relaxation.....	71
4.9 Examples of inspirational shapes of shell structures.....	72
4.9.1 Aichtal Outdoor Theatre	72
4.9.2 Tessellated shell pavilion.....	73
4.9.3 The concrete grid shell	73
Chapter 5: Literature review conclusions and derived criteria	76
5.1 Design and manufacturing Choices (Literature Review Conclusions)	76
5.1.1 Type of glass.....	76
5.1.2 Moulding and manufacturing method	76
5.1.3 Form finding method.....	77
5.1.4 TO Method	77
5.1.5 TO approach.....	77
5.1.6 TO Software	77
5.2 Design Criteria	77
5.2.1 Minimum distance between separate parts.....	77
5.2.2 Correct edges geometry for connections.....	77
5.2.3 Even distribution of material (mass and volume).....	78
5.2.4 Max annealing time (less 3 months).....	78
5.2.5 Thickness range of shell	78
5.2.6 Thickness range of dissected elements.....	78
5.2.7 Size of subdivided elements.....	78
5.2.8 Maximum deflection	78
5.2.9 Case study limitations.....	78
5.2.10 Redundancy (safety factors) /Discussion	78
Chapter 6: The design process: Topology Optimisation, Structural verification, and Design Evolution of the Shell	78

6.1 Procedure (as followed)	79
6.2 Verifying the legitimacy of the Ansys model	81
6.3 Topology optimisation and analysis conclusions and notes	81
6.4 Shape evolution after TO	83
6.5 Manual design modifications based on TO result and deflections analysis.....	83
6.6 Workflow along a variation of software (discussion)	90
Chapter 7: Subdivision of elements	90
7.1 Subdivision tessellation criteria:	91
7.3 Refining the chosen subdivision pattern.....	94
7.4 Will they fit in a truck dimension? How many trucks needed?	95
Chapter 8: Connection possibilities between cast glass elements.....	96
8.1 Connection Types	96
8.1.1 Mechanical Connections (sub-structural metal bars or braces)	96
8.1.2 Adhesive Connections	96
8.1.3 Embedded Magnetic Connections (proposal, currently under research by Grammatiki Dasopoulou) 96	
8.1.4 Embedded titanium connections (currently under research).....	97
8.1.5 Interlocking-based geometrical connections	97
8.2 More about interlocking connections	97
8.3 Challenge arising from combining the interlocking system with the subdivision pattern	98
8.4 Connection system criteria	99
8.5 Interlayer Material	102
8.6 Foundation.....	104
Chapter 9: Mould design	106
9.1 Mould logistics.....	107
9.2 Mould design criteria:	107
9.3 Mould design and manufacturing procedure	108
Chapter 10: Assembly	113
10.1 Assembly order.....	113
10.1.1 Holding method	113
10.1.2 Logistics	113
10.1.3 Temporary support.....	113
10.1.4 The assembly order procedure.....	114
Chapter 11: Redundancy (safety factors) - discussion	118
Chapter 12: Conclusion discussion and recommendations.....	120
12.1 Answer to research question.....	120
12.1.1 To what extent can topological optimisation and new fabrication methods be employed to create a compressive free-form glass structure?	120
12.2 Answers to sub-questions (Recommendations included).....	120

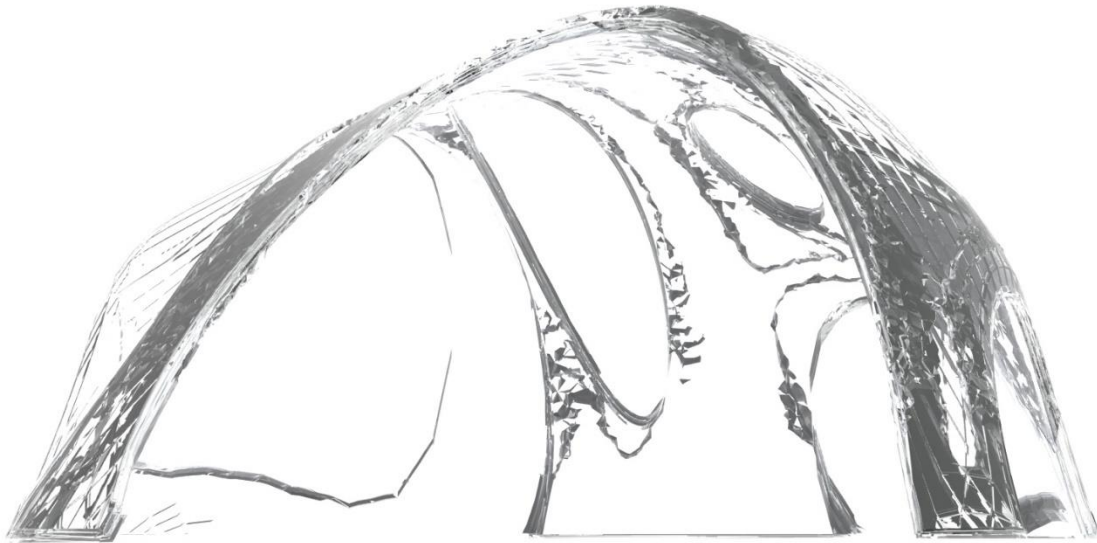
12.2.1 What are the main considerations and properties that define the feasibility of large-scale cast glass components?	120
12.2.2 What design criteria can be drawn from existing glass, topology optimisation and shell projects?	120
12.2.3 What challenges does glass present to topology optimisation, and which method is the most suitable for glass TO for shell structures?	121
12.2.4 What are the most suitable manufacturing, transportation, and assembly methods for a large cast glass free form structure?	122
12.3 Further applications	123
Reflection	126
Appendices	128
Appendix A: Structural and mechanical explanations	128
Density	128
Stress, Strain and Elastic Modulus	128
Stiffness and elasticity	130
Strength	130
Strength vs toughness	130
Fracture toughness mechanics	130
The fracture toughness–Young’s modulus chart	132
The fracture toughness–Yield strength chart	133
Appendix B: Dynamic relaxation of the shell using Particle-Spring form finding Method	135
A.1 Dynamic relaxation	135
A.2 Meshing	148
Appendix C: FEA Results from Ansys	157
C.1 Original 10cm thick shell – Deformations	157
C.2 Original 10 cm shell – Normal Elastic Strain	159
C.3 Original 10 thick shell – Shear elastic strain	162
C.4 Original 10 cm shell – Normal stress	166
C.5 Original 10 cm shell – Maximum Principal Elastic Strain	168
C.6 Original 10 cm shell - Maximum shear stress	170
C.7 Original 10 cm shell – Minimum Principal Stress	172
C.8 Original 10 cm shell – Shear Stress	174
C.9 First Topology optimisation – Results	176
C.10 Second Topology optimisation – Results	178
C.11 First Simplified Topology optimisation – Deformations	180
C.12 First Simplified Topology optimisation - Max Principle Elastic Strain	184
C.13 First Simplified Topology optimisation – Max Principal stress	186
C.14 First Simplified Topology optimisation – Minimum Principal Stress	189
C.15 First Simplified Topology optimisation – Normal Stress	192
C.16 First Simplified Topology optimisation – Shear Stress	194

C.17 The 2 cm shell – Minimum Principal Stress.....	197
C.18 The 2 cm shell – Deformation.....	200
C.18 The 2 cm shell – Maximum Principal Stress.....	203
C.19 The 2 cm shell – Maximum Principal Elastic Strain.....	207
C.20 The 2 cm shell – Maximum Shear stress.....	207
C.21 The 2 cm shell – Minimum Principal Stress.....	208
C.22 The 2 cm shell – Normal Elastic Strain.....	208
C.23 The 2 cm shell – Normal Stress.....	209
C.24 The 2 cm shell – Shear Elastic Strain.....	210
Appendix D Extra pictures from during the design process.....	211
Appendix E Connections archive.....	220
Bibliography.....	235



This thesis is dedicated to my parents, loving fiancé, and supportive family.

My beloved father has instilled in me the love for science, intellect, design, knowledge, and education. He spent endless hours explaining how things work, stuff is made, and nature behaves the way it does. The endless hours he has spent with me, including building Lego and kids-science-kits, were not in vein. Despite him being a biochemist, his hobbies always involved product design and engineering. My dad spoke passionately about nature and his belief in a creator. During my studies, I have experienced the complexity of designing optimal integrated products; thus, I became personally more convinced of an intelligent designer and engineer for our complex yet beautiful universe. Now we enjoy talking about this common ground from two different perspectives; biochemistry and building engineering. My late mother's passion for interior and architectural design inspired me to become an engineer. She has always encouraged us to study. Her love, care, positivity, compassion, empathy, and support kept on motivating and strengthening me. Sadly, she met her demise the same month I graduated from my bachelor's degree in architecture, urbanism, and building sciences. I followed this master's program in fulfilment of her wish, and I'm so happy I did. My parents made sure my brother and I receive the best education possible from kindergarten till university. I am forever grateful for their investment in time, money, and energy in us. Last, but not least, to my fiancé, the one who has supported and cheered me on while writing my thesis. He is a beam of sunshine that warms my heart and brightens my day!



Daniella Naous: Author

Delft, July 6 2020

Chapter 1: Introduction

Elegance is a quality highly desired by humans. It is expressed with good quality, simplicity, and purity. Unfortunately, though, at times elegance is compromised in complex projects. This compromise should not be taken as a given penalty of complexity. The ability to strike both elegance and complexity cannot be more eloquently expressed than how Constantin Brancusi expresses it, “simplicity is complexity resolved”. The field of design and engineering has some exemplary projects where the complexity of the project is almost invisible due to the elegant look of the final product. Glass is a material which can be seen as a double-edged sword. Its monolithic, smooth, and transparent look transmits a sense of elegance and simplicity. However, due to its brittle mechanical property, it can create complex engineering challenges when intended for a structural load-bearing application. Many forget glass has a comparable compression strength to steel and excels when compared to the mechanical properties of unreinforced concrete. (Oikonomopoulou, 2019; Ashby, 2006) The question arises then, can simple elegance be achieved by resolving the complex challenges accompanying the use of glass structurally?

Sometime an architectural plan and design is created before thinking of the building material. The question arises midway through the process, when it is time for dimensioning and detailing the design for construction. Which materials can best be used to build this construction? Ashby et al. (2019) describes a strategic thinking process of matching material to design. When designing for a material like glass the design process is reversed. The material is chosen first, then it is time to think: which design can best utilize the strengths of glass and avoid testing its weakest limitations? Since glass can withstand high compression forces but is weak when tension is present, a compression only design would be the most suitable structure. Shells and relaxed catenary arch networks, like that of what Antoni Gaudí used, result in compression-only forms. Therefore, a free form shell structure will be designed to further investigate the potential of glass.

So far, float glass has been commonly used architecturally and structurally. However, float glass maximum thickness is limited to 25mm (AGC, 2019). Cast glass can provide the freedom of form and a wide range of thickness flexibility missing in float glass. Nevertheless, since cast glass has not been as widely used as float glass, much needs to yet be investigated. Production methods of cast glass are still on the verge of new developments. There is no industrialized manufacturing method for cast glass. Another challenge casting glass presents is the lengthy annealing (cooling) time that could last for months, if not years, as the volume increases. Topological Optimisation (TO) is explored in this thesis as a potential solution to lower the annealing time of cast glass. TO reduces the amount of material to the minimum required to sustain the load cases the structure is required to sustain. This in return will remove unnecessary material from the element, decrease the thickness and increase the exposed surface area of glass, which in return will decrease the annealing time.

This thesis answers the question: To what extent can topological optimisation and new fabrication methods be employed to create compressive free-form glass structures?

1.1 Case study (context selection and design)

This research is going to focus on designing a shell (freeform) exhibition booth out of cast glass for the Material District exhibition. Since shells are ideally loaded primarily vertically through self-weight, with no asymmetric horizontal forces such as wind, an indoors case study design has been chosen. This is also fitting for the pioneering ambition for cast glass within the industrialized material world. Since cast glass is not industrialized yet, it is appropriate to design with it an exhibition booth for the Material District Exhibition that features new material innovations. The size of a booth is ideal for a giant element that is still realistic for prototyping in case funds become available.

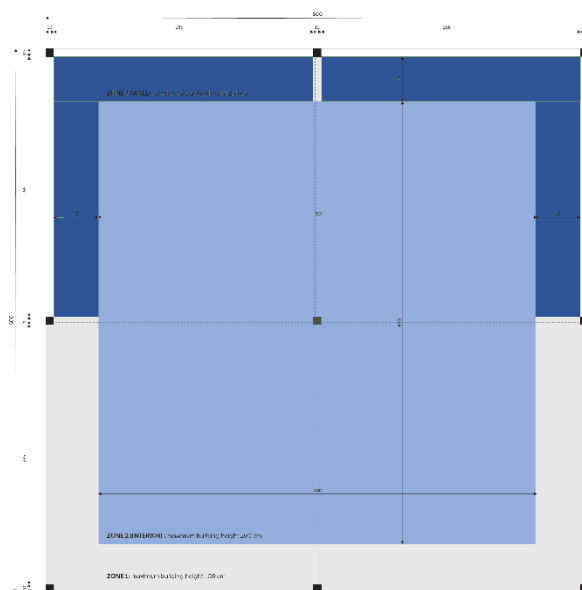
1.1.1 Bounding dimensions of the booth

The Material District 17-19 March 2020 Exhibition in Rotterdam Ahoy website provides the following guidelines for the design.

- All booths require a closed back to back booth partition. This means no openings into the neighbour's booth.
- All booths require a door-like opening at the front and from the sides. Dimensions can deviate practically by a maximum of 5%

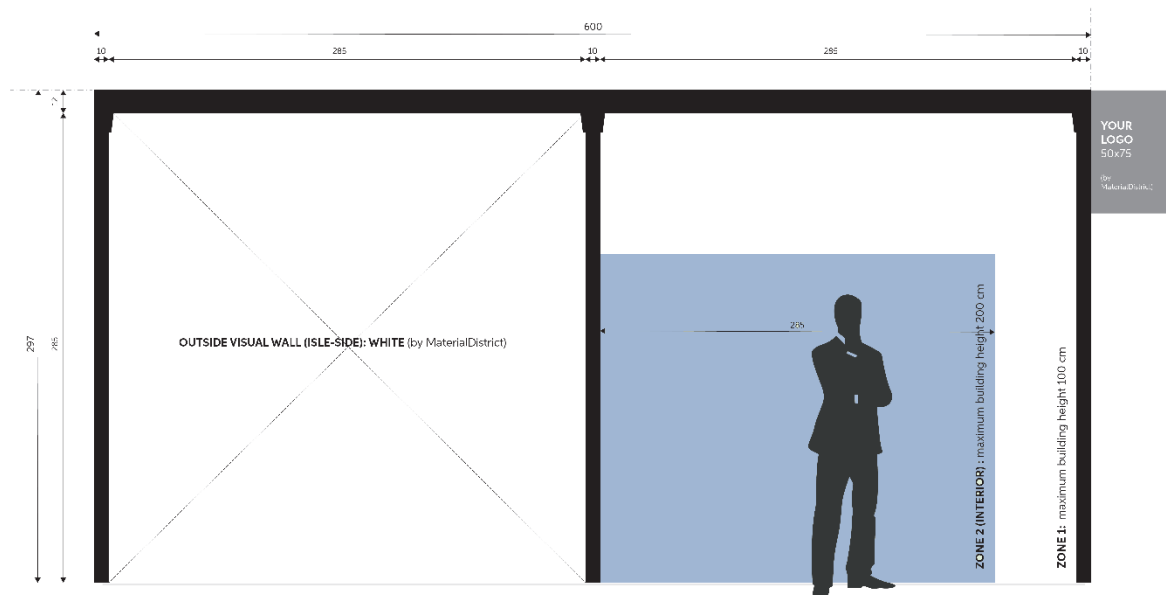
The chosen option offers a 600 x 600 x 297cm rectangular volumetric boundary.

MATERIALDISTRICT ROTTERDAM



Top View (overview)

Figure 1 Top view of the 600 x 600 x 297cm MaterialDistrict (2020) booth



Side Views (left & right)

Figure 2 Front View of the 600 x 600 x 297cm MaterialDistrict (2020) booth



Figure 3 Quick illustration of what a shell structure booth could look like in the Material district exhibition (edited by author from MaterialDistrict, 2020)

1.2 Problem statement

1.2.1 Research question:

To what extent can topological optimisation and new fabrication methods be employed to create compressive free-form glass structures?

1.2.2 Sub-questions

1. What are the main considerations and properties that define the feasibility of large-scale cast glass components?
2. What design criteria can be drawn from existing glass, topology optimisation and shell projects?
3. What challenges does glass present to topology optimisation, and which method is the most suitable for glass TO for shell structures?
4. What are the most suitable manufacturing, transportation, and assembly methods for a large cast glass free form structure?

1.3 Outline of thesis

To be able to design, manufacture and build this booth this research needs to first address three main topics:

- Properties and applications of glass
- Topology optimisation
- Shell structures

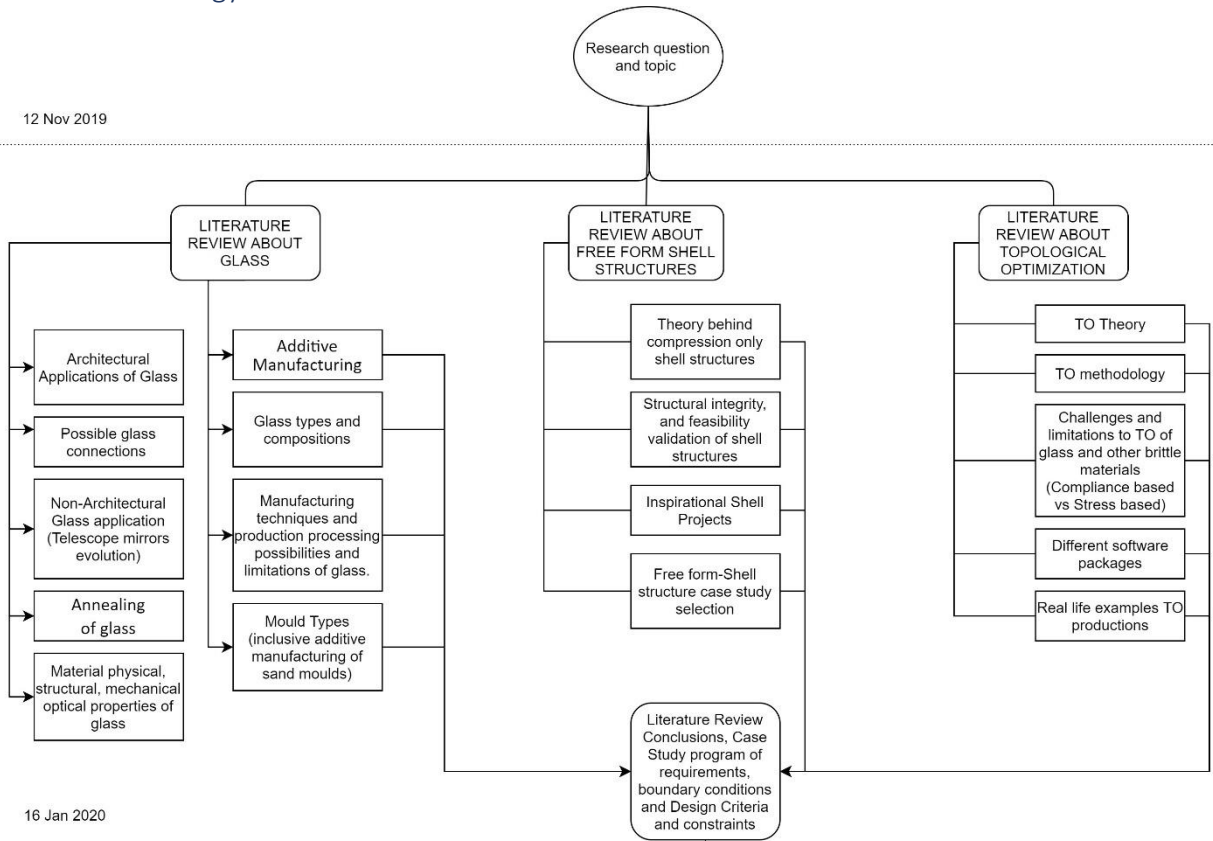
The report starts with a literature review. The first section will discuss glass applications, different compositions, annealing time, production methods, challenges and properties. The second section will explain structural optimisation, evaluate different topological optimisation approaches and software. The third section will handle the theory behind shell structures and form-finding methodology. Subsequently the case study will be presented. The design criteria are set based on the conclusions derived from the literature review findings. Then the design process begins and ends with the following:

1. Shell form will be determined.
2. Solid shell is structurally verified.
3. Topology optimisation is iterated.
4. The design evolution of the shell with the result of TO will be presented.
5. Then options are compared, and a method is developed regarding tessellation patterns and connection.
6. Finally manufacturing, transportation and assembly procedure is defined regarding connection (interlayer), cast glass mould, shell elements and foundation.

1.3.2 Research Methodology Scheme

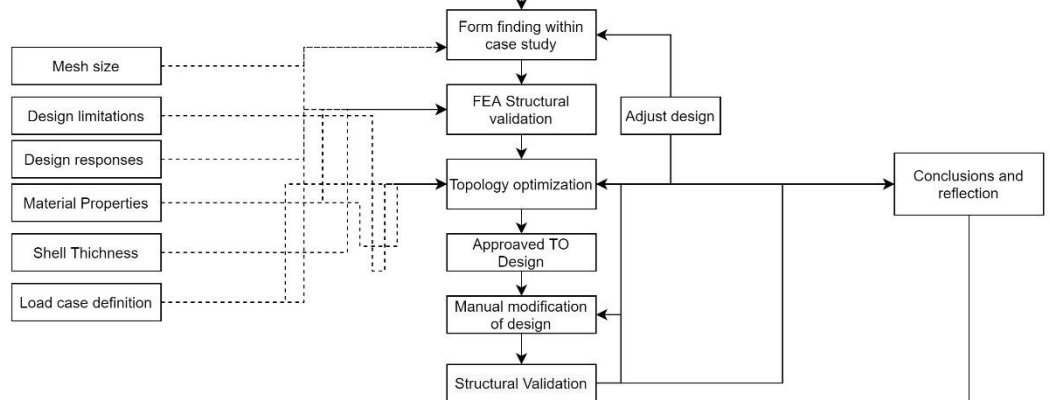
P1

12 Nov 2019



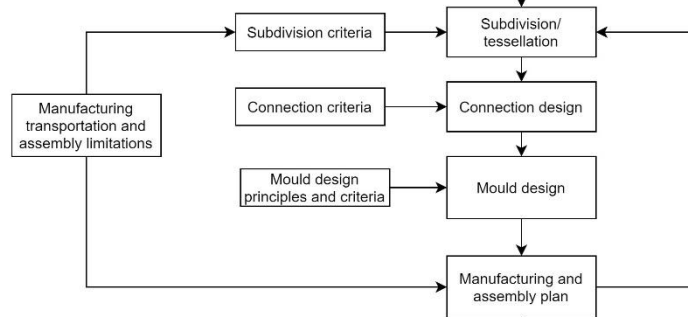
P2

16 Jan 2020



P3

26 March

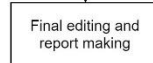


P4

21 May

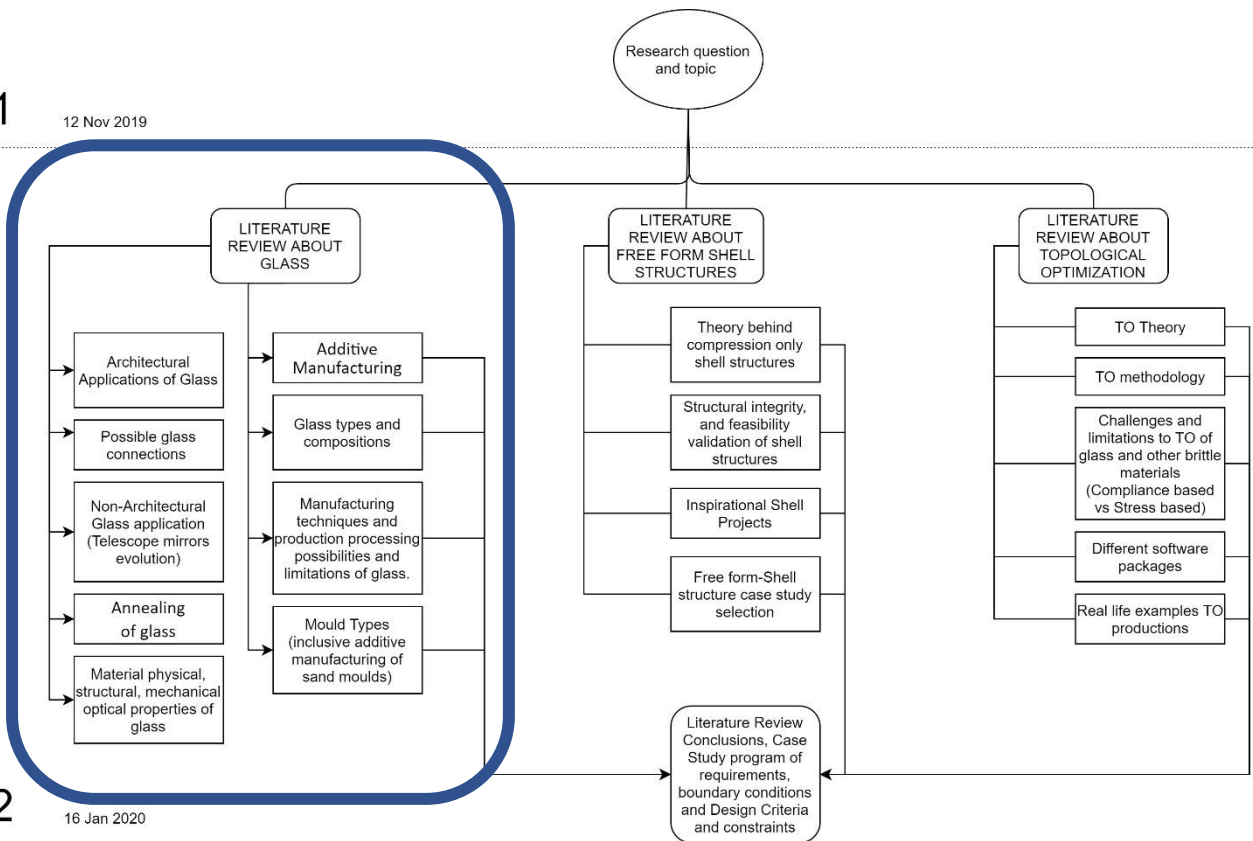
P5

6 July



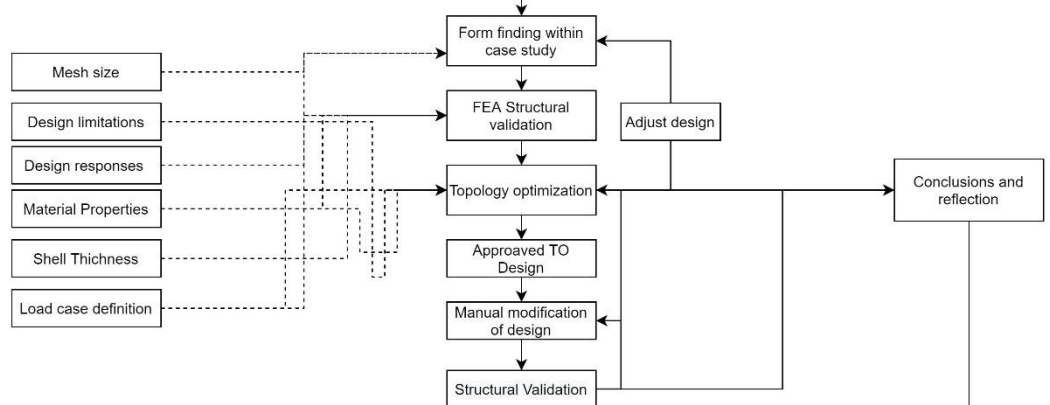
P1

12 Nov 2019



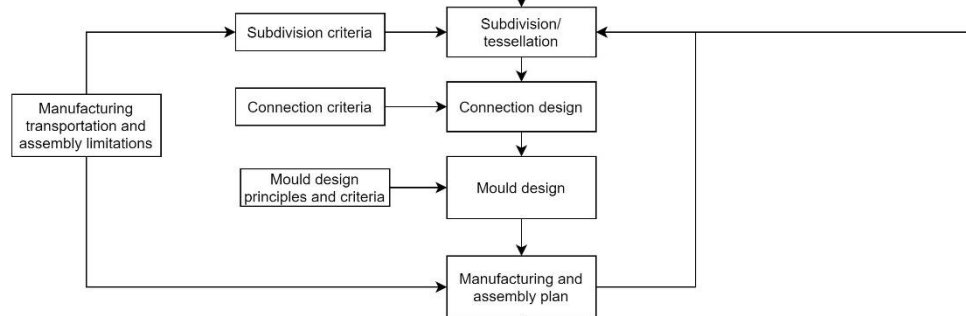
P2

16 Jan 2020



P3

26 March

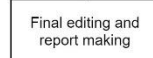


P4

21 May

P5

6 July



Chapter 2: About Glass

- 2.1 The potential of glass in structures
- 2.2 Properties of glass
- 2.3 Glass types and compositions
- 2.4 Glass Manufacturing Methods
- 2.5 Annealing of Glass
- 2.6 Glass Moulds
- 2.7 Mass optimisation in cast glass: The telescope mirrors
- 2.8 Conclusions

2.1 The potential of glass in structures

As discussed in the introduction, glass has the potential to be used in structural applications, due to its high compressive strength. Its optical transparency makes it attractive for designers and architectural applications. Among all manufacturing methods of glass, only cast glass has the potential of producing giant, monolithic, thick and complex 3D geometries that can be structurally validated. On the other hand, some mechanical properties present challenging limitations. These will be elaborated upon in this chapter.

2.2 Physical, structural, mechanical optical properties of glass

Each material has its own sets of strengths and limitations. Each design has its own sets of load cases and requirements. The design is usually driven based on the most important requirement and/or weakest attribute of the material. The property and requirement forcing the design to change in shape or increase in dimension despite already having achieved the minimum requirements of all other criteria is called the dominant determining factor. In this section some relevant values and properties will be explained. Appendix A includes a more elaborate explanation. Ashby et al. (2019) provides guidelines to a “Strength-limited” design and a “Fracture- and Fatigue-limited” design.

Glass is a homogeneous isotropic material, but it is not ductile. It is a brittle, fracture-limited design driven material. (Ashby et al., 2019, p. 60) To understand this one must understand simple mechanical terminologies and material properties. Some will be explained in this section and others in Appendix A.

2.2.1 Homogeneous material

A homogeneous material is a mixture with one “pure” material with uniform composition throughout the sample. The material cannot be split into different materials by mechanical force. (Ashby et al., 2019)

2.2.2 Isotropic material

Isotropic materials have identical properties in all directions. Glass and metals are isotropic materials. (Ashby et al., 2019)

2.2.3 Compressive strength vs tensile strength

Glass has a high compressive strength that exceeds 1000MPa. As shown in figure 4 this is even higher than many types of steel (Pye et al., 2005). The limitation in glass results from its low tensile strength. Glass might break due to local tensile stresses before it could ever reach its allowable compressive level. Hence the real allowable compressive limit cannot be verified through tests. (Emami, 2013)

Compressive Strength: 800- 1000 MPa (Saint Gobain, 2018)

Borosilicate glass Tensile Strength: 25.2 – 27.8 MPa (Granta Design Limited, 2019)

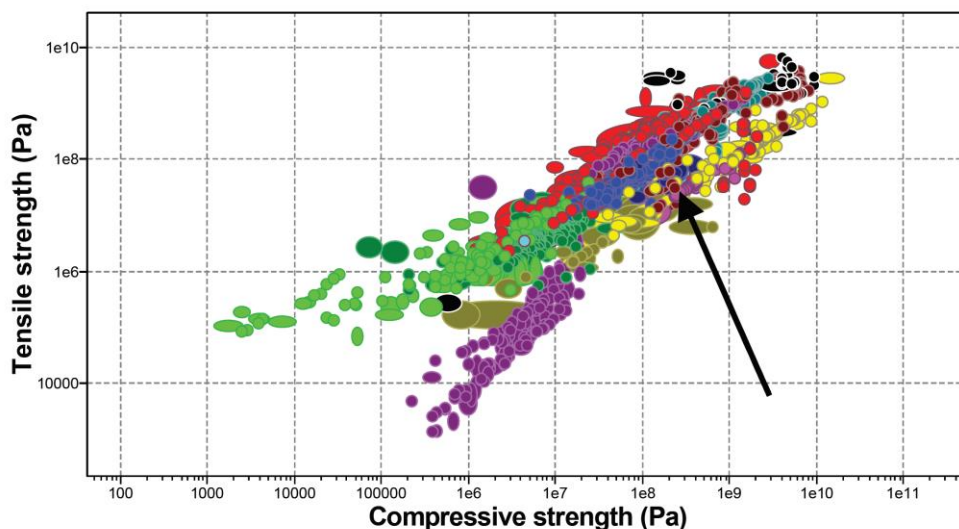


Figure 4 Compressive vs Tensile strength. Glass position in comparison to other materials. (Granta Design Limited, 2019)

2.2.4 Strength vs toughness

Strength of a material is its resistance to permanent deformation or complete failure. (Ashby, 2019, pp.48)

According to Ashby et al. (2019, pp.204) strength is a material’s resistance to plastic flow, while toughness is a material’s resistance to propagate a crack. If the material is not tough, it means that it lacks plasticity and is brittle.

A brittle material fractures at a stress level below its yield strength if a crack is present due to propagation. See figure 5. Fracture toughness is a property separate from yield strength. Understanding this is important because mostly designs are based on yield strength charts. For a brittle material like glass failure could “unexpectedly” occur even when the load is lower than what the material’s strength could withstand. (Emami, 2013). In other words, a brittle material would always break before it could ever permanently deform. One should assume that at least small cracks exist and consider a fail-safe design. (pp.263) Another consideration is to design with a shape that allows the object to fulfil its function without fracturing. (pp.259)

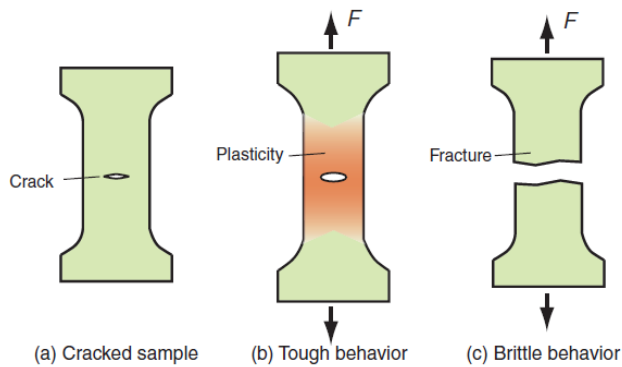


Figure 5 Tough and Brittle behaviour. in the crack in the material is shown. In b the material is tough, and its plasticity prevents the crack from immediately propagating when loaded. c depicts a brittle material like glass where a crack propagates at a stress lower than its yield strength (Ashby et al., 2019, fig 8.1 p. 205)

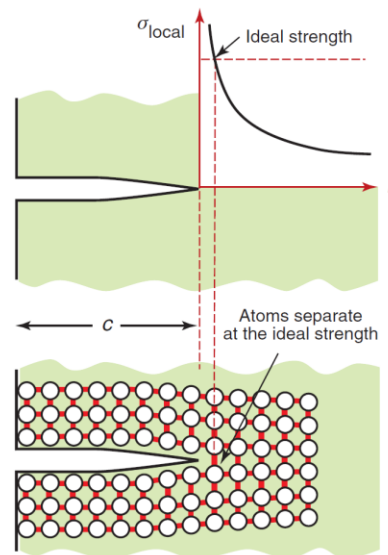


Figure 6 Cleavage fracture. Once the ideal strength is reached inter-atomic bonds are broken and molecules are pulled apart (Ashby et al., 2019)

2.2.5 Fracture toughness mechanics

Fracture Toughness is measured as K_{Ic} . This measure indicates the material’s resistance to cracking and fracture. Fracture toughness K_{Ic} is the value at which the stress intensity surpasses the critical value. Glass is brittle and has a low K_{Ic} . (Emami, 2013; Ashby, 2019)

Brittle fracture is typical behaviour of glass. Glass cracks at about $E/15$. This is the strength required to break apart atomic bonds as illustrated in Figure 6. In contrast to plastic materials, there is no plasticity at the crack tip. If the material is ductile a plastic zone forms at the crack tip. Glass however has a very high yield strength. This prevents glass to release stress through plastic flow at the tip. (Ashby et al., 2019) Nevertheless, fracture cannot be measured and therefore we can only design based on tension stress and deflection. However, it is important to understand fracture to understand glass behaviour and then understand why fracture is not used as a design criterion.

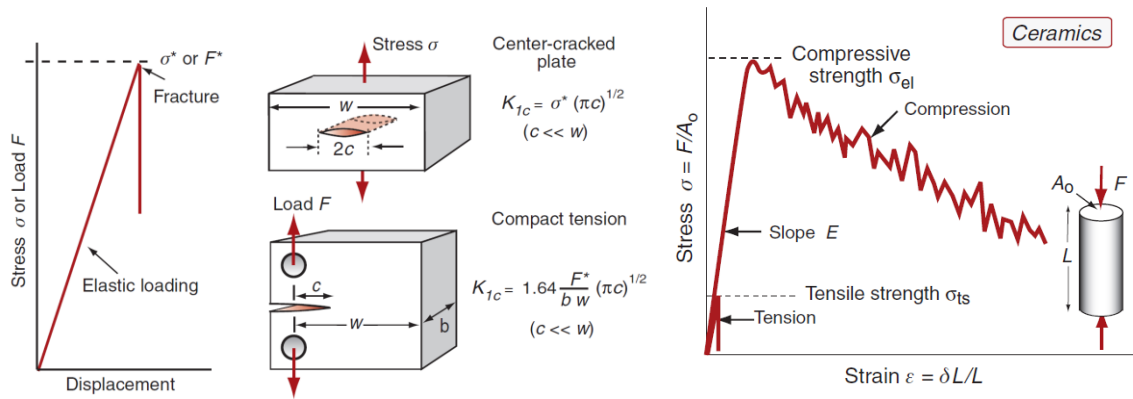


Figure 7 Fracture toughness, K_{Ic} , measurement. Only two tests are shown here as an example. (Ashby et al., 2019) Other tests and scenarios are described in chapter 8 and 10 of the referenced book, but any further explanation goes beyond the scope of this research. The point of this graph is to show how fracture toughness leads to a sudden crack in the material lacking plasticity. The failure happens abruptly without any warning. In comparison a tough material would deform gradually and fail by means of the yield stress before it fractures. Stress-strain curve for brittle material. Right: in compression. Left tension test

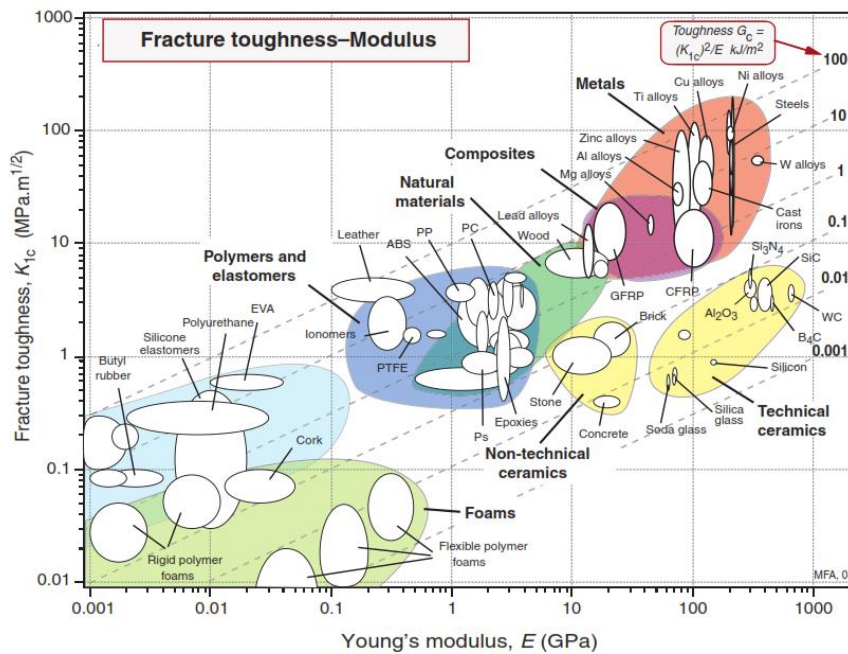


Figure 8 Fracture toughness K_{Ic} against Young's Modulus E . G_c , the toughness is shown as contours. Soda lime and silica glass are placed at the lower right corner of the graph in the Technical ceramics group (Ashby et al., 2019)

According to CES Edupack borosilicate glass fracture tensile strength ranges between 22-32 MPa and its fracture compressive strength ranges between 260-350 MPa (Granta Design Limited, 2019). These values drastically differ from one source of literature or experiment test to the other (Oikonomopoulou, 2019)

2.2.6 The fracture toughness-Young's modulus chart

Figure 8 plots the fracture toughness K_{Ic} against modulus E with Toughness contours lines, G_c . The lower part of the chart plots brittle materials with a low fracture toughness K . These materials maintain these elastic behaviours until fractured. Just as in figure 8 above. With the Toughness logarithmic scale, glass and ceramics have a lower G_c than polymers.

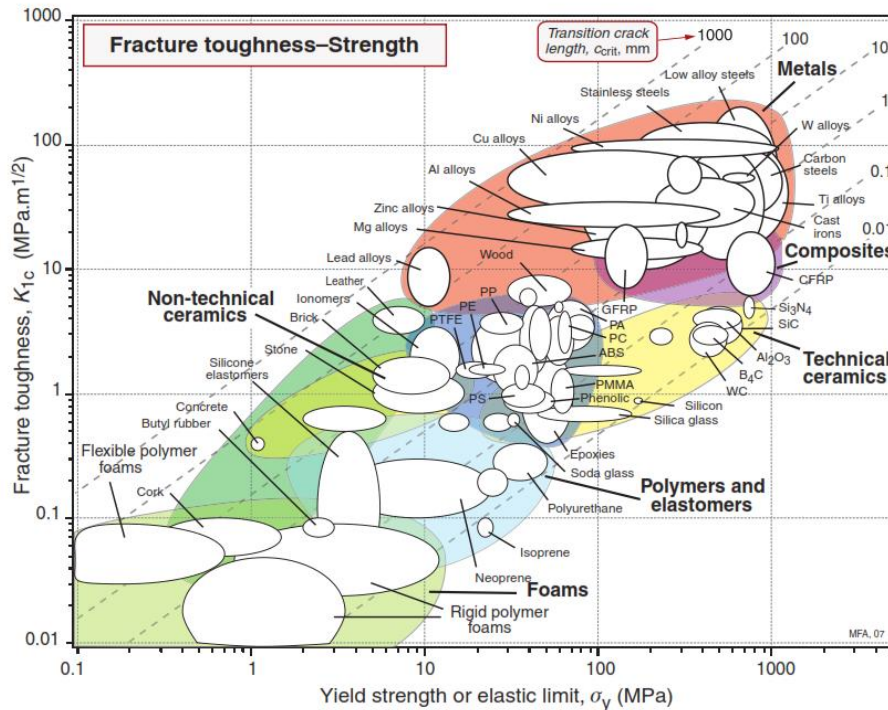


Figure 9 Fracture toughness plotted against yield strength. The transition crack size is shown, c_{crit} is shown in by the contours (Ashby et al., 2019)

2.2.7 The fracture toughness– Yield strength chart

When the material is strength-limited for design, then the yield prior to fracture becomes a crucial figure to account for. Figure 9 plots fracture toughness against yield strength. Materials at the bottom right have low toughness but high strength. Hence, they fracture before they yield. Soda lime glass is in this region (bottom right), meaning that it will fracture before it yields. This can also mean that designing with glass would be a fracture-limited design, not a strength-limited design. (Ashby et al., 2019)

More about the mechanical and structural properties is explained in appendix A.

2.2.8 Conclusion on glass mechanical and structural properties

Glass is a homogeneous isotropic material, but it is not ductile. It has a high compressive strength but low tensile strength. Therefore, it should be used in structures where only compression loads are present. Glass has a low fracture toughness, which means that it is a brittle, fracture-limited design driven material. (Ashby et al., 2019, p. 60) Nevertheless, fracture cannot be measured and therefore the design will be based on tension stresses and deflection limited. It is important to understand fracture to understand glass behaviour, but it will not be used as a design criterion. Numerical properties of borosilicate glass are summarised in table 1.

Table 1 Summary of properties of 7740 Borosilicate glass based on CES EduPack' averages (Granta Design Limited, 2019) ***
 Since glass would break due to local tensile stresses before it could ever reach its allowable compressive level. That is why the real allowable compressive limit cannot be verified through tests. (Emami, 2013) Compressive Strength: 800- 1000 MPa (Saint Gobain, 2018)

Property	Units	7740 - Borosilicate glass
Composition	%molecules	81% SiO ₂ 2% Al ₂ O ₃ 13% B ₂ O ₃ 4% Na ₂ O
Density	kg/m ³	2225
Elasticity (Young's modulus)	GPa	62.95
Yield strength (elastic limit)	MPa	26.5
Yield Strength	MPa	26.8
Fracture Toughness	Pa.m ^{0.5}	6.1 e5
Tensile strength	MPa	26.5
Compressive strength	MPa	265 – 1000 ***
Toughness (G)	J/m ²	6.01
Flexural strength (modulus of rupture)	MPa	34.5
Shear modulus	GPa	26.25
Poisson's ratio	-	0.2
Thermal expansion coefficient	strain/°C	3.245 e-6
Specific thermal capacity	J/kg.°C	780

2.3 Glass types and compositions

Commercially, there are 6 main types of glass based on their composition. As summarized in the table 2 below, these are 96% silica, Soda-lime, Lead-oxide Silicate, Aluminosilicate, Sodium Borosilicate, and Fused Quartz/ Silica. (Oikonomopoulou, et al., 2018). Table 2 presents each type's melting, softening, annealing, and strain points. Table 3 summarizes all types in relation to their common uses along with each pros and cons.

Table 2 Approximate properties of different types of glass (Oikonomopoulou, 2019)

Glass type	Mean melting Point at 10 Pa.s*	Softening Point	Annealing Point	Strain Point	Density	Coefficient of Expansion 0°C - 300°C	Young's Modulus
	[°C]	[°C]	[°C]	[°C]	Kg/m ³	10 ⁻⁶ /°C	GPa
Soda-lime (window glass)	1350-1400	730	548	505	2460	8.5	69
Borosilicate	1450-1550	780	525	480	2230	3.4	63
Lead silicate	1200-1300	626	435	395	2850	9.1	62
Aluminosilicate	1500-1600	915	715	670	2530	4.2	87
Fused-silica	>>2000	1667	1140	1070	2200	0.55	69
96% silica	>>2000	1500	910	820	2180	0.8	67

* These values are only given as a guideline of the differences between the various glass types. In practice, for each glass type there are numerous of different recipes resulting into different properties.

2.3.1 Soda-lime glass composition

This composition is the most commonly produced and the cheapest. The higher the manufacturing temperature the higher the production cost. Soda lime can be manufactured at a low cost because it has a low melting temperature (1350–1400 °C Mean melting Point at 10 Pa). It is durable but inferior when faced with sudden change in temperature (thermal shock), exposed to high temperatures, or strong alkali due to its weak thermal and chemical resistance. Façade glass and bottles are two common applications of soda lime glass. (Oikonomopoulou, et al., 2018)

2.3.2 Lead-oxide silicate glass composition

This is the second least expensive glass after soda lime. Its consistence of 20% lead contributes to its soft characteristic and attributes to having a low melting point (1200–1300 °C Mean melting Point at 10 Pa). It is relatively easy to shape and play with when cold because it is softer than other glass types. Artists find this appealing to work with because they can easily post process it by grinding and polishing. Artists find it visually alluring due to its high refractive index. It is used to block nuclear radiation as it can absorb x-rays as a result of its high PbO %. However, its vulnerability to thermal shock and high temperatures, and easily scratched surface, makes it not suitable for architectural applications (Oikonomopoulou, 2019, p54; Damen 2019, p18; Oikonomopoulo, 2018)

2.3.3 Aluminosilicate glass composition

As indicated by its name, this type contains alumina (Al₂O₃) This type of glass has a high manufacturing cost in relation to its high melting point (1500–1600 1300 °C Mean melting Point at 10 Pa). Nevertheless, it is a strong glass and is comparatively highly resistive to chemicals, high temperatures and thermal shocks. Some application where aluminosilicate is used are mobile telephone screens, combustion tubes, fibre glass, and high temperature thermometers.

2.3.4 Fused quartz/ 99.5% silica composition and 96% silica glass composition

These two types are almost entirely made out of silica, which makes them have a very high melting temperature. The additives in the composition of the other types of glass contribute to lowering their melting temperature. In reality, fused silica and 96% silica glass melting temperature is above 2000 °C at 10 Pa. It is heated to a state that glass can be shaped but producers do not reach a complete molten state of these glasses. Hence it allows for limited shapes. This extremely high manufacturing temperature makes these glass types the most expensive. On the other hand, the lack of additives reduces the internal stresses and allow for a high thermal temperature

resistance. Fittingly then, space craft windows are made of this thermal shock resilient glass. (Oikonomopoulou, 2019)

2.3.5 Sodium borosilicate glass composition

Borosilicate glass is discussed last because it is considered to be the most suitable for cast glass. It requires a shorter annealing time than others and therefore larger cast glass volumes can be moulded. For example, the Giant Magellan Telescope mirror, the Dennis Altar glass slab, the “Optical house”, and the “Atocha memorial” were all cast glass projects that used Borosilicate glass. It is also resilient to thermal shock and chemicals. Thanks to boron oxide attributes to Borosilicate glass its thermal expansion rate is low. Its processing costs slightly more than soda-lime and lead-oxide glass but is considerably less than that of aluminium-silicate, 96% silica, and fused silica glass. This manufacturing cost corresponds to its Mean melting Point at 10 Pa of 1450–1550 °C, which lies in between that of the aforementioned types of glass. (Oikonomopoulou, et al., 2018)

Table 3 Different types of glass, their estimate of the chemical composition, common applications glass as derived from (Shand, Armistead 1958; and presented by Oikonomopoulou, 2019)

Glass type	Approximate Composition	Observations	Typical applications
Soda-lime (window glass)	73% SiO ₂ 17% Na ₂ O 5% CaO 4% MgO 1% Al ₂ O ₃	Durable. Least expensive type of glass. Poor thermal resistance. Poor resistance to strong alkalis (e.g. wet cement)	Window panes Bottles Façade glass
Borosilicate	80% SiO ₂ 13% B ₂ O ₃ 4% Na ₂ O 2.3% Al ₂ O ₃ 0.1% K ₂ O	Good thermal shock and chemical resistance. More expensive than soda-lime and lead glass.	Laboratory glassware Household ovenware Lightbulbs Telescope mirrors
Lead silicate	63% SiO ₂ 21% PbO 7.6% Na ₂ O 6% K ₂ O 0.3% CaO 0.2% MgO 0.2% B ₂ O ₃ 0.6% Al ₂ O ₃	Second least expensive type of glass. Softer glass compared to other types. Easy to cold-work. Poor thermal properties. Good electrical insulating properties.	Artistic ware Neon-sign tubes TV screens (CRT) Absorption of X-rays (when PbO % is high)
Aluminosilicate	57% SiO ₂ 20.5% Al ₂ O ₃ 12% MgO 1% Na ₂ O 5.5% CaO	Very good thermal shock and chemical resistance. High manufacturing cost.	Mobile phone screens Fiber glass High temperature thermometers Combustion tubes
Fused-silica	99.5% SiO ₂	Highest thermal shock and chemical resistance. Comparatively high melting point. Difficult to work with. High production cost.	Outer windows on space vehicles Telescope mirrors
96% silica	96% SiO ₂ 3% B ₂ O ₃	Very good thermal shock and chemical resistance. Meticulous manufacturing process and high production cost.	Furnace sight glasses Outer windows on space vehicles

2.3.6 Conclusion regarding glass compositions

Borosilicate glass is considered to be the most suitable composition for cast glass of large elements. This is because it has a low thermal expansion coefficient and melting temperature. Further in the report annealing will be explained to one of the most challenging aspects of cast glass. Choosing the borosilicate glass contributes to lowering the time and temperature of annealing. Borosilicate glass is also resilient to thermal shock and chemicals. This is also a relatively affordable type of glass for large size manufacturing.

2.4 Glass manufacturing methods

Until now there have been 4 primary discovered manufacturing techniques for glass. Mainly, float glass (figure 10), extruded glass (figure 17), 3D printed (figure 24), and cast glass. These 4 techniques are comparatively summarized in table 4 by Oikonomopoulou (2019).

Table 4 Comparative summary of the 4 known glass manufacturing techniques for building purposes within their size limitations (Oikonomopoulou, 2019)

Glass process	Optical Characteristics	Main type of glass applied	Standard size [mm]	Thickness [mm]
Float	Smooth Transparent	Soda-lime	3210 x 6000 ^a	2-25
Extruded	Smooth Transparent	Borosilicate Silica	1500-10000 in length	Hollow: 460 Ø Solid: 300 Ø
3D-printed	Layered Transparent	Soda-lime	currently up to 30 kg	currently approx. 30 mm ^b
Cast	Smooth Transparent	Soda-lime Borosilicate Lead	currently up to 20000 kg ^c	n/a

^a The max. panel size is continuously stretching. At present, up to 20 m long panels have been produced.

^b Based on the work of (Klein 2015)

2.4.1 Float glass

According to Pilkington (n.d.) float glass is produced through 6 stages as follows:

Stage 1: Melting, refining and homogenising of raw glass in a controlled quality at 1550 °C.

Stage 2: The Float bath Stage. Molten glass is gently poured over molten tin. The temperature in this stage is 1050 °C. Glass exits this stage solidified at 600°C. The sheet thickness is limited within the range from 6.8 mm to 25 mm.

Stage 3: Coating. Coating can significantly affect optical quality. Chemical vapour deposition (CVD) is the most advanced method preventing major optical effects. These coatings, depending on their type, can be wavelength selective. For example, reflect infrared while allowing visible light to pass through.

Stage 4: Annealing as discussed previously allows for stress release while cooling.

Stage 5: glass is inspected

Stage 6: it is cut into the ordered length

raw material

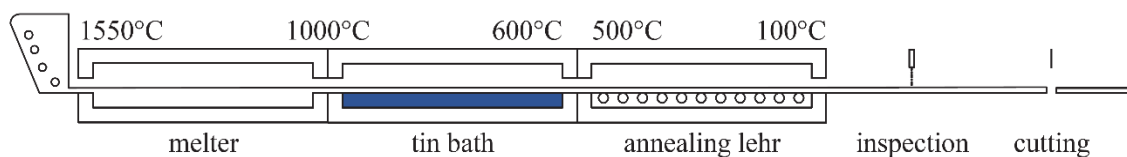


Figure 10 schematic illustration of float glass production by means of a tin bath (Oikonomopoulou, 2019)

2.4.1.1 Structural applications of float glass in architectural projects

Glass is commonly utilized in non-structural functions in the architectural world. Such applications include windows and non-structural separative walls. However, throughout the past years, some engineering pioneers have been using glass for structural purposes. The evolution of float glass in structural applications will be demonstrated using a few examples, followed by inspiring extruded, 3D printed and cast glass projects.

2.4.1.1.1 Apple stores

Apple has invested in architectural designs that reflect the morphological characteristics of their products. Glass was chosen as a representative building material for Apple stores due to its elegant transparency, simplicity and

minimalistic look. Apple persuaded engineers to push the boundary of glass to be used in staircases, beams, columns, facades and roofs. Steve Jobs was excited to see James O'Callaghan's glass design for the New York City Apple flagship store in SoHo. Jobs encouraged O'Callaghan make the entire box from glass. As a result, the designs evolved by having larger glass elements leading to less connections. Elegance was enhanced as the connections got striped down says O'Callaghan. Eventually in 2011, the 5th Avenue glass cube was refurbished consisting of only 15 10-meter-high-panels and 40 fittings. (Devlin, 2019) O'Callaghan later designed another glass box with Forester + Partners for the Apple store at the Zorlu Center in Istanbul, Turkey. This box has just 4 panels and no fittings at all. Each panel is 10-meter-long and 3 meters high. (Hein, 2014) See Figure 11 and 12.



Figure 11 Apple Store Glass Cube on Fifth Avenue, NYC, USA by Foster + Partners. Renovation started 2017 and reopened door September 2019 (Baldwin, 2018; Devlin, 2019)



Figure 12 Apple store glass box in Zorlu, Istanbul, Turkey by Foster + Partners and Nous Studio built in 2014 (Baldwin, 2018)

2.4.1.1.2 Museum aan de stroom (MAS)

ABT have made some ambitious glass designs. Museum aan de stroom in Antwerp is one of them (2009). MAS is a good example of how corrugating glass can make it stronger. The alteration of geometry enables this façade to withstand strong wind forces.



Figure 13 Museum aan de Stroom (MAS) in Antwerp, BE – built in 2009 (ABT, 2013)

2.4.1.1.3 Burgers Zoo glass stairs and bridge in Arnhem, NL (1996)

In 1996, ABT demonstrated how laminating multiple layers to each other can increase glass strength. The structure is resting on glass beams and connected with structural silicon. The stairs connect two buildings, while on the other side a bridge connects another two buildings. In 2012, a truck ran into the beams of the bridge. This case study shows that lamination protects parts from falling apart. It also shows that partial collapse did not cause damage to the bridge which was still hanging on the silicone. This is an interesting case study displaying the safety of glass when partially damaged. The use of lamination and structural silicone protected the structure from complete failure. (Louter et. al, 2014)



Figure 14 Burgers Zoo, Arnhem, NL - 1996 (ABT, 2013)



Figure 15 Burgers' Zoo, Arnhem, N L (1996, damaged: 2012)

2.4.1.1.3 Glass bridge design, Nieuw-Vennep, NL (2002)

The abt glass bridge design in Nieuw-Vennep is an example of maximum utilization of material. In collaboration with Glas-Cl, using Glastik and other computational software, the small structural components were tested, and connections were optimised. This is a good example on how meticulous detailing results in fine glass results (ABT, 2013)

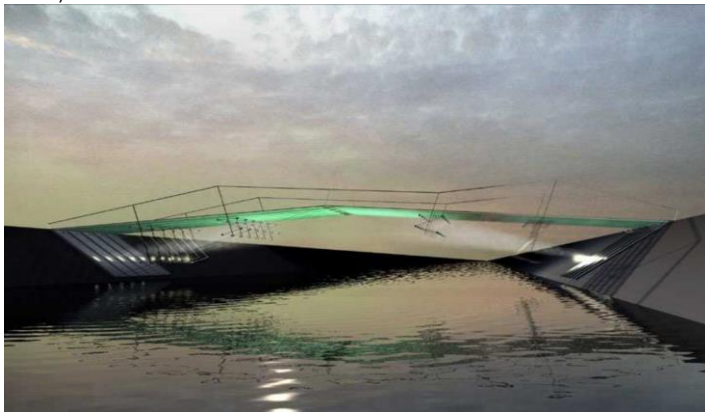


Figure 16 ABT Glass bridge design, Nieuw - Vennep, N L (2002)

2.4.2 Extruded glass

This method is mostly suitable for glass with a high softening point, tendency to crystalize and sharp viscosity curve. On the other hand, Fused Silica or 96% silica glasses can also be used despite having a very high melting temperature because extrusion can be done at a low working temperature. Hollow circular tubes or non-circular solid cross sections are usually produced using this method. (Roeder, 1971)

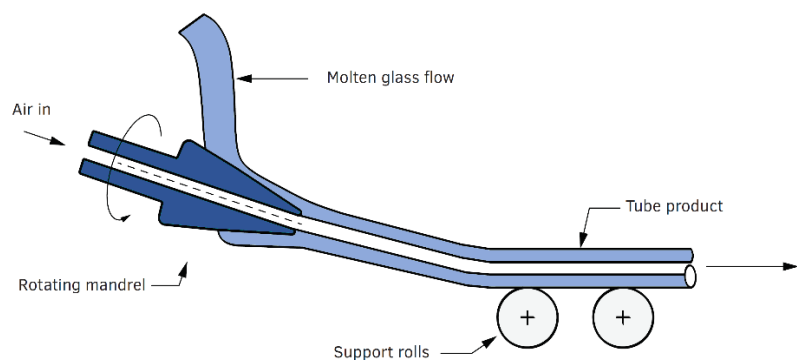


Figure 17 Principle of the Dannner process of extruded glass (Oikonomopoulou, 2019)

2.4.2.1 Structural extruded glass architectural examples

2.4.2.1 The bundled glass column

The bundled glass column was realized using extruded borosilicate rods and 2 component adhesive bond. It was initially designed for the Arnhem office of ABT but was never used due to an issue with lamination. Years later this was solved, and it was built. The final design includes a metal rod running through the middle for pre-stressing purposes. (Oikonomopoulou et al., 2017b). See figure 18.



Figure 18 Right: Extruded glass bundled column with adhesive bond. Left: CONTURAX® and DURAN® extruded profiles by SCHOTT 2012 retrieved from Oikonomopoulou et al., 2017b

2.4.2.1.2 The Tubular Column (layered)

The cylindrical shape of this column makes it excel in stiffness and more resilient against torsion and buckling. These tubes were also used in a structural application by ARUP in London's Tower Place. It was not a column in this case. The tubes functioned as wind load carriers being horizontal façade elements. Steel cables pre-stressed them allowing for tensile forces. See figure 19. (Oikonomopoulou et al., 2017b) Another example of these tubular columns was the setup of a tree-shaped compression only structure in Aachen, Germany for Glassbaum. See figure 20. (Knaack, 1998)



Figure 19 Tower Place in London. Pre-stressed structural glass tubes (Bhatia, 2019)



Figure 20 Tubular extruded glass column tree structure in Aachen, Germany for (Knaack, 1998)

2.4.2.1.3 The glass truss bridge

On the Green Village on the campus of Delft university of Technology (TU Delft), the Glass & Transparency Research group from the faculties of Architecture and Civil engineering, built a Glass Truss Bridge. To the extent structural feasibility made possible the use of glass components was maximized. This means that the fitting nodes are made of cast glass, and the truss diagonals are made of glass bundle struts. The extruded glass bundle struts are pre-tensioned by means of a 12 mm diameter steel rod. Pre-stressing offers a solution in case to enable tensile forces to occur. The safety of the structure has been verified by a series of load testing. Twice the maximum expected load case was used to validate the glass bundles prior to their installation. After installation the entire bridge has been proof-loaded for a variety of both static and dynamic critical load combinations. Strains were measured during load testing and passed acceptable limit requirements. (Snijder et al., 2018).

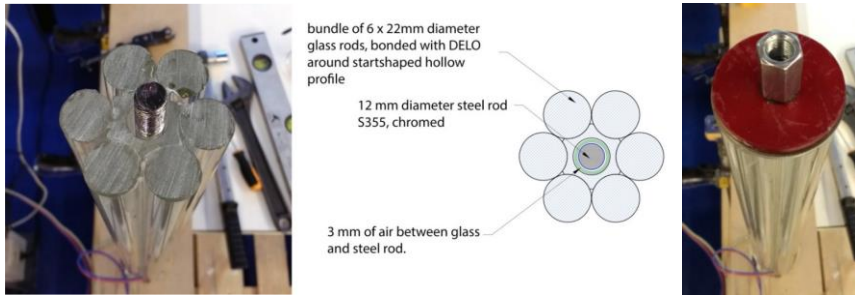


Figure 21 Cross-section of the bundles on the left. On the right extension nut to apply pre-stress (Snijder et al., 2018).



Figure 22 The glass truss bridge (Snijder et al., 2018).

2.4.2.1.4 The Glass Swing

The glass swing was designed to have all forces transferred axially like in spatial struts or vertical columns. The geometry was found by structural optimisation. A safety factor was implemented so that in case two rods break the swing will remain by means of force transfer through the rest of the bundle. More about it can be found in the TO chapter of this report. (Snijder et al., 2019).



Figure 23 The Glass Swing at Delft University (Snijder et al., 2019)

2.4.3 Additive Manufacturing of glass (3D Printed)

This method, just like any other 3D printing, adds viscous glass layer by layer on top of each other through a nozzle. Klein et al. (2015) has managed to additively manufacture several optically transparent glass objects. The methods offer shape flexibility. However, it is a slow process in comparison to others. The structural integrity of the objects is not validated. Size is limited by manufacturing machines. Due to the required annealing time for stress release, the 3D printed object must remain in a 600- 800°C heated oven while being printed. (Klein, 2015)

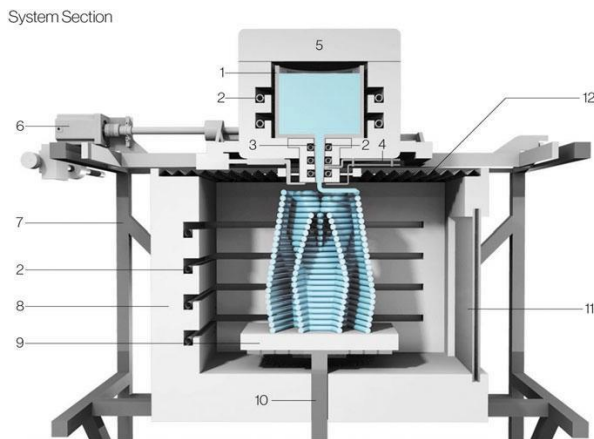


Figure 24 A cross sectional render of 3D printed glass. These are the numbered parts: 1. crucible 2. heating elements. 3. nozzle. 4. thermocouple. 5. removable feed access. 6. stepper motor. 7. printer frame. 8. print annealer. 9. ceramic print plate. 10. z-driven train. 11. ceramic viewing window. 12. Insulating skirt (Klein et al., 2015)



Figure 25 Object printed using the platform in figure19 (Klein et al., 2015)

2.4.4 Cast glass

In this process glass molten then poured into a mould that enables glass to take the form of an irregular complex organic 3D geometry. For melting and pouring of glass there are two methods; hot forming (melt quenching) and kiln casting. (Oikonomopoulou, 2019)

2.4.4.1 Hot forming/ melt quenching

This is a form of primary processing, because glass is made from raw ingredients in this procedure. Glass is first made by mixing the raw ingredients in a very high temperature oven (~1200°C). Afterwards, at 850°C it is poured into the mould, and the mould is transferred into another oven for annealing. The temperature in the second for annealing starts from 600°C and cools down gradually till room temperature. This could take hours, days or months depending on the size of the cast element. Mass production can be realized by means of the process. (Bhatia, 2019) See figure 26.

2.4.4.2 Kiln casting

This is a form of secondary processing because solid pieces of glass are reheated till molten. This method requires a lower temperature. This process uses one kiln from melting the glass pieces to the annealing of the in-mould glass. Therefore, it requires one oven and one setup. It is suitable for prototyping, (Bhatia, 2019)



Figure 26 Hot Forming / Melt Quenching (Wheatonarts, n.d.)



Figure 27 Kiln Casting at TU Delft lab (Bhatia, 2019)

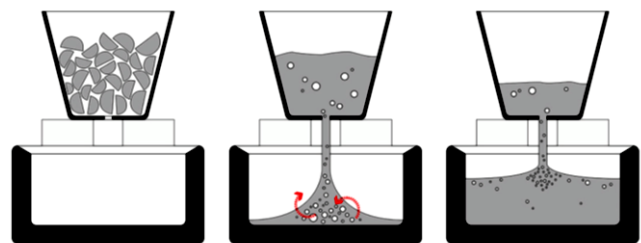


Figure 28 Kiln Casting (Bhatia, 2019)

2.4.4.3 Structural use of cast glass in the architectural domain

Despite the evolution and developments taking place with float glass, it still has its limitations. The main limitation that motivates engineers to investigate the potential of cast glass is float glass limited maximum thickness of 25mm. This disproportional (length /thickness) dimensioning drawback makes float glass more vulnerable to buckling. While float glass can be perceived as a 2D object, cast glass has the potential of forming a proportional length/thickness ratio. This 3D cast glass element would be more resistive to buckling than float glass. Cast glass easy free form casting would have the winning comparative argument against float glass' inflexibility of extensive free forming. (Oikonomopoulou, 2019)

The Crystal House façade in Amsterdam (Stevens, 2019), Crown Fountain in Chicago (Minner, 2011), Optical House in Japan (Hiroshi Nakamura & NAP, 2017), and the Atocha Memorial in Madrid (SCHOTT,2007) are referred to in almost every literature review on cast glass. This is probably due to the lack of other architectural projects employing cast glass structurally. This scarcity of projects is a result of the non-industrialized production method of cast glass. The process is manual. In order to ensure meeting the structural requirements of the assembly, proper connections are researched and developed. Therefore, they are rather real scale prototypes of experimental engineering exploring the potential of cast glass structurally (Oikonomopoulou, 2019, pp.108).

2.4.4.4 Architectural examples on cast glass

2.4.4.4.1 Crystal House façade in Amsterdam

This façade has been developed by MVRDV in collaboration with TU Delft and ABT engineers for in-depth research and development. Later Wessels Zeist was the contractor. The bricks mimic the traditional Amsterdam masonry bricks with glass bricks that were bonded using Poesia Delo industrial adhesives. Originally designed for Chanel, but currently accommodating Hermès store (Stevens, 2019). See figure 29 and 30

The envelope is 10 x 12 meters. The bricks were composed of low-iron soda-lime glass. Mould in open steel moulds (moulds will be explained later). There were 3 types of brick variations; namely, 210x210x65 mm, 210x257.5x65 mm, and 210x105x65 mm. This led to a range of 8 to 38 hours of annealing time. (More about annealing time will be explained later) (Oikonomopoulou et al., 2017).

Some concerning challenges arose in this project, mainly that the glue was too thin and could not accommodate any size deviations. This required meticulous and high accuracy demanding construction. For the low tolerance allowability the blocks had to be post-processed in order to achieve high level of accuracy. (Oikonomopoulou et al., 2017).



Figure 29 Crystal House Facade ABT TU Delft (Stevens, 2019)



Figure 30 Christal House ABT TU Delft (Stevens, 2019)

2.4.4.4.2 Crown Fountain

The Crown family commissioned the Spanish artist Jaume Plensa to design a gift for the Chicago community that reflects the qualities of water and light. They are two 50-foot-high LED lit towers, but most importantly made out of glass. (Minner, 2011) See figure 31. The envelope dimension is 12.5x7x4.9 m and it weighs 50.6 tonnes. Low-iron soda-lime glass bricks were casted in open steel moulds. Each brick weighs 4.5 kg. The towers are supported with a substructure. (Oikonomopoulou, 2019)



Figure 31 Glass Crown Fountain at night in Chicago, USA (Minner, 2011; Ermengem, 2019)

2.4.4.4.3 Optical House in Japan

Hiroshi Nakamura & NAP architects designed this project in Hiroshima, Japan, while Equitone manufactured the façade in 2012. The architects thought of cast glass to achieve privacy and tranquillity. As glass is translucent day light can protrude the interior without fully exposing the indoor scene to the public eye. Press steel moulds were used to cast 2.2 kg Borosilicate glass bricks. The façade is supported with a substructure. The blocks were threaded in a steel mesh that takes the tensile forces, resulting in a slender construction. (Oikonomopoulou, 2019) When pictures are taken from a distance the translucency is perceived pure, however the closer one gets, the clearer the impact of the substructure is. (Hiroshi Nakamura & NAP, 2017) See figure 32



Figure 32 The Glass Optical House in Hiroshima, Japan (Hiroshi Nakamura & NAP, 2017)

2.4.4.4.4 Atocha Memorial in Madrid, Spain

This masonry cylinder memorial was meant to commemorate the shock people experienced after the terrorist attack on March 11, 2004. Linking the devastating event that took place on September 11, 2001, the number 11 started to represent a meaning for Studio FAM five architects. Therefore, the cylinder was built to be 11 meters tall. (SCHOTT, 2007)

The memorial is a cylinder with envelope dimension of 8x 11m. The entire glass cylinder weighs circa 135,000 kg. It contains 15,600 borosilicate glass blocks and bonded using UV hardened acrylic adhesive bonds. One repetitive brick type was used dimensioning 300 x 200 x 70 mm. To accommodate a tolerance cylindrical form, each brick was convex from one side and concave on the other. (SCHOTT, 2007) The bricks were fabricated using press steel moulds, and took 20 hours for annealing (Oikonomopoulou, 2019, pp 109) See figure 33



Figure 33 Atocha Memorial in Madrid, Spain with SCHOTT Borosilicate Glass (SCHOTT, 2007)

2.4.4.5 Conclusion regarding cast glass in relation to other manufacturing methods

Table 5 Assessment of glass manufacturing methods based of criteria. information based on Schott (2016), Klein et al. (2015), AGC (2019), and Oikonomopoulou (2019).

	Thickness >25mm	Can be formed into very complex 3D geometry	Structurally validated	Smooth Transparent
Float glass	No	No	Yes	Yes
Extruded glass	Yes	No	Yes	Yes
3D printed glass	Some nozzles resulted in wall diameter of 85mm or more, but the average was 19.5 mm. The answer is not clear.	Yes	No	No, it's layered transparent
Cast glass	Yes	Yes	Yes	Yes

Until now, there have been 4 primary discovered manufacturing techniques for glass. Float glass is limited with a maximum thickness of 25mm. Extruded and float glass cannot form complex 3D geometries. Additively manufactured glass is not structurally validated. Cast glass can offer a solution to all of these limitations. Cast glass can be casted into complex 3D geometries with a significantly higher range of thicknesses and is structurally reliable, resulting with a smooth and transparent finish.

2.5 Annealing of glass

In the kiln-casting process glass is first heated to 800°C – 1100°C. After molten viscous glass fills the mould it is ready to cool down. The initial cooling stage is called quenching. This is a relatively fast drop in temperature (until it reaches 700°C) to prevent crystallization. If glass is permitted to cool down within the window between 1100 °C and 700°C at a slow rate, it might acquire a crystal molecular arrangement. If glass arranges in a crystal formation it loses its optical transparency. This clear optical quality is satisfied due to the lack of need for post processing like cutting. Internal stresses are avoided by allowing glass to relax during the low viscosity window. Afterwards the cooling process is slowed down. The annealing process starts when the viscosity of the glass is thick enough so as not to deform under self-weight. Below the softening temperature point the shape is preserved given that there are no external forces acting on it. With very slow rate cooling at the annealing point glass is

permitted to gradually relax towards equilibrium by releasing any internal differential strains and residual stresses. (Shand & Armistead, 1958) This can be achieved at the annealing point because glass is still able to rearrange on a molecular level. The longer glass is maintained at the annealing point the more internally stable it will be. If the cooling process is not slowed down the surface layer will cool down fast while the core is still liquid. The inside glass will then have a different thermal expansion rate coefficient than the outside layers. This might cause tension or even failure in the form of cracks. (Cummings, 2001). At the strain point stress relief takes longer than at the annealing point. While it can take hours to release stress at the strain point, below that point residual stresses remain permanent. The relationship between viscosity and temperature of soda lime glass is depicted in figure 34 (Oikonomopoulou, 2019)

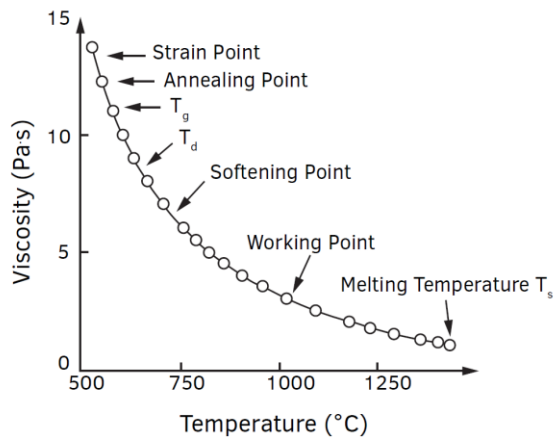


Figure 34 As function: the relationship between viscosity and temperature of soda lime glass (Oikonomopoulou, 2019)

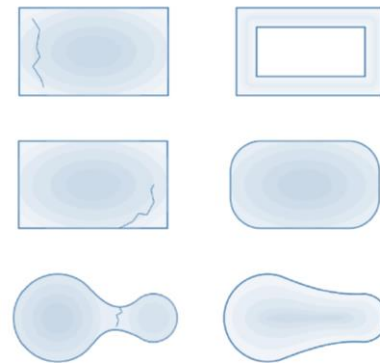


Figure 35 design principles for a strong glass, and faster homogeneous annealing time using smart design. From top and bottom: reduced weight or thickness, rounded forms with especially no sharp edges, and an even distribution of mass (Damen, 2019)

2.5.1 Design principals for strong cast glass and annealing

According to Shand & Armistead (1958) a homogeneous even distribution of mass and volume contributes to homogeneous cooling. A homogenous exposure to temperature differences plays a key role in preventing internal stresses. The mould serves as an insulating cover. Therefore a “lid”-covered mould would prevent the surface from cooling faster than the rest of the object. In this case one could speak of a homogenous cooling process. On the other hand, if one or more surfaces are exposed, the cooling process would be faster. A design lacking sharp edges and with smooth rounded corners can help avoiding large temperature gaps between warm and cold areas. This would prevent thermal shock in glass (Oikonomopoulou, 2019) Damen (2019) suggests some design principles for a strong glass, and faster homogeneous annealing time using smart design. See Figure 35

2.5.2 What affects annealing?

The telescope examples show that there are two prevailing factors affecting the annealing time. Type of glass and the Mass/Volume ratio. See Figure 36 and 37

Figure 36 shows that as the volume/mass increases the time for annealing increases exponentially. From the architectural cast glass examples this can be clearly seen. As a reminder, the crystal house 210x210x65 mm brick took 8 hours. One brick of 300 x 200 x 70 mm for the Atocha Memorial took 20 hours for annealing. The crystal house 210x105x65 mm cast glass brick took 38 hours of annealing time. However, the examples of cast glass telescope mirrors show that despite the increase in volume and mass, annealing time can decrease through smart design. Topological optimisation can facilitate a solution. (Damen, 2019). The 2.5 diameter solid disk of 4 tonnes took 12 months. The 20 tonnes 5m in diameter Hale telescope took 10 months of annealing. A significant decrease in annealing time was achieved with the Giant Magellan. The Giant Magellan is 16 tonnes and 8.4m in diameter and it took 3 months to cool. (Oikonomopoulou, 2019)

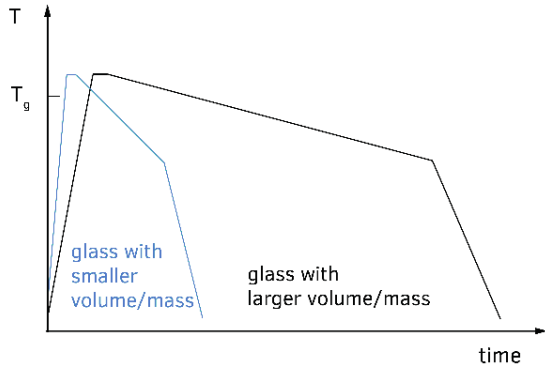


Figure 36 A scheme showing how annealing time can be reduced by decreasing the volume (Schott AG, 2004; as presented by Oikonomopoulou, 2019)

Figure 26 shows that different types of glass has a different the level of viscosity at every temperature. This means that the melting point, strain point and annealing point differs for every glass type. Henceforth, the next subheading will compare the most common compositions of glass. Melting temperature and annealing time required will be part of the evaluation for the different glass compositions.

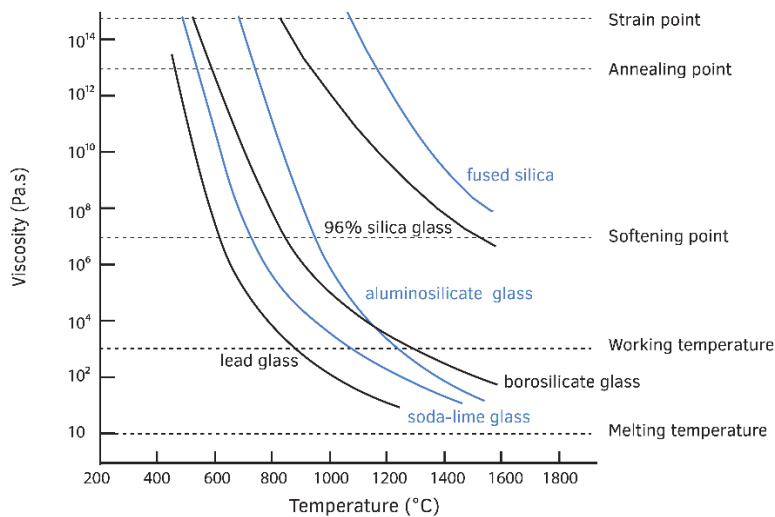


Figure 37 approximate viscosity vs temperature curvatures for different types of glass (Shand, Armistead 1958; as presented by Oikonomopoulou, 2019)

2.6 Mass optimisation of the glass giants: lessons learned from the cast glass blanks of the giant ground telescopes.

Non-architectural cast glass examples provide this research insight into the potential and limitations of giant monolithic elements regarding size and form in relation to annealing time. Annealing time is in other words cooling time, but it will be further explained under the next subheading. The lessons learned about the design, manufacturing process and its implications are practical to use when casting glass with a comparable component size for architectural purposes.

2.6.1 Hooker telescope

The Hubble telescope was built in 1979 and is 2.4 meter in diameter. Ultra-Low Expansion (ULE®) glass was cast. It was a solid cast that required 12 months of annealing. 3 years of post-processing took place to achieve the precision level required despite achieving concavity directly when cast. (Oikonomopoulou, 2019)

2.6.2 Hale Telescope mirror in Mt. Palomar

This is a 5m diameter telescope mirror cast in 1936. It is made from Pyrex® glass. In comparison with ordinary glass, Pyrex® low thermal expansion was appealing for use at the time. A custom-made furnace was made to fit the geometry and to achieve the required high temperature. A high temperature of 1482 °C was necessary to secure proper flow through narrow canals and a homogeneous distribution. It was the first honeycomb formed mirror. While weighing 15 tonnes, an 80% weight reduction was achieved by this design. It lasted for about 10 months in an annealing oven. The outer flat mirror surface was ground to become concave. The grinding process consumed more than a decade. (Oikonomopoulou, 2019)

2.6.3 Giant Magellan Telescope mirror

This is a 16 tonnes glass mirror that took only 3 months to anneal. E6 borosilicate glass was melted into a honeycomb structured silica-alumina mould. E6 borosilicate glass has a lower thermal expansion coefficient and is less viscous than Pyrex®. The honeycomb structure achieved a 90% weight reduction.

Spin casting is the procedure of rotating the object mould while still in the melting oven and during annealing. This was done in the same oven since kiln casting was implemented. This procedure was used for the 8.4m diameter monolithic Giant Magellan Telescope. Spinning the blank resulted in a concave geometry without post-processing. (Oikonomopoulou, 2019)

2.6.4 Conclusions regarding the annealing of cast glass

The Telescope examples show that there are two determining factors affecting the annealing time. Type of glass and the Mass/Volume ratio.

From existing cast glass projects, we learn that homogenous cooling is crucial in order to avoid cracks due to thermal gaps. As the volume/mass ratio increases the annealing time increases exponentially. This means careful consideration should be attributed to decreasing this time. Annealing is the process of cooling down glass as at a very slow rate. Gradual cooling at the annealing point, allows glass on a molecular level to rearrange and release internal strains and stresses. This would prevent crack in glass. Annealing has an impact on my design criteria

- The design should follow some design principles for strong glass, and faster homogeneous annealing time.
- These include avoiding sharp edges and ensuring an even distribution of mass in the volume.
- Thickness should not exceed 10cm
- And the annealing time must be shorter than 3 months

The telescope examples show that the smallest in diameter solid disk took up to 12month of annealing, while this time significantly dropped to only 3 months with the largest mirror. Two major factors can cut down the cooling process. First, by choosing low volume/mass (thickness) of the object. Second, by using a composition with a low thermal expansion coefficient and melting temperature.

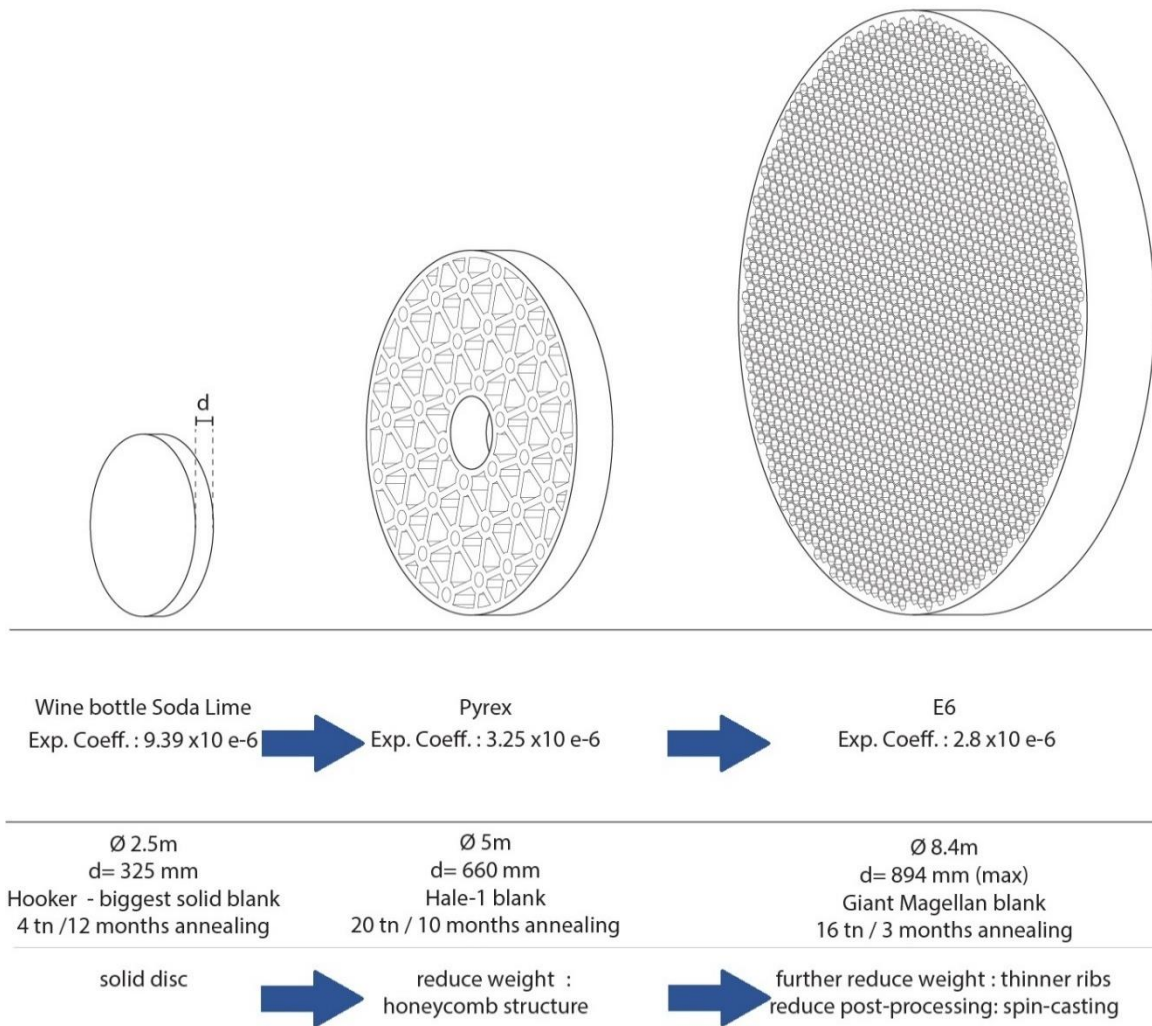


Figure 38 Cast glass evolution in increased size and a reduced annealing time. (Zirker, 2005; as presented in Oikonomopoulou, 2019)

2.7 Mould types

Molten glass is poured into a mould before annealing. For the most suitable mould one must consider accuracy tolerance allowed, batch size, time and cost. There are two major categories of moulds; Permanent moulds and disposable ones.

2.7.1 Disposable moulds

The product of these moulds is rough. The coarse surface demands postprocessing for smoothness and transparency. These moulds cannot be reused. Their form is non-adjustable. These moulds cost less because the materials they are made of are cheaper than those of permanent ones. These materials are Alumina-silica (high performance) and Silica Plaster fibre (castings below 1.000 °C to). Alumina-silica fibre yields higher precision than Silica Plaster. Such materials are brittle and cannot withstand very high temperatures. Therefore, disposable moulds are mostly used for kiln casting. The moulds are inserted into the furnace with the glass at the same time. Complex geometries are possible without excessive manufacturing cost. (Oikonomopoulou, et al. 2019)

Additive manufacturing (discussed below) introduces a new set of moulds that can be disposable or used up to 3-4 times, depending of the binder and material used. (Bhatia)

2.7.2 Permanent moulds

Large batch size production favours permanent moulds. They are made of steel, stainless-steel, or graphite. These are more durable and expensive materials. Non-stick agents, Boron nitride or graphite, coat the surface of the moulds which result with a clear transparent fine finish and no postprocessing is necessary. Permanent moulds are ideally paired with the melt-quenching/ hot forming technique for high efficiency. Adjustable shape moulds and press moulds are two possible variations. However, each variation differs in precision. Precision is the highest in press steel moulds, then it deteriorates to a high level in fixed moulds, and moderate/ high level in adjustable moulds. To avoid surface chills when pouring the molten glass in, the moulds are preheated. Proper preheating is crucial for a crisp surface finish. Complex geometries are possible but are accompanied by an increase in cost. (Oikonomopoulou, et al. 2019)

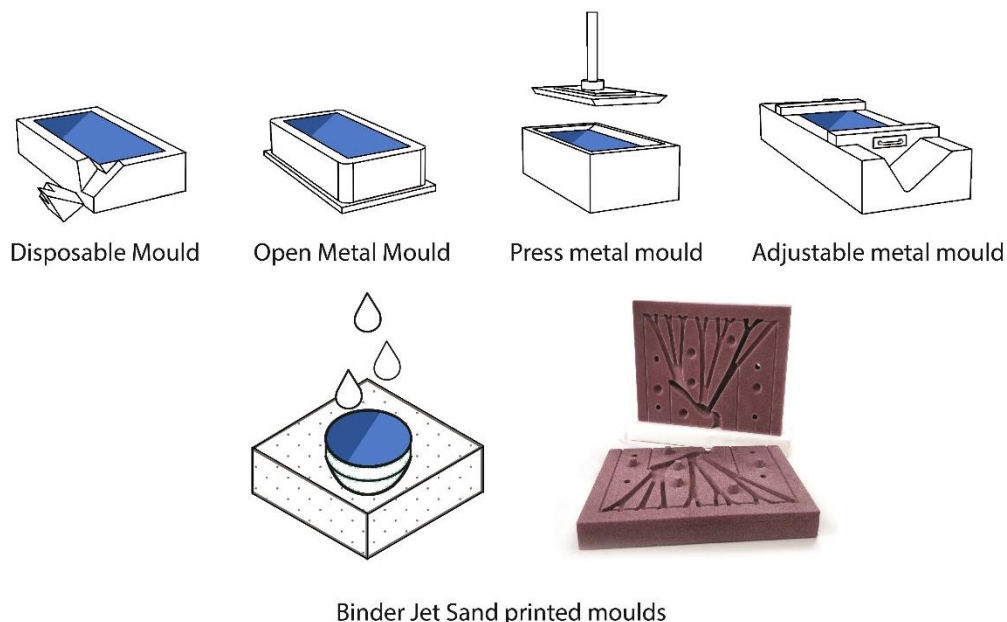


Figure 39 most popular mould types (Oikonomopoulou, 2019; Bhatia, 2019)

With the aforementioned mould types, one cannot have one very affordable mould for a very complex geometry that results in a high level of accuracy and precision. However, it is made possible by means of additive manufacturing. Arup and 3Dealise worked on a complex node project involving 3D printed sand moulds for steel. Bhatia (2019), among others, have already researched the potential of using 3D printed sand moulds for cast glass and have yielded promising results. (Oikonomopoulou, et al. 2019, p.76)

2.7.3 Additive Manufacturing (3D-Printing)

Additive manufacturing is another term for 3D printing. The process takes a computerized CAD model of a 3D geometry and builds it up by adding material one layer at a time. The joined 2D layers on top each other create the 3D object. (Bhatia, 2019)

There are many processing methods for 3D printing moulds. Each process is best paired with a different set of materials. The comparison between these different methods and materials is summarized in table 6. However, Bhatia (2019) research concluded that the most suitable 3D printed moulds for cast glass are those made out of sand using the Binder Jetting technology.

2.7.3.1 Binder Jetting: Additive manufacturing of sand moulds

This research is going to adopt the same sand mould manufacturing approach as Bhatia (2019) did due to the similarities between this project's requirements and the selection criteria Bhatia used. Bhatia selection criteria before selecting binder jetting of sand included the following:

- High precision
- Affordable cost
- Resilient material to high temperatures for the annealing time
- No support needed or dissolvable intermediate
- Smooth finish or treatable surface

Additive manufacturing of sand moulds comes with great advantages including adhering to the above-mentioned criteria. It has a very high accuracy of ± 0.1 mm, as influenced by the size of sand grains. (Oikonomopoulou, et al. 2019) It also facilitates the potential of complex geometries. Not to mention the reusability potential of excess sand during printing and destroyed used moulds. By using CHP binder system, the mould can be dissolved. In addition to the silica-plaster mould surface coating, using a water-soluble binder makes the cast glass object easy to detach from the mould. The application of surface quality coating can be challenging in deep narrow areas. (Damen, 2019) Once the object is hardened the mould can be simply immersed in water. Once cleaned it can be reused. (Damen, 2019) The mould is closed from all directions ("has a lid") and therefore allows for homogenous cooling.

The 3D printed object is anisotropic regardless of whether the material itself is isotropic in nature or not. This means that one cannot depend on the mechanical properties of the material in assessment of the 3D printed object. The process is slow and therefore not suitable for mass production. (Bhatia, 2019)

The printers are expensive, so investment in capital is required. If it is a onetime project ordering from a supplier will be cheaper. Current suppliers have a limit on the 3D printed object's maximum dimensions. VX4000 VoxelJet in the US, Germany, UK, China, and India can 3D print Sand Moulds up to 4,000 x 2,000 x 1,000 mm. (Voxeljet, 2018b). If money is not an issue, this facility can be used. To say the least, it indicates that these dimensions are possible. However, for prototyping purposes here is Delft, the facilities available in Rotterdam by CONCR3DE (2019) allows for 650 x 1400 x 800 mm sand moulds using their Hippo 3Dprinter. Ivneet Bhatia (2019) proved that several pieces of 3D printed sand mould can be connected together to make a larger mould. Bhatia (2019), achieved a tall mould by connecting smaller 3D printed sand moulds together via bolts and nuts. Nevertheless, since Covid-19 pandemic social distancing and the intelligent lockdown in the Netherlands, prototyping is not possible at the moment. Therefore, the only limitation that will be considered is that of the VX4000 VoxelJet of 4 x 2 x 1 m. The same concept of vertical stacking and multi sand mould bolt and nut connection can be applied to the 1:1 scale mould. By stacking 3 moulds on top of each other the mould limitation can be multiplied to 3 to reach a 4 x 2 x 3 m limitation.

Table 6 Comparative Analysis of 3D printing technologies based on inferences from “The 3D Printing Handbook” (Bhatia, 2019)

PROCESS OF 3D PRINTING	MATERIAL EXTRUSION	VAT POLYMERIZATION	POWDER BED FUSION	MATERIAL JETTING	BINDER JETTING	POWDER BED FUSION
MATERIAL GROUP	Thermoplastic filaments	Photopolymer resin	Thermoplastic powder	Photopolymer resin	Sand or Metal powder	Metal Powder
COMMON MATERIALS	PLA ABS PEI TPU	Standard Castable Transparent High Temp.	Nylon 6 Nylon 11 Nylon 12	Standard Castable Transparent High Temp.	Stainless/ Bronze Silica (sand casting)	Aluminum Stainless Steel Titanium
DIMENSIONAL ACCURACY	+/- 0.5 mm	+/- 0.5 mm	+/- 0.3 mm	+/- 0.1 mm	+/- 0.2 mm (metal) +/- 0.3 mm (sand)	+/- 0.1 mm
SUPPORT MATERIAL	Dissolvable available	Support required	No support required	Dissolvable	No support required	Support required
STRENGTH	<ul style="list-style-type: none"> Low cost Non-commercial functional parts 	<ul style="list-style-type: none"> Smooth surface finish Fine feature details 	<ul style="list-style-type: none"> Functional parts, good mechanical properties Complex geometries 	<ul style="list-style-type: none"> Best surface finish Full color and multi-material available 	<ul style="list-style-type: none"> Low Cost Large Build volumes Functional metal parts 	<ul style="list-style-type: none"> Strongest, functional parts Complex geometries
WEAKNESS	<ul style="list-style-type: none"> Limited dimensional accuracy for small parts Visible print layers 	<ul style="list-style-type: none"> Brittle Not suitable for mechanical parts 	<ul style="list-style-type: none"> Longer lead times Higher cost than material extrusion for functional application 	<ul style="list-style-type: none"> Brittle, not suitable for mechanical parts Higher cost compared to Vat Polymerization 	<ul style="list-style-type: none"> Mechanical properties not as good as metal powder bed fusion 	<ul style="list-style-type: none"> Small build sizes Most expensive of all
COMMON APPLICATION	<ul style="list-style-type: none"> Electrical/Housing enclosures Prototyping Jigs and fixtures Investment Casting patterns 	<ul style="list-style-type: none"> Injection mold-like prototypes Jewelry Dental Application Hearing aids 	<ul style="list-style-type: none"> Functional polymer parts Complex ducting (hollow) Low run part production 	<ul style="list-style-type: none"> Injection mold-like prototypes Low run injection molds Medical models 	<ul style="list-style-type: none"> Functional metal parts Sand casting Sand moulds for metal casting 	<ul style="list-style-type: none"> Automotive & Aerospace functional metal parts Medical Dental

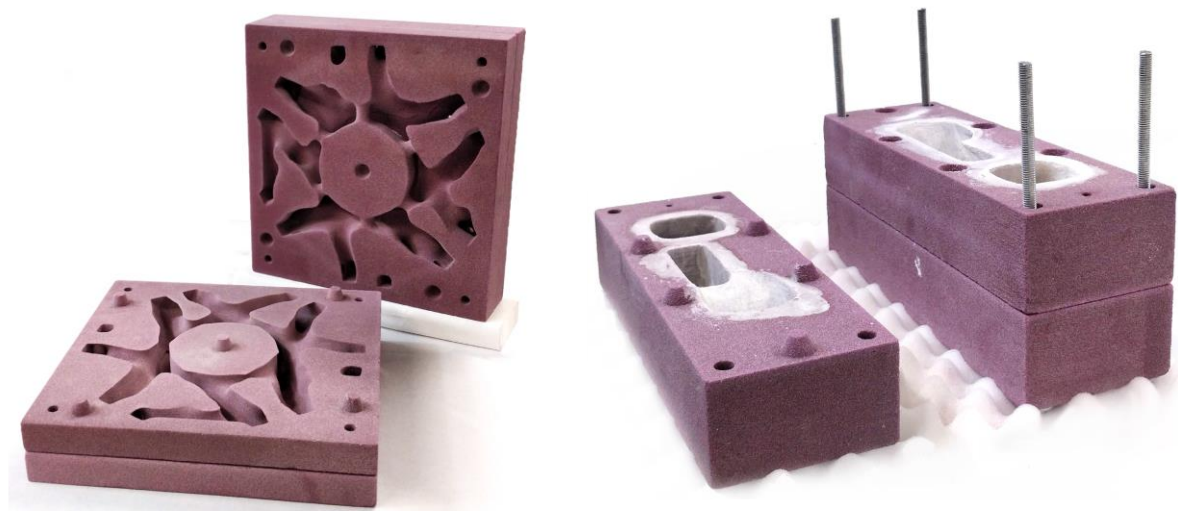


Figure 40 Stackable 3D printed sand mould. Mould dimension extended by bolt and nut connection (Bhatia, 2019)

2.8 Conclusions and decisions regarding glass

As a conclusion, cast glass has the potential of forming 3D complex geometries with a variation and a wide range of thicknesses that exceeds the limitation imposed by other manufacturing techniques. The process is not yet industrialized but both hot forming and kiln casting are promising techniques. Expectedly the real full-scale design would be casted using Hot Forming/ Melt Quenching. However, at the TU lab kiln casting would be implemented for prototyping, especially if recycled glass is to be used.

With different types of moulds on the market ranging from permeant to disposable ones, fixed and adjustable, the additively manufactured sand moulds by means of binder jetting are found to be the most suitable. This is due to:

- High Precision ± 0.1 mm
- Affordable cost
- Resilient material again high temperatures for a long time period.
- No support needed or dissolvable intermediate
- Smooth finish or treatable surface
- Facilitates the potential of complex geometries
- Reusability potential of excess sand during printing and destroyed used moulds
- In the CHP binder system is in used, then it can be dissolved. In addition to the crystal cast mould surface coating, using a water-soluble binder makes the cast glass object easy to detach from the mould.
- Once the object is hardened the mould can be simply immersed in water. The cleaned again sand can be reused for printing another mould.
- The moulds can be closed from all directions ensuring homogeneous cooling

The size limit for prototyping is 1m x 1m x 1m due to the available sand mould printers available.

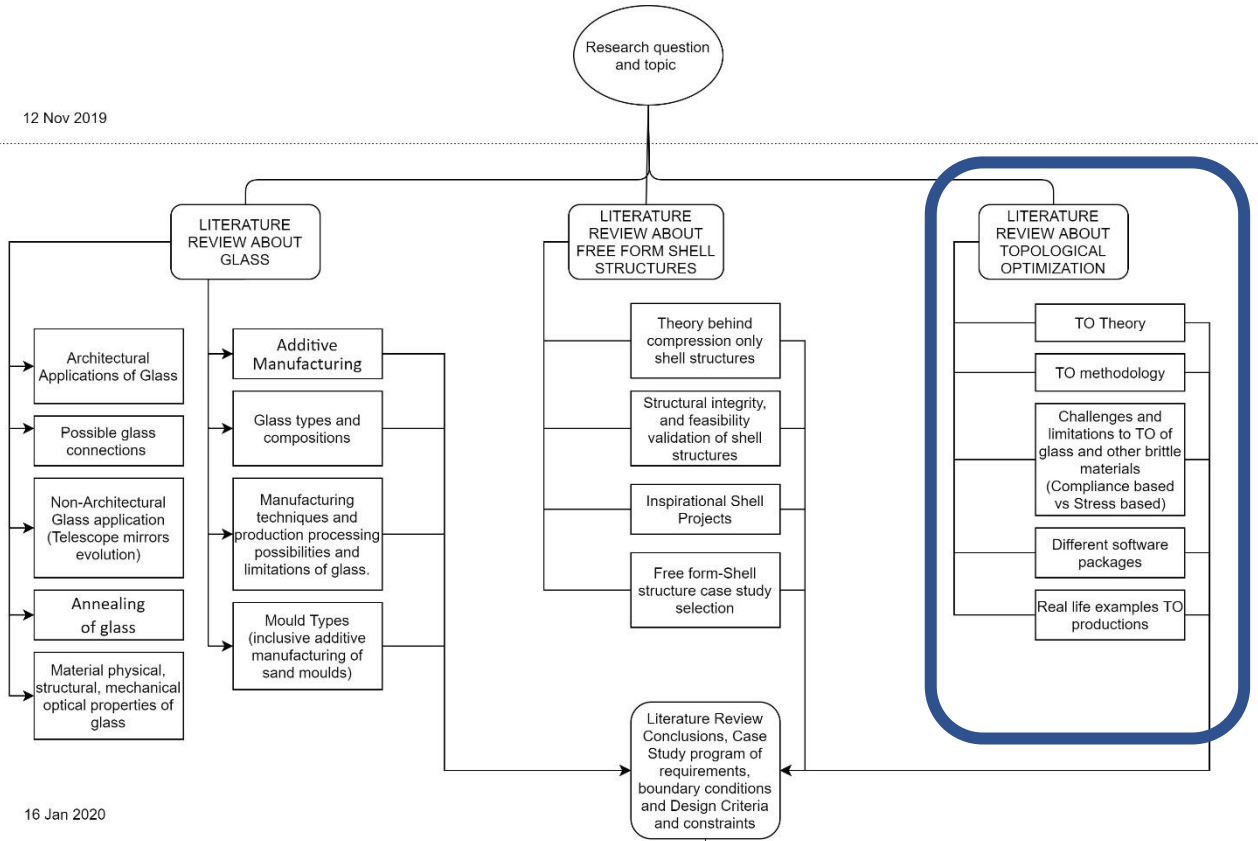
Annealing time is one of the most challenging aspects of cast glass. As the volume/mass ratio increases the annealing time increases exponentially. This means careful consideration should be attributed to decreasing this time. Two major factors can cut down the cooling process. First, by choosing low volume/mass (thickness) of the object. Second, by using a composition with a low thermal expansion coefficient and melting temperature. Therefore, borosilicate glass is considered to be the most suitable type for cast glass. Borosilicate glass is also resilient to thermal shock and chemicals. This is also a relatively affordable type of glass for large size manufacturing.

Homogenous cooling is crucial in order to avoid cracks due to thermal gaps. The design can ensure that by avoiding sharp edges and ensuring an even distribution of mass in the volume.

Since glass is strong in compression but weak in tension a compression only structure is found to be fitting. To avoid tension, or fracture, one must avoid moments and therefore deflection.

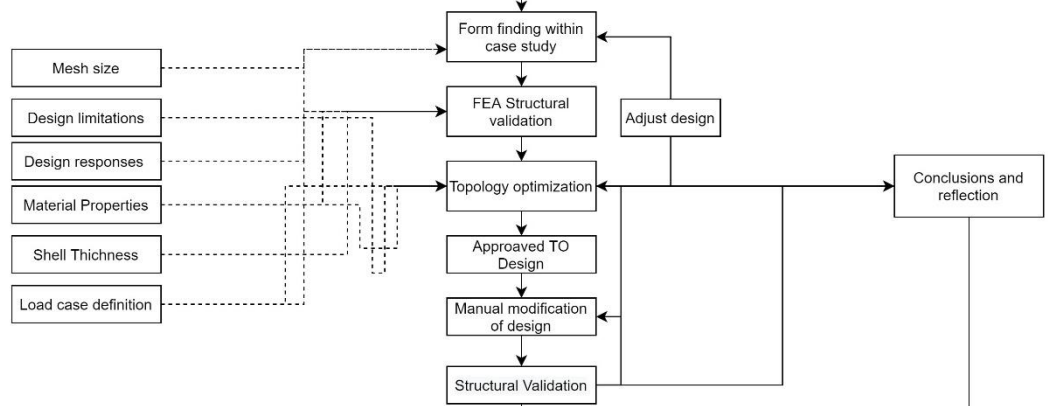
P1

12 Nov 2019



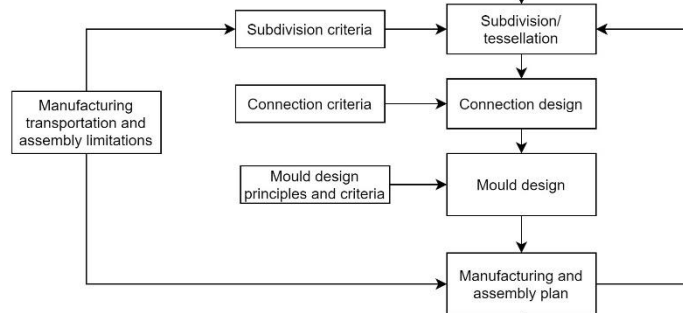
P2

16 Jan 2020



P3

26 March

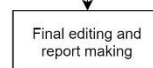


P4

21 May

P5

6 July



Chapter 3 About Topological Optimisations (TO)

"The art of structure is where to put the holes" Robert Le Ricolais, 1894-1977 (as quoted in Bendso and Sigmund, 2003)

3.1 Structural optimisation theory

A structural element is intended to fulfil a functional criterion to sustain loads. An optimal solution is one that finds the middle ground of contradictory objectives. For example, cheapest best quality, while quality usually comes at a cost. Structural elements' main functional quality is their capability to withstand all loads the structure might experience. Structural optimisation (SO), is a process that takes a structural geometry and optimises it by means of reducing its weight, volume, machining time, or any other cost objective the engineer finds fit to achieve, while preserving its intended structural integrity. Constraints indicating the minimum required mechanical properties within the minimization formula ensure preserving the minimum structural requirements of the elements. These constraints might be minimum required stiffness or strength, or a maximum allowable deflection and vibration. The process determines the most efficient distribution of material placement in order to achieve its serviceability objective. If the structure can be made using less material, or can weigh less than originally, and yet be able to sustain the same amount of forces the original design was capable of, then the design is structurally optimised. In cases where the opposite takes place, one could speak of over engineering; hence, a waste of material. One could optimise for multiple objectives. In the case of multi-objective optimisations, the objectives are prioritized based on their relative importance evaluation. (Adriaenssens et al., 2014, pp.3; Christensen & Klarbring, 2008)

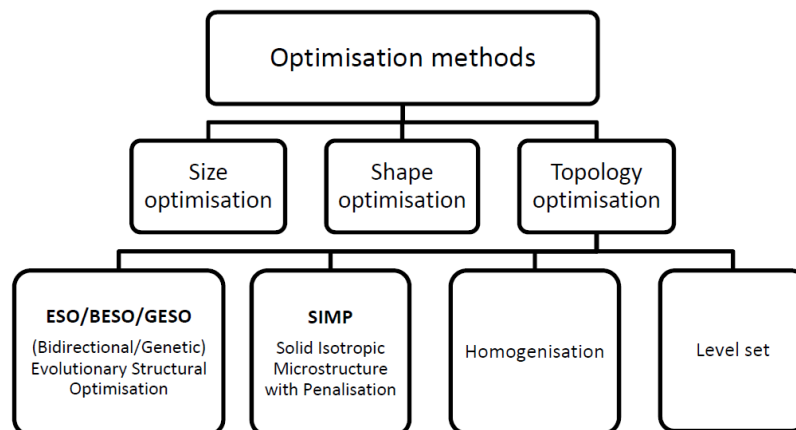


Figure 41 Optimisation Methods (Lundgren & Palmqvist, 2012)

There are three main structural optimisation categories; size, shape, and topology. See figure 42.

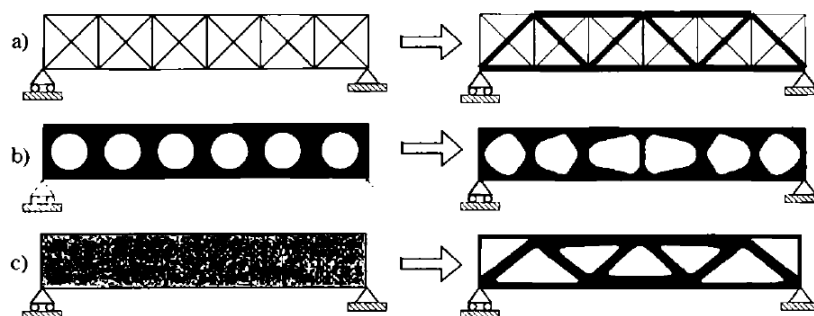


Figure 42 original form is on the left side. The optimised result is presented on the right-side a) size optimisation. b) shape optimisation. c) Topological optimisation (Bendso and Sigmund, 2003)

3.1.1 Size optimisation:

This optimisation can be used to reach the optimal thickness of a sheet or a plate. In other cases, it yields with the optimal cross-sectional area of a beam or any structural profile like a column or truss beam. (Christensen & Klarbring, 2008) See figure 43

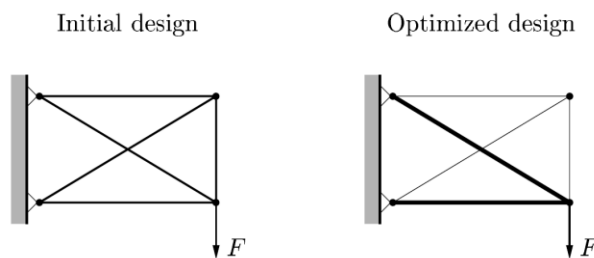


Figure 43 Size optimisation shows dimensioning the profiles of the trusses. Original form on the left. Size optimised on the right (Christensen & Klarbring, 2008).

3.1.1 Shape optimisation:

Shape optimisation finds the optimal integral solution of a differential equation. For example, if the original cantilever beam had originally a uniform height along the length. Shape optimisation will find the optimal shape of the beam and thus vary the height across the length. This optimisation does not change the connectivity of the geometry and therefore the topology remains the same. (Christensen & Klarbring, 2008) See figure 44.

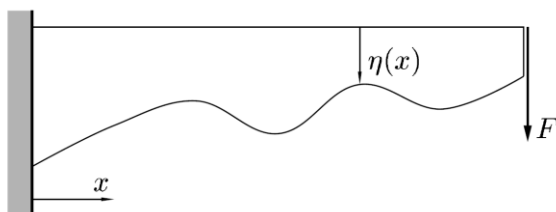


Figure 44 Shape optimisation. This is an optimal integral solution of a differential equation. Function $f(x)$ defines the shape of the structure. A cantilever beam height can get smaller gradually in correspondence to the moment. (Christensen & Klarbring, 2008).

3.1.3 Topological optimisation

In this method the most efficient distribution of material is determined within a spatial domain, given a load case and a number of constraints the structure must adhere to. After topological optimisation the original number of elements the objects consisted off changes. Usually the amount is less, as elements are eliminated through optimisation. This optimisation method changes the topology and connectivity of the structure. If spoken of a truss or a beam, certain elements of the structure will be assigned the value 0. See figure 45. In case of a sheet, the function assigns certain volumes a value of 0. The zero value leads to elimination. See figure 46. Sheets, beams and trusses are examples of 2D geometries. 3 dimensional geometries might be optimised by means of density in correspondence to stiffness. Through several iterations some algorithms might also add material to a more favourable location within the predefined spatial domain (Rozvany, 2001; Christensen & Klarbring, 2008)

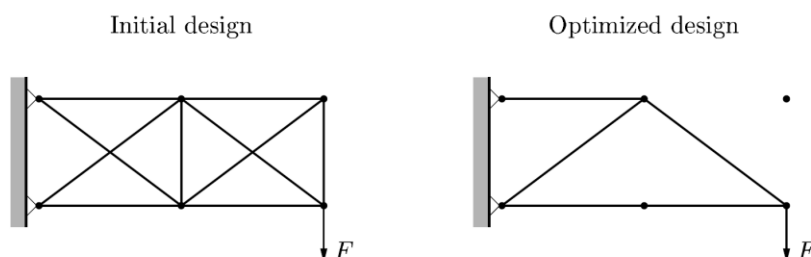


Figure 45 through topological optimisation of trusses some elements can be eliminated (Christensen & Klarbring, 2008).

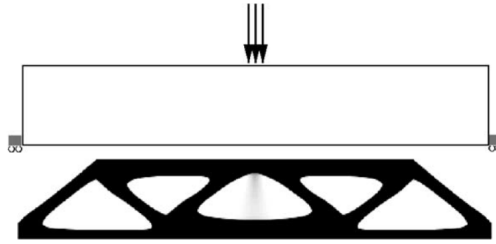


Figure 46 Topological Optimisation: top box is the spatial domain of the element. the bottom is the result (Christensen & Klarbring, 2008).

Topology optimisation can be divided into two approaches based on the first step. The object can either be represented by a meshed or a boundary by defined with lines running through it. In case of a mesh each subdivision will be assigned a material, void or an intermediate. In case of a boundary it will be defined by lines and surfaces. Most common methods use meshing and therefore these are the methods explained below. (Lundgren & Palmqvist, 2012)

In a broad sense, all TO approaches carry out the following general steps. First, the geometry is meshed. Meshing the geometry means computationally representing it through a network of subdivided spaces and cells. This means the mechanical structure being optimised gets divided into small elements. (Lundgren & Palmqvist, 2012) This is then computationally voxelated. Voxels are a form of 3D pixilation that finite element discretization uses to represent the geometry. A finer (less coarse) mesh, leads to more precise simulation and analyses results. This is especially crucial when analysing peak stresses, strains and deformations in critical areas like corners, joints and openings. A coarse mesh might mislead the conclusions and result in an unsafe structure. (Bendsø and Sigmund, 2003) Second, using finite element analyses (FEA) tools, the internal stresses strains deformations and other relevant calculations are simulated. Each voxel is now judged where it contributes to the intended structural performance or not. If removing the voxel (piece of material) will not decrease the structural integrity of sustaining the loads on the structure, the material is removed eventually. The process leading to the final TO design, can be done though several approaches. The algorithm judging the whether a voxel is relevant to the structural integrity of the structure varies from one approach to the other. (Christensen & Klarbring, 2008)

Categorization can be based on the general algorithm (and functions) the software processes in order to achieve the optimal geometry. These functions (f) usually aim to minimize any of the factors affecting cost and time of manufacturing. This could be by achieving the lightest structure, minimum thickness, or minimum volume. Other objectives might be minimum compliance, or maximum stiffness. (Beghini et al., 2013) The function takes a variable (x), which defines the geometry boundary, shape, thickness, area, volume, or any other function that would define the geometry of the original design. This could include the material mechanical properties such as density and young's moduli. This geometry variable will change during the optimisation process as elements are deleted in every iteration. Finally, the optimisation minimization function considers a behavioural constraining variable (y). This constraining variable ensures adhering to the minimum structural requirements. These constraints may include the maximum displacement, stain, and stress allowed by the structure. Other merits can be verified for qualification requirements such as natural frequencies, ductility, eigenmodes, P-D effects, buckling or stability limits. These constraining requirements are checked in the design during and after the minimization function is run. The equilibrium conditions are usually provided by a FEA. The minimized structure should still be able to sustain the expected loads and forces by the structure. The minimizing objective function (f) the geometrical design variable (x) and the behavioural constraint (y) of the general structural optimisation algorithm are illustrated below (Christensen & Klarbring, 2008). It is crucial to choose a suitable objective function goal and the right constraints depending on the material and design structure problem. (Beghini et al., 2013)

$$\text{(SO)} \quad \left\{ \begin{array}{l} \text{minimize } f(x, y) \text{ with respect to } x \text{ and } y \\ \text{subject to } \left\{ \begin{array}{l} \text{behavioral constraints on } y \\ \text{design constraints on } x \\ \text{equilibrium constraint.} \end{array} \right. \end{array} \right.$$

(Christensen & Klarbring, 2008).

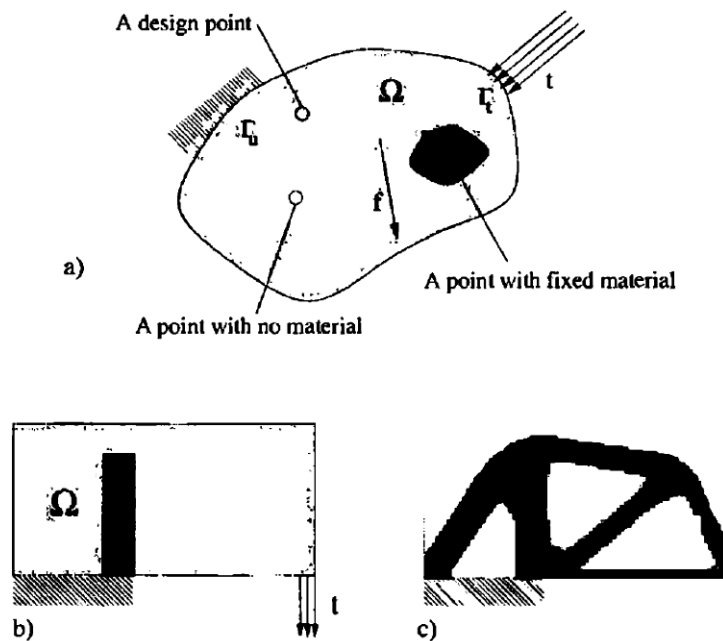


Figure 47 Finding an optimal material distribution. There is a point with fixed material. a is a generalized shape. B is a defined rectangular with defined constraints. C is the result with 50% volumetric reduction (Bendsø and Sigmund, 2003)

In a multi-objective optimisation with prioritized ranks constraints on architectural and manufacturing variables can be set. These could include constraints allowing for electrical and water plumbing to run through the structure. These constraints could indicate the size of pipe hole diameter. For manufacturing, transportation and assembly purposes the “pick-weight” and maximum length, width and height could be applied. Aesthetically oriented the architect might add a morphology-based restriction based on a density filter or in other scenarios constraints defining a pattern or symmetry. (Beghini et al., 2013)

3.2 Topological optimisation approaches

Throughout the years multiple algorithms for TO have been developed. Some use less iterations than others and are thus faster, some yield closer results to the desired goal, others are based on a gradual filtration of the voxels, while others adopt what is called a hard-kill approach. These algorithms form the backbone to commercially available TO software. Each algorithm has its own set of pros and cons, and therefore there is no one ideal algorithm that fits all TO cases. (Rozvany, 2001)

TO of glass raises a new challenge because the common algorithms were designed for isotropic, homogeneous, and ductile materials. Glass is a homogeneous¹ isotropic material, but it is not ductile. (Ashby et al., 2019, p. 60) A new algorithm is needed to meet the need for topologically optimising brittle material. Nevertheless, this development goes beyond the scope of this research. If this thesis were to focus on developing a new algorithm that solves TO challenges and FE glass related limitations, it would be wise to delve into each current algorithm. However, in this research, commercial software will be used with existing algorithms. Therefore, only a brief

¹ A Homogeneous material is a mixture with one “pure” material with uniform composition throughout the sample. The material cannot be split into different materials by mechanical force.

comparison between the most common algorithmic methodologies within the available commercial software will be discussed. This will guide the choice of software for this research. A PhD or a separate MSc thesis can be recommended to develop focus on developing a new algorithm that might solve some of the missing features present with the current ones. (Personal contact with Jackson Jewett)

A full comparative review of all TO approaches is beyond the scope of this paper and thus, only the relevant potential methods for this case study will be reviewed.

3.2.1 Level set method

This is an iterative method, which means that the algorithm keeps on looping until the optimal result has been achieved. It does not only subtract material but can also create new typologies within the set level of design domain. With every iteration material is either added or subtracted, even from places where the reverse was just done by the previous iteration. This is due to the geometry constantly changing. Thus, every iteration forces taking a different path as the material responds differently in different locations. The material is either added or subtracted based on whether it passes the minimum response criterion. For instance, that could be min stress capacity. (Wang, Wang & Guo, 2003; Lundgren & Palmqvist, 2012; Sigmund & Maute, 2013) The method is relatively new and therefore resources mention it as still being under development. Beghini et al. (2014) wrote that topological derivative-based, and phase-field and level-set methods, despite their great potential, are yet to be further developed for industrialized use.

3.2.2 Generalized Shape Optimisation (GSO) using Isotropic-Solid or Empty elements (ISE) - TO for isotropic materials

Isotropic materials have identical properties in all directions. Glass and metals are isotropic materials. (Ashby et al., 2019). These methods fix boundaries for ISE topologies with Isotropic Solid or Empty elements. One or a number of finite elements compose each of these isotropic solid or empty elements. This means that the topology optimisation deal with either fully filled solids with an isotropic material or a completely empty void. There are many algorithms, but these are the top used approaches for ISE topology optimisation (Rozvany, 2001):

- SIMP (Solid Isotropic Microstructure with Penalty for intermediate densities)
- OMP (Optimal Microstructure with Penalty for intermediate densities)
- NOM (Non-Optimal Microstructures)
- DDP (Dual Discrete-Value-Programming)
- Sequential Element Rejections and Admissions (SARA) (also known Evolutionary Structural Optimisation (ESO))

Only SIMP and SARA methods will be elaborated upon since they are among the most well-established and industrialized methods of structural topology optimisation (Rozvany, 2007) OMP was proven “uneconomical, without significant advantages” (Rozvany, 2009). On the other hand, NOM fails to produce a completely black and white solution. Both OMP and NOM require a considerable number of extra variables per element, while SIMP requires only one. (Rozvany, 2009) DDP is not very much elaborated upon in literature.

3.2.3 SIMP (Solid Isotropic Microstructure with Penalty for intermediate densities)

SIMP is a numerical FE-based topology optimisation method. In this method pseudo density material values are assigned to each voxel. The value ranges from 0 to 1 corresponding to its level of stiffness. 0 elements are displayed in white and are eliminated. 1 elements are represented in black and are preserved. Shades of grey correspond to the values in between 0 and 1. (Bendsø and Sigmund, 2003) A compliance or displacement-based function would result in predominantly grey elements. (Rozvany, 2009) Since only one material, with one specific density will be used, the density may not vary. Therefore, all shades of grey should ultimately be rounded up or down. A penalization system handles this process. Each voxel is assigned a property formulated as follows (Bendsø and Sigmund, 2003; Sigmund & Maute, 2013) A multi priority ranked criterion is possible with SIMP

$$E_{ijkl}(x) = x^p E_{ijkl}^0, \quad p > 1$$

Whereas E is the material stiffness of any other property, p is the penalization threshold, and x is the variable of design. (Bendsø and Sigmund, 2003; Damen, 2019)

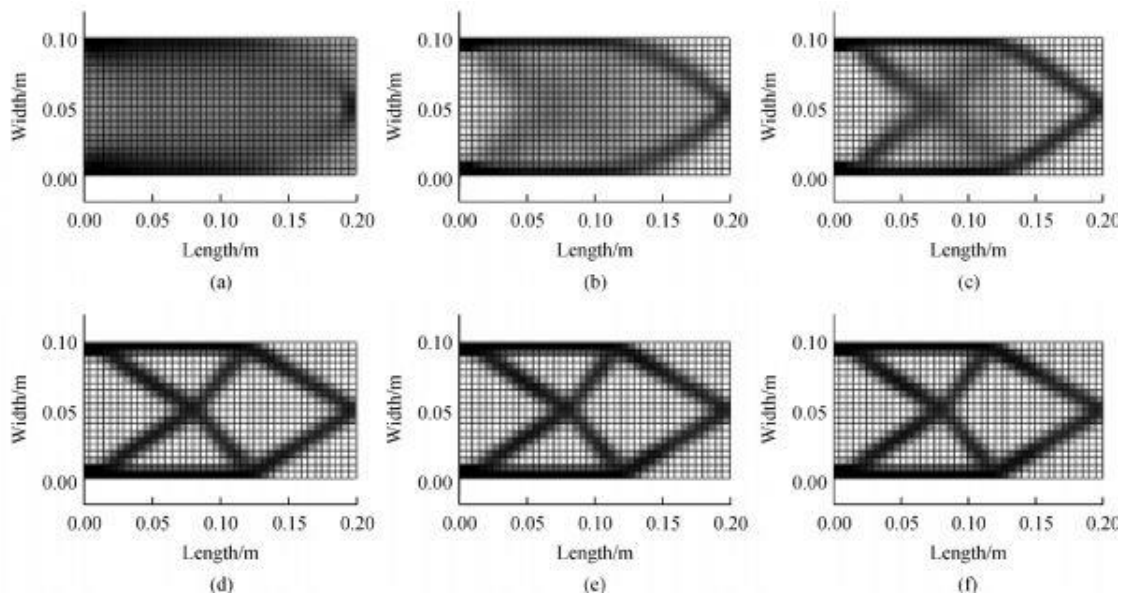


Figure 48 SIMP the element is optimised through many iterations. The element transforms from black (solid fill), to a combination of grey voxels (semi-filled areas), to finally a black (solid fill) and white (void) object by means of the Penalization factor. (Source)

3.2.4 Sequential Element Rejections and Admissions (SARA) (also known as “Hard-Kill” Methods

3.2.4.1 Evolutionary Structural Optimisation (ESO) (also called Adaptive Biological Growth (ABG) methods and Generalized Stress Design (GSD))

The name of this method is rather confusing. While E for evolutionary eludes to Darwin’s genetic process, the algorithm of ESO is not evolutionary. The O stands for optimisation, but the result of the process is not an absolute computationally optimal solution. Therefore, SARA, Sequential Element Rejections and Admissions is a more appropriate name. However, since it applies to ESO and BESO, in this paper it is the name heading both subheadings. (Rozvany, 2009)

ESO shows the outcome with black for completely material-filled elements and white for hollow volumes. One function in ESO checks for the calculated criterion value the model must comply to. This could be Mises stress or energy density for instance. With every iteration elements with a value below the required threshold are eliminated. (Rozvany, 2009)

In a two staged ESO, alternative solutions are evaluated and ranked by means of a “performance index” or “objective function” then the “global optimum” is numerically calculated for sorting out the best solution. (Rozvany, 2009)

Every method has its own shortcomings. Some criticize ESO for being simply a heuristic method that does not yield an optimal solution. Others criticize it for having no direct link between the criterium function and the objective function. The comparison between alternative to find a global optimum might take great computational power and processing time is cases were the comparison is vast. The same is to be said regarding the lengthy numerous amounts of iterations the method has to run. Not to mention that it does not guarantee an optimum solution. With a two stage ESO optimisation process there is no control over the volume of the result. In case of a multi load scenario, or a need for a multi constraint optimisation function ESO falls short and is limited. (Rozvany, 2009)

3.2.4.2 BESO: Bi-directional Evolutionary structural optimisation method

As with ESO elements are ranked according to a criterion function based on, for example, Mises stress or energy density. In BESO elements are inserted in addition to elements with the predefined high value. (Rozvany, 2009)

3.2.5 Homogenisation method (TO for Anisotropic Materials)

This method, as evident in its name, it unifies the entire object by means of a 3D grid. Homogenisation reconstructs the entire object into a linear elastic matrix of microscopically small and numerous amounts of unit cells of either material or voids. There are grey areas where it has an undefined material density. These densities are determined by the needed material property at this location given the load cases present and design domain. These partial voids are called intermediate materials. If the stiffness tensor formula for the given scenario exists, it will be calculated. The stiffness tensor will be compared to the proportion of the effective density and help push the TO result to an all-black and white design. This is necessary because an intermediate material cannot be produced. In this matter homogenisation is similar to SIMP by having an intermediate grey material density that will be eventually ruled as either full material or void. (Bendsøe and Sigmund, 2004)

Homogenisation has proven to be a good tool for anisotropic materials. Past applications for this approach were done for material that is reinforced, layered up, laminated or a composite. (Hassen, Bleyer & Buhan 2017) Anisotropic materials are those that have different properties with the change of direction. (Bendsøe and Sigmund, 2004) There is a greater chance of reaching an optimal solution with homogenisation than with numeric methods because of the use of the intermediate densities. More precise feedback is expected regarding the optimal use of material on a local scale, thanks to the finely defined material limits and their potential effective behaviour. (Fernandes et al., 1999) In comparison with SIMP, homogenisation demands extra design variables to define the material and structure. (Bendsøe and Sigmund, 2004) This method was also criticized for being “uneconomical, without significant advantages” above SIMP (Rozvany, 2009).

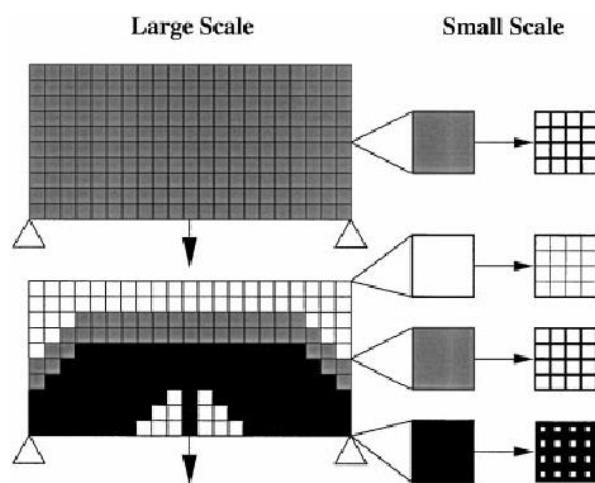


Figure 49 Homogenization method starts with representing the entire element with homogenous micro voids (TOP), and later optimising it with by means of grey intermediate voxels, white voids, and black material fills. (Source)

3.3 Examples of TO productions

Table 7 Comparison of TO projects objectives software and results (Jipa et al., 2016; Bhatia, 2019; Damen, 2019; Snijder et al., 2019; apworks,2020)

	ETH Zurich Concrete slab prototype A	ETH Zurich Concrete slab prototype B	The light Rider	The Glass Swing	Bhatia's Column	Damen shell node
Material	Concrete	Concrete	Scalmalloy® (APWorks)	Extruded Glass Bundle Struts	Cast borosilicate glass	Cast borosilicate glass
Software	Millipede (grasshopper plug-in)	ABAQUS	Altair	Karamba 3D (grasshopper plug-in)	ANSYS	ANSYS
TO Approach	Homogenisation	SIMP	Level set	BESO	SIMP	SIMP
Criterion / objective	reduce material to a 0.2 set fraction of the initial amount while minimizing deformation s of the slab under uniform surface load	reduce material to a 0.18 set fraction of the initial volume while minimizing the stress of the slab under uniform surface load	Stresses von- misses		Minimum compliance (Maximize stiffness)	Minimum compliance (Maximize stiffness)
Mass reduction	70%	70%	30%		40.3 %	70%

3.3.1 ETH Zurich concrete slabs

ETH Zurich used the Millipede plugin for grasshopper in the TO of one concrete slab (figure 50), and Simulia ABAQUS for another (figure 51). The results proved that a large scaled building component can be additively manufactured. A minimum of 30 mm thickness of concrete was achieved. This is a 70% weight reduction. Both slabs required manual post processing. Narrow tubes, very close parts, and non-smooth surfaces had to be refined. (Jipa et al., 2016)



Figure 50 Prototype A ETH Zurich used the Millipede plugin for grasshopper for TO for this slab. Supported by 3 points. (Berhard et al., 2019)



Figure 51 Prototype B ETH Zurich slab ABAQUS software was used for TO. It is designed to be supported at the four corners (Jipa et al., 2016)

3.3.2 The light rider

This motorcycle weighs 35kg, but the frame alone is just 6kg. This TO example reduced the entire bike's weight by 30% without decreasing its strength and stiffness. This is beneficial for energy consumption. (Damen, 2019)



Figure 52 Light Rider: The 3D printed TO motorcycle (Grolms, 2016)

3.3.3 The Glass Swing

The glass swing was designed to have all forces transferred axially like in spatial struts or vertical columns. The geometry was found by structural optimisation. A safety factor was implemented so that in case two rods break the swing will remain by means of force transfer through the rest of the bundle. Rhino plug-in Grasshopper was used for form finding. Structural optimisation was done using Karamba3D by means of the Bidirectional Evolutionary Structural Optimisation (BESO). Oasys GSA was used for final verification checks. The organic result of TO was stripped down and translated into a wireframe model through discretization.

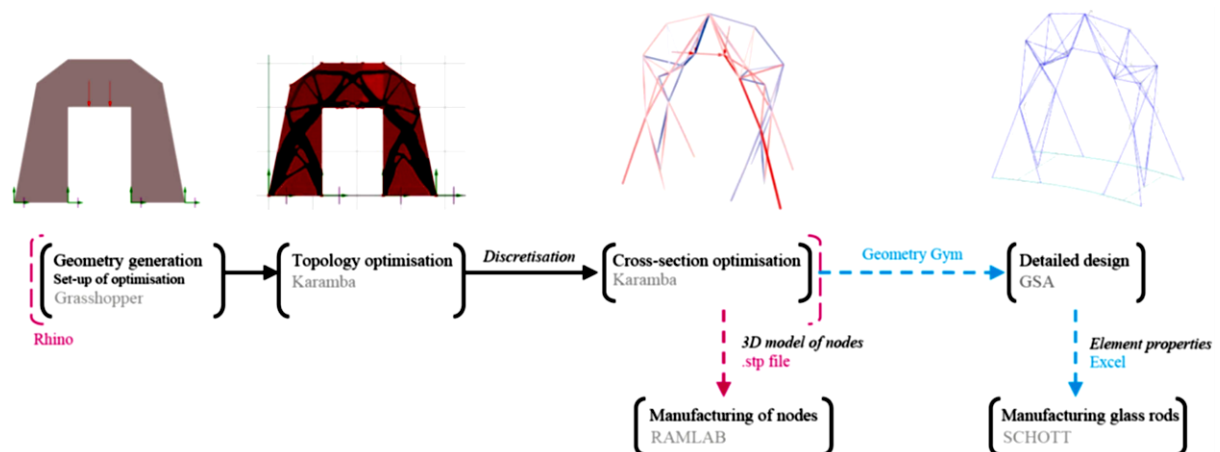


Figure 53 Overview of the applied digital workflow for the design and manufacturing process of the Glass Swing (Snijder et al., 2019)

Overview of the applied digital workflow for the design and manufacturing process of the Glass Swing (Snijder et al., 2019)

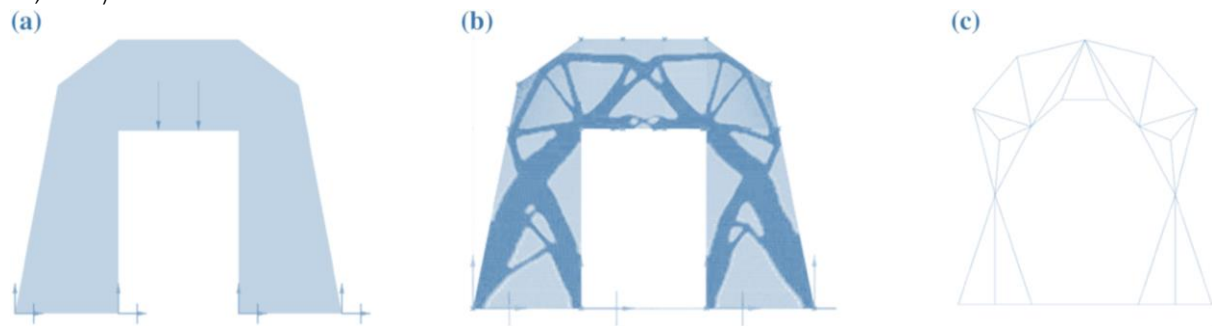


Figure 54 a Initial material envelope and loads for BESO optimisation. b Result of BESO optimisation. In black the material that has not been removed in the process. c Discretization and rationalization of the result from the BESO procedure to a static truss structure (Snijder et al., 2019)

3.3.4 Kolumba museum cast glass column

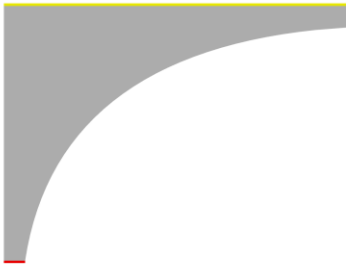
Bhatia (2019) ran 3 trials of optimisation, two of which will be discussed here. The first trial was with an arch like form column. 8175 mm x 6000 mm and a foot of 500mm in width. The thickness was also 500 mm. Results are shown in figure 55-56. By the third optimisation the mesh stopped reducing. The or mass of original geometry was 20369 kg, and the mass of the optimised geometry became 8221.6 kg. That achieved a 40.3 % of mass retention from the original geometry. Bhatia used ANSYS as a software.

Bhatia (2019) optimised with the objective of minimum compliance (Maximize stiffness). And constrained the process by limiting the maximum number of iterations to 500 and minimum normalized Density to 0.001.

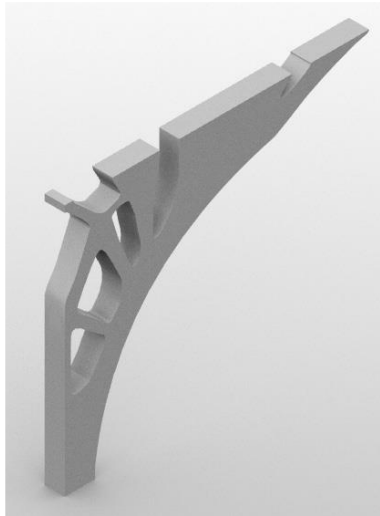
From Kolumba museum cast glass column topology optimisation Bhatia (2019) drew a few conclusions:

- Manual changes to the geometry may result in better TO. For example, introducing the arch design to the column and splitting its thickness. These are positive interventions that are only possible by means of the engineering eye.
- Ansys student licence does not allow for reducing the mesh. At times the mesh can be too large for TO and therefore a manual intervention. The mesh size of the optimised geometry was even bigger than the original because of the introduced curvatures. Therefore, remeshing and extruding the silhouette of the structure before importing it again for another run of TO was necessary.

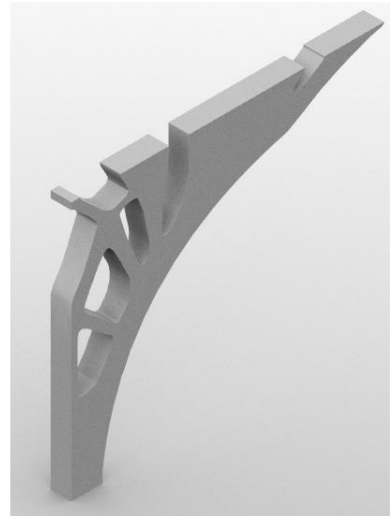
Original shape before the lit in thickness



First optimisation



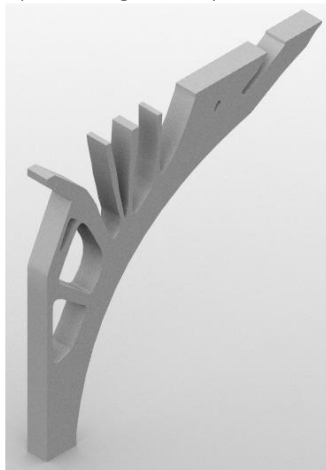
Extrusion of silhouette of 1st optimised geometry



Second optimisation



Extrusion of silhouette of 2nd optimised geometry



Third Optimisation



Post processing of the optimised geometry

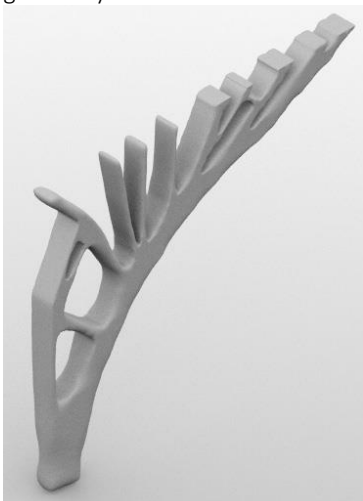


Figure 55 Topology Optimisation of the solid ergonomic arch design by Bhatia (2019)

New split geometry with 200 thk member and 100 thk gap in between the 2 geometries



First Optimisation of split geometry
No. of iterations: 51
Percentage of mass retention: 52.4 %



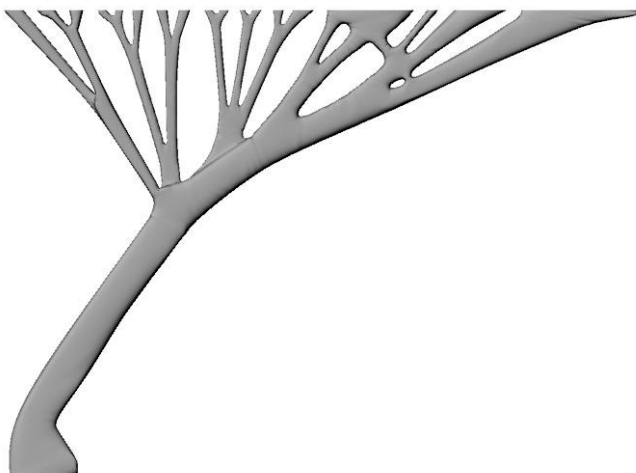
Second Optimisation of split geometry
No. of iterations: 41
Percentage of mass retention: 50.81 %



Third Optimisation of split geometry
No. of iterations: 28
Percentage of mass retention: 50.22 %



Forth Optimisation of split geometry
No. of iterations: 33
Percentage of mass retention: 51.22 %



Final Optimised Geometry for fabrication

Figure 56 TO process of the split geometry by Bhatia (2019)

3.3.5 The shell node

Damen (2019) topologically optimised a cast glass node connection for a grid shell structure. See figure 57-59. These nodal connections were optimised using Ansys with a minimum compliance approach with the goals of decreasing volume of material used. Aside assembly port connection design constraints there were other constraints specified regarding thickness and maximum allowable stresses. The minimum element size ranged from 15-20 mm and the maximum element size ranged from 30-50mm. However, this was later on scaled up because the entire node was too small for easy screw of a bolt. In tension the allowable stress was set for 20 N/mm² while 200 N/mm² in compression.

Some practical decisions were made based on the following realizations. First the contact surface area where the loads are, and the beams make contact for connection are better left out of the optimisation. Otherwise the area would become too thin and sharp edges may occur. These might be applicable in this research too. In other words, excluding the edges of the subdivided elements or the connection ports. Later on, during post processing the optimising geometry can be welded into the excluded parts from optimisation for smoother connections. Another critical factor to account is the load cases. If there are only deadload some unexpected horizontal or asymmetric loads might lead to failure. Setting up only self-weight would result in a very thin structure which is dangerous if wind loads are present. Therefore, Damen set up bending moments in the beams as a safety factor.

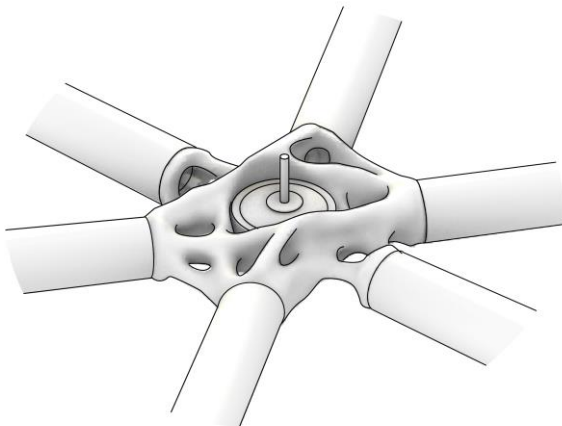


Figure 57 assembly ready node connected to rods of the grid shell (Damen, 2019)



Figure 58 Casted TO node for light structure (Damen, 2019)

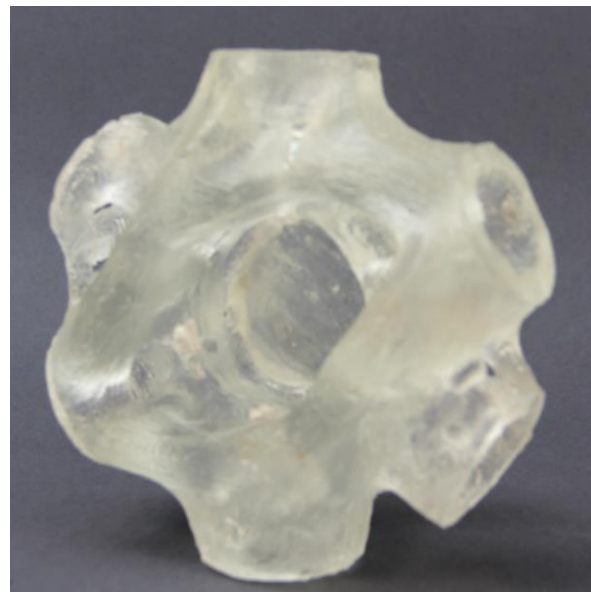


Figure 59 Casted TO node for heavy structure (Damen, 2019)

3.4 Challenges and limitations to TO of glass and other brittle materials

Stress-based optimisation using Von-Mises stress vs principle stresses and strain-based compliance-based optimisation for brittle material such as glass.

3.4.1 What is minimum compliance (compliance based TO)?

Minimizing compliance is equivalent to maximizing stiffness for linear elastic materials.

$$\begin{aligned} & \underset{\phi_i}{\text{minimize}} \quad f(\rho) = \mathbf{F}^T \mathbf{d} \\ & \text{subject to} \quad \mathbf{K}(\rho) \mathbf{d} - \mathbf{F} = \mathbf{0} \\ & \quad c(\rho) = \sum_{e \in \Omega} \rho^e v^e - V \leq 0 \\ & \quad \phi_{\min} \leq \phi_i \leq \phi_{\max} \quad \forall i \in \Omega, \end{aligned}$$

Whereas, ϕ_i is the design variable controlling the density ρ . The design variables are controlled by bounded and continues using ϕ_{\min} and ϕ_{\max} . $c(\rho)$ is the volume constraint. ρ^e is the element density. v^e is the volume of the element. V is the max allowable amount of material in the element. Static equilibrium should be achieved where $\mathbf{K}(\rho)$ is the global stiffness matrix, \mathbf{F} is the global load vector and \mathbf{d} contains the free displacements. (Jewett & Carstensen, 2019)

3.4.2 What is von Mises stress (stress-based optimisation)?

Von Mises stress (aka maximum distortion energy criterion) is a criterion that predicts whether a material would fracture or yield. The estimated yield failure criteria are given either a positive or negative sign based on the dominant principle stress. While principle stresses are a real value, von Mises is a theoretical one. Von Mises is commonly used and designed for ductile materials. Von Mises best works with ductile materials because they have comparable tensile to compressive strength levels. However, brittle materials like glass have a large difference between their tensile and compressive strength which might lead to misleading von Mises conclusions. von Mises is unreliable for brittle materials such as glass. Von Mises is based on that ductile materials behave differently when under tension or uniaxial stress. It takes into account the elastic limit, lower and upper yield limits and the rupture or fracture point. (Ugural & Fenster, 2012; Simscale, 2019) von Mises suggests that fracture would take place if the stresses in an element exceed the following:

$$\frac{1}{6} [(\tau_{11} - \tau_{22})^2 + (\tau_{22} - \tau_{33})^2 + (\tau_{33} - \tau_{11})^2 + 6(\tau_{12}^2 + \tau_{23}^2 + \tau_{13}^2)] = k^2$$

Whereas k is a constant and τ is the stress tensor. K can be rewritten as:

$$\frac{\tau_y^2}{3} = k^2$$

And when τ_y reaches S_y which is the elastic limit, the following applies:

$$\frac{S_y^2}{3} = k^2$$

And the first formula can be rewritten with the substitution as:

$$\frac{1}{6} [(\tau_{11} - \tau_{22})^2 + (\tau_{22} - \tau_{33})^2 + (\tau_{33} - \tau_{11})^2 + 6(\tau_{12}^2 + \tau_{23}^2 + \tau_{13}^2)] = \frac{S_y^2}{3}$$

Von Mises is defined as:

$$\tau_v^2 = 3k^2$$

Or expressed by:

$$\tau_v \geq S_y$$

(Ugural & Fenster, 2012; Simescale, 2019)

In comparison with compliance based TO Literature also suggests that a stress-based optimisation yields clearer designs that do not need a lot of post-processing.

3.4.3 What is Drucker-Prager?

“The Drucker–Prager failure criterion is a three-dimensional pressure-dependent model to estimate the stress state at which the rock reaches its ultimate strength. The criterion is based on the assumption that the octahedral shear stress at failure depends linearly on the octahedral normal stress through material constants.” (Alejano & Robet, 2012)

This criterion can be perceived as an altered continuation to the von Mises criterion that makes it more suitable for brittle material. The Drucker–Prager failure criterion is designed to deal with materials with both equal or imbalanced behaviour in tension and compression. (Bruggi & Duysinx, 2012) It was developed as a criterion for soil which can only take compression loads. Drucker-Prager criterion can be defined as:

$\sqrt{J_2} = \lambda I_1' + \kappa$ Whereas J_2 is the second invariant of the stress deviator tensor. I_1' is the first invariant of the stress tensor defined as such:

$$I_1' = \sigma_1' + \sigma_2' + \sigma_3'$$

$$J_2 = \frac{1}{6} [(\sigma_1' - \sigma_2')^2 + (\sigma_1' - \sigma_3')^2 + (\sigma_3' - \sigma_2')^2]$$

Whereas σ_1' , σ_2' , and σ_3' , are the effective principal stresses.

3.4.4 Dilemma: Should this research opt for a compliance-based or a stress-based topological optimisation?

The first question is: would the structure be expected to be stress driven or deflection driven? Engineer Dimitris Vitalis advised for a glass floor a deflection driven TO, but this is not necessarily true and depends on a plethora of parameters. So, for a floor slab a compliance model with minimising the strain energy as an objective function and with volume reduction the opposing constraint. Natural frequency of the floor should be also taken into account. So, for a floor slab a compliance-based method should be more suitable. However, for a design like the shell node of Damen (2019) Engineer Dimitris Vitalis expected a stress-limited design to be more suitable. Stress-based models give cleaner results but require high computation time and resources to achieve that. Stress based optimisation poses also the challenge of stress singularities. (Source: personal correspondence with engineer Dimitris Vitalis)

Regardless of which method one uses, it is always necessarily to go back and check all the other failure modes. Dimitris Vitalis suggested writing a compliance routine with a stress check on every step. But in general, a minimum compliance model is expected to yield better results if the design is expected to be deflection driven.

Nevertheless, new and different optimisation models are on demand for development. However, this goes beyond the scope of this research and is considered suitable for a separate thesis. (Source: personal correspondence with Dimitris Vitalis)

On TO Dimitris Vitalis (2019) commented that it is a process followed during concept design stage to preliminary assess the optimal material distribution. TO is not a process to achieve compliance and it will never result by the press of the button a neat, smooth and tidy ready-to-produce model. Post processing is always required. Engineering judgement remains a vital part of the process. Literature suggests that a stress-based optimisation yields clearer designs that do not need a lot of post-processing.

In theory it is possible to setup a principal stress based TO but it will unlikely converge. That von-Mises are applicable to ductile material is not the only reason they are widely used in TO software. Von Mises is more prevalent than principle stresses because von Mises combines multiaxial stress states into a uniaxial stress. This can then be compared against experimental results and singular derived value per element of uniaxial strengths. It is a problem that can therefore converge and does not easily result in matrix singularities. Principal stresses- which indeed shall be used for glass design- are dependent on the reference plane which changes every time the geometry changes e.g. s_{11} of one element is related to s_{22} of the adjacent element. If one element is deleted, this will affect the principal planes of the adjacent element. Vitalis expressed that von Mises might just be a way to overcome the challenge of converging without guaranteeing an optimal result. Nevertheless, Vitalis did not think that von Mises is the right choice for glass as a brittle material.

One of the reasons von-mises is perceived as a trick method is its strong dependency on the mesh. If the mesh differs in size and definition the results will vary as well. Artificial stress concentrations are created. von Mises or any type of stress, especially in brittle materials, is not a metric of how well the mass of a domain is distributed according to set loading and boundary conditions. It is a yield/failure criterion. Vitalis explains even though stress based TO is the most practical and real method, it has received much criticism the above reasons and more. (Source: personal email correspondence with ir. Dimitris Vitalis)

Jackson Jewett, an MIT structural engineer graduate has also shared some thoughts about the matter (through personal correspondence). Jewett said that compliance based TO by means of minimizing deflection is a more "typical" approach in comparison to a stress-based optimisation via reducing maximum stress in the system for glass. Jewett explained how stress-concentrations can be avoided even with a compliance-based optimisation. Therefore, both Vitalis and Jewett are in line with using compliance-based approach instead of a stress based one for glass.

3.4.5 Conclusion on TO for glass

For a shell structure deflection are more influential than stresses. This is because a large deflection might lead to eccentricity and therefore moments. Deflections lead to tension which it neither good for a shell structure not for glass as a material. Therefore, a deflection driven compliance based TO for a glass made shell form make more sense than a stress based (von-mises) TO.

Druker-Prager criterion can be an interesting path to try out if time is at hand because it is designed to deal with materials with both equal or imbalanced behaviour in tension and compression. (Bruggi & Duysinx, 2012) It was developed as a criterion for soil which can only take compression loads. However, this research will not adopt it as the main and first TO approach due to the lack of experience among the experts consulting this paper. If in due time more information and time is at hand, this promising criterion might be experimented with. However, the main approach will remain the compliance-based criterion.

3.5 Different software packages

3.5.1 ANSYS

This is a certified structural FEA software that has an extensive various analysis package, and TO is one of them. Therefore, TO and FEA can be executed in the same software. This tool gives the user control over material settings, the objectives of the functions, and its constraints. The SIMP approach is used by ANSYS. Manufacturing constrains and post processing are possible features with ANSYS. (Damen, 2019)

3.5.2 Ameba

This is a plugin for McNeel Rhinoceros Grasshopper. Two optimisation goals are made available next to volume reduction by means of Ameba, namely, minimizing displacement or Mises stress. The Plug-in uses the BESO methodology. In settings Young's modulus and Poisson ratio can be set as material properties. Thanks to the cloud online remote Ameba servers, computing can be done relatively faster. The plugin includes smoothing and remeshing components. (Damen, 2019)

3.5.3 Millipede

Millipede is a Grasshopper plug-in that incorporates the homogenization method for TO. It also allows a collaborative work with another grasshopper plugin called Galapagos. The later uses an evolutionary TO approach. The objective function is designed to achieve a sought-after density requirement within a set volume limit. It is restrictive considering options customizations. (Damen, 2019) ETH Zurich used this plugin in the TO of a concrete slab. (Jipa et al., 2016)

3.5.4 Autodesk Fusion 360

This is a design, optimisations and analyses software that integrates several Autodesk software in one. The software uses SIMP approach for TO. Fusion 360 has an elaborate material library, that allows one to add a customized new material to. Fast computing is made possible via their cloud servers' facility. (Damen, 2019) The latest Autodesk Forum discussion from 2018 said that the Drucker-Prager yield criterion is only supported in the Nonlinear Static analysis materials.

3.5.5 Autodesk Generative Design

This software is capable of handling a multi-objective set of criteria. This includes a vast range on manufacturing goals such as production time, cost and machining limitations. It uses the Level Set TO algorithms. A powerful cloud server availability enables fast computing time. The program generates several alternative solutions for the engineer to choose from instead one optimal result. (Autodesk, n.d.; Damen, 2019)

3.5.6 Karamba3D

This is a Rhinoceros3D plugin that uses the BESO method for TO. It is also a structural validation plugin, so one can check for stresses and deflection. However, it is not a licensed FEA software that can certify a project at structurally validated. Nevertheless, it is by practice proven to be accurate and comparable to results from FEA certified software. If the design domain is parametrically defined, then tweaks in the design can be done easily. This means that variations of the design can be instantly structurally checked and topologically optimised before setting on a final result. (Snijder et al., 2019)

3.5.7 Optistruct (Altair Hyper Works)

This software offers a vast manufacturing constraints options, such as extrusion related constraints, pattern and symmetry constraints. It also gives one the option to choose between Level Set and SIMP methods. (Bhatia, 2019)

Table 8 Different TO software packages

	ANSYS	Ameba	Millipede	Autodesk Fusion 360	Autodesk Generative Design	Optistruct (Altair Hyper Works)	Karamba 3D
TO Method	SIMP	BESO	Homogenisation	SIMP	Level set	Can choose between Level Set and SIMP	BESO
Objective function goal and constraints	Comprehensive user-controlled settings customization (incl. manufacturing constraints)	Minimizing displacement or Mises stress, while minimizing volume	Desired density within a volume	Stress based and compliance based.	Handles multi-objective criterion including a vast range on manufacturing goals such as production time, cost and machining limitations.	Vast manufacturing constraints options, such as extrusion related constraints, pattern and symmetry constraints.	
Material options	Extensive Library and open for additional custom created ones	Young's modulus and Poisson ratio can be set as material properties	Limited	Extensive Library and open for additional custom created ones	Elaborate Material Library with custom additions made possible.		
Special Features	Post processing made possible with ANSYS	Cloud Computing. + Includes smoothing and re-meshing components.	Allows a collaborative work with another grasshopper plugin called Galapagos.	Easy post processing via ReCap	Generates several alternative solutions for the engineer to choose from instead one optimal result. + Offers fast cloud computing.		

3.6 Conclusions and decisions regarding TO

3.6.1 TO Method

SIMP

This method has been chosen because it is a well-established and industrialized methods of structural topology optimisation (Rozvany, 2007) It is the method used by the top two available software's with student licences. Ansys and Fusion 360. SIMP is a numerical FE-based topology Optimisation method. Other methods are either not yet fully developed or do not yield optimal solutions.

3.6.2 TO approach

Deflection driven compliance based.

For a shell structure deflection are more influential than stresses. This is because a large deflection might lead to eccentricity and therefore moments. Deflections lead to tension which it neither good for a compression-only shell structure not is it for glass as a material. Therefore, a deflection driven compliance based TO for a glass made shell form make more sense than a stress based (von-mises) TO.

Drucker–Prager

Druker-Prager criterion can be an interesting path to try out if time is at hand because it is designed to deal with materials with both equal or imbalanced behaviour in tension and compression. (Bruggi & Duysinx, 2012) It was developed as a criterion for soil which can only take compression loads. However, this research will not adopt it as the main and first TO approach due to the lack of experience among the experts consulting this paper. If in due time more information and time is at hand, this promising criterion might be experimented with. However, the main approach will remain the compliance-based criterion for the time being.

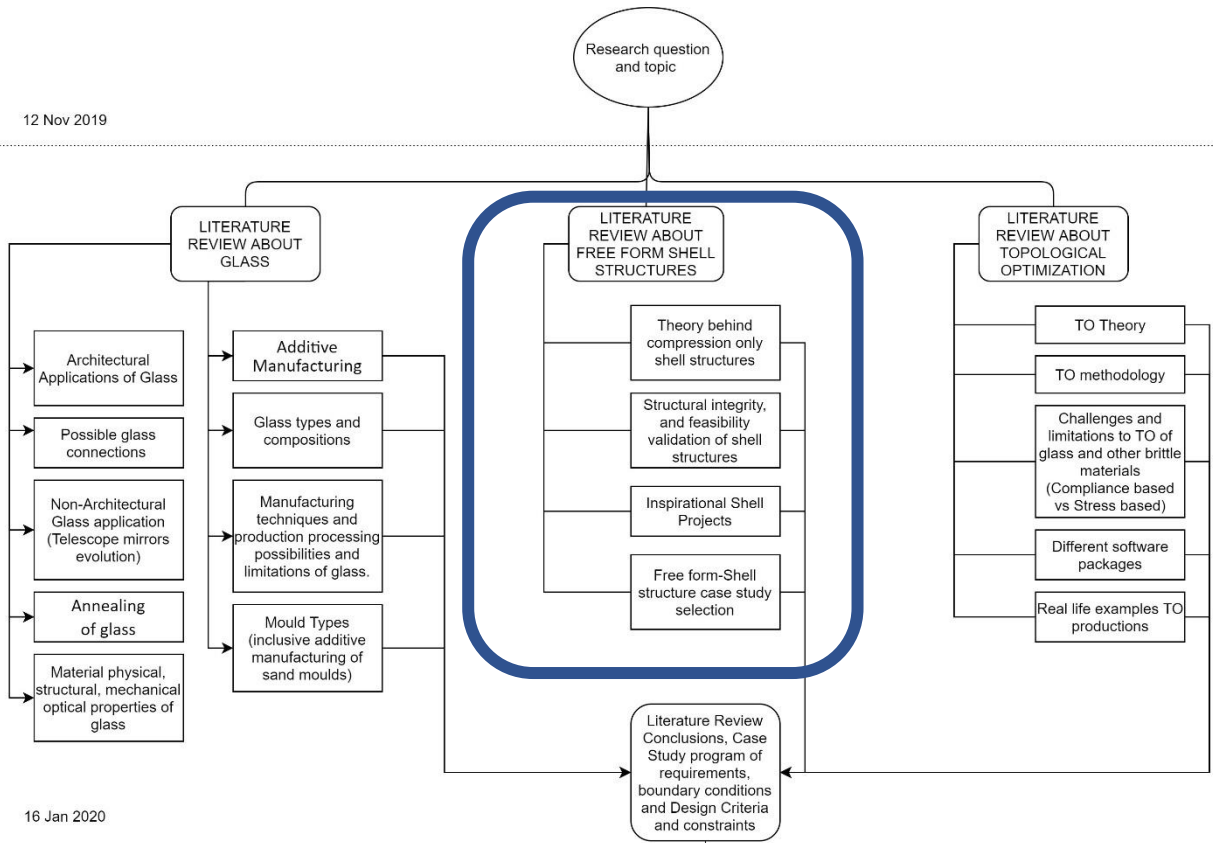
3.6.3 TO Software

ANSYS (TO and FEA Software)

This is a certified structural FEA software that has an extensive various analysis package, and TO is one of them. Therefore, TO and FEA can be executed in the same software. This tool gives the user control over material settings, the objectives of the functions, and its constraints. The SIMP approach is used by ANSYS. Manufacturing constrains and post processing are possible features with ANSYS. (Damen, 2019) Deflection driven compliance based is possible using Ansys.

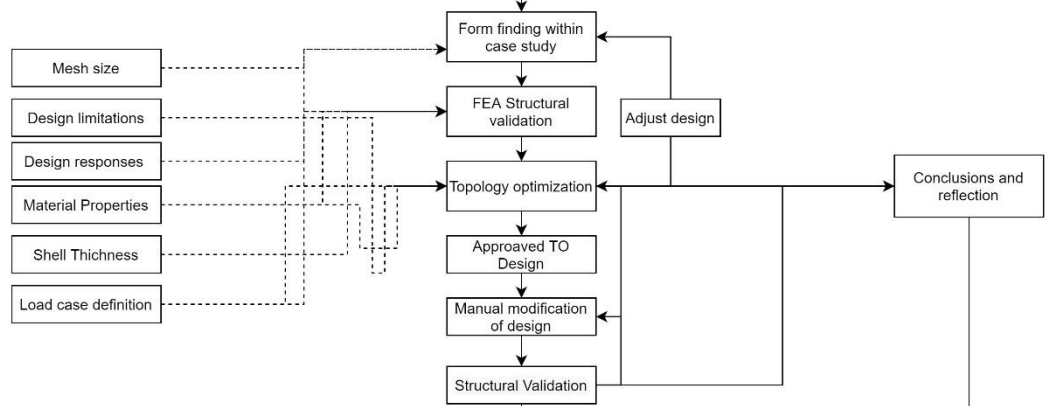
P1

12 Nov 2019



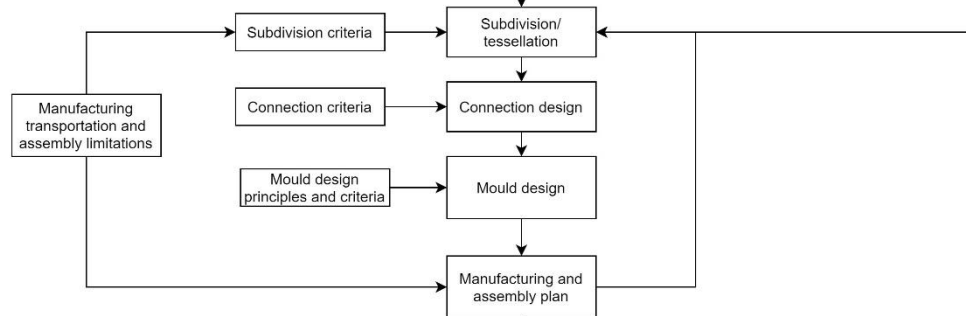
P2

16 Jan 2020



P3

26 March

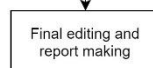


P4

21 May

P5

6 July



Chapter 4: About free form shell structures

4.1 What is a shell?

Shells are singular or double curved structural surface whereas the thickness is unquestionably thinner than the dimension of the span in both directions. Their slenderness is possible due to the transfer of loads by means of axial forces normal to the thickness of the structure through membrane plane stresses. This could mean pure tensile stresses when speaking of a tension-only fabric material, or compression-only “membrane” structure out of steel, concrete, brick, or glass. Tensile structures are called form-active shell structures, because they change shape to adjust for the varying applied load cases. A compression-only glass shell would be a form-passive structure. This shell would not adapt its shape in accommodation for different load cases. The only deformation expected is deflection or bending within a maximum allowance before the structure would buckle. (Adriaenssens et al., 2014, pp.1, 21-26).

4.2 Why building a shell structure is ideal for Glass?

Shell structures are ideal for glass for three reasons; namely, due to its compressive-only loads, its thin cross-section, and aesthetical simple elegance.

1. Glass is brittle. This means that it fractures without warning when tension is applied to a crack. Glass has a low tensile strength but has a very high compressive strength. That is why shell structures are ideal for glass utilization as they experience compression only loads. Shells best utilize the strengths of glass and avoid testing its weakest limitations.
2. To decrease the annealing time, the structure volume/mass ratio should be as low as possible. They achieve large spans while maintaining an optimised slender light weight. Shell structures are thin structures that allow for shorter annealing and cooling time.
3. Shells are attractive, not only because they resist loads efficiently, but because their simple elegance is appealing to the eye. Architects appreciate the floor plan design flexibility provided by the unobstructed free space thereunder. Glass is an elegant material as introduced in the report. Using it to build a simply elegant structure according to architects will just enhance its aesthetical application. (Adriaenssens et al., 2014, pp.7)

4.3 Hooke’s Law and Antoni Gaudi

Robert Hooke wrote a mathematical riddle that when solved, could be interpreted simply by saying the following: An arch subject to pure compression and free of tension can be obtained by inverting the shape of a hanging chain that is purely tensioned. Antoni Gaudi applied the same technique when designing Sagrada Familia using inverted catenary curves. See figure 60 (Adriaenssens et al., 2014)

The shape is formed by gravity’s influence on each particle. Just like the ball in figure 61 if the ball on top of the hill is pushed horizontally by a gust of wind, it will no longer be stable and fall to position c where it reaches stability equilibrium again. Therefore, ideally a shell structure should not be prone to asymmetric horizontal forces. (Adriaenssens et al., 2014, pp.15).

A shell structure is there by achieved after all particles reach equilibrium stability when pulled by gravity. The ratio between the span and the height (L/h) is mostly between 2 and 10 among existing shells, but this range can be very diverse. Perhaps the ratio is influenced by non-structural factors like the ease of construction process and assembly sequence. (Adriaenssens et al., 2014, pp.8).

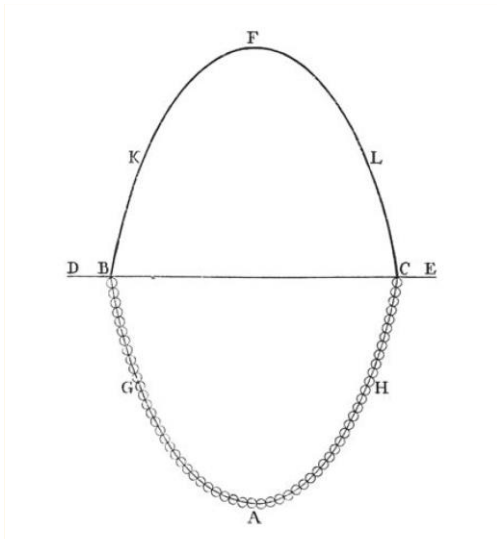


Figure 60 Poleni's illustration of Hooke's hanging chain and the catenary arch (Adriaenssens et al., 2014, pp.8).

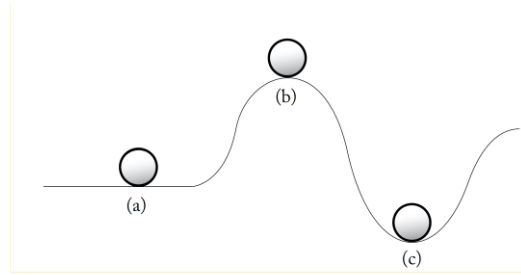


Figure 61 a) a neutral state, b) an unstable state, and c) is a stable equilibrium state of a ball (Adriaenssens et al., 2014, pp.16).

4.4 Structural mechanics of shells

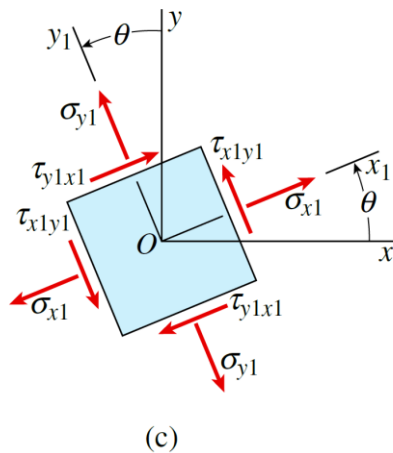
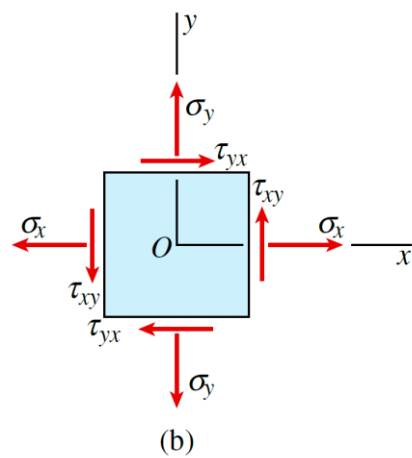
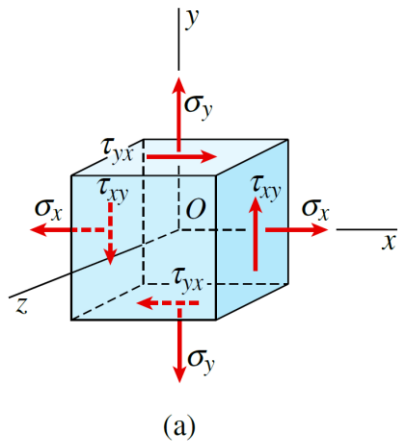


Figure 62 Elements in Plane Stresses. (Goodno & Gere, 2018, pp.669)

In order to understand how do shells mechanically work, one must understand isotropic homogenous plates and plane stresses. This is crucial to comprehend before conducting mechanical finite element analysis. (Adriaenssens et al., 2014, pp.23).

Usually plane strains are spoken of when dealing with thick bodies, while plane stresses are dealt with if the body is thin as a shell. This assumption is useful when placing the object into a FEA model from 3D to 2D. In this case the z direction is the thin dimension. With a plane stress mechanical scenario, the assumption is made to have all the stresses are in the xy plane direction. This means that there are zero out of plane stresses. There are normal stresses in the x and y directions, $\sigma_x \sigma_y$ respectively. Reciprocally, Shear stresses perpendicular to the x and y directions occur; $\tau_{xy} \tau_{yx}$ respectively. This is depicted in the diagram below.

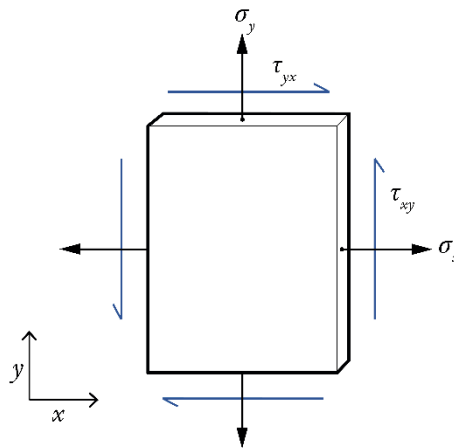


Figure 63 Plane Stress (Goodno & Gere, 2018)

Even though all objects are 3D it can be assumed for this level of shell engineering that all forces are transferred in 2D in-plane membrane stresses or axial stresses in case of an arch. If this 2D scenario is substituted in the 3-dimensional equation of Hooke's law, one could get

$$\begin{aligned} \sigma_{zz} = \sigma_{zx} = \sigma_{zy} &= 0 \\ \epsilon_{xx} &= \frac{\sigma_{xx}}{E} - \nu \frac{\sigma_{yy}}{E} \\ \epsilon_{yy} &= \frac{\sigma_{yy}}{E} - \nu \frac{\sigma_{xx}}{E} \end{aligned}$$

If π_{xx} is assumed to be zero ($\pi_{xx} = 0$) Then

$$\epsilon_z = \nu \left(\frac{\sigma_{xx} - \sigma_{yy}}{E} \right) \text{ whereas } \nu \text{ is Poisson ratio}$$

$$\pi_{zx} = \pi_{yz} = 0$$

Maximum in-plane shear stresses are called principal stresses because they are in principal axes. (Goodno & Gere, 2018, pp.671)

Since there is an equilibrium state of moments around the normal axes $\tau_{xy} = \tau_{yx}$. Therefore, the loads exerted per unit area on the plate, q_x and q_y are in equilibrium according to the following equations:

$$\frac{\partial \sigma_x}{\partial x} + \frac{\partial \tau_{yx}}{\partial y} = q_x$$

$$\frac{\partial \tau_{xy}}{\partial x} + \frac{\partial \sigma_y}{\partial y} = q_y$$

This leads to three unknown stresses and two equilibrium equations which results in a statically indeterminate model. In shell structures one more unknown and one more equilibrium equation added to that of a flat plate membrane stresses scenario. In this case the two plate-like plane stresses are just along the tangent of the shell curvature. The third membrane stress, however, is multiplied with the curvature. The curvature in this case is 1/radius of curvature. This equates up to 3 unknowns and 3 equilibrium equations, which makes it very hard to solve. (Adriaenssens et al., 2014, pp.23,24).

If both loads, q_x and q_y are null, then the Airy stress function (Φ) applies:

$$\sigma_x = \frac{\partial^2 \phi}{\partial y^2}$$

$$\sigma_y = \frac{\partial^2 \phi}{\partial x^2}$$

$$\tau_{xy} = \tau_{yx} = - \frac{\partial^2 \phi}{\partial x \partial y}$$

This is handy when a shell is loaded only vertically. Since horizontal loads are zero, horizontal equilibrium can be solved then by means of the Airy stress function (Φ). Henceforth, the shell's vertical equilibrium can be calculated via

$$w = \frac{\partial^2 \phi}{\partial x^2} \frac{\partial^2 z}{\partial y^2} - 2 \frac{\partial^2 \phi}{\partial x \partial y} \frac{\partial^2 z}{\partial x \partial y} + \frac{\partial^2 \phi}{\partial y^2} \frac{\partial^2 z}{\partial x^2},$$

Whereas w is load per unit area and z is the shell's height. (Adriaenssens et al., 2014, pp. 24,25).

When dealing with flat plates, out of plane stresses would lead to bending moments. Bending moments cause tension stresses. Look at figure 64 diagram below. In a shell, out of plane loads, bending moments, and tensile stresses are avoided by curving the plates along the direction of the load transfer. That way all loads will be transferred normal to the thickness; which means through plane membrane stresses. (Adriaenssens et al., 2014

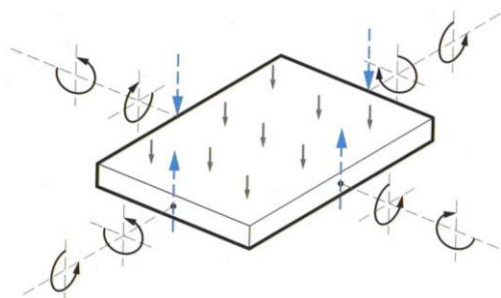


Figure 64 A flat plate with bending moments counteracting out of plane loads

4.5 Eccentricity, deformation and bending in shell structures

When a shell is properly defined and engineered bending stiffness and membrane reactions should be sufficient to sustain deformations with a certain margin. This margin is linked to eccentricity of the forces. Engineers account for such deformations by adjusting the thickness of the shell and choosing for a more tolerant materials if possible. In principle the deformation causing eccentricity of the forces from the axial plane should not exceed 1/6 of the thickness of the shell. Otherwise, bending moment will occur, and the structure will no longer act like a shell. Look at Figure 65 (Adriaenssens et al., 2014, pp.25,26).

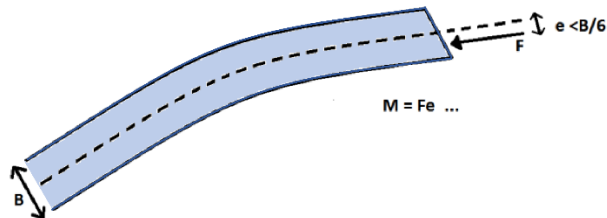


Figure 65 Normal Force Eccentricity Limit in Section view of a shell (Source: Author)

4.6 Buckling

According to Goodno et al. (2019), buckling is the sort of deformation a slender element under compression would bend into when excessively loaded. For a simple element like a column, the threshold loads an element would buckle at can be calculated using Euler's formula. This is also called the critical failure load of buckling.

$$F_c = \frac{\pi^2 EI}{L_e^2}$$

Whereas, F_c is the buckling critical failure load

E is the Material's Young's modulus

I is the second moment of area of the profile

L_e is the effective length dependant on the type of end supports (fixed, hinged, or pinned)

The designed shell's bending stiffness should be high enough to resist buckling. FEA can assist in assessing this requirement's verification. However, hand calculation through simplification is recommended due to FEA limitations in simulating buckling (Source: personal contact with Dr. Eng. Fred Veer).

4.7 Shell geometries

Adriaenssens et al. (2014, pp.2) describes 3 geometries for shell structures:

- **Free-form** or free curves geometries are usually designed before any structural evaluation is considered. When designed computationally these are called NURBS (Non-Uniform Rational Basis Splines). (Adriaenssens et al., 2014, pp.2)
- **Mathematically** the form can be determined by means of predefined analytical functions. This method is proven useful for post processing calculations regarding manufacturing subdivision. Usually, this method is restricted to non-complex shapes derived from low degree polynomials, trigonometric, or hyperbolic functions like ellipsoids and catenary curves. (Adriaenssens et al., 2014, pp.2)
- **Free found shells** are what this thesis is going to implement as the exhibition booth is designed. This is based on Hooke's law and Antoni Gaudi method of the hanging cloth of set of chains. When the tension-based hanging model is mirrored horizontally, the structure becomes a compression-only form. This could be done computationally, and this is the method adopted within this research. The high degree polynomial is parametrized. The parametric model is "relaxed", and the shape is attained once the model reaches a state of static equilibrium. The process is called form finding and will be elaborated upon further on. (Adriaenssens et al., 2014, pp.2)

4.8 Form finding methods of shell structures

There are several methodologies for form finding and shell structures, such as soap film method, force density method, cloth hanging, catenary chain hanging and other. However, it is handy to have responsive and controllable form finding method computationally. Rhino, Grasshopper, Weaverbird, and Kangaroo allow for a parametric meshing, tessellation and dynamic relaxation. In this project the Particle-Spring method is used with the aid of rhino and its plugins. (Adriaenssens et al., 2014)

In order to achieve a state of static equilibrium where all external forces are predominantly transferred within the plane of the curvature thickness, an optimal shape must be found. This form finding process is conducted by means of controlling the parameters of the geometry. These parameters may define the support points, the topology of the geometry and internal forces. By controlling the parameters, the desired length and height can be attained. (Adriaenssens et al., 2014, pp.2)

4.8.1 Particle-spring method: Rhino grasshopper meshing, Weaverbird tessellation, and Kangaroo dynamic relaxation

This method will be the most elaborated upon approach because this research design will be developed by means of this methodology. It is a parametric computational form finding method. The form is made up of particles and springs. Each particle is a control point in grasshopper which has a mass-representative attribute and responds according to Newton's second law ($\text{Force} = \text{mass} * \text{acceleration}$). The springs act like rubber bands. Although the grasshopper relaxed model looks erected upwards, the model algorithm simulates the behaviour of an upside-down hanging model. Therefore, it results with a tension-only relaxed structure. However, it becomes a compression-only structure when taking the same shape and flipping it horizontally. The challenge with rubber-like springs is that rubber has some resistance against compression (tension when flipped). Therefore, the parametric model compensates for this tendency of resisting any compression forces by splitting the springs in two with a particle in between. While a non-split rubber-like spring might withstand a small amount of compression, a split spring would buckle. This would ensure a reliable tension-only relaxed model, hence a compression-only structure when flipped. (Eigenraam, 2018) see figures 66-68 below

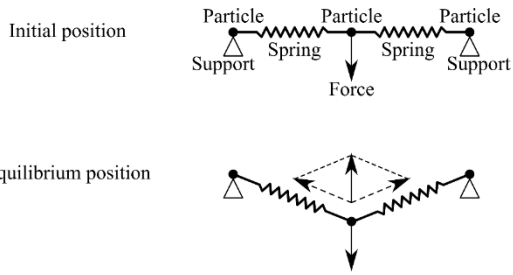


Figure 66: Particle Spring reaching equilibrium according to Newton's 2nd law. Source: (Eigenraam, 2018)

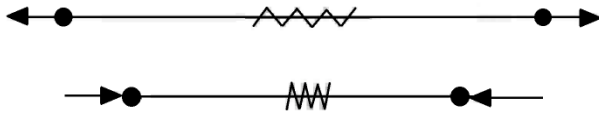


Figure 67 A normal "rubber" spring would take both tension and compression. Source (Eigenraam, 2018).

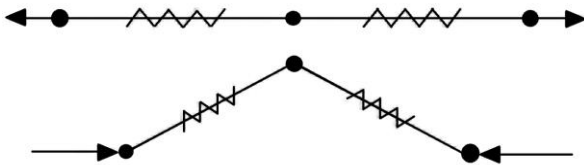


Figure 68 A split parametric spring would take tension but would buckle under compression (reversed in reality). Source: (Eigenraam, 2018).

This method can be applied using computer program Rhinoceros, some of its plug-ins like Grasshopper, Kangaroo, and Weaverbird. These parametric tools will be used for the form finding procedure. Meshes will be produced using these plugins by means of NURB.

The Algorithmic Grasshopper Procedure is described in Appendix B: Dynamic relaxation of the shell using Particle-Spring form finding Method. See figure 69

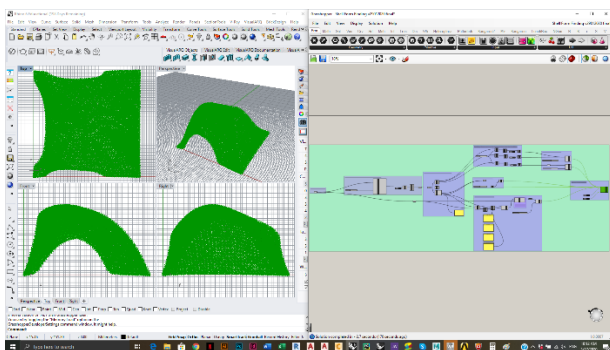


Figure 69 Dynamic relaxation using spring-particle grasshopper method for form finding. The procedure and algorithm script are explained in appendix C

4.9 Examples of inspirational shapes of shell structures

4.9.1 Aichtal Outdoor Theatre

In the world there are very huge shell structured buildings like the Funicular shell, Aichtal Outdoor Theatre in Germany. (Adriaenssens et al., 2014) However, the two other small-scale examples are more relevant for this

paper.

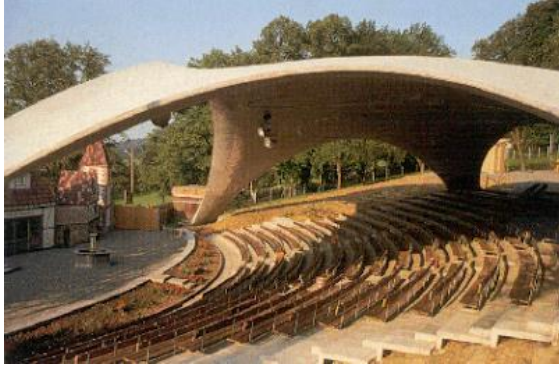


Figure 70 Funicular shell: Aichtal Outdoor Theatre (Naturtheater Aichtal-Grötzingen) in Grötzingen, Aichtal, Esslingen (Landkreis), Baden-Württemberg, Germany. Completed in 1977 (Clark, 2009)

4.9.2 Tessellated shell pavilion

This project used tessellation design logic along with “friction-fit-connection-system” to avoid mechanical connections and adhesives. The form was found using RhinoVault. The triangles were made to be equilateral looking so that a hexagonal pattern would emerge. Openings were introduced into the design before form finding was run and the shape was optimised (Tepavčević et al., 2016)



Figure 71 The Tessellated Shell Pavilion (Tepavčević et al., 2016)

4.9.3 The concrete grid shell

This project presented “a method for the construction of non-uniform precast concrete shell structures from unique parts. A novel method of discontinuous post-tensioning is introduced which allows tension to be taken through the connections.” (Pedersen et al., 2014)



Figure 72 The Concrete Grid shell (Pedersen et al., 2014)

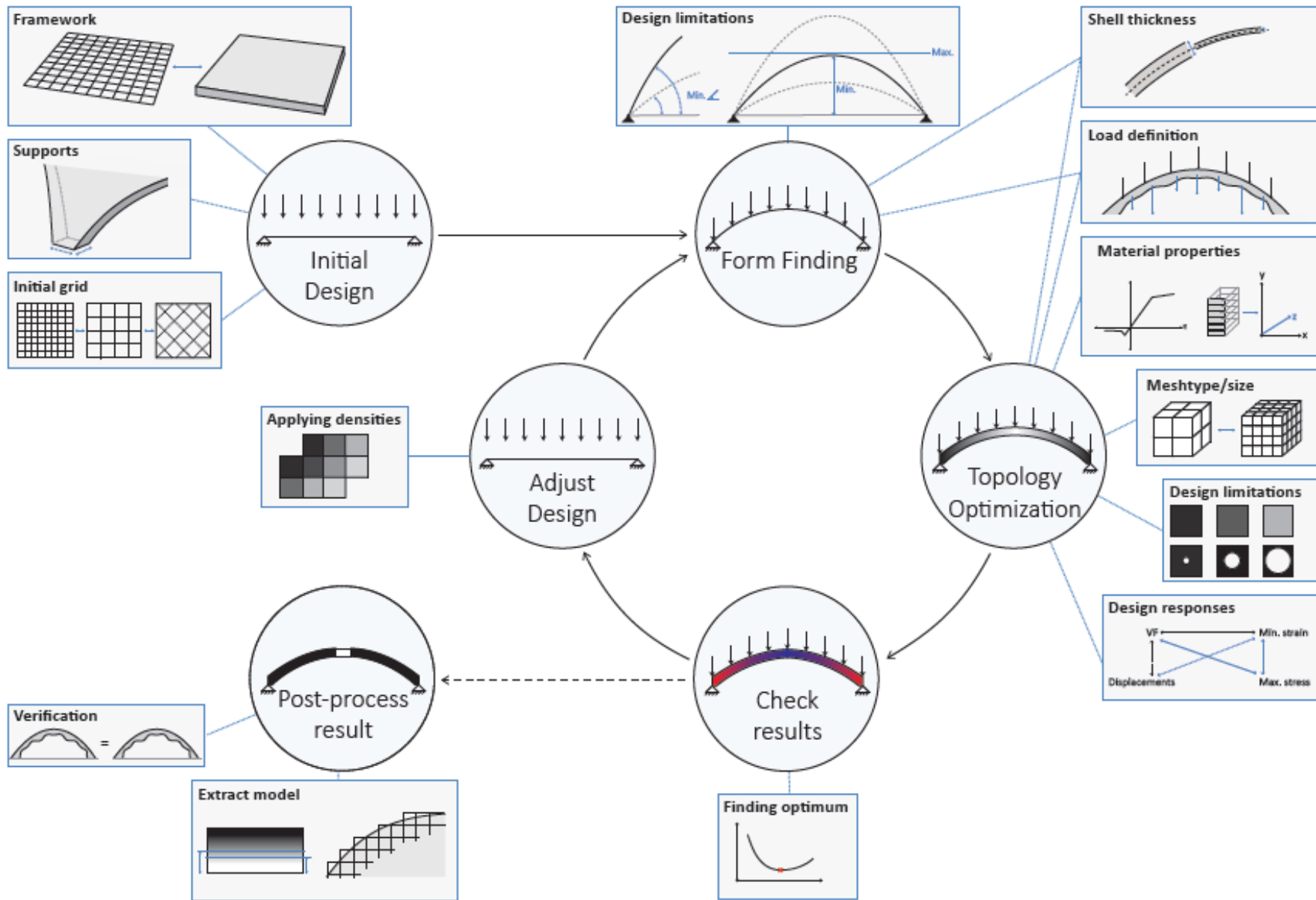
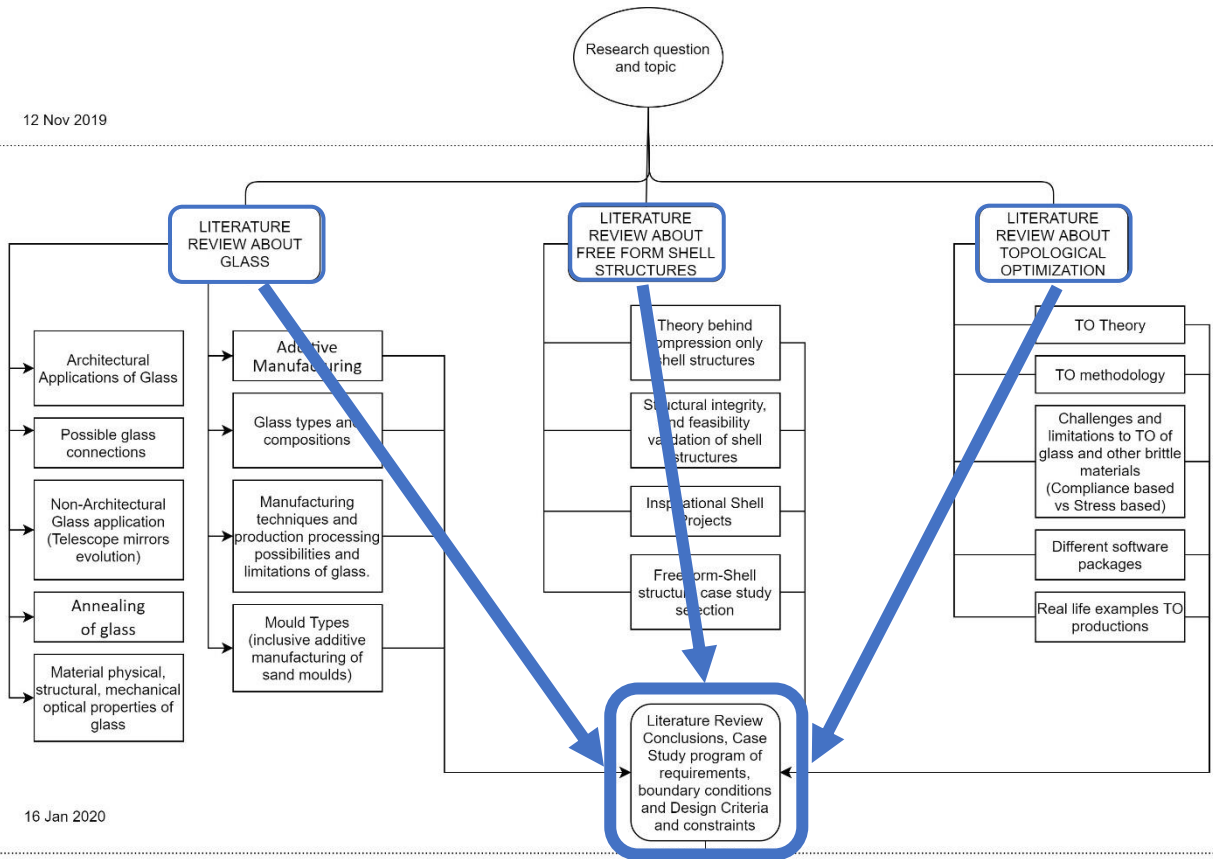


Figure 73 Overview of the process from form finding to Topology Optimisation (Bartels & Houben, 2016)

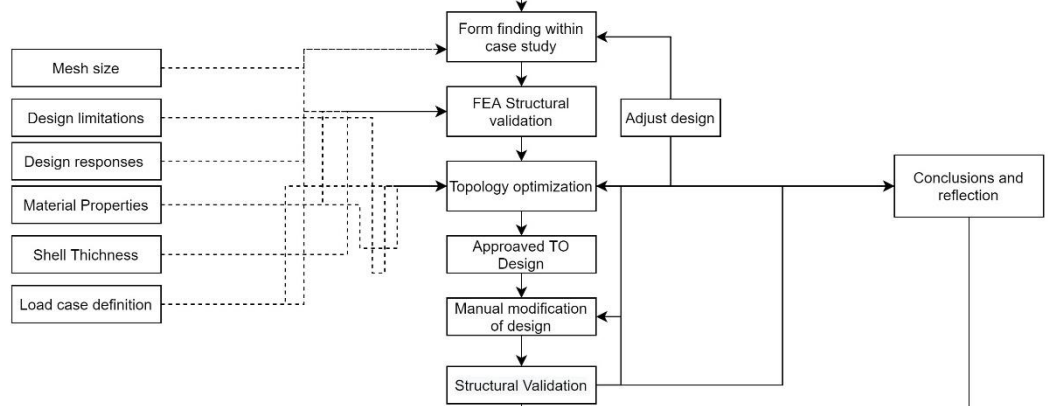
P1

12 Nov 2019



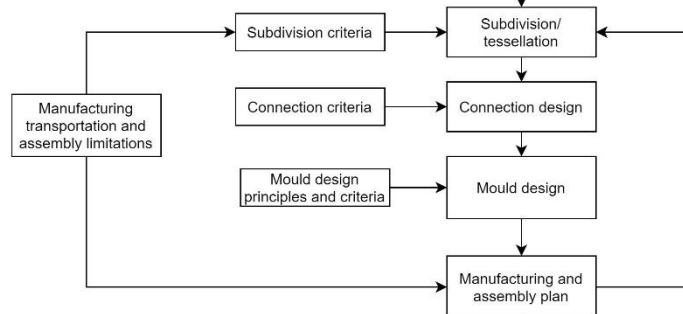
P2

16 Jan 2020



P3

26 March

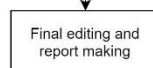


P4

21 May

P5

6 July



Chapter 5: Literature review conclusions and derived criteria

This chapter presents no new information. Rather it summarizes the design choices made based on the literature review findings in chapter 1 to 3 in the first section. The second section of this chapter lists the design criteria

5.1 Design and manufacturing Choices (Literature Review Conclusions)

5.1.1 Type of glass

Sodium Borosilicate glass

Borosilicate glass is considered to be the most suitable type for cast glass. This is because it requires a shorter annealing time than other glass compositions, and therefore, larger cast glass volumes can be moulded. For example, the Giant Magellan Telescope mirror, the Dennis Altar glass slab, the “Optical house”, and the “Atocha memorial” were all cast glass projects that used Borosilicate glass. It is also resilient to thermal shock, and chemicals. Thanks to the contribution boron oxide attributes to Borosilicate glass, its thermal expansion rate is low. Its processing process costs slightly higher than soda-lime and lead-oxide glass but lower than that of aluminium-silicate, 96% silica, and fused silica glass. This manufacturing cost corresponds to its Mean melting Point at 10 Pa of 1450–1550 °C, which lies in between that on the aforementioned types of glass. (Oikonomopoulou, et al., 2018)

5.1.2 Moulding and manufacturing method

Expectedly the real full-scale design would be casted using Hot Forming/ Melt Quenching. However, at the TU lab kiln casting would be implemented for prototyping, especially if recycled glass is to be used.

Kiln casting requires lower temperatures. But since all moulds yet to be cast are vertical, placing recycled glass on top of the mould as part of kiln casting would not be practical. If the moulds were to be placed horizontally then kiln casting would be more suitable, especially if recycled glass is to be used kiln casting would be the preferred method.

The size limit for prototyping is 1m x 1m x 1m due to the available sand moulds printers available.

Additively manufactured sand moulds (by means of binder jetting)

As Bhatia (2019) Damen (2019) and Oikonomopoulou, et al. (2019) concluded that additively manufactured sand moulds are the most suitable for large size cast glass production because it passed the following criteria:

- High Precision ± 0.1 mm
- Affordable cost
- Resilient material against high temperatures for a long time period.
- No support needed or dissolvable intermediate
- Smooth finish or treatable surface
- Facilitates the potential of complex geometries
- Reusability potential of excess sand during printing and destroyed used moulds
- In the CHP binder system is in used, then it can be dissolved. In addition to the silica-plaster mould surface coating, using a water-soluble binder makes the cast glass object easy to detach from the mould.
- Once the object is hardened the mould can be simply immersed in water. The cleaned again sand can be reused for printing another mould.

5.1.3 Form finding method

Spring-Particle method using Kangaroo, Grasshopper and Rhino.

It is a method where tension is avoided, and the user has control over the height, cross sectional area, and 2D shape of the shell. Since the method is parametric it can be easily exported and imported into TO and FEA software.

5.1.4 TO Method

SIMP

This method has been chosen because it is a well-established and industrialized methods of structural topology optimisation (Rozvany, 2007) It is the method used by the top two available software's with student licences. Ansys and Fusion 360. SIMP is a numerical FE-based topology Optimisation method. Other methods are either not yet fully developed or do not yield optimal solutions.

5.1.5 TO approach

Deflection driven compliance based.

For a shell structure deflection are more influential than stresses. This is because a large deflection might lead to eccentricity and therefore moments. Deflections lead to tension which it neither good for a compression-only shell structure not is it for glass as a material. Therefore, a deflection driven compliance based TO for a glass made shell form make more sense than a stress based (von-mises) TO.

5.1.6 TO Software

ANSYS (TO and FEA Software)

This is a certified structural FEA software that has an extensive various analysis package, and TO is one of them. Therefore, TO and FEA can be executed in the same software. This tool gives the user control over material settings, the objectives of the functions, and its constraints. The SIMP approach is used by ANSYS. Manufacturing constrains and post processing are possible features with ANSYS. (Damen, 2019)

5.2 Design Criteria

Minimum distance between separate parts	5 mm
Max annealing time	3 months
Thickness range of shell	Max 10cm
Size of subdivided elements	3T x 3.4m
Fits in truck	12 x 4 x 2.5 m
Case study limitations	6x6x2.97 m

5.2.1 Minimum distance between separate parts

This is related to the mould design. Minimum thickness of 5mm in any section of the mould. If the gap between two elements is very narrow and long, the sand mould in-between these two elements will be fragile or not even able to withstand the pressure. This can be achieved by inserting a code indicating the following logic: (if distance < min, then join parts by deleting separation or increase separation), or by manually adjusting the results of TO.

5.2.2 Correct edges geometry for connections

Curved shapes (no sharp edges). This can be achieved by a fillet constraint in the software. The most ideal shape glass would be shaped in is the shape of an egg, a sphere or an ellipsoid. Therefore, ideally the more rounded the elements are the better for homogenous cooling and transfer of forces.

Molten glass is a viscous material that should be able to flow smoothly through the mould cavities. This is another reason not to have sharp edges. From a mould design perspective this means a minimum of 3mm fillet as recommended by 3Deals. 3 Deals is a steel casting company; however, the same principle applies.

5.2.3 Even distribution of material (mass and volume)

A homogenous distribution of material is important for an even and gradual cooling during annealing. Otherwise, the narrow thin areas will cool faster than the thick massive volumes and cracks will occur due to the change of thermal expansion coefficient.

5.2.4 Max annealing time (less 3 months)

It is essential to aim for a short annealing time due to the high costs accompanying the process. Calculating annealing time is a complex simulation. However, the design can be compared to existing projects like telescope mirrors. The annealing time will be influenced by different factors including volume, thickness, and thermal expansion coefficient. Therefore, borosilicate glass will be used as it has an appealing thermal property in this regard. A homogenous mass distribution can contribute to a short annealing time as well. Maximum thickness is a crucial factor limiting annealing time. Therefore, a maximum thickness of 10 cm will be initially adopted.

5.2.5 Thickness range of shell

The shell must be able to avoid moments. This means a starting point range of 5-10cm to prevent eccentricity. This will ensure a compression-only shell. Structural verification results are allowed to lower this number.

5.2.6 Thickness range of dissected elements

Through optimisation dissected separate ribs-like elements will emerge, each of these separate elements should be able to resist buckling. Therefore, as a starting point a range between 5-10cm is chosen.

5.2.7 Size of subdivided elements

The elements should be able to fit into standard transportation means. The weight should be safe and feasible to carry through and assembled by common interior cranes.

1. Fits in trucks. (truck dimension 12 x 4 x 2.5 m Diagonally it is 4.74m.)
2. Can be lifted by interior spider crane. (limit 3T x 3.4m). See figure 113. (Uniccranes, 2020)

5.2.8 Maximum deflection

Max deflection should not exceed $1/6$ the thickness of the shell so as to avoid eccentricity.

5.2.9 Case study limitations

Dimensions of the booth. There should be an opening for the door. 6x6x2.97 m.

5.2.10 Redundancy (safety factors) /Discussion

Glass breaks without notice, therefore it can be dangerous for people surrounded by it. People might not have time to notice the crack and move away before it fails. Therefore, safety factors should be in place. One of the safety factors might be placing a net in the cast, not as reinforcement, but to hold up any broken pieces from falling. Another way is to subdivide the shell in a way where if one element fails all other elements will be able to carry the load.

Choosing borosilicate glass makes the structure more firesafe than soda-lime due to its thermal shock resistivity. Please read the redundancy discussion at the end of the report.

Chapter 6: The design process: Topology Optimisation, Structural verification, and Design Evolution of the Shell

6.1 Procedure (as followed)

1. First, the shell is dynamically relaxed in form using the spring-particle method. The mesh was given a thickness of 10 cm. This was done using Rhino, grasshopper and Maya. See appendix B for this procedure in details.
2. Second, the original 10cm shell was structurally verified using finite element analyses (FEA) via Ansys with regard to deflection, tensile and compressive stresses. See appendix C for all FEA results.
3. Third, TO was generated using Ansys. See result in Figure 74.
4. Fourth, the TO result was simplified to a shell with elliptic wholes at the locations TO removed material. The simplification was done for 2 reasons. First to improve the aesthetics, and second, because the rough result of TO was not a clean mesh and could not be computed.
5. Fifth, the simplified shell from the first TO was structurally verified using FEA with regard to deflection tensile and compressive stresses.
6. Sixth, a second TO was run on the first simplified TO shell.
7. In step 7, the entire shell dynamically relaxed again and was given a mesh thickness of 2 cm.
8. In step 8, FEA was run on the 2 cm thin shell. The structural verification passed the required limit in regard to deflection tensile and compressive limits
9. Step 9, here manually manipulation of the shell surface topology took place. Each area was assigned a different thickness. In light blue, where the first TO removed material, the thinnest layer of 2cm was placed. The shape of second TO was given a 8cm thickness because these are the most structurally functioning ribs. In between the red area and yellow are 4 and 6cm respectively. The transition between the varying thicknesses is done gradually to ensure homogeneous cooling.
10. At the end, the shell is subdivided, the connections are designed, transportation is accounted for, the mould is developed for casting, and the plan for assembly is elaborated.

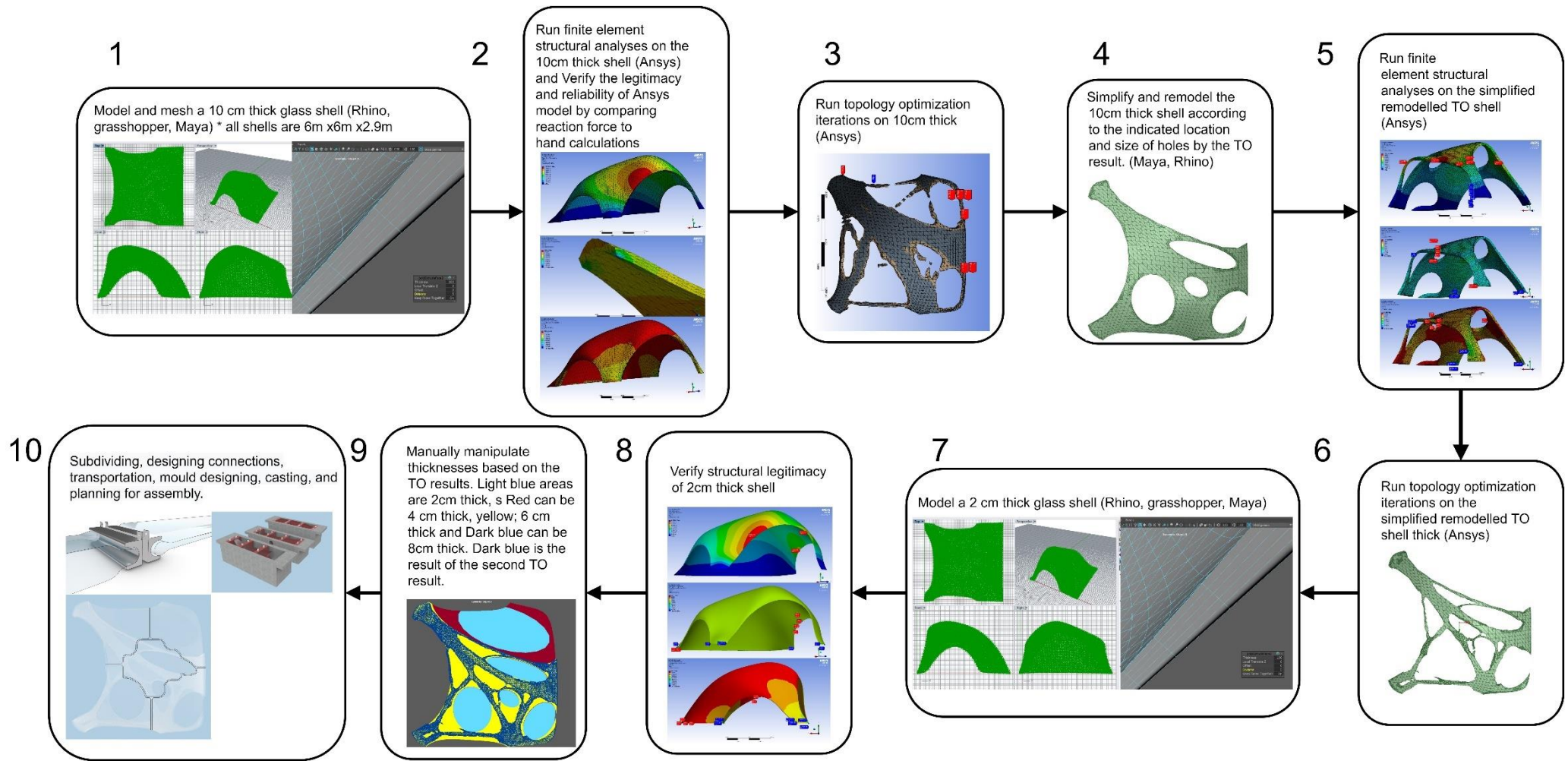


Figure 74 Topology Optimisation, Structural verification, and Design Evolution of the Shell

6.2 Verifying the legitimacy of the Ansys model

After the Model was form-found and meshed it was imported into Ansys. (See Appendix A: Dynamic relaxation of the shell using Particle-Spring form finding Method). With such a complex geometry it is hard to do manual calculations, however some calculations can verify whether the Ansys model is reliable or not. If the hand calculation of reaction forces does not deviate more than 5% from the Ansys model fixed support force reaction forces, then the other results from the Ansys model can be taken to be reliable. The comparative calculation verified that the Ansys model is reliable. The results can be seen in table 9.

Table 9 hand calculation comparison to Ansys FEA result of reaction forces for verification of the model

Borosilicate glass Density	2120 kg/m ³
Volume	4.1173 m ³
Mass	8728.7 kg
Gravitational Force	-9.8066 m/s ²
Mass x Gravitational Force	85598.9 N
Ansys result of total reaction forces	85599 N
Deviation	~ 0%

6.3 Topology optimisation and analysis conclusions and notes

- For the structure to maintain its shell behaviour, all forces must continue acting as normal forces along the structure's neutral axis. If deflection exceeds the limit of 1/6 the thickness, the bending moment will take place due to eccentricity. The maximum occurring deflection in all directions is less than the required limit. This means that all forces will continue acting as normal forces within the structure. Therefore, the structure will continue acting as a shell in consideration of the required deflection and eccentricity limits. See table 10.
- Foundation of shell should be a fixed support. A ring that takes outwards forces
- Although glass has nonlinear material properties (incomparable compression and tension strengths), in order to be able to run the TO iterations successfully, nonlinearity of material had to be ignored.
- For a more accurate FEA result mesh size was small leading high mesh count 23 million mesh count was reduced to 1.5 million mesh count for faster computation. TO took 1200 iterations to converge towards a result. This took half a day.
- All compressive stress and tensile stresses occurring in all three shells lie under the allowable stress limit glass can take. See table 10.

Table 10 FEA results from Ansys regarding the 3 different analysed shells. Please look Appendix C for all FEA results

	Permitted limit by Material properties or shell dimensions	Ansys Shell analyses results before TO 10cm thick	Ansys Shell analyses results After TO 10cm thick	Ansys Shell analyses results before/without TO 2cm thick
Maximum Principle stress (tensile stress) [MPa]	26.5	0.050007	0.11716	0.086317
Minimum Principle stress (compressive stress) [MPa]	265 – 1000 ***	0.0026977	0.0085319	0.020139
Deformation m	(1/6) * thickness for the 10 cm thick shells it is 16.67mm, and for the 2cm it is 3.33mm	0.0163 mm	0.0277 mm	0.0222 mm

- The 10 cm shell is over dimensioned by a factor of 530 is tensile strength capacity, and by a factor of 1000 in deflection. The 2cm thick shell is over dimensioned by a factor of 150 in deflection and a factor of 300 in tensile capacity.
- These results show that the 10cm and the 2 cm thick shell before and after creating the wholes based of the TO results are structurally sound.
- Since both shells are over dimensioned it can be concluded that a shell structure is an optimised structure to begin with. Thickness is not needed since it's a compression only structure and glass are

strong under compression. The difference in thickness would then be made for aesthetics, and safety factors. Cast glass would still be needed for a n organic free form. due to time and lengthy computational processes no further reduction in mass will be done. Recommended is to investigate how thin can one make the shell.

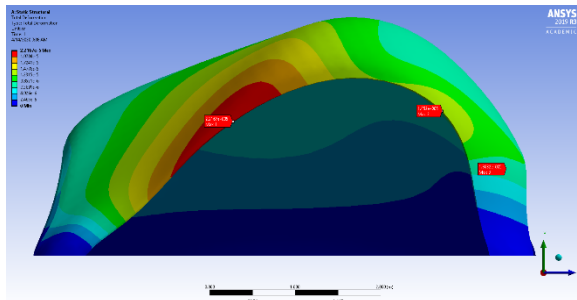


Figure 75 FEA results from Ansys: 2 cm thick shell deformation

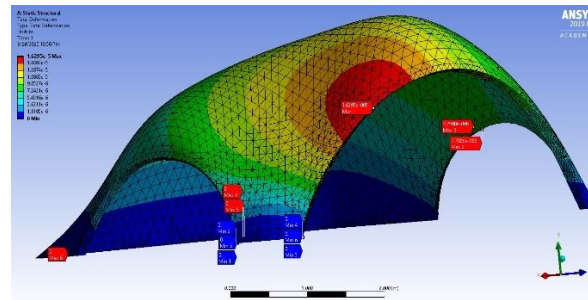


Figure 79 FEA results from Ansys: 10 cm thick shell deformations

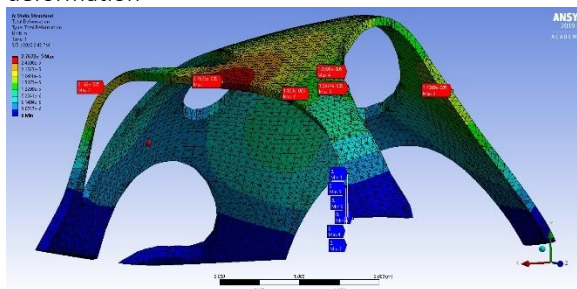


Figure 76 FEA results from Ansys: Simplified TO shell deformations

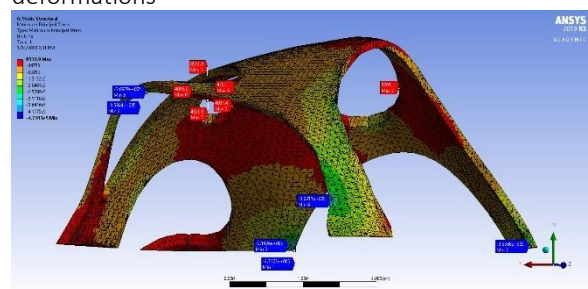


Figure 80 FEA results from Ansys: Simplified TO shell minimum principal stress (compressive stress)

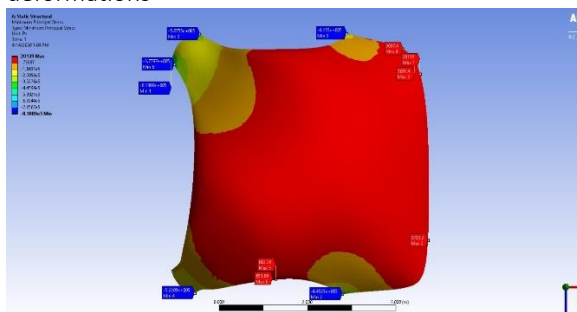


Figure 77 FEA results from Ansys: 2 cm thick shell minimum principal stress (compressive stress)

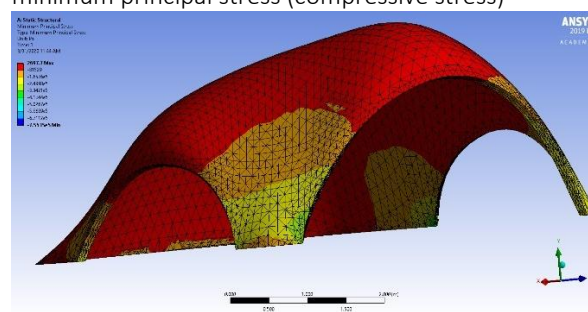


Figure 81 FEA results from Ansys: 10 cm thick shell minimum principal stress (compressive stress)

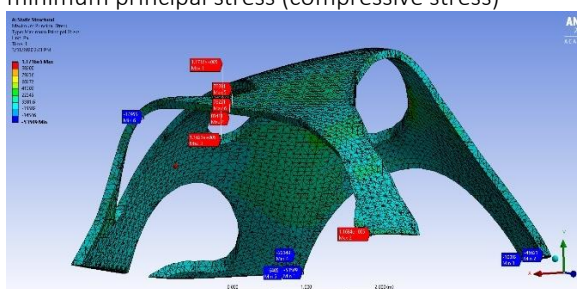


Figure 78 FEA results from Ansys: Simplified TO shell maximum principal stress (tensile stress)

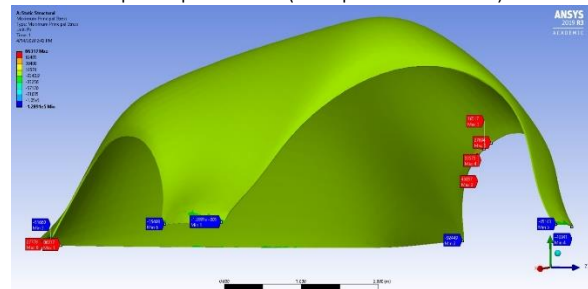


Figure 82 FEA results from Ansys 2 cm thick shell maximum principal stress (tensile stress)

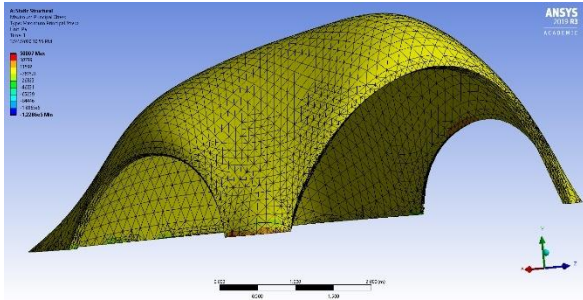


Figure 83 FEA results from Ansys; 10 cm thick shell maximum principal stress (Tensile stress)

More finite element analyses results are to be found in appendix C

6.4 Shape evolution after TO

The rough result from Ansys TO was subjectively perceived by some to be an ugly looking shape. This is due to its roughness, utter scatter and organic mess. See figure 85, 94-97. First TO Results. Therefore, and for easier analysis purposes, a simplified version was made by cutting ellipse wholes at the locations TO removed material. Both versions, the original TO and the simplified elliptical cuts shell were rendered in glass. The conclusions were that the original TO shell looked from a personal perspective better in glass than the simplified one. See figure 86-87. The asymmetric organic structure looks ugly in an opaque material; however, it looks like splashing water when rendered in translucent glass and therefore subjectively amazing. By maintaining an organic shape, it will be obvious that it is topologically optimised as a revolutionary design out of glass.

The challenge with this organic shape is the potential stresses at the free-form protrusions. These might lead to failure during annealing. Stress in edges will also be a dangerous consequence of the considerable uneven cross-section. Therefore, the question now is how can the organic design be realized while avoiding these problems? To do so, the design had to go back to the basic design principles for a strong glass, and faster homogeneous annealing. Manual design modifications were made. These are discussed next. Meanwhile though, a second TO was run on the simplified first TO result. The result is depicted in figure 90, 104-108.

6.5 Manual design modifications based on TO result and deflections analysis.

The first TO result was organic and flowing in shape. It looked when rendered in glass as splashing water. There were two problems regarding this result. First, the directly exported TO mesh from Ansys was complicated to clean up and re-mesh as a manifold for analysis. Second, due to its uneven distribution of mass throughout its cross-section, local stresses would lead to failure during annealing. See figure 84 design principles for a strong glass, and faster homogenous annealing time using smart design. Therefore, a simplified mesh was made based on the location and size of the holes in the TO result from Ansys. See figure 76 and (New simplified TO simplified shell).

The simplified shell with holes could be run through FE analyses for stresses and deflection. The simplified version with elliptic holes was run for a second TO. The result of the second TO indicated where the thickest ribs should be

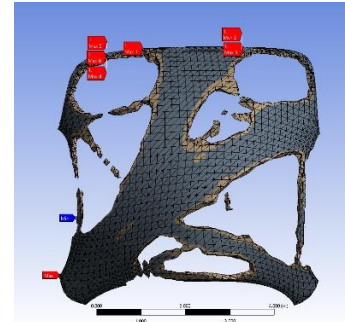


Figure 85 First TO Result Top. 50% mass reduction



Figure 86 Original TO result rendered in Glass



Figure 87 simplified TO result rendered in glass



Figure 88 Simplified TO result with elliptic holes

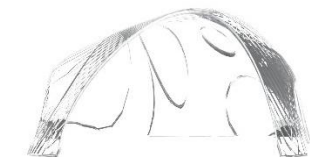


Figure 89 first and second simplified TO results rendered in glass together

located. See figure 90. A hybrid version was made using mesh mixer sculpting tool and Autodesk Maya meshing. It combines the simplified shell with ecliptic holes and the organic shapes that resulted from Ansys TO process. That way both the splashing water organic effect can be achieved while also adhering to the smart design principles for a strong glass, and faster homogeneous annealing time. See Figure 84.

Bullseye (glass producer for art glass mainly) provides a sheet indicating how long glass will need to cool depending on different thicknesses. This is summarized in table 11. This indicates that the cooling time for the shell will be between 9 and 120 hours because it varies in thickness ranging between 20mm and 80 mm. The increase in thickness should be very gradual in order to ensure an even distribution of material ensuring no cracks during annealing according to the design principles depicted in Figure 84 The gradient ensures a homogenous cooling preventing cracks. However, the entire piece should be annealed according to the lengthiest annealing time. So, the entire thing will take about 120 hours.

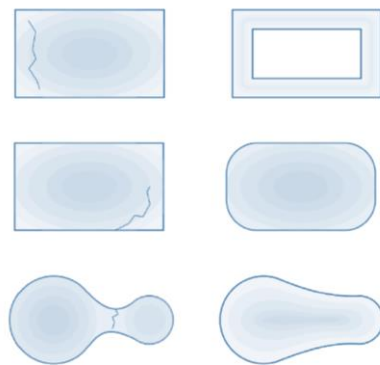


Figure 84 design principles for a strong glass, and faster homogeneous annealing time using smart design. From top and bottom: reduced weight or thickness, rounded forms with especially no sharp edges, and an even distribution of mass (Damen, 2019)

Table 11 Annealing time of slabs corresponding to different thicknesses (Bullseyeglass, 2019)

THICKNESS (mm)	Annealing soak time @482 °C	TOTAL MINIMUM TIME (Hours)
19	3 hrs	~9
25	4 hrs	~14
38	6 hrs	~28
50	8 hrs	~47
75	12 hrs	~99
100	16 hrs	~170

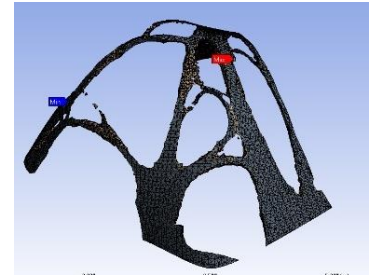


Figure 90 Second TO result perspective 60% mass reduction of the 1st TO simplified result

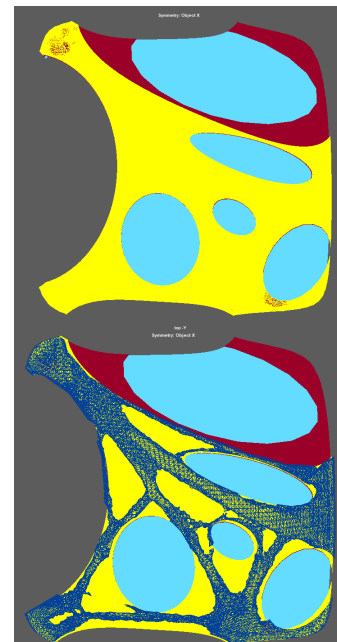


Figure 91 Manually manipulated thicknesses based on the TO results. Light blue areas are 2cm thick, since these are the areas where material was removed the first TO. Red can be 4 cm thick, yellow; 6 cm thick and Dark blue can be 8cm thick. Dark blue is the result of the second TO result. (Dark blue result is exported from Ansys, all other layers are modelled using Autodesk Maya based of the baked geometry in Rhino using Grasshopper dynamic relaxation.)



Figure 92 shell with different layers of thickness, manually adjusted, rendered in glass

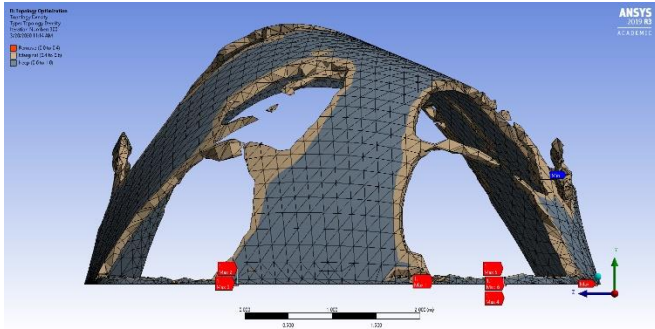


Figure 93 First TO Result Back. 50% mass reduction



Figure 94 Original TO result rendered in Glass

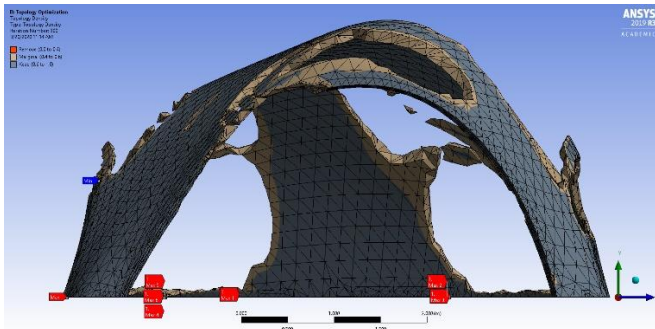


Figure 99 First TO Result Front. 50% mass reduction



Figure 95 simplified TO result rendered in glass

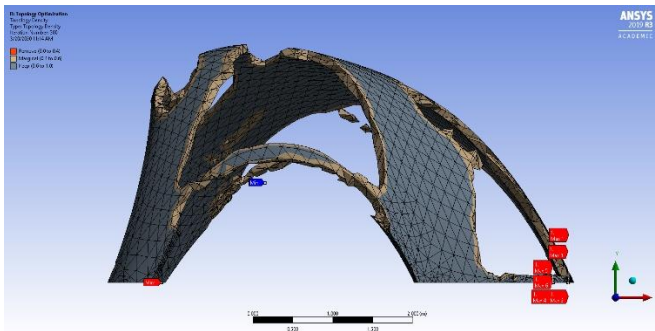


Figure 100 First TO Result Left. 50% mass reduction

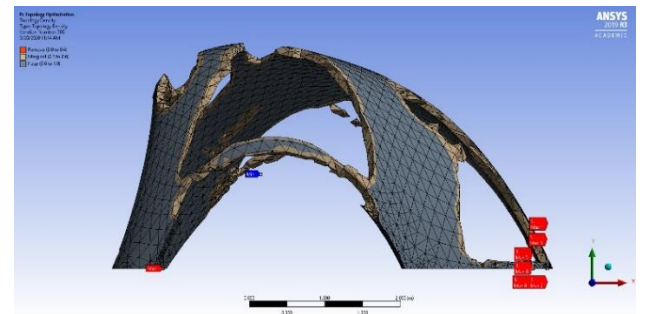


Figure 96 First TO Result Left. 50% mass reduction

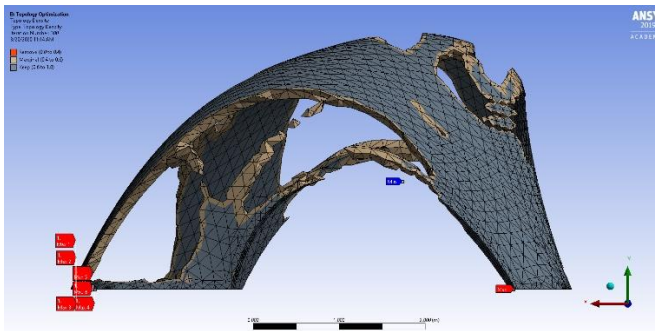


Figure 101 First TO Result Right. 50% mass reduction

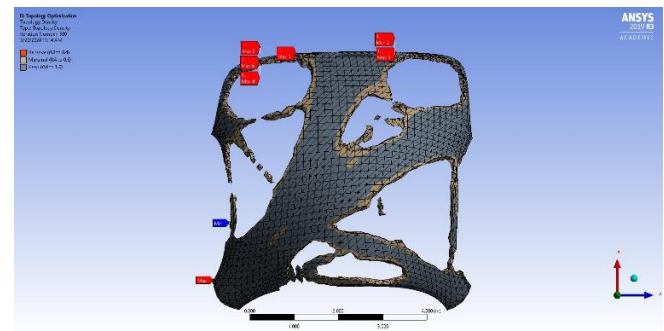


Figure 97 First TO Result Top. 50% mass reduction

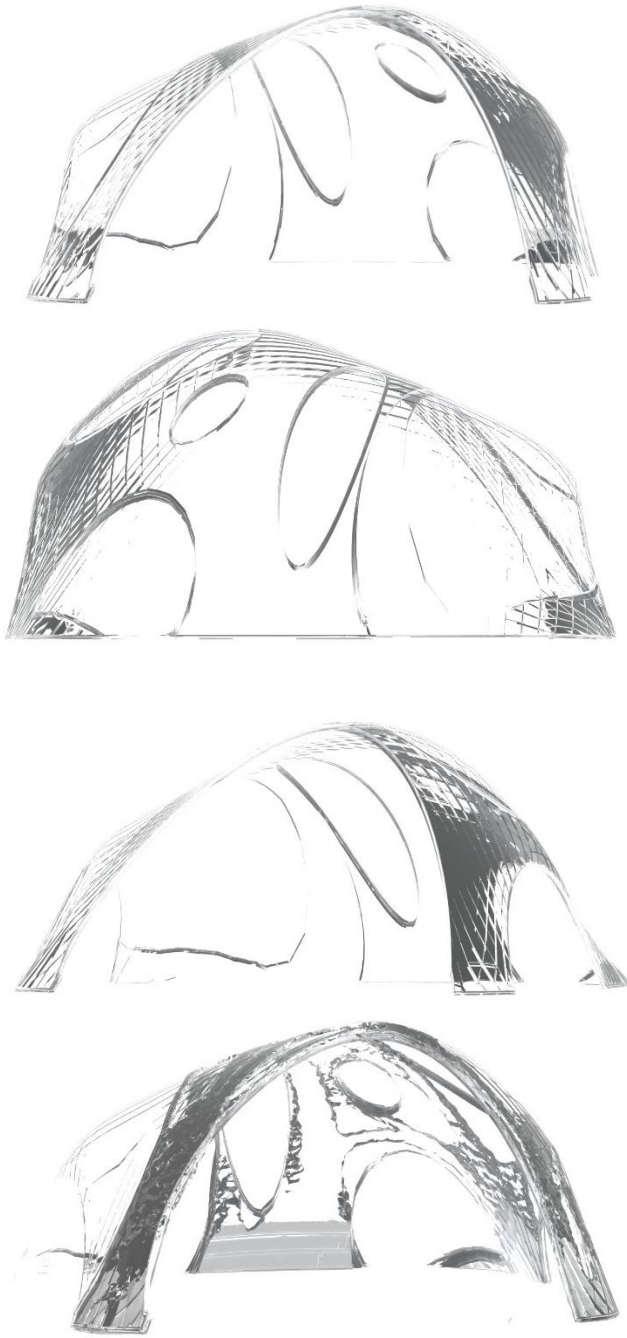


Figure 102 first and second simplified TO results with the ribs from second TO added rendered in glass together

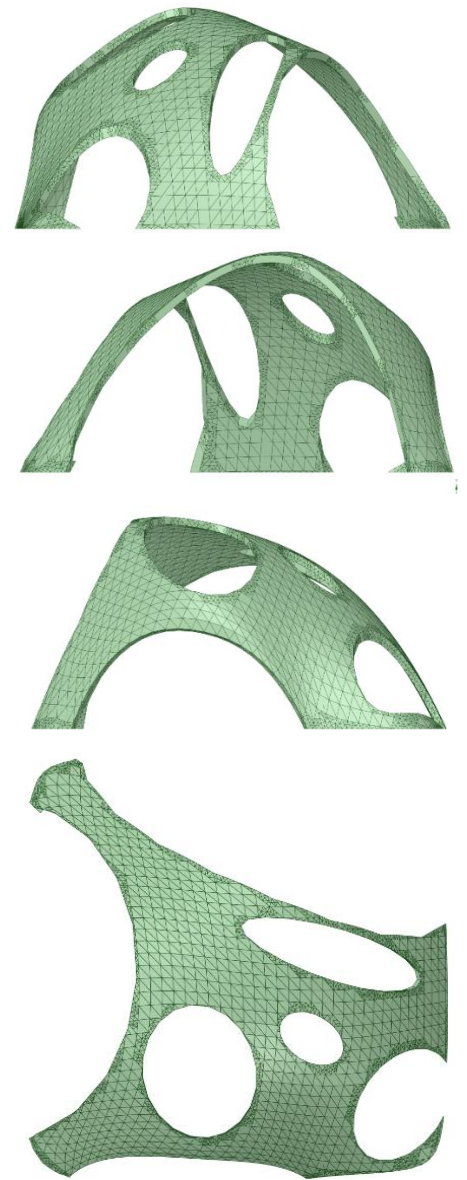


Figure 98 Simplified TO result with elliptic holes

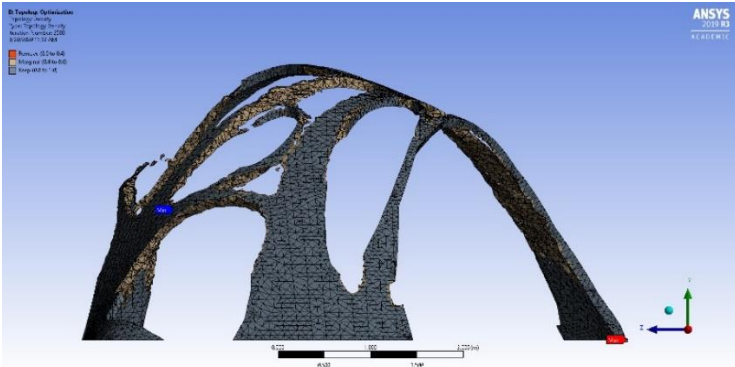


Figure 103 Second TO result back. 60% mass reduction of the 1st TO simplified result

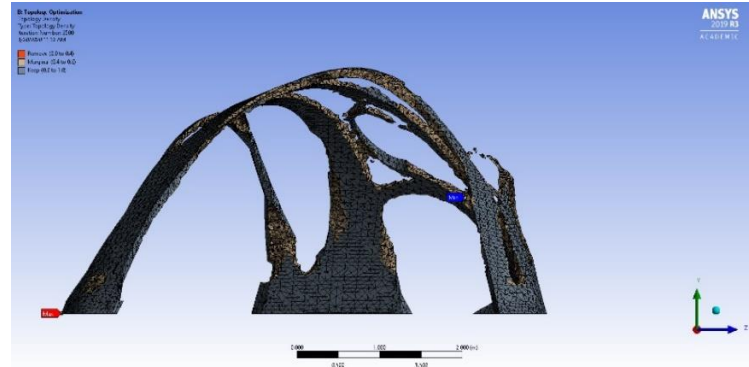


Figure 106 Second TO result front

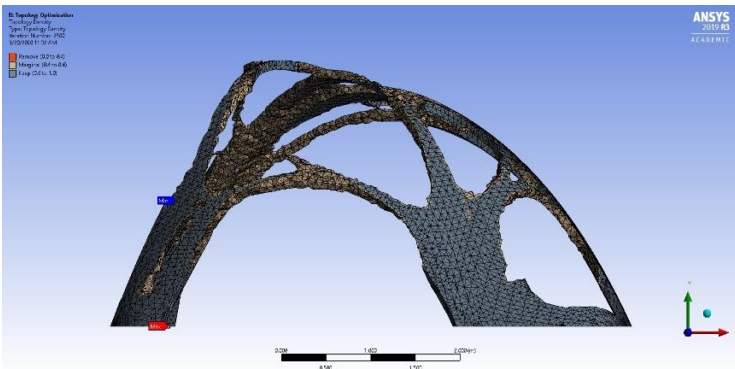


Figure 104 Second TO result left. 60% mass reduction of the 1st TO simplified result

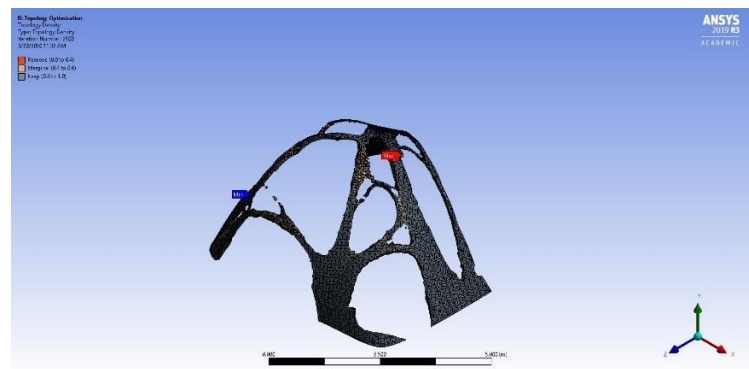


Figure 107 Second TO result perspective 60% mass reduction of the 1st TO simplified result

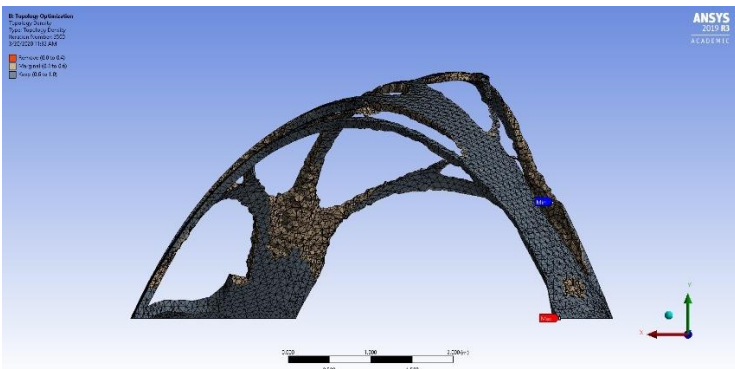


Figure 105 Second TO result right



Figure 108 first and second simplified TO results with the ribs from second TO added rendered in glass together

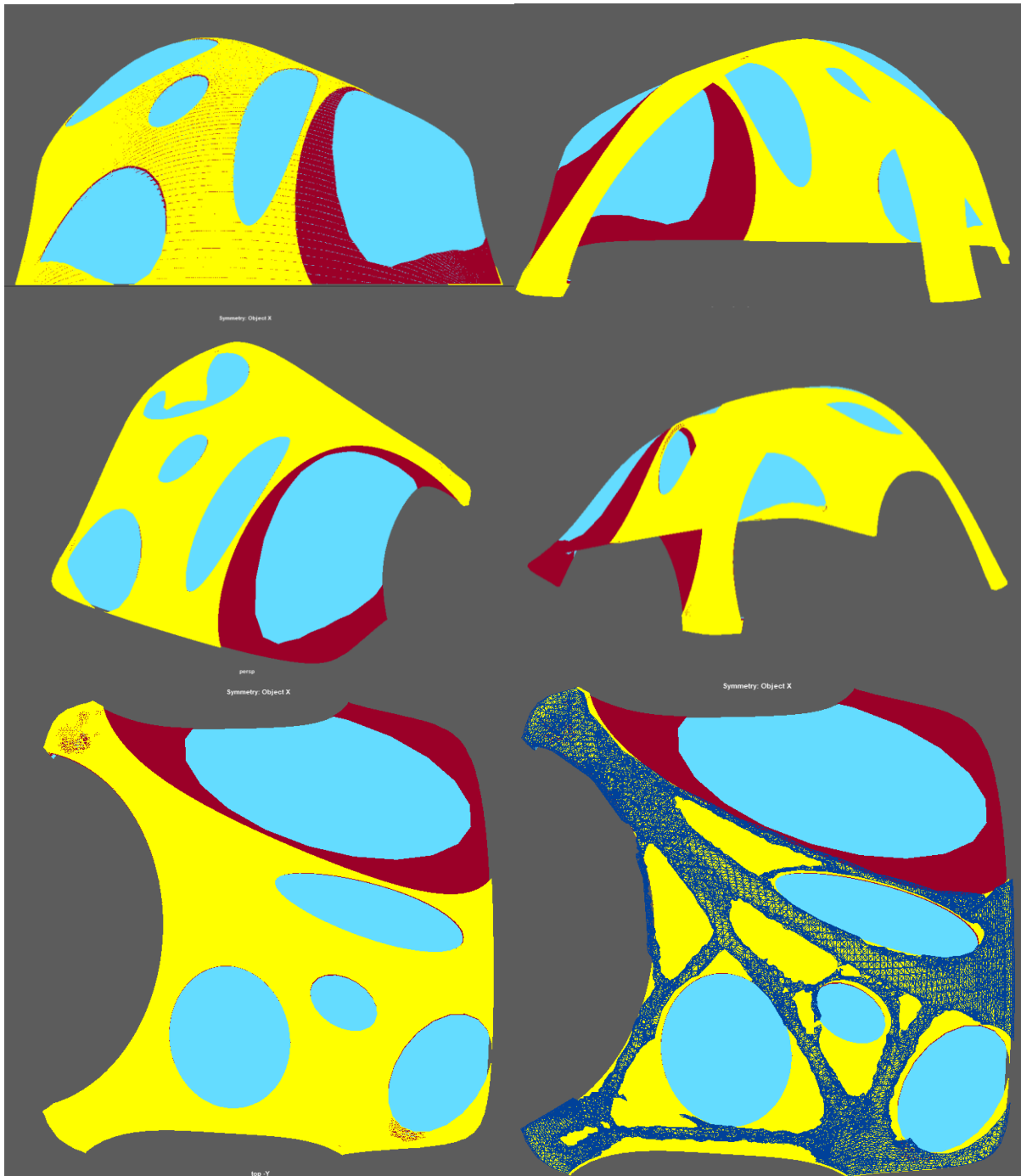


Figure 109 Manually manipulated thicknesses based on the TO results. Light blue areas are 2cm thick, since these are the areas where material was removed the first TO. Red can be 4 cm thick, yellow; 6 cm thick and Dark blue can be 8cm thick. Dark blue is the result of the second TO result. (Dark blue result is exported from Ansys, all other layers are modelled using Autodesk Maya based of the baked geometry in Rhino using Grasshopper dynamic relaxation.)

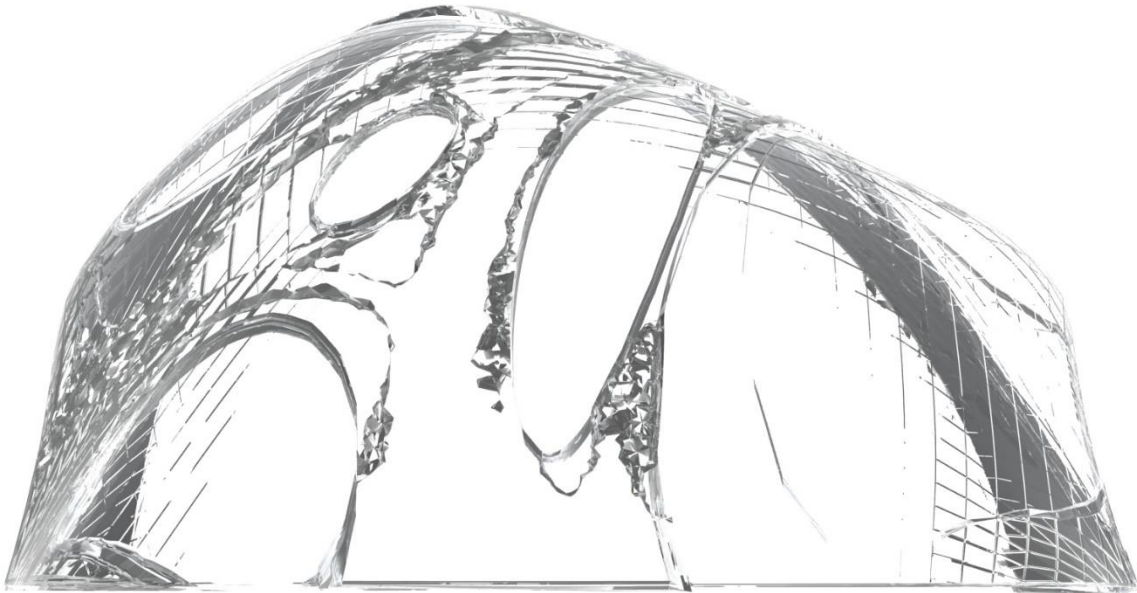
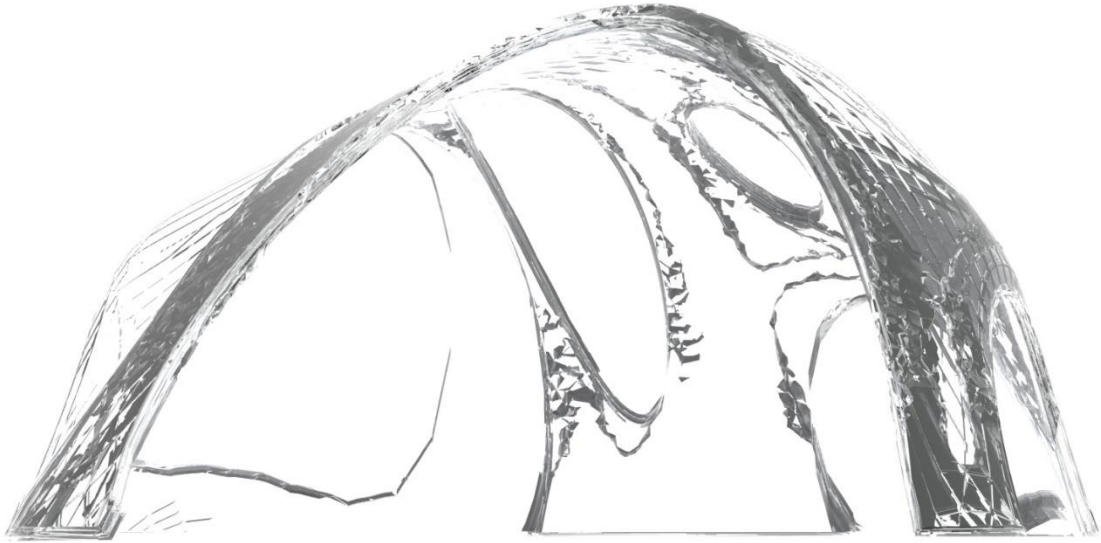


Table 12 mass reduction comparison

Shell version	Mass [Tonnes]	Mass reduction percentage
Original 10 cm solid shell	8.729	0%
8 cm shell with wholes at TO indicated areas	3.175	64%
4 cm shell with cut away material at TO indicated areas	1.906	78%
Solid 2 cm shell	1.598	82%
The manually adjusted shell with varying thickness from 8,6,4, to 2cm	4.138	53%
The manually adjusted shell with varying thickness from 8,6,4, to 2cm including additional ribs for extra reinforcement at connections	4.998	43%

6.6 Workflow along a variation of software (discussion)

The model was processed throughout the different platforms. The form of the shell was found using dynamic relaxation in Grasshopper (with Kangaroo plugin). The shell mesh without any thickness was baked into Rhino. Then the shell had to be given a thickness for topology optimisation purposes. Rhino was not able to exclude the thickness properly. In retrospect that might be due to that vector normals were not properly oriented. At the time the understanding was that Rhino can best handle NURBS, while Autodesk Maya is a better equipped software for handling complex meshes.

Extruding the mesh via Maya worked flawlessly, with an additional advantage of subdividing the thickness into segments. Space Claim, a geometry editor from Ansys, proved to be compatible with the same method Ansys regenerates the mesh for analyses. Having a clean reduced mesh from either Maya or Rhino is crucial to import into Ansys Space Claim.

Some meshing processes took hours, and these were solved by reducing the recount from 2 million to about 1 million.

Chapter 7: Subdivision of elements



The division can be done based on a variety of reasonings. First, one might subdivide the shell into elements of max 40 kg so that they can be lifted by 2 people. Or, second, subdivided based on transportation dimensions limitation and production mould size limitations. With the second approach large pieces will be produced. More research has been conducted on brick-like glass structures than giant elements. Therefore, the second approach was adopted.

7.1 Subdivision tessellation criteria:

3. No sharp corners allowed.
4. No scaffolding needed (preferably)
5. Consists of max 6 pieces so that the assembly procedure can be done fast and does not distort other booths in the surrounding.
6. Fits in trucks. (truck dimension 12 x 4 x 2.5 m Diagonally it is 4.74m.)
7. Can be lifted by interior spider crane. (limit 3T x 3.4m). See figure 113. (Uniccranes, 2020)
8. All elements have a comparable annealing cycle.
9. Can be manufactured within mould size (4 x 2 x 1 m) and mould design criteria
10. Tessellation does not interfere with force flow lines.

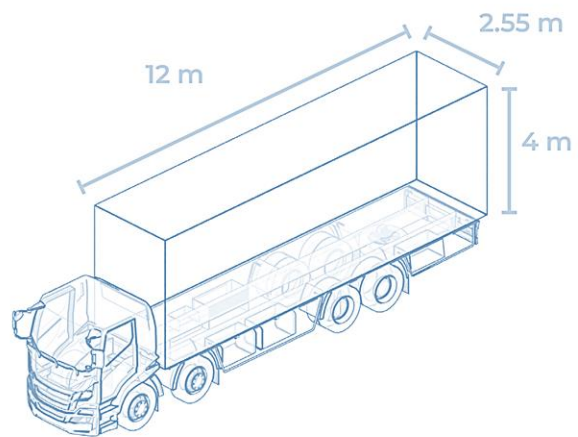


Figure 110 Max permissible dimension of a truck on German roads (Bhatia, 2019)

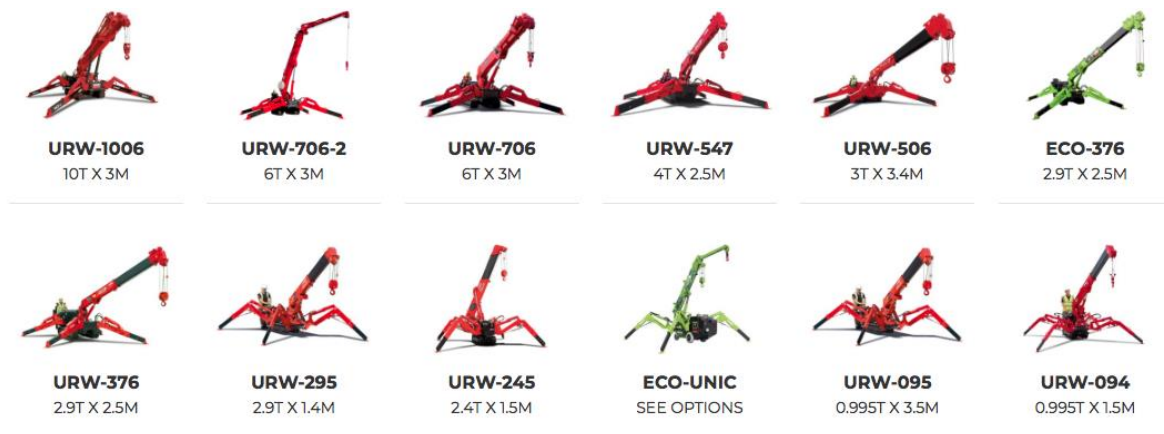
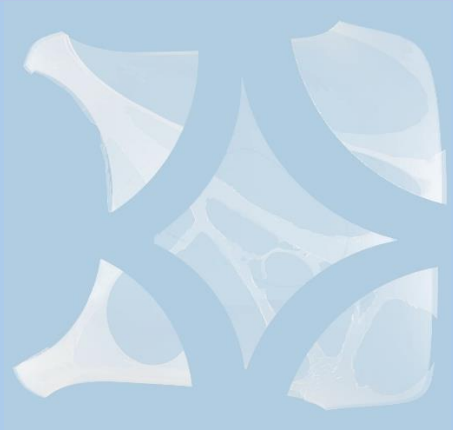
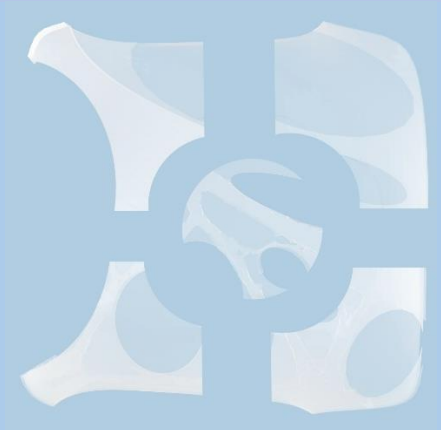
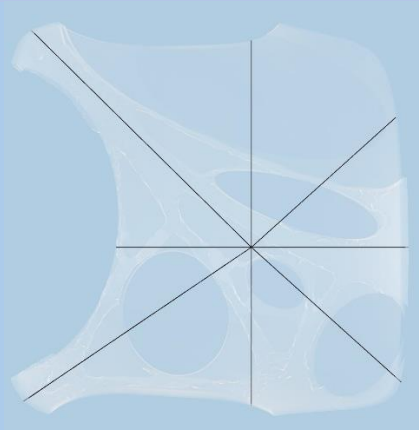
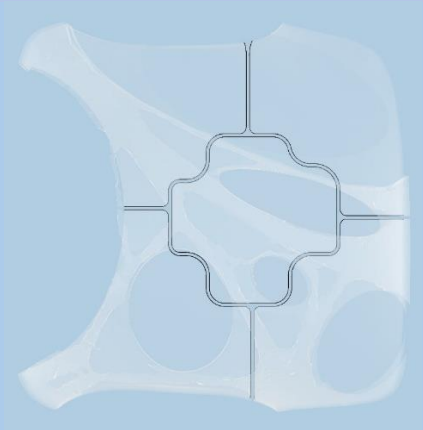


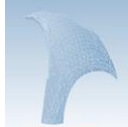
Figure 111 Specs, capacity, and limitations of Spider Cranes (Uniccranes, 2020)

Table 13 Subdivision pattern options

<p>Tessellation option</p>	 <p>Figure 112 Diamond cut.</p>	 <p>Figure 113 round keystone cut.</p>	 <p>Figure 114 Pie cut</p>	 <p>Figure 115 curvy cut with keystone</p>
<p>Avoid sharp corners.</p>	<p>Contains sharp corners.</p>	<p>Contains sharp corners.</p>	<p>Contains sharp edges</p>	<p>No sharp corners.</p>
<p>No scaffolding needed</p>	<p>Scaffolding required</p>	<p>No scaffolding needed</p>	<p>No scaffolding needed</p>	<p>No scaffolding needed</p>
<p>Max 6 pieces</p>	<p>5 pieces</p>	<p>5 pieces</p>	<p>7 Pieces</p>	<p>5 pieces</p>
<p>Fits in trucks. (12 x 4 x 2.5 m)</p>	<p>Diamond element does not fit in truck</p>	<p>Fits in truck</p>	<p>Fits in truck</p>	<p>Fits in 2 trucks with some adjustment in orientation</p>
<p>Can be lifted by spider crane (3T x 3.4m)</p>	<p>Key stone cannot be lifted by spider crane (3T x 3.4m)</p>	<p>Can be lifted by spider crane (3T x 3.4m)</p>	<p>Cannot be lifted by spider crane (3T x 3.4m)</p>	<p>Can be lifted by spider crane</p>
<p>All elements have a comparable annealing cycle.</p>	<p>All elements have a comparable annealing cycle.</p>	<p>Elements have large difference in size and thus don't have a comparable annealing cycle.</p>	<p>All elements have a comparable annealing cycle.</p>	<p>All elements have a comparable annealing cycle.</p>
<p>Can be manufactured within mould design limitations & criteria</p>	<p>Can be manufactured within mould size and mould design criteria</p>	<p>Can be manufactured within mould size (4 x 2 x 1 m) and mould design criteria</p>	<p>Can be manufactured within mould size (4 x 2 x 1 m) and mould design criteria</p>	<p>Can be manufactured within mould size (4 x 2 x 1 m) and mould design criteria</p>
<p>Tessellation does not interfere with force flow lines.</p>	<p>Tessellation does not interfere with force flow lines.</p>	<p>Tessellation does not interfere with force flow lines.</p>	<p>Tessellation interferes with force flow lines.</p>	<p>Tessellation does not interfere with force flow lines.</p>

The chosen tessellation pattern shown in figure 116 has is made up of sub elements. The specifications of each sub-element are summarized in table 14

Table 14 Specifications of the shell's sub-divided components

	Piece location	Volume [m ³]	Mass [Tonnes]	Bounding box Size/ Dimensions [m]	Mould Size limitation	Total Annealing time
	Front left leg	0.4552	0.965	3.5 x 2.9 x 2.87	Requires 5 connected moulds	~120 hours
	Front right leg	0.5648	1.197	3.6 x 3.1 x 3.1	Requires 5 connected moulds	~120 hours
	Back right leg	0.5102	1.082	2.4 x 2.3 x 3	Requires three connected moulds	~120 hours
	Back left leg	0.5091	1.079	3 x 2.3 x 2.6	Requires three connected moulds	~120 hours
	Centre Piece	0.3186	0.675	2.4 x 1.3 x 2.7	Requires 3 connected moulds	~120 hours

7.3 Refining the chosen subdivision pattern

The pattern was made without considering the pattern of the shell thicknesses and relief. As a result, two elements would have to connect via a 2cm thick glass area in some areas. This is because the cut runs through the 2cm area. The 2cm glass areas are not considered to be structural as TO suggested removing all material from these areas leaving them void. However, they are strong enough to absorb the forces during assembly to avoid temporary scaffolding. In this scenario the interlayer should play a role of holding the two elements in the right position and ensure proper connection. See figure 117.

One solution is creating an indent where load transfer is not crucial (2cm thick areas) and an offset some areas where contact is essential for load transfer. Then the connection is interrupted and concentrated on structural ribs. However, this will lead to gaps that are not very aesthetically pleasing.

Another solution is to increase the thickness at all edges to 8cm gradually. This way the pattern is preserved. Also mould dimensions and homogenous annealing are kept intact. And the connection area is unified along all edges making assembly, and interlayer design and manufacturing easy. However, from a design and aesthetics perspective it imposes a significant and undesirable impact for an architect. Another negative aspect associated with this solution is the increased mass. With topology optimisation the goal is to decrease mass. A 43% mass reduction has been achieved with TO and it would be counter-productive to add mass at this point. See figure 118

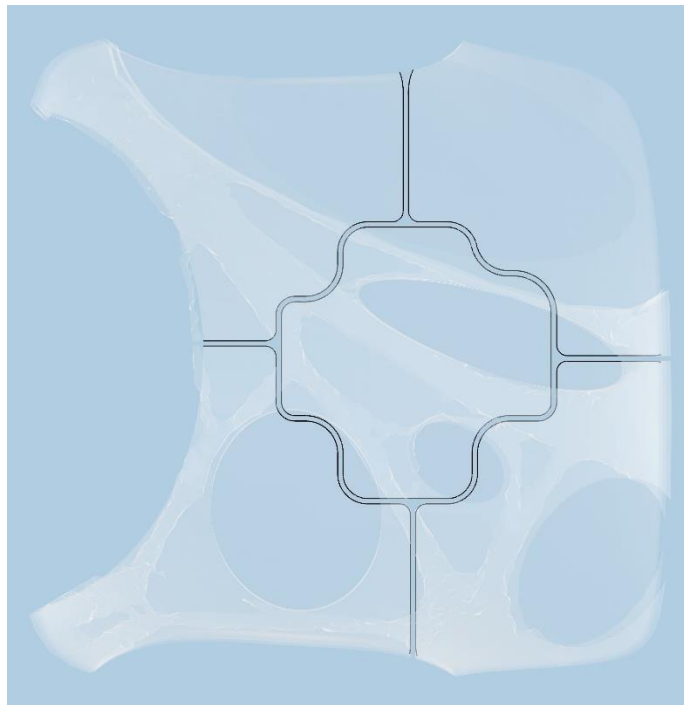


Figure 116 original subdivision clashing with surface topology of glass shell

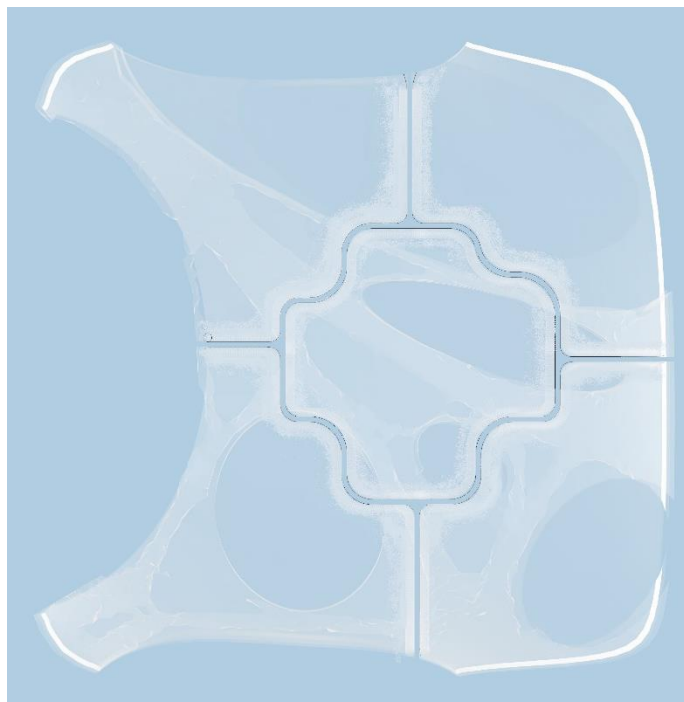


Figure 117 Added thickness around edges of connections

Another solution is to manipulate the division borders to wrap around the entirety of oval 2cm thick areas. This way 2cm thin areas will not be split in two. This will lead to abnormal mould size and design. Nevertheless, 3D printing allows for such forms. This might also lead to non-homogeneous annealing process as the average mass in every element would greatly vary. In this case the addition to each element has been checked and is verdict not to have a significant additional amount of surface area. For aesthetics reasons this will be the chosen option accompanied with a solution provided by the interlayer. See figure 119

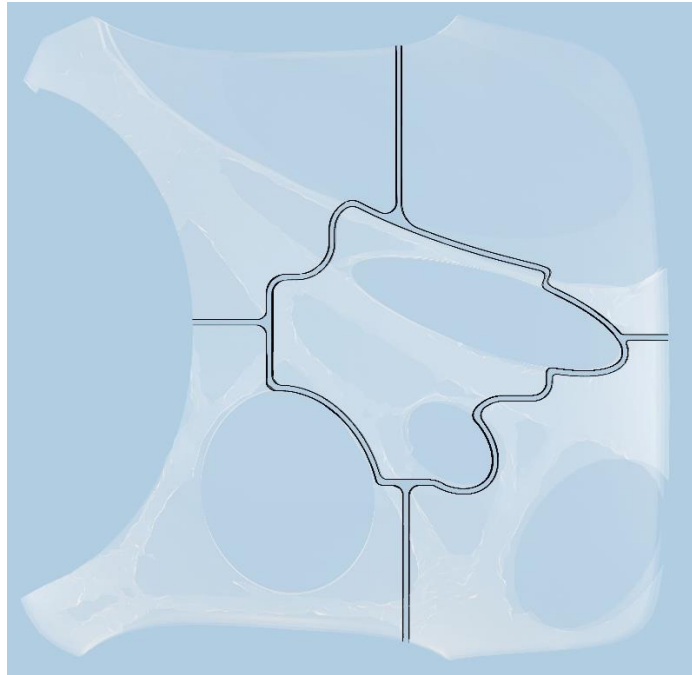


Figure 118 manipulating subdivision borders to wrap around thin ovals

7.4 Will they fit in a truck dimension? How many trucks needed?

The design allows for each sub-element to fit in a standard sized truck (12 x 4 x 2.55 m). They will fit in two trucks if they are rotated at an angle. See figure 120. CNC Styrofoam will hold the elements in position within wooden boxes. The CNC foam work can be a grid supporting the edges just as a TV and other appliances are packaged. See figure 121.

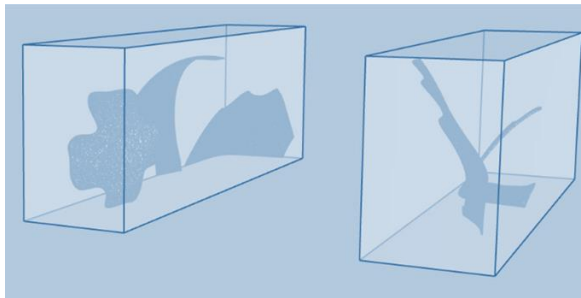


Figure 119 The shell elements can fit in two trucks with dimension 12 x 4 x 2.5m with adjusted orientation



Figure 120 CNC milled formwork of Styrofoam to support shape negative shape of shell elements in wooden boxes transported in trucks

Chapter 8: Connection possibilities between cast glass elements

Now that the shell design, dimensions and weight are known, subdividing it into smaller elements is necessary. Connections come hand in hand with subdivision and assembly methods. Connection methods and subdivision patterns were interchangeably discussed during the design process. That is why some of the arguments and options overlap subdivision options.

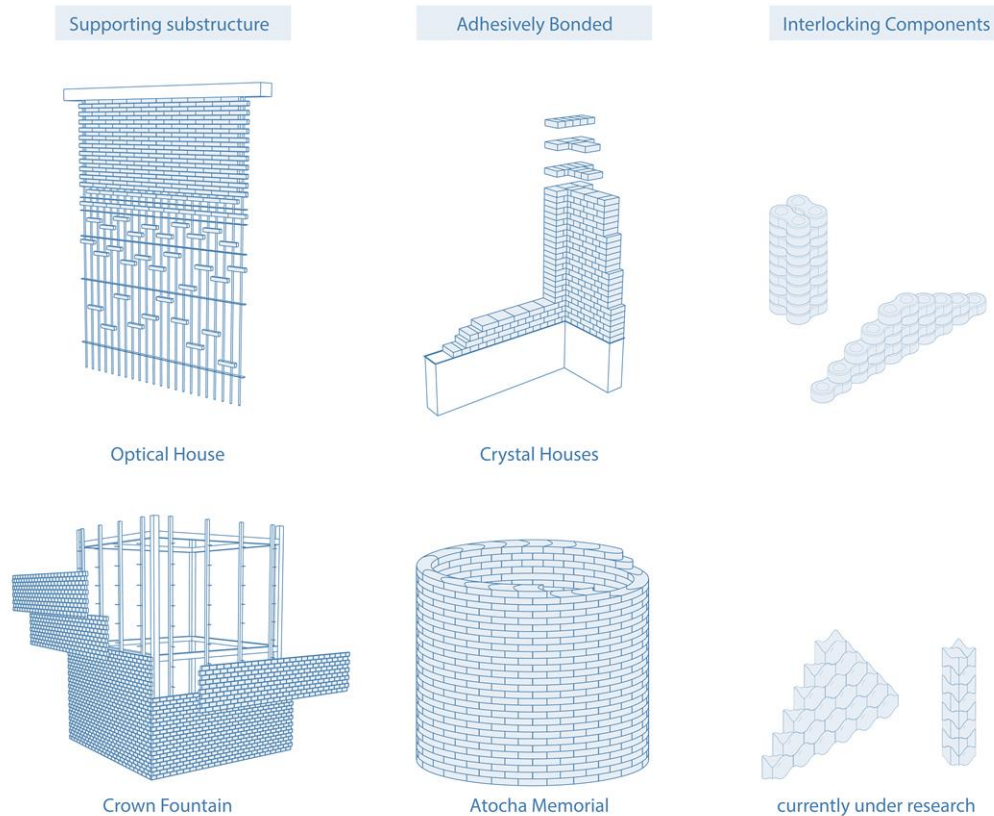


Figure 121 Connection Methods currently present for cast glass components (Oikonomopoulou, 2019)

8.1 Connection Types

8.1.1 Mechanical Connections (sub-structural metal bars or braces)

Holes of metal bars and metal bar connections cause peak stresses. Metal bars also hinder transparency. A dry assembly is easier and quicker than a wet connection. Demounting and reusing the building elements is possible. This makes maintenance and component replacement relatively easy. (Bhatia, 2019. P77-78) See figure 122.

8.1.2 Adhesive Connections

This method cannot be reversed but it allows for a very high level of transparency. Adhesive bonds do not cause peak stresses and ensure an even distribution of load transfer. The process should be executed with precision and care. A minimum thickness is essential to ensure a strong bond. The need for low tolerances means that each component would require extra post processing labour. (Bhatia, 2019. P77-78; Van der Weijst, 2019, P.46) See figure 122

8.1.3 Embedded Magnetic Connections (proposal, currently under research by Grammatiki Dasopoulou)

This is a proposal for a research topic. Some of the considerations that might be taken into consideration are the strength of the magnet, type of magnet (permanent/controlled), metal type (expansion coefficient), and location of embedment (Personal correspondence with Dr. F.Oikonomopoulou and currently developed by Grammatiki Dasopoulou).

8.1.4 Embedded titanium connections (currently under research)

Commonly used in laminated float glass, yet to be explored within cast glass applications. Titanium is ideal to use because it has the same thermal expansion coefficient. However, Titanium cannot just be sunk into the molten glass during casing because of the different expansion coefficient during the various stages of cooling (Granta Design Limited, 2019).

8.1.5 Interlocking-based geometrical connections

This method allows for high transparency. Since elements can be easily demounted it makes circularity possible. When an interlayer is added, the connection can accommodate for more tolerances. (Bhatia, 2019. P77-78) A variation of interlocking systems has been compared and developed as depicted in figure 122. However, these were intended for easy connection between a vast number of elements. Some of them require meticulous and lengthy postprocessing. They were compared in terms of their resistivity to shear stress. However, for a compression-only shell-structure, only membrane stresses should be assumed, shear and moment stresses can be neglected.



Figure 122 A variety of demountable dry-assembly structural cast glass interlocking systems as investigated by Oikonomopoulou et al. (2018a).

8.2 More about interlocking connections

Since interlocking-based geometrical connections offer a demountable dry-assembly solution, they are the most suitable option for this exhibition booth shell. Therefore, this thesis will delve deeper into the different types of experimented interlocking systems.

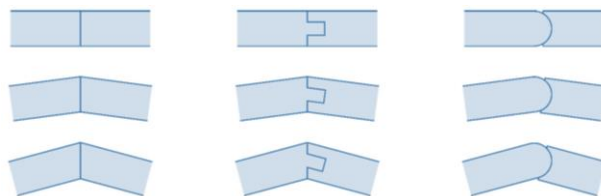


Figure 123 "Voussoirs connection a) planar interfaces, b) tongue and groove and c) convex-concave interface" (Van der Weijst, 2019)

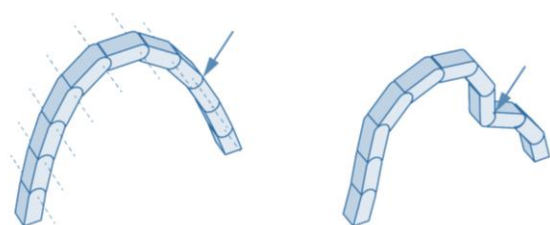


Figure 124 convex concave collapse mechanism (Van der Weijst, 2019)

Van der Weijst (2019) investigated different interfaces connecting two Voussoirs. Figure 123 displays the three main systems. The tongue in groove system has sharp edges and therefore is not suitable for glass. It also requires extra tolerances to fit in the right position. However, it offers extra out of plane support. The concave convex system allows for movement and is therefore the easiest to assemble and design for meeting at different angles. Nevertheless, it might collapse due to the hinge mechanism it is accompanied with as demonstrated in figure 124. Planar interfaces do not support out of axes (outward) forces.

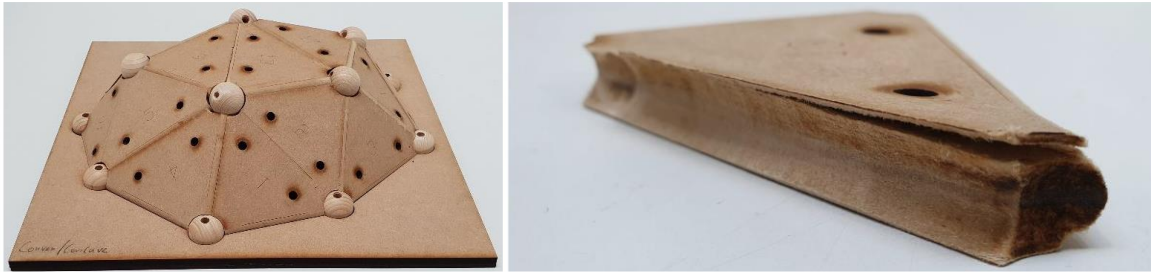


Figure 125 One of the test models. Shell divided and connected using convex-concave bonded elements (Van der Weijst, 2019)

Van der Weijst (2019) made 2 models of domes with the two different mechanisms. One was planar the other was concave convex. The results concluded that, the planar interface model could withstand higher loads than the concave-convex model when a point load is applied to one of its nodes. However, when gradual and evenly distributed load is applied, the concave convex interface could withstand more loads. Ideally the interlocking system should prevent out of plane forces or sliding outwards. Van der Weijst (2019) finally chose for a rounded version of the tongue and groove interlocking system, which is a hybrid of the concave convex project. This can be seen in figure 126. This is the system is adopted and further developed for this design project.

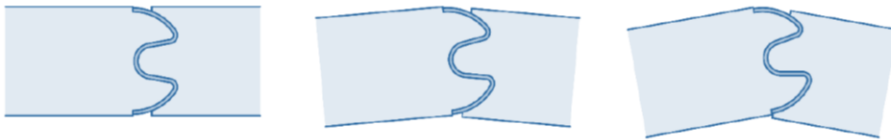


Figure 126 hybrid version of the concave convex and tongue in groove interlocking system (van der Weijst, 2019)

8.3 Challenge arising from combining the interlocking system with the subdivision pattern

When the connection was applied to the subdivision pattern. For simplification, the tongue will be represented by the convex shape and the groove will be the concave dent. Figure 127 shows the challenge of transitioning from tongue to groove.

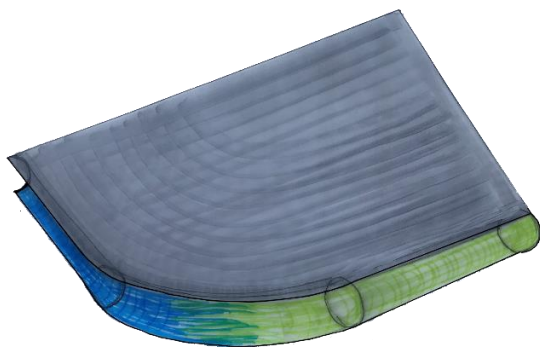


Figure 127 This shows how the challenge of transitioning from tongue to groove direction on one element. For simplification, the tongue is represented by the convex shape and the groove is the concave dent

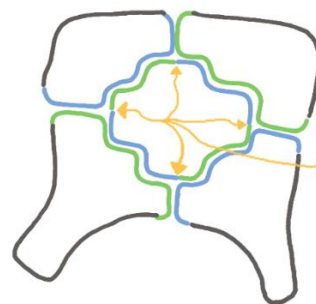


Figure 128 both scenarios would lead to elements with two different edges. green is tongue (convex) and blue is a groove (concave). Yellow arrows point out the location of the transition.

This could be solved by means of creating a gap at the corners and inserting a disc like fill at van der Weijst (2019) did as shown in figure 129. One solution in creating gaps in the mould for titanium inserts to be glued in afterwards. This will create embedded connections.

Another option is by means of an interlayer. The interlayer can define and unify the shape of the connection at the all edges of glass elements. If the interlayer is concave (groove) then glass is convex (tongue). With this option

the benefit is that glass is smoother, but the interlayer is more visible. If the interlayer is convex (tong) and glass edges are concave then glass have narrow edges (less even distribution of material), but the interlayer is less visible. The later solution will be chosen due to its consistency, ease of manufacturing and assembly that will be discussed in the choice of interlayer.



Figure 129 sphere at the nodes as a solution for transitioning between connection direction

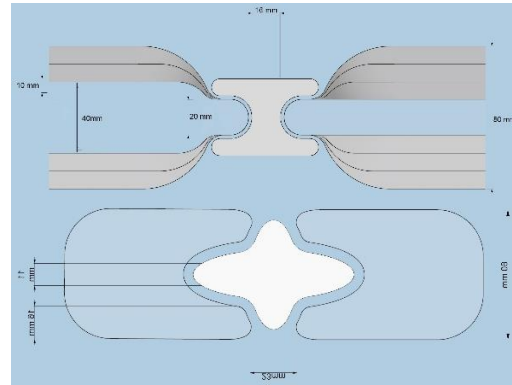


Figure 130 the other solution can be achieved by an interlayer that unified all glass connection shapes into either all tong or all groove

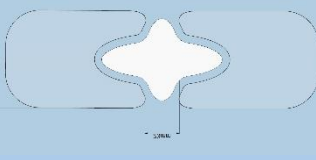
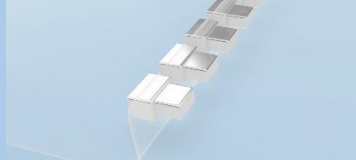
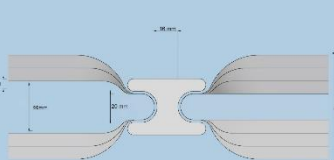
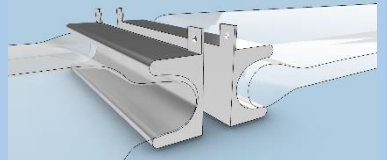
Another solution is creating an indent where load transfer is not crucial (2cm thick areas) and an offset in some areas where contact is essential for load transfer. Then the connection is interrupted. However, this will lead to gaps that might not be aesthetically pleasing. The last option is a combination with implementing embedded titanium insert connections where structural rubs come in contact. This method is the least visible and most safe regarding annealing because it does not include any abrupt extrusion of a thin object causing uneven mass distribution. Holes on both sides can be designed within the 3D printed mould. During postprocessing the titanium inserts can be glued into the wholes with an interlayer of Pom to avoid concentration of stress. Nevertheless, it will be rejected according to the connection criteria to follow.

8.4 Connection system criteria

1. Easy assembly
2. Easy manufacturing
3. High tolerance for variation in 3D orientation (curvature friendly)
4. Accommodating for the varying glass thicknesses around the edges of the tessellation
5. Does not force glass to have sharp edges
6. Does not force glass to change thickness abruptly causing a non-gradual change and uneven distribution of mass.
7. Connection should facilitate load transfer normal to the thickness; which means through plane membrane stresses.
8. Connection can prevent out of plane forces.
9. Demountable and reusable for the same booth

A series of connection types have been developed, compared and assessed according the aforementioned criteria. A summary of the assessment can be found in table 15

Table 15 Connection options assessed based on criteria

Connection design option					
Criteria	Figure 131 Option 1	Figure 132 Option 2	Figure 133 Option 3	Figure 134 Option 4	Figure 135 option 5 (concept)
Easy assembly	Only if profile is split in half	No. Only possible if all are in the same direction	Yes	Only if profile is split in half	Yes, since it is split
Easy manufacturing	Yes	Yes, but requires more postprocessing to glue into glass	Yes, but requires more postprocessing to glue into glass	Yes	Yes
High tolerance for variation in 3D orientation (curvature friendly)	Yes	No	Yes	Yes	Yes
Accommodating for the varying glass thicknesses around the edges of the tessellation	In this option all glass edges will be increased to 8 cm. This will also add mass prior to the edge for gradual inclination	They will only be placed in 6 and 8 cm thick edges, assuming that these are the only significant load bearing structures	They will only be placed in 6 and 8 cm thick edges, assuming that these are the only significant load bearing structures	In this option all glass thicknesses will be reduced at the edge to 2cm to fit into profile	Yes, 8 and 6 thickness will gradually narrow to 4 cm. 2 cm edges will increase to 4 cm
No Sharp glass edges	Yes	Yes	Yes	Yes	Yes
Gradual change in glass thickness and even distribution of glass mass.	Since the interlayer is the tongue, and glass is the groove glass is split into two narrow edges.	Yes	Yes	NO, since the opening of the groove is 2cm, all other thick edges would have to be narrowed to 2cm abruptly.	YES, since the groove opening is the mid-way thickness, gradual increase from 2 to 4cm and gradual decrease from 8 to 4 is possible
Load transfer preserves shell behaviour	Yes	No, point stresses might occur. The connection is interrupted along the edge.	No, point stresses might occur. The connection interrupted along the edge.	Yes	Yes, since it is a continuous line with contact along the normal axis of shell
Connection can prevent out of plane forces.	Yes, since curvature is parabolic not circular	Yes	Yes	Yes, since tongue and groove profile are achieved	Yes, since the tongue entering the groove is greater than the curvature's diameter.
Demountable	Yes	Yes	Yes	Yes	Yes
Additional remarks	Counter acts topology optimisation by adding mass significantly	In the picture the embedded connection is too close. In reality they will be 1m apart	In the picture the embedded connection is too close. In reality they will be 1m apart	Gradual decrease not possible for structural 8cm thick glass	In comparison to option 4 the difference between 8 and 4 is more doable.

The chosen connection design concept is option 5. This was developed into the following detailed connection.

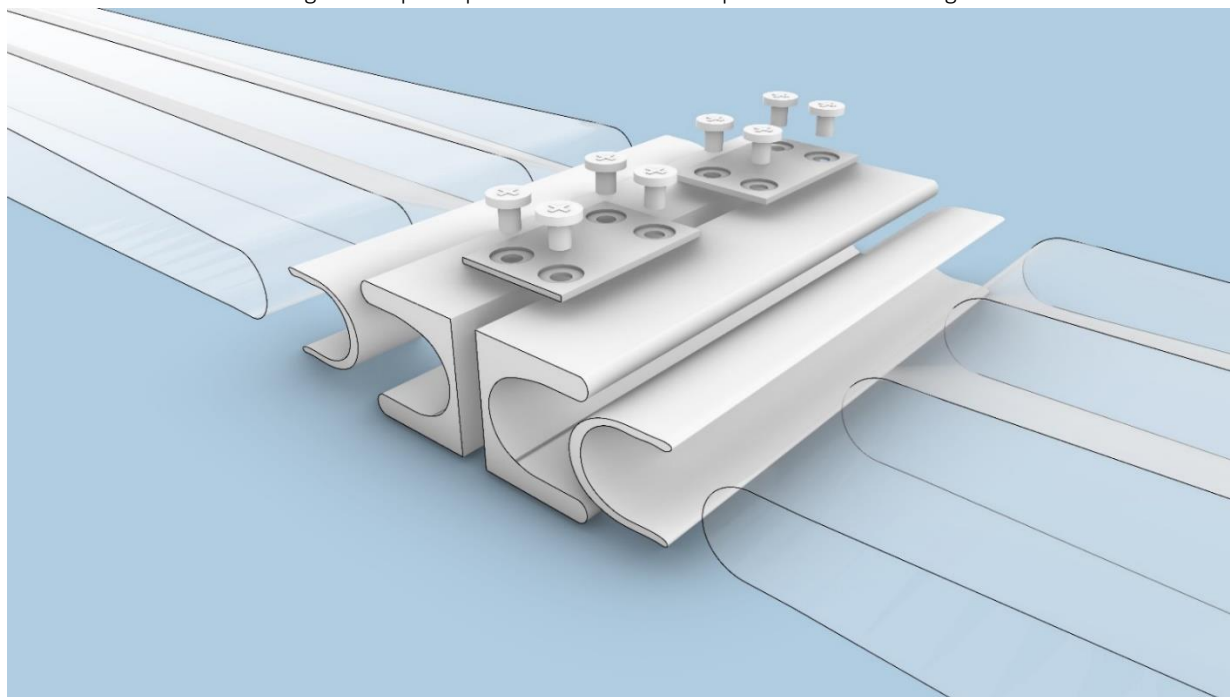


Figure 136 exploded view of connection.

Half the part of the connection will be connected to the glass with structural silicon. Silicon will prevent the sub element of the interlayer from falling of the glass element during assembly with over hanging. By attaching the aluminium profiles onto the glass edges prior to transportation and assembly, the edges will be protected.

This connection design allows for easy assembly as each element has its own sub element connected to it. The bolts are embedded into the connection profile making it less visible.

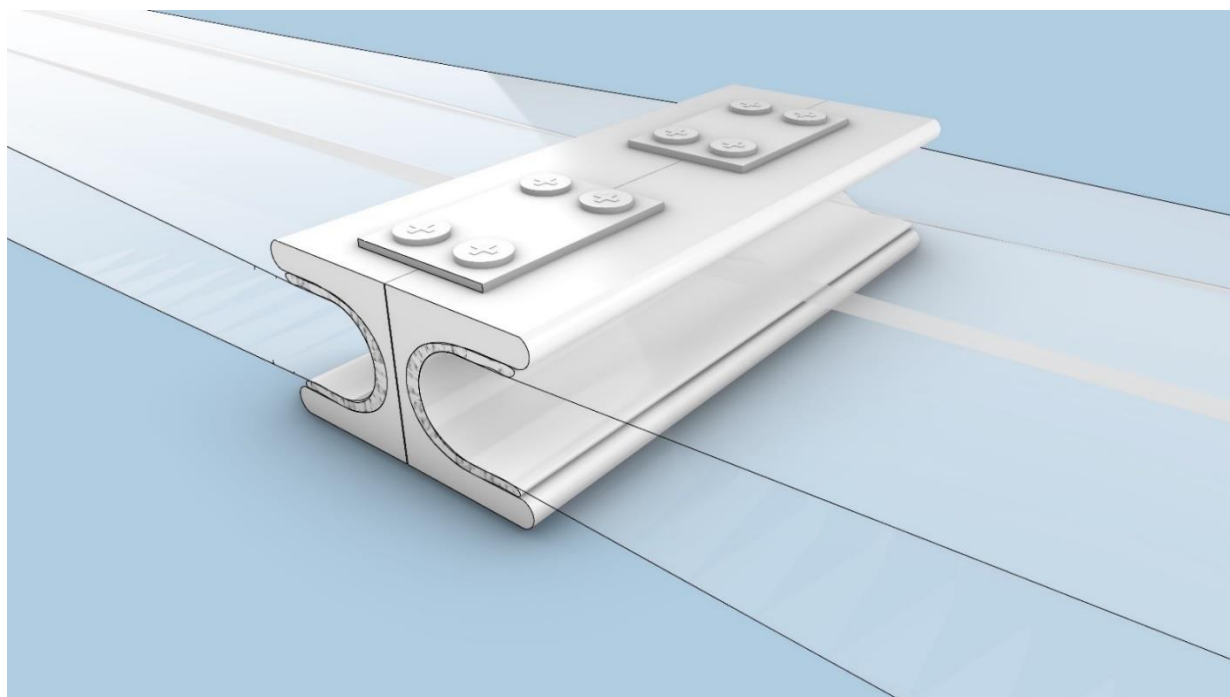


Figure 137 Illustration how two elements will be connected by means of bolts

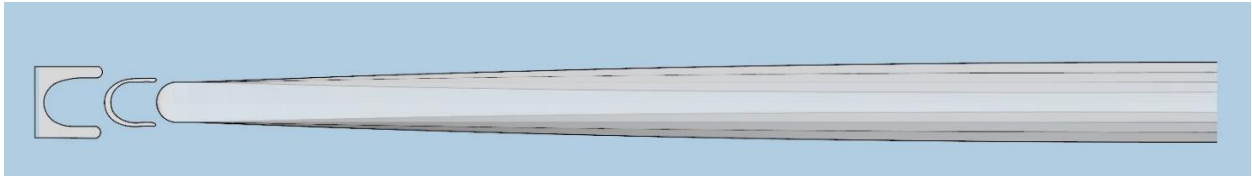


Figure 138 This illustration shows how glass gradually increases or decreases in thickness from 2, 6, 8 cm to 4 cm at the tongue insert of the connection.

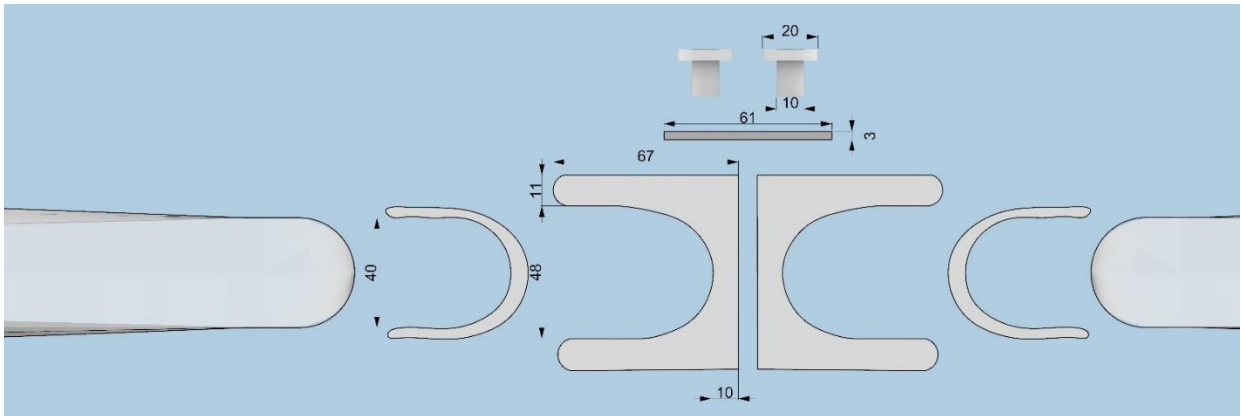


Figure 139 Dimension of connection. Exploded view

8.5 Interlayer Material

To prevent local stress due to glass to glass direct contact an interlayer will be used in between the glass connections. Interlayer materials vary in properties. The main criteria for choosing the right one given that the interlayer will also need to have a fixed tongue shape are the following:

1. Does not creep or deform (shrink or expand)
2. Compressive strength greater than the stress applied by weight of the elements.
3. Less stiff than glass so that it can take the contact force
4. Can be shaped into the connection cross section geometry and 3D curvature of edge.

Based on Dimas (2020) comparison between interlayers in table 15 aluminium is the most suitable interlayer material for this project. It can be manufactured into the desired cross-sectional profile by means of extrusion and into the 3D curvature by means of CNC tube bending. (Private correspondence with Dr. ir. M. Bilow; CESEduPack, 2019)

This will achieve shape of interlayer and connection depicted in figure 140

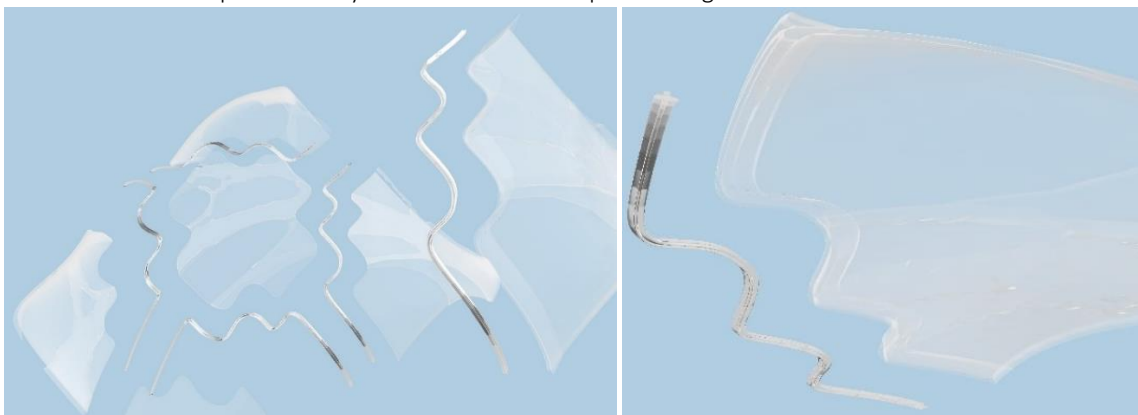


Figure 140 interlayer 3D shape (Illustration based on a different connection profile. However, the same principle of 3D CNC bending applied)

Table 16 summary comparison between interlayer options (Dimas, 2020)

	POLYMERS			ELASTOMERS			METALS			HYBRIDS			
	PU	PVC	VIVAK®	NEOPRENE	SILICONE	TEFLON	COPPER	ALUMINIUM	LEAD	METAL FOAM SANDWICH	LAMINATED PU	SOFT CORE ALUMINIUM	
PRIMARY	COMPRESSIVE STRENGTH $\geq 20\text{MPa}$	YES	YES	YES	YES	YES	YES	YES	YES	YES	YES	YES	
	CREEP RESISTANT	UNKNOWN	NO	UNKNOWN	UNKNOWN	NO	MAYBE	YES	YES	YES	MAYBE	YES	
	SLIGHTLY LESS STIFF THAN GLASS	NO (MUCH LESS)	NO (MUCH LESS)	YES	NO (MUCH LESS)	NO (MUCH LESS)	MAYBE	NO (MORE)	YES	YES	YES	MAYBE	YES
	ABILITY TO BE SHAPED IN FINAL GEOMETRY & THICKNESS	YES INJECTION MOLDING	YES INJECTION MOLDING	YES VACUUM FORMING	NO N/A	YES INJECTION MOLDING	MAYBE/ NO MILLING	YES PRESS FORMING	YES PRESS FORMING	YES PRESS FORMING	MAYBE/ NO *COMBINATION*	MAYBE *COMBINATION*	MAYBE *COMBINATION*
	CIRCULARITY	YES	YES	YES	YES	NO	MAYBE	YES	YES	NO	MAYBE/ NO	MAYBE/ NO	MAYBE/ NO
SECONDARY	OPTICAL QUALITY	TRANSPARENT/ TRANSLUCENT	TRANSPARENT/ TRANSLUCENT	TRANSPARENT/ TRANSLUCENT	OPAQUE WHITE	TRANSLUCENT	TRANSLUCENT	REFLECTIVE RED-BROWN	REFLECTIVE SILVER	OPAQUE ASH GRAY	REFLECTIVE	TRANSLUCENT/ OPAQUE	REFLECTIVE
	THERMAL EXPANSION COEFFICIENT* GLASS: 4-10 MSTRAIN/ °C	90-92	45-180	120-130	110-240	250-300	120-180	15-23	18-26	18-30	UNKNOWN	UNKNOWN	UNKNOWN
	DURABILITY: WATER, FIRE & UV	YES	YES	YES	YES	WATERTIGHT FOR APPROX. 20 YEARS YES YES	YES	YES *DISCOLORATION FROM WATER*	YES	YES	MAYBE *CONSIDER THE EDGES*	YES	YES

*The values for the thermal expansion coefficient have been retrieved from CES EduPack 2019

8.6 Foundation

The foundation for the shell could be a pile or spread footing. Other alternative includes a tension ring or a ring beam. See figure 141. Forces even though compressive all the way through the shell are, at the end of the shell, at the bottom part of the shell's leg forces start pushing outwards forming lateral forces. These lateral forces create stress and places an expansive force that pushes the legs outwards to spread. To prevent this spreading the Pantheon dome increases in thickness as it comes closer to the bottom. To preserve the thinness of the structure modern projects, use a tension tie member. (Rahman, 2016). This project is a temporary structure that needs to be dismantled after the exhibition is over. Plus, the foundation should only be above ground. No permanent drilling can be done on the floor of the exhibition hall. Therefore, either above ground tension cables or a tension ring should be implemented. An example of such a foundation can be seen in figure 143 by the Armadillo Vault. The foundation will be covered by creating a wooden stage platform.

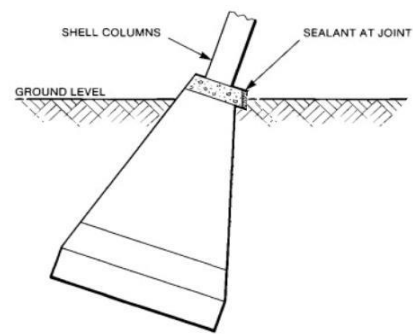


Figure 141 Spread plus pile foundation for shell structure (Rahman, 2016)

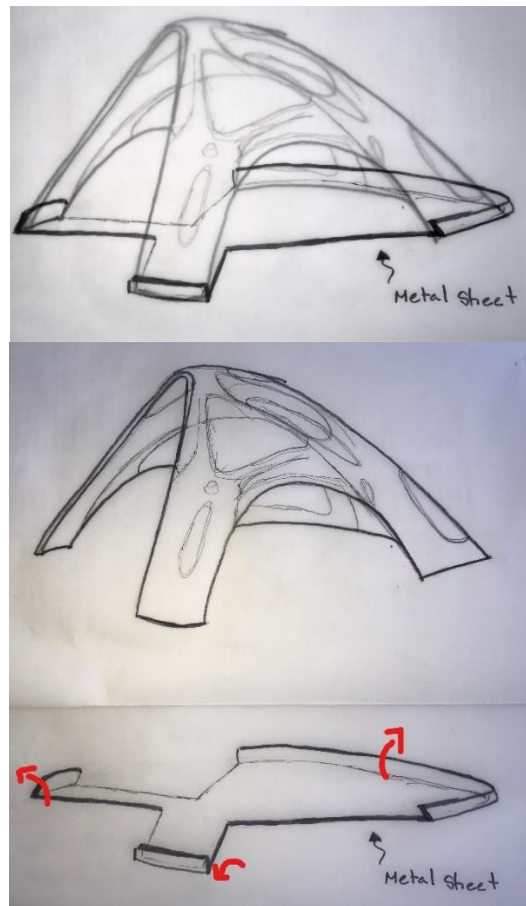


Figure 142 first option for foundation design. The problem with this design is that the bended flat metal sheet can bend in the direction of the red arrows as the out of plane forces push outwardly.



Figure 143 The Armadillo Vault, showing a fixed support and tension-based foundation creating a compression ring effect (Frearson, 2017).



Figure 144 wire rope clipper. rope knotted into a loop (Kimball Midwest, 2018)



Figure 145 turnbuckles. Ropes can be tightened

An offset of the shell will create the foundation a structural steel base plate cap. This will include nodes with holes in them for rope. See figure. The metal wire rope will run through the wholes encircling the shell base. The rope ends will be knotted into a loop using wire clips after being inserted into the eye of a turnbuckle. See figure 145 for turnbuckles and figure 144 for wire rope clips. The foundation will be covered over by means of a 22cm high stage.

Chapter 9: Mould design

Mould size limitations: VX4000 VoxelJet in the US, Germany, UK, China, and India can 3D print Sand Moulds up to 4,000 x 2,000 x 1,000 mm. (Voxeljet, 2018b) The same concept of vertical stacking and multi sand mould bolt and nut connection can be applied to the 1:1 scale mould. By stacking several moulds on top of each other the mould limitation can be multiplied to reach 4m x 2m x height = number of moulds stacked on top of each other.

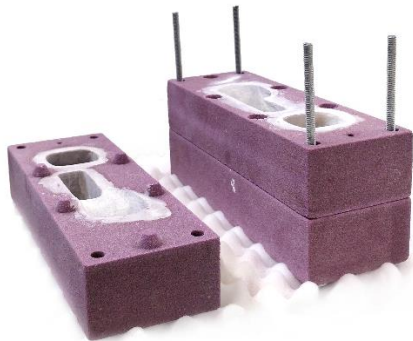


Figure 146 stackable mould. Mould dimension extended by bolt and nut connection (Bhatia, 2019)

Autoclaves are available in larger dimensions than the shell's subdivided elements and therefore they are not a restricting factor. (ASC, n.d.; Akar, n.d) This also means that all 5 pieces can be in the furnace at the same time. Therefore, it was economic to choose for all pieces to have a comparable annealing cycle. Concerning lamination the need for metal moulds in order to withstand the pressure should be further investigated.



Figure 147 ASC Process Systems is the manufacturer of the World's Largest Autoclave System. Inside working diameter: 30ft. (9.26M). Inside working length: 76 ft. (23.5M)

9.1 Mould logistics

The complete mould with connected sub moulds will be lifted, rotated and transported on the factory with an overhead crane. An example of such a crane is the QDX Series Double Girder Overhead Crane (Dongqi Group, 2016). This has the following limitation

- Lifting Capacity: 1-100 ton
- Span: 7.5-31.5 m
- Lifting Height: 6/9/12/18 m

the factory included the note “We can design and manufacture the crane according your requirements and working conditions.” (Dongqi Group, 2016)

Table 17 largest mould dimensions, mass and volume

Front right leg (Requires 5 connected moulds)	Glass piece Volume	Glass Mass	Bounding box dimensions	sand volume in mould	Volume of concrete mould 100mm thick	Mass of concrete based on density of 2400 kg/m ³	Mass of sand based on density of 1631 kg/m ³	Total mass of mould
	0.5648 m ³	1.197 Tonnes	3.6 x 3.1 x 3.1m	34.596 - 0.5648 = circ. 34 m ³	37.888- 0.5648 - 34.596 = circ. 2.7 m ³	6480 kg	55454 kg	6.5 tonnes

9.2 Mould design criteria:

1. Ventilation pipes. These should be placed at a higher lever preceded by a lower level cavity to prevent trapped air.
2. Min 50mm shell surface thickness of the mould
3. Casting pouring opening
4. Minimum thickness of 5mm in any section of the mould
5. Moulds should include interlocking nodes for a precise connection
6. Each sub-element mould is split into connectible moulds of max 4x2x1m. The mould is designed to be printed on its side to avoid steep curvatures and hollow foundation while printing. This way temporary support filling. See figure 150 and 151

- To decrease printing time only ribs will be creating for correct alignment, the rest will be added by hand.

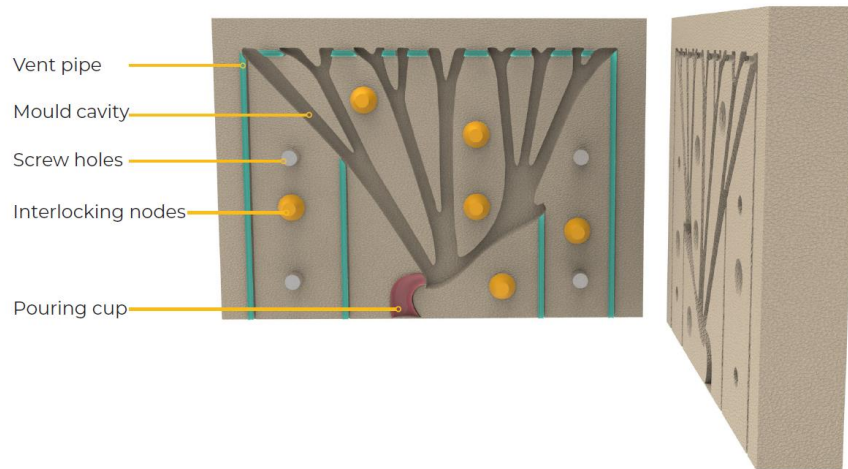


Figure 148 final computer design. Ventilation pipes are present to prevent air from trapping and thus ensure a complete fill on mould when molten glass is poured in. (Bhatia, 2019)

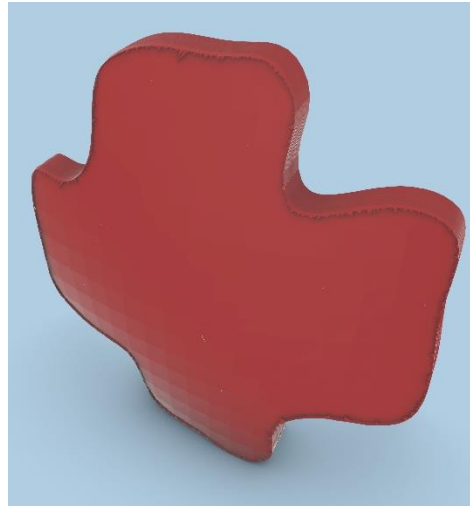
9.3 Mould design and manufacturing procedure

This represent the original design of the glass piece yet to be casted. The following steps apply to any other piece.

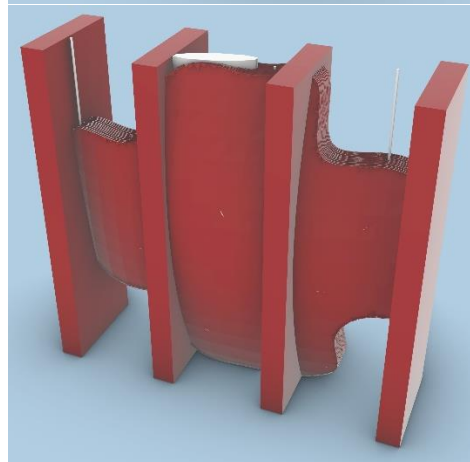
The glass element negative is created by means of an offset. This will create an envelope with a cavity as the base of the mould



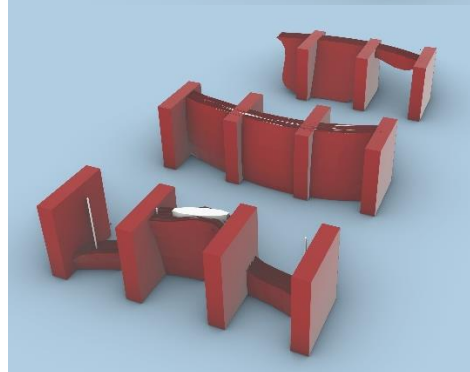
The relief on the exterior of the mould will be smoothed. This ensures manually added sand will slide easily filling all gaps.



Ventilation pipes are added next to the pouring opening and at locations with a higher level preceded by a lower level cavity to prevent trapped air



The mould is divided into pieces with max dimensions of 4x2x1m. whereas the 1-meter limitation is the height.



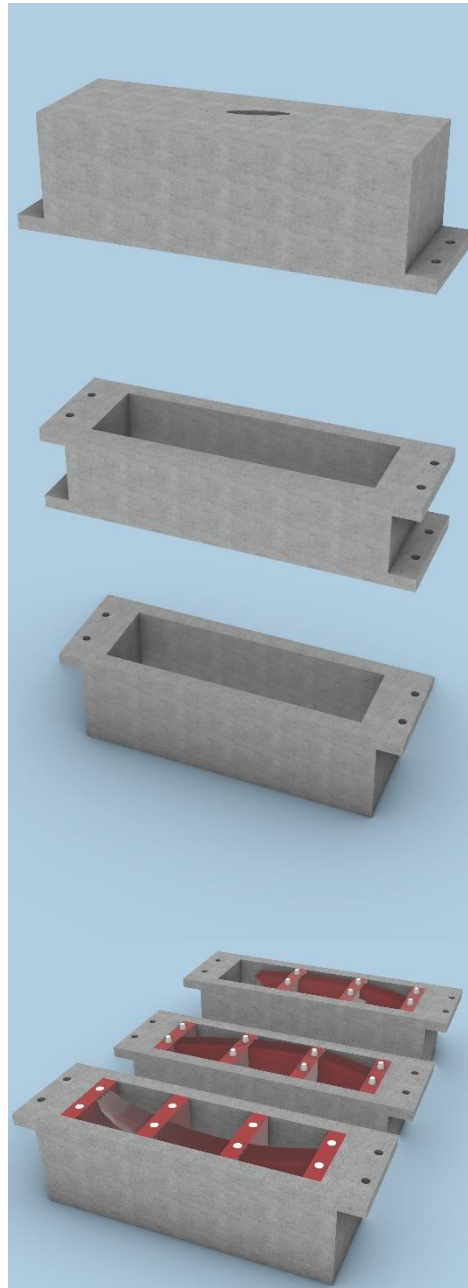
Concluding the computational design of the mould, interlocking nodes are added. These make sure the mould pieces are aligned



The sand mould will be additively manufactured using CHP binder system. Bhatia (2019) concluded that CHP was the most suitable binder for this project. This is because it loses its strength when exposed to high temperatures for a long time. It is also water solubility. These characteristics make it easy to detach the cast glass element from the mould. It makes it ideal for a one time use of mould. Image source VX4000 (VoxelJet, 2018b)



A hard silicon carbide cement tub is prefabricated. This needs to be preheated in furnace to stabilize the expansion and contraction of the cast.



After hand through sand is added to the bottom of the concrete mould, the 3D printed sand mould will be placed according to the appropriate orientation and position.

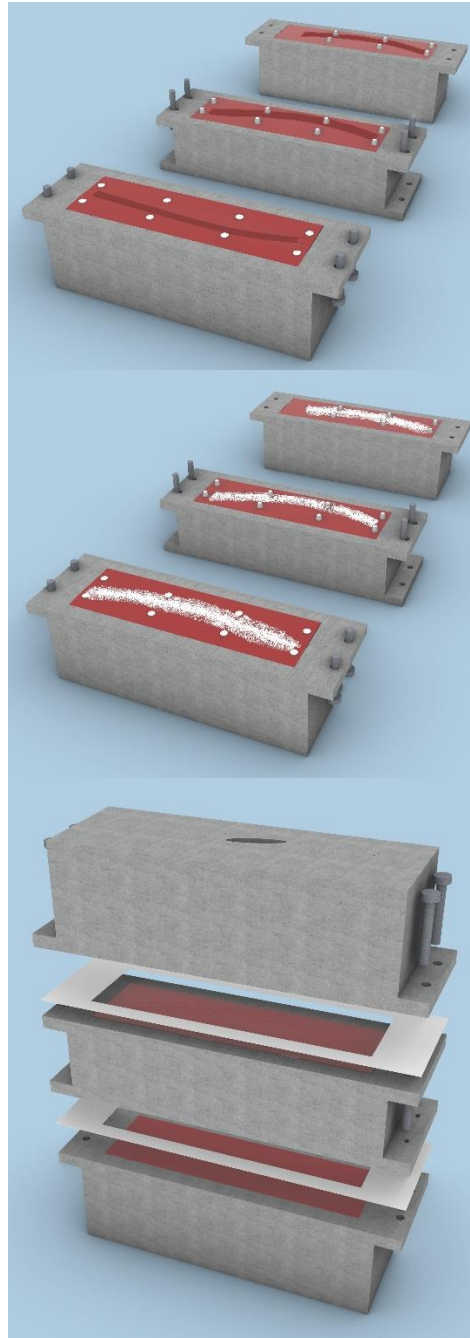
Extra sand will be added to fill in the gaps in the concrete box and add height.

The moulds will be coated with crystal cast for a smooth finish. Crystal cast has been tested to be result with the most polished surface quality by Bhatia (2019).



Figure 149 Applied crystal cast coat for a smooth finish (Bhatia, 2019)

Ceramic fibre will cover the seams between connections. Ceramic fibre can be easily detached from glass in case of a leak



Molten glass will be poured from the cast opening at the highest point of the cavity.

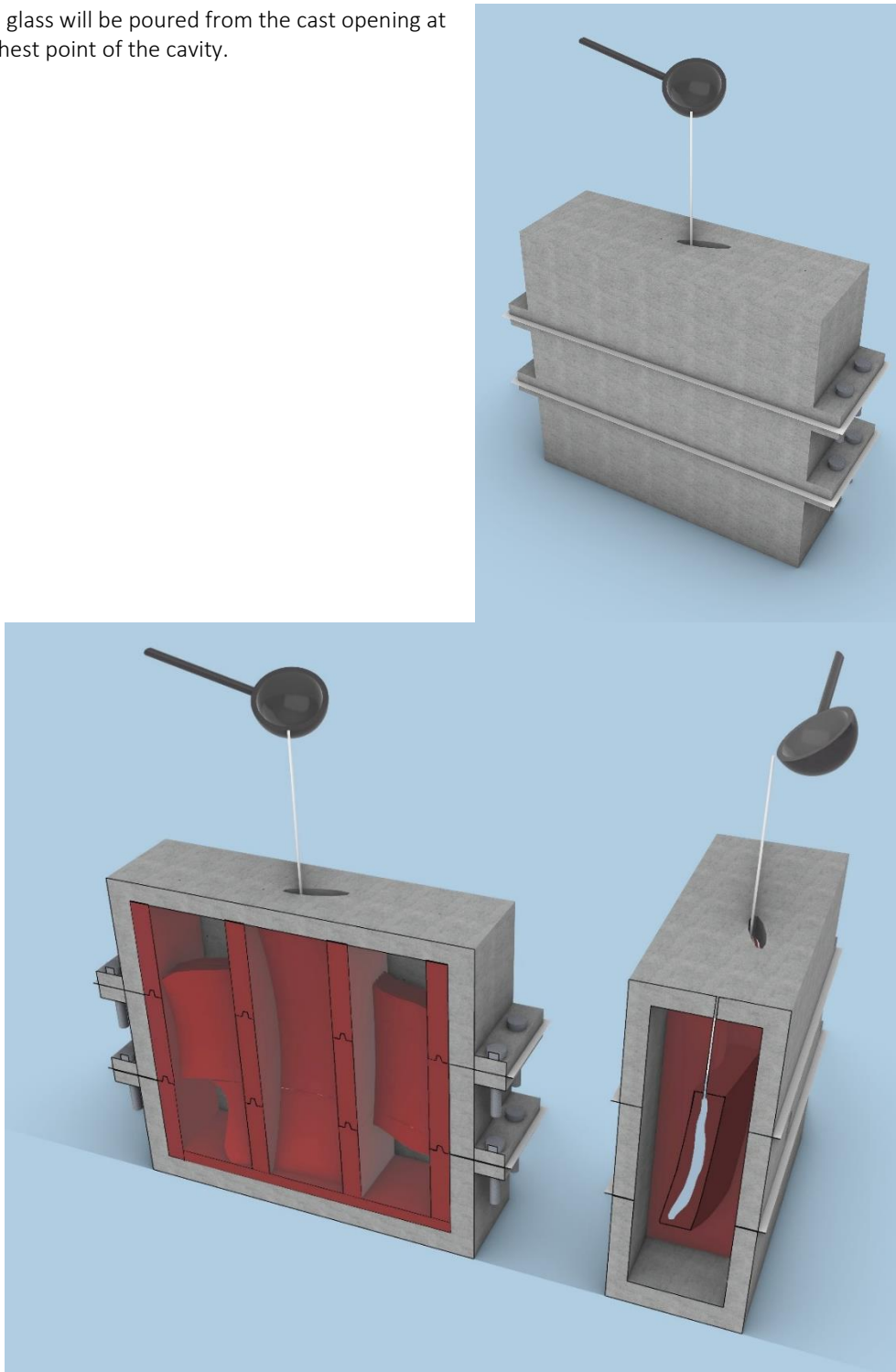


Figure 150 Mould cross section showing only the 3D printed sand, while hiding the added sand by hand

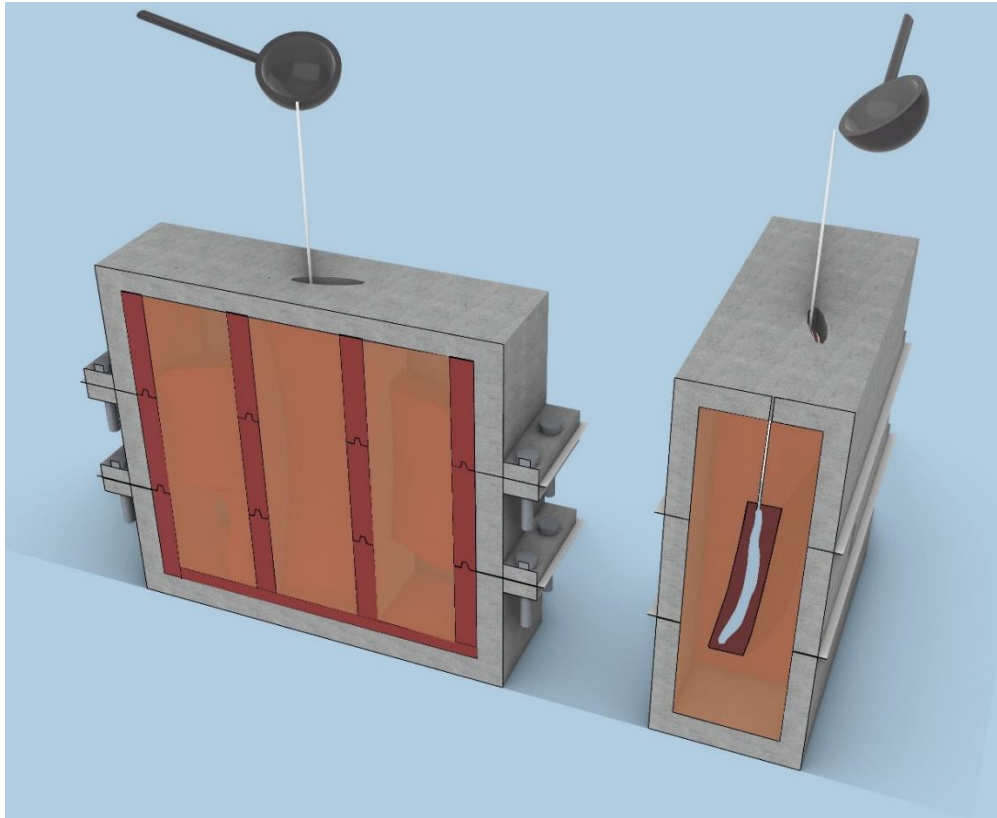


Figure 151 Mould cross section showing 3D printed sand in dark red and hand pressed sand in brown

Chapter 10: Assembly

10.1 Assembly order

10.1.1 Holding method

There are several ways for holding the elements during manoeuvring. Prior to transportation and assembly, the glass elements can be smoothed (postprocessed) at specific locations for suction cups. Another method can be by means of ropes that go around every corner of the element. The third method is by using the connection bolt holes in the aluminium connection after fixing it to the glass element using structural silicon. Temporary eye bolts can be inserted into these holes for transportation. The latter method will be the one illustrated in the assembly order.

10.1.2 Logistics

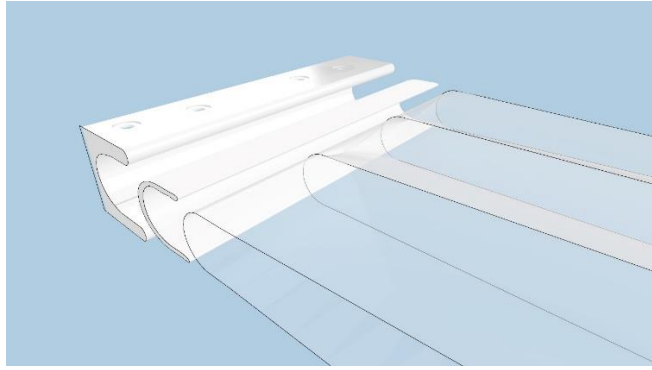
Prior to transportation, permission should be granted to assemble the glass booth before any other booths arrive into the exhibition hall. One crane is enough if a temporary scaffolding is to be used. More than one crane can be used to place the elements at the same time for better stability while lacking a temporary scaffolding. To decrease cost one crane will be used with the aid of scaffolding.

10.1.3 Temporary support

Initially the need for temporary scaffolding was not desired as part of the tessellation criteria. The chosen tessellation does not require scaffolding theoretically if the keystone is placed last. However, because of the connection type, it is better not to place the keystone last. Therefore, temporary support will be needed. Support for the foundation will also be needed to prevent the elements from moving. Sandbags will be placed surrounding the foundation of the elements placed while assembly is under process. This is to prevent the elements from moving before the foundation cords are tensioned. To support the elements from tipping over, vertical tripods with adjustable heights will be used. The top part will be from anti-slip silicon to take the form of the glass element it is supporting and prevent it from slipping. The anti-slip silicone pads come in different forms. Some resist slipping by friction, while others have suction pads.

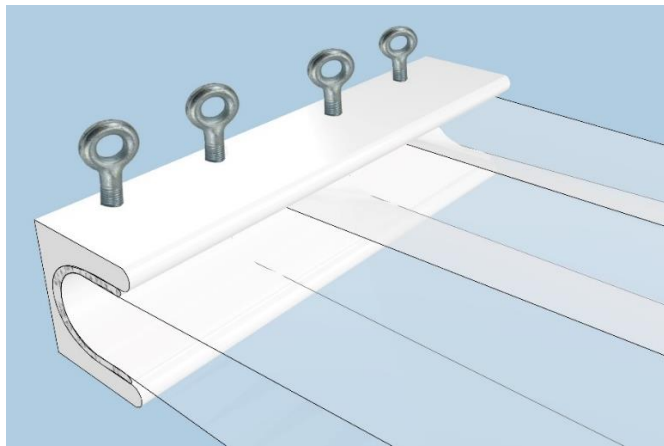
10.1.4 The assembly order procedure

1. Attach every side of the interlayer on the edge of the glass piece it belongs to. Structural silicon is applied to attach the interlayer aluminium connection to glass element.

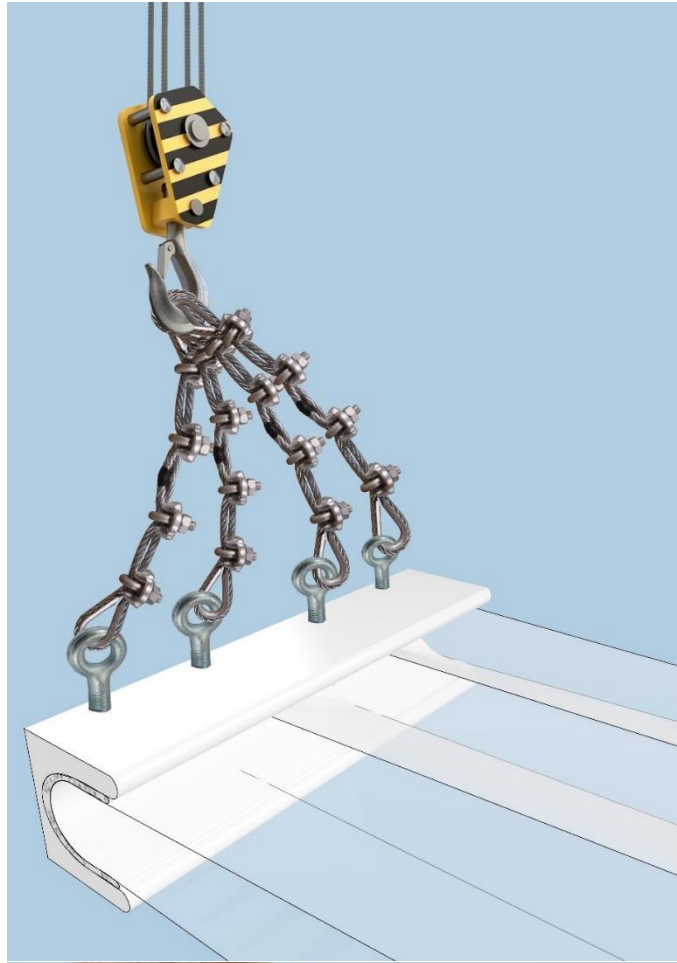


2. Place the cap of the foundation onto the glass foundation edge using structural silicon.

3. Place eye bolts in the holes of the aluminium connections for manoeuvring.



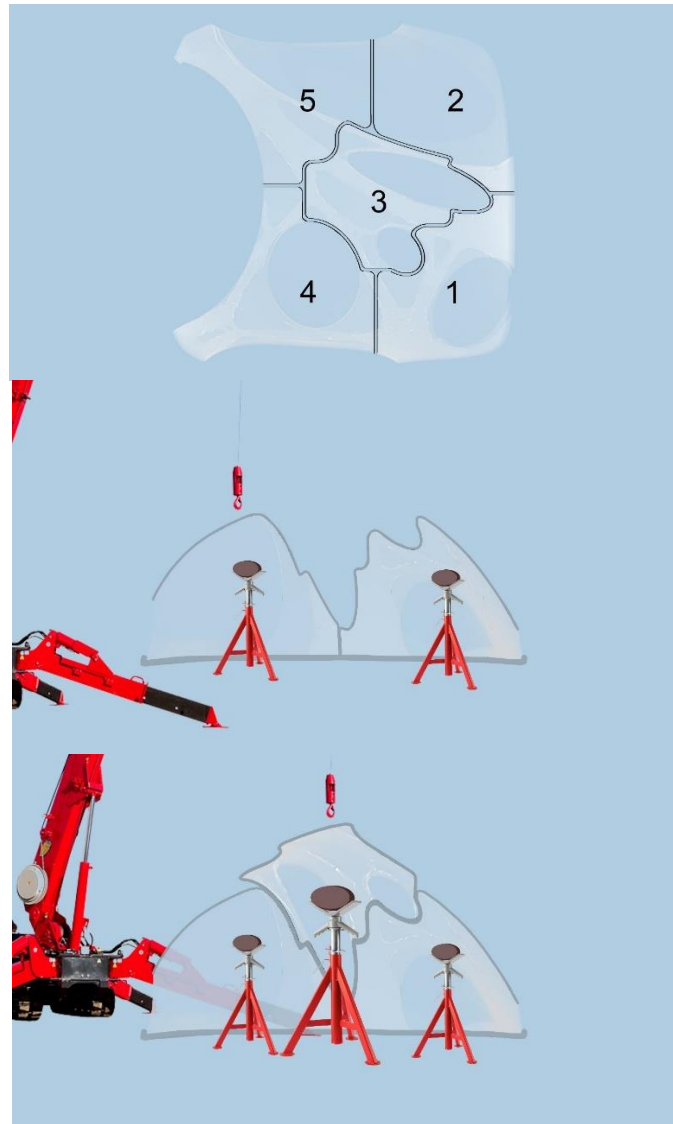
4. Connect the glass element through the eye bolts to the crane's hook via steel cables



5. Place sandbags ready in place to surround the feet of the glass element. The sandbags should weigh more than the glass elements. Sandbags will prevent the elements from sliding off before the entire structure is stable and foundation is tightened.



- Place vertical supports in place to support the elements about to be placed. Then place the elements using a spider crane in the designated location. Start with the most stable glass components. The elements should be placed in the following order from 1 to 5.





7. Connect the foundation cables and but do not fully tighten them.

8. Connect the glass elements by means of bolts and connection plates

9. Fully tension the foundation cables using turnbuckles.



10. Last, the stage is mounted to hide foundation and for people to walk on.



Chapter 11: Redundancy (safety factors) - discussion

Glass breaks without notice, therefore it can be dangerous for people surrounded by it. People might not have time to notice the crack and run away before it fails. Therefore, safety factors should be in place. One of the safety factors might be placing a net in the cast, not as reinforcement, but to hold up any broken pieces from falling. Another way is to design the subdivide the shell in a way where if one element fails all other elements will be able to carry the self-load.

Choosing borosilicate glass makes the structure more firesafe than soda-lime due to its thermal shock resistivity. However, fire safety and other safety factors can be a separate thesis topic on its own.

However, one might rethink these safety factors and wonder, are they really needed in this particular case? Banding and cracks are usually dangerous in float glass, due to their very thin nature. This shell form is designed to have only compression forces. It is over dimensioned for safety, aesthetic and manufacturing factors, but is there anything else needed to be implemented? (source)

Float glass is usually made stronger by full tempering or heat strengthening. These treatments make glass deform less than annealed glass. This procedure mainly rapidly cools down the surface. Cooling the surface faster than the core leads to sucking inwards and closing the cracks on the surface. When cracked, it shatters very small pieces that could be considered safe if it falls on a person. This is because unlike untampered float glass, no large sharp pieces would fall and hurt anyone. This method cannot be used in cast glass that is enveloped through a mould.

Another way float glass is provided with a measure of safety is through lamination, but this lowers the easement and chance of recyclability. due to the PVB interlayer. (Van der Weijst, 2019). By laminating either one layer of glass of multiple layers of glass to each other, broken pieces would stick to the lamination and be prevented from falling. (O'Regan, 2014). Laminating multiple layers of glass to each other increases the thickness and therefore its stiffness. (Van der Weijst, 2019). By laminating an extra layer of glass that has not been included in structural validation calculation one would be introducing a spare layer that could be sacrificed. (Kaiser et al., 2000) The protective sacrificial layer breaks in that case protecting the other structurally needed layers. Standard Lamination autoclaves like that in turkey withhold glass up to 3.210m x 8.000 m in sizes. (Akar, n.d.). The largest lamination autoclave was built by ASC (n.d.) Process Systems manufactures. This one has a Inside working diameter: 30ft. (9.26M) and Inside working length: 76 ft. (23.5M). The standard ones are big enough to fit the pieces of this shell, however the question would be first, would lamination on a double curved surface be successful? Second, would the lamination be strong enough to carry a 1 ton broken piece of cast glass? The latter is proven by lamination projects and tests of float glass that weight no less than the pieces if this shell. For this project lamination would be rather a perplex procedure due to the curvature and relief. The need of metal moulds in order to withstand high pressures should be investigated (Kaiser et al., 2000)

Impact forces are another safety factor that are usually taken into consideration. An impact and vandalism test were set-up by Oikonomopoulou (2019). The mock-up consisted of a 1230 mm wide and 580mm tall wall made of 22 N adhesively bonded blocks. This could be comparable to one of the sub-elements of the shell. The test was conducted using two different methods. First, using a solid concrete brick of 65 x 102.5 x 215 mm in dimensions and 3.4 kg in weight, that was released from two angles, 45 and 90 degrees. See figure 152. Second, using a 4 Kg

sledgehammer reflecting a vandalism act. The results lead to no worries regarding this project. Both concrete blocks suspensions from 45- and 90-degree angles led to no damage on the glass brick while in both cases the concrete specimen lost a chip of its corner. The result of the hammer vandalism test resulted in an internal crack of the targeted brick but no other damage to surrounding bricks. See figure 153.

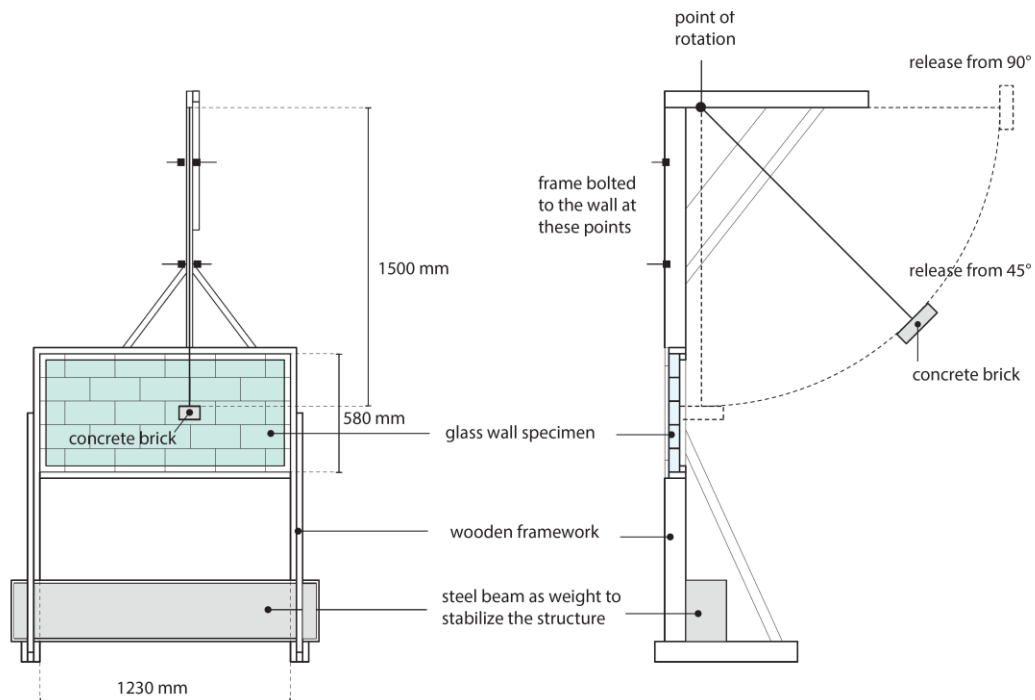


Figure 152 Concrete brick suspension test scheme (Oikonomopoulou, 2019)



Figure 153 Vandalism test result (Oikonomopoulou, 2019)

What if someone leans on it? It is a 4 tonnes sable construction. Does anyone worry about leaning on the pyramids, a truck or a car? No

If engineers are not worried about any of the above-mentioned safety factors if the construction were to be made from non-reinforced concrete, then why should it be an issue with glass? Non-reinforced concrete and glass have similar property strengths and mechanical weaknesses. When in doubt whether a safety measure is necessary or not for a glass structure, Dr.ir Faidra Oikonomopoulou suggests asking oneself whether the same worry would take place if the construction were to be made from non-reinforced concrete. Reason is, even sound-minded engineers can be swayed from reason once the material is transparent. If non-reinforced concrete shells are considered safe enough, so is a glass shell given that it has better mechanical properties and higher strength than non-reinforced concrete which has similar brittleness.

Chapter 12: Conclusion discussion and recommendations

In conclusion, this thesis answered the following main research question and sub-questions.

12.1 Answer to research question

12.1.1 To what extent can topological optimisation and new fabrication methods be employed to create a compressive free-form glass structure?

This thesis has proven that the design, manufacturing and assembly of a large glass structure such as a shell is feasible from an engineering perspective. The knowledge, facilities, ovens, moulds, and other needed equipment and services are already existing. This is especially proven with additive manufactured sand moulds and large autoclaves.

It can be concluded that the topology optimisation is a valuable solution to decreasing the annealing time of cast glass by decreasing the mass/volume. However, this could have been more effective in other in combination with other structures. Combining TO with shell structures was not as effective as it could have been with another structure because shell structures are already optimised structures. Shells are significantly thin in comparison to the span they could stretch over. TO in that case was a tool to see where material is really needed for safety and aesthetic manipulations. Hole could have been made, but the program of requirements by the exhibition booth did not allow for it.

Shell structures were found to be an ideal structural typology that utilizes glass compressive strength. Shells can freely over span a lengthy surface area while maintaining a slender thickness. This has proven to be beneficiary to decreasing annealing time of glass by decreasing the mass/volume. It is therefore recommended to make shells out of cast glass.

In regard to manufacturing methods, additively manufactured sand moulds were ideal for this project. They are recommended to non-identical, unique cast elements. They were also ideal for this project because the components consisted of 3D complex geometries. However, if the project consists of the mass production of a simple geometrical component like a brick, then other permanent moulds like steel moulds would be more suitable.

12.2 Answers to sub-questions (Recommendations included)

12.2.1 What are the main considerations and properties that define the feasibility of large-scale cast glass components?

Glass is a strong in compression but weak in tension. Therefore, the structure glass is made of should be a compression only structure.

Cast glass has a very lengthy annealing time that increases the cost of production significantly. Annealing time can be reduced by choosing a glass composition with a low thermal expansion coefficient and low melting temperature. Therefore, borosilicate glass has been chosen. The other method for reducing the annealing time is by reducing the Mass/Volume ratio, or the thickness of the object. Therefore, Topology optimisation and the characteristics of shell structures aid into solving these challenges.

12.2.2 What design criteria can be drawn from existing glass, topology optimisation and shell projects?

Since glass is a brittle material, tension should be avoided. This leads to a maximum deflection limitation requirement to prevent eccentricity of forces that would lead to moments and tension stresses within the glass shell structure.

The design should follow smart design principles for a strong glass, and faster homogeneous annealing time. To avoid cracks during annealing the design should be reduced in weight or thickness (max 10cm), it should have rounded forms with especially no sharp edges, and it should have an even distribution of mass.

Other criteria are specific to the mould design, transportation limitations, and assembly requirements.

12.2.3 What challenges does glass present to topology optimisation, and which method is the most suitable for glass TO for shell structures?

It can be concluded that the topology optimisation is a valuable solution to decreasing the annealing time of cast glass by decreasing the mass/volume.

This thesis chose for a deflection-driven and compliance based TO approach. Compliance based TO approach is chosen rather than the von-mises criterion because the von-Misses criterion is designed for ductile materials with comparable tensile and compressive strengths.

Compliance based topology optimisation for deflection lead to structurally valid forms. However, it was noticed that the shape is not as neat and ready to go. A considerable amount of post processing is required. Advised is to investigate and compare different TO approaches like the Drucker–Prager in future theses papers. The Drucker-Prager criterion is designed to deal with materials with incomparable tension and compression strengths, like soil. It is a newly developed criterion and on the verge of development.

Advised is to investigate and compare different TO approaches like the Drucker–Prager. Drucker-Prager criterion can be an interesting path to try out if time is at hand because it is designed to deal with materials with both equal or imbalanced behaviour in tension and compression. (Bruggi & Duysinx, 2012) It was developed as a criterion for soil which can only take compression loads. However, this research will not adopt it as the main and first TO approach due to the lack of experience among the experts consulting this paper. If in due time more information and time is at hand, this promising criterion might be experimented with. However, the main approach will remain the compliance-based criterion for the time being.

Recommended is to compare and explore the advantages of different software like AutoDesk 360. This is a design, optimisations and analyses software that integrates several Autodesk software in one. The software uses SIMP approach for TO. Fusion 360 has an elaborate material library, that allows one to add a customized new material to. Fast computing is made possible via their cloud servers' facility. (Damen, 2019) The latest Autodesk Forum discussion from 2018 said that the Drucker-Prager yield criterion is only supported in the Nonlinear Static analysis materials.

TO of glass raises a new challenge because the common algorithms were designed for isotropic, homogeneous, and ductile materials. Glass is a homogeneous² isotropic material, but it is not ductile. (Ashby et al., 2019, p. 60) A new algorithm is needed to meet the need for topologically optimising brittle material. Nevertheless, this development goes beyond the scope of this research. If this thesis were to focus on developing a new algorithm that solves TO challenges and FE glass related limitations, it would be wise to delve into each current algorithm. However, in this research, commercial software will be used with existing algorithms. Therefore, only a brief comparison between the most common algorithmic methodologies within the available commercial software will be discussed. This will guide the choice of software for this research. A PhD or a separate MSc thesis can be recommended to develop focus on developing a new algorithm that might solve some of the missing features present with the current ones. (Jackson Jewett, through personal correspondence)

At the end this project reached a 43% mass reduction. Despite the 43% mass reduction the shell can be further optimised. Due to time limitation TO was run only twice and FEA was conducted in on three versions of the shell. From the FEA results it can be concluded that a shell structure is an optimised structure to begin with, therefore further reduction in thickness is possible. Since it's a compression only structure and glass is strong under

² A Homogeneous material is a mixture with one "pure" material with uniform composition throughout the sample. The material cannot be split into different materials by mechanical force.

compression, thickness is not needed as in other structural typologies. Nevertheless, the variation in thickness has a good effect on aesthetics, and safety factors. Even if the thickness can be reduced below 25 mm, cast glass (as a production method) would still be needed to achieve the 3D geometry and variation in thickness. Here it can be recommended to investigate how thin can one make the shell?

12.2.4 What are the most suitable manufacturing, transportation, and assembly methods for a large cast glass free form structure?

Cast glass

Until now, there have been 4 primary discovered manufacturing techniques for glass. Float glass is limited with a maximum thickness of 25mm. Extruded and float glass cannot form complex 3D geometries while 3D printed glass is not structurally validated. Cast glass can offer a solution to all of these limitations.

Additively manufactured sand moulds

With different types of moulds on the market ranging from permeant to disposable ones, fixed and adjustable, the additively manufactured sand moulds by means of binder jetting are found to be the most suitable. This is due to:

- High Precision ± 0.1 mm
- Affordable cost
- Resilient material against high temperatures for a long time period.
- No support needed or dissolvable intermediate
- Smooth finish or treatable surface
- Facilitates the potential of complex geometries
- Reusability potential of excess sand during printing and destroyed used moulds
- In the CHP binder system is in used, then it can be dissolved. In addition to the crystal cast mould surface coating, using a water-soluble binder makes the cast glass object easy to detach from the mould.
- Once the object is hardened the mould can be simply immersed in water. The cleaned again sand can be reused for printing another mould.
- The moulds can be closed from all directions ensuring homogeneous cooling

Subdivision for transportation

Due to transportation and casting size limitations the structure had to be split into components. The subdivision had to adhere to the following criteria.

1. No sharp corners allowed.
2. No scaffolding needed (preferably)
3. Consists of max 6 pieces so that the assembly procedure can be done fast and does not distort other booths in the surrounding.
4. Fits in trucks. (truck dimension 12 x 4 x 2.5 m Diagonally it is 4.74m.)
5. Can be lifted by interior spider crane. (limit 3T x 3.4m). See figure 102. (Unicranes, 2020)
6. All elements have a comparable annealing cycle.
7. Can be manufactured within mould size (4 x 2 x 1 m) and mould design criteria
8. Tessellation does not interfere with force flow lines.

Aluminium connections with structural silicon, bolts and cable tensioned foundation.

The chosen connection was selected based on the following criteria

1. Easy assembly
2. Easy manufacturing
3. High tolerance for variation in 3D orientation (curvature friendly)

4. Accommodating for the varying glass thicknesses around the edges of the tessellation
5. Does not force glass to have sharp edges
6. Does not force glass to change thickness abruptly causing a non-gradual change and uneven distribution of mass.
7. Connection should facilitate load transfer normal to the thickness; which means through plane membrane stresses.
8. Connection can prevent out of plane forces.
9. Demountable and reusable for the same booth

Assembly

Spider cranes, trucks and overhead cranes capacity were taken into consideration and will be used for transportation and assembly.



Figure 154 Render of glass shell in the Material district exhibition booth (background image source: MaterialDistrict., 2020)

12.3 Further applications

1. This thesis has proven that large cast glass elements can be produced by reducing the annealing time using topology optimisation, thin shell structures (compression-only structures) and 3D printed moulds. This means that any large element can be produced using cast glass given the considerations accommodated for in this thesis.
2. Glass shell structures and domes are appealing as a restaurant's roof or a vacation glass room. However, in case of application in a desert high temperature should be taken into account. In case of a cold location like Iceland, thermal stress should be accounted for. When building outdoors asymmetric horizontal loads should be calculated.
3. Shell structures and topology optimisations are great tools for other architectural applications with other brittle materials like earthy architecture using sand, and clay.
4. The same tools and skillset can be used to design cast glass, columns, slabs, telescope mirrors, arch bridges, walls, or just art. The same technology can be applied to design and build cast glass arch bridges. Hybrid designs can be made by creating "windows" or other separate elements out of float glass and connecting them to cast glass elements during assembly.

With this vision in mind this thesis' finding open the door to many other applications!



Figure 155 Further application. Glass shells are appealing in areas where rain protection is needed but sunlight is desired like in restaurants and bars. This is a proposal for the Bouwpub Faculty bar. (background image source: Braaksma & Roos, n.d.)



Figure 156 Cast glass has the potential of forming arch bridges (background image source: Doyle, 2018)



Figure 157 A glass shell under a waterfall. Cast glass has the potential to be used in vacation destinations. (background image source Andres, 2016)

Reflection

In beginning the topic has been chosen out of passion, interest and goals to learn more in this field. By P2 it was evident that the plan was over ambitious and unrealistic to achieve within the limited time the thesis needs to be completed within. Therefore, the goals had to be adjusted to a procedure excluding any comparisons between different designs or TO software. Throughout the process, I was confronted with a lot of challenges. One would think that the most difficult thing in this thesis is engineering glass and structurally validating a shell structure. Engineering glass is indeed challenging, but to my surprise the number one challenge was meshing and sculpting the model in a controllable way. The mesh models were, more often than desired, not able to be read, mesh, or process by Ansys for analyses or topology optimisation. So, I have not been able to structurally verify a lot of different models. I ended up learning more about the strengths of software what about structural mechanics after P2. I learned a bit of linear algebra that explained how computational geometry is represented and modelled. This explained why a certain geometry might look ok for the naked eye but is algorithmically ill defined as a computational geometry. After understating a bit of the logic behind computational geometries, I was able to overcome most glitches that were occurring throughout the procedure. I'm happy to say that by now I am more than ever confident with my skills in grasshopper Maya Auto desk and Rhino. Other tools like mesh mixer and Lumion where interesting to experiment with and useful for rendering and sculpting. For example, I learned that rhino is powerful in handling NURBS but is not very handy when working with complex meshes. Maya is better equipped at editing meshes. This was important to have an accurately meshed shell, with a uniform thickness, subdivided into layers for TO, and with a clean trim at the bottom for the foundations. These were design informatics challenges, that caused a long delay in my progress, but I had happily overcome them with a wide set of computational skills that I would never have had the chance to practice without encountering these challenges.

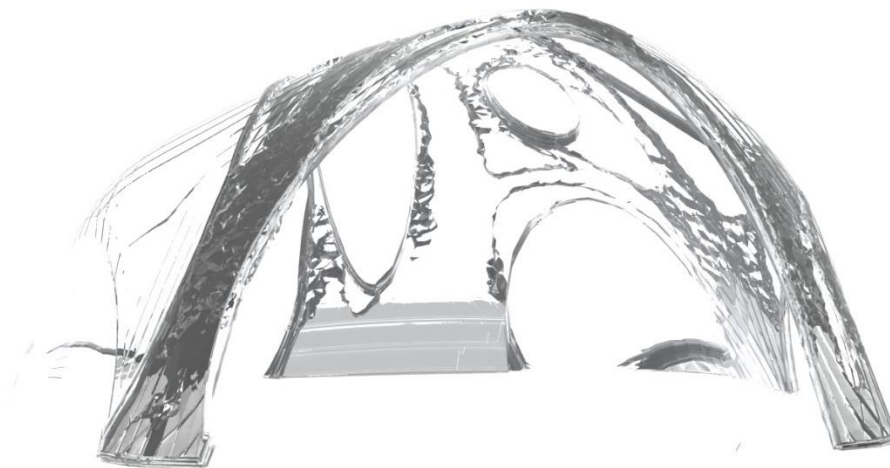
As usual, software are tools, they are not our intellect, cognitive power, or creative mind. I learned that if after a reasonable amount of computational trials my mesh was not processed enough to be usable, I should start thinking of primitive alternative ways for TO. Cutting holes in hanging waxed cloth was one idea. Another idea was using actual clay. I did not need to resolve to these methods eventually, but I was happy to realize that I can always use common sense to achieve my goal regardless of the available means. Perhaps using primitive tools would not lead to legal structural verification of the model, but it would surely proof that I understand the engineering principles behind the design. This applies to interpreting the finite element analyses results. The software provides numbers and a colour scheme that looks nice, but what does it really mean? I wanted to delve into the requirements and be able to discern whether a certain amount of deflection is acceptable or not. I wanted to be able to execute judgment regarding the level of stress in this design. Can these stresses be handled by this material given the dimensions? Is the model safe or over dimensioned? I have enjoyed further developing my skill of analyses assessment. The results generated by the software mean nothing without the keen knowledge and experience of an engineer. Hopefully my future career would give me the opportunity to further develop my experience and skill. I have way much more to learn, but I'm happy with where I am now at for the time being.

One challenge that I have faced is creating one model that is ideal for all purposes. I have realized that a model for rendering might need to be slightly different than the one for FEA. The reason is that the model for rendering and later on additive manufacturing of mould can be more complex in shape and organic than that for FEA. FEA is sensitive to any nonlinearity, non-manifold, overlap, or misconnection that the model should be simplified enough to ensure a smooth FEA run. This means again that an engineer's eye is needed to judge whether an alteration in the design would be within the margins of the structurally validated simplified model or not. Therefore, the procedure was as follows. The shell was topologically optimised. This result was too complicated to run through FEA. Therefore, a simplified shell with ecliptic wholes was created under inspiration from the TO result of the first shell. This simplified shell with TO ecliptic wholes was topologically optimised again. The result inspired me to know where the thickest ribs should be located. The final result was manually drawn indicating the shape, and with colour codes the variation in thicknesses. This means that I needed to be modest and realize that for a MSc thesis I do not have the time to structurally verify the final model using FEA. However, this meant that I needed to be creative and rely on my understanding of deflections, and stresses shown in previous simplified versions of the model.

I have also experienced the vitality of organization, file naming, time management, multi-scenario-based procedure flowcharts, backup, and general planning. At times creating a flowchart with all the probable solutions was handy to make sure that all possibilities have been tested. Going back the literature review and design criteria helped me stay in check with the requirements. Dealing with frustration of lost VPN connection midway through a 16-hour long iteration simulation is just part of the job. Take a deep breath then restart the optimisation, meshing or analyses procedure anew.

At times I got stuck for days in something, but as soon as I reached out to an expert in the field, I received a solution within minutes. Sometimes, emailing, posting a question on an online forum, or just paying someone an office visit was all the shortcut to the solution I needed. I have experienced the truth of the following words: "Knock and you will be answered, ask and you will be given." It made me realize that complex projects are possible at engineering firms because they work in teams. There is always someone who can help, inspire, or provide a new perspective. Now it is the time for me to prove that I am adequate to work independently, and I am confident that I can. However, I look forward to work in a team where everyone helps each other, brainstorm together at times, share knowledge and experience. Teamwork is also healthy for moral support and encouragement that we have surely missed during the corona virus social distancing experience. One should not be too proud to ask for help or think that he/she can do everything on his/her own. After graduating I will be an adequate, and confident engineer, but I do not want to be a presumptuous, haughty, or overconfident one that thinks to know everything. Nobody knows everything, and we can always learn something new. Modesty is a beautiful quality to have in balance with confidence.

I hereby would like to seize the opportunity to thank my wonderful supervisors, for their insightful and knowledgeable feedback, constructive criticism and support. Faidra Oikonomopoulou's knowledge and experience with glass was very informative inspiring and useful. She did not hesitate to connect us with her network of expertise around the world for extra consultation. Marcel Bilow's focus on adaptability regarding the procedure was liberating. His focus on practical production and assembly will definitely be of practical use in the upcoming stages. Thanks to Paul de Ruiter who, even though is not my supervisor, was willing to help me with Autodesk Maya. F. Oikonomopoulou and M. Bilow, are very encouraging and supportive morally as well, which was encouraging for me to keep up the pace even when facing challenges. Both Faidra and Marcel really want us to succeed and learn the most from our experience and this is evident in their word and action.



Appendices

Appendix A: Structural and mechanical explanations

Density

The microstructure insensitive property of density depends of packing, weight of atoms, and type of molecular bonding. (Ashby, 2019, pp. 48)

Density³: 2.2e3 - 2.25e3 kg/m³ (Granta Design Limited, 2019)

Stress, Strain and Elastic Modulus

Strain is a consequence of stress. When force is applied to a body of material, the material is stressed. Strain is the deformation responses of the material caused by stress. The elastic modulus of a material represents its measure of resilience against deformation when stressed. (Ashby, 2019, pp. 48)

Stress σ :

$$\sigma = \frac{F}{A}$$

; whereas F is force and A is the cross-sectional area the force is applied to. This could be compressive stress (negative sign), or tensile stress (positive sign). Or in another form when experience in membrane or plane, then it is shear stress τ (more about that later in the section about shells):

$$\tau = \frac{F_s}{A}$$

Strain ϵ

$$\epsilon = \frac{\delta L}{L_o}$$

; Whereas L_o is the original length, L is the length after deformation, and δL is the difference between L and L_o . See illustration below

³ All values in this section will be based on 7740 Borosilicate glass:

Al₂O₃ (alumina) 2 %

B₂O₃ (boric oxide) 13 %

Na₂O (sodium oxide) 4 %

SiO₂ (silica) 81 %

The characteristics of this glass type are discussed in the section handling glass compositions.

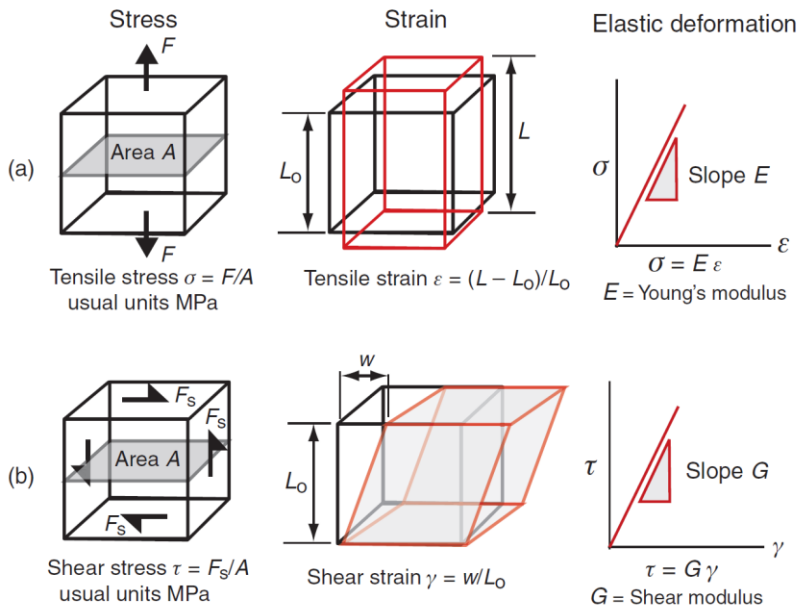


Figure 158 Strain (deformation) as a result of Stress due to a) Tensile force b) Shear stress (Ashby, 2019, pp. 50)

Borosilicate glass 7740 Shear modulus: 25.6 - 26.9 GPa (Granta Design Limited, 2019)

Compressive strength vs Tensile strength

Glass has a high compressive strength that exceeds 1000MPa. As shown in the graph this is even higher than many types of steel (Pye et al., 2005). The limitation in glass results from its low tensile strength. Glass might break due to local tensile stresses before it could ever reach its allowable compressive level. Hence the real allowable compressive limit cannot be verified through tests. (Emami, 2013)

Compressive Strength: 800- 1000 MPa (Saint Gobain, 2018)

Borosilicate glass Tensile Strength: 25.2 – 27.8 MPa (Granta Design Limited, 2019)

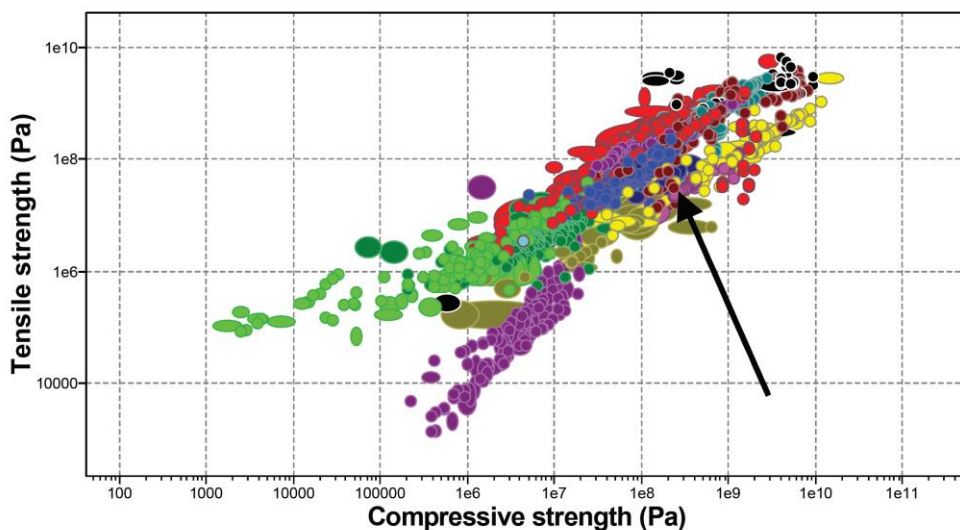


Figure 159 Compressive vs Tensile strength. Glass position in comparison to other materials. (Granta Design Limited, 2019)

Yield Strength

Yield can mean two things. One is to bear fruit or give product as a result. The other meaning is to give in or surrender. Yield strength is the stress which beyond a material becomes plastic. In metals plasticity is a beneficial attribute and is linked to being ductile. This makes them capable of being shaped and absorb energy at impact.

However, when the material starts acting with plasticity unwillingly the structure becomes unreliable and does not serve its purpose. (Ashby et al., 2019, pp. 134)

Borosilicate glass Yield strength (elastic limit): 25.2 - 27.8 MPa (Granta Design Limited, 2019)

Stiffness and elasticity

Elasticity allows the material to deform under stress but go back to its original shape when the load is no longer present. Stiffness is the resistance to elastic deformations when stressed. Some have assumed that stiffness requirements would be achieved anyway when strength-limited analysis and compliance is achieved. This is an assumption where some structures and materials dominant mechanical requirement is strength. However, this is proved to be wrong for some structures. One example is the Millenium bridge spanning the river Thames. Its strength adhered to requirements but started wobbling once pedestrians placed foot onto it because it was not stiff enough. (Ashby et al., 2019, pp. 98)

Borosilicate glass⁴ Elasticity (Young's modulus): 61.4 - 64.5 GPa (Granta Design Limited, 2019)

Strength

Strength of a material is its resistance to permanent deformation or complete failure. (Ashby, 2019, pp.48)

Strength vs toughness

According to Ashby et al. (2019, pp.204) strength is a material's resistance to plastic flow, while toughness is a materials resistance to propagate a crack. If the material is not tough, it means that it lacks plasticity and is brittle. A brittle material fractures at a stress level below its yield strength if a crack is present due to propagation. Fracture toughness is a property separate from yield strength. Understanding this is important because mostly designs are based on yield strength charts. For a brittle material like glass failure could "unexpectedly" occur even when the load is lower than what the material's strength could withstand. (Emami, 2013). In other words, a brittle material would always break before it could ever deform permanently. One should assume that at least small cracks exist and consider a fail-safe design. (pp.263) Another consideration is to design with a shape that allows the object to fulfil its function without fracturing. (pp.259)

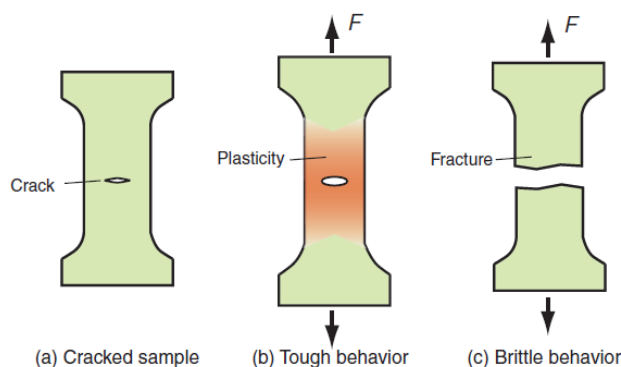


Figure 160 Tough and Brittle behaviour. in the crack in the material is shown. In b the material is tough and its plasticity prevents the crack from immediately propagating when loaded. c depicts a brittle material like glass where a crack propagates at a stress lower than its yield strength (Ashby et al., 2019, fig 8.1 p. 205)

Fracture toughness mechanics

Fracture Toughness is measured as K_{Ic} . This measure indicates the material's resistance to cracking and fracture. Fracture toughness K_{Ic} is the value at which the stress intensity surpasses the critical value. Glass is brittle and has a low K_{Ic} . (Emami, 2013; Ashby, 2019)

⁴ Based on CES EduPack 2019: Borosilicate - 7740 Compositional summary: 81% SiO₂/2% Al₂O₃/13% B₂O₃/4% Na₂O

Brittle fracture is typical behaviour of glass. Glass cracks at about $E/15$. This is the strength required to break apart atomic bonds as illustrated in Figure 12. In contrast to plastic materials, there is no plasticity at the crack tip. If the material is ductile a plastic zone forms at the crack tip. Glass however has a very high yield strength. This prevents glass to release stress through plastic flow at the tip. (Ashby et al., 2019) Nevertheless, fracture cannot be measured and therefore we can only design based on tension stress and deflection. However, it is important to understand fracture to understand glass behavior and then understand why fracture is not used as a design criterion.

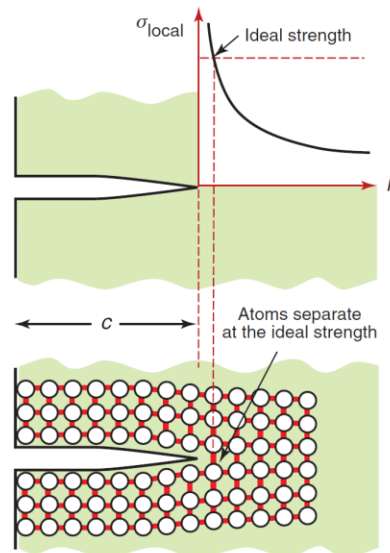


Figure 161 Cleavage fracture. Once the ideal strength is reached inter-atomic bonds are broken and molecules are pulled apart (Ashby et al., 2019)

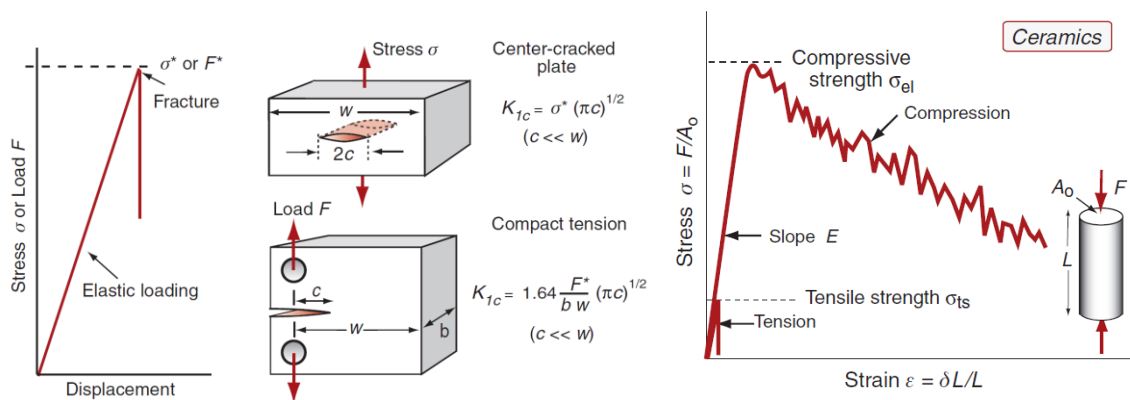


Figure 162 Fracture toughness, K_{Ic} , measurement. Only two tests are shown here as an example. (Ashby et al., 2019) Other tests and scenarios are described in chapter 8 and 10 of the referenced book, but any further explanation goes beyond the scope of this research. The point of this graph is to show how fracture toughness leads to a sudden crack in the material lacking plasticity. The failure happens abruptly without any warning. In comparison a tough material would deform gradually and fail by means of the yield stress before it fractures. Stress-strain curve for brittle material. Right: in compression. Left tension test

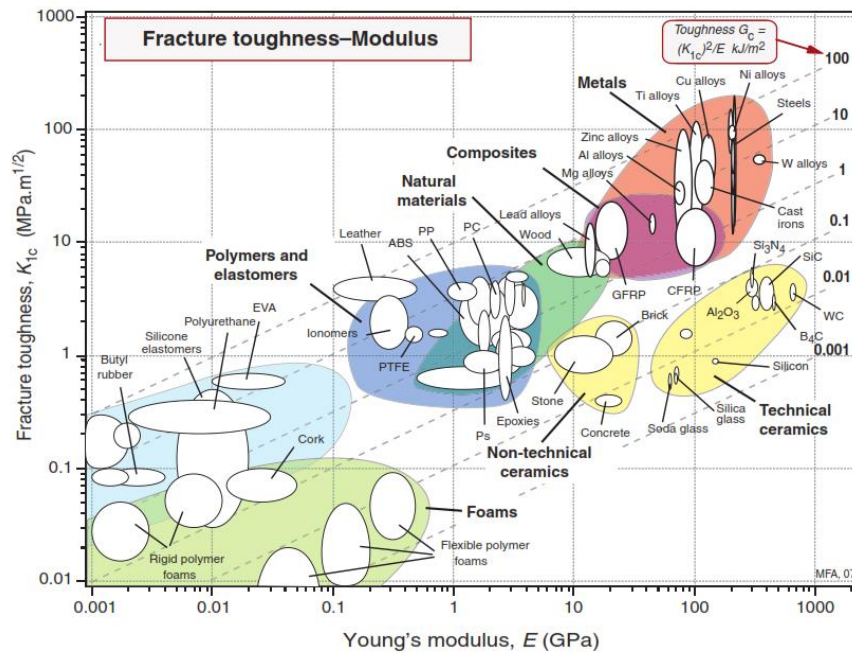


Figure 163 Fracture toughness K_{1c} against Young's Modulus E . G_c , the toughness is shown as contours. Soda lime and silica glass are placed at the lower right corner of the graph in the Technical ceramics group (Ashby et al., 2019)

According to CES EduPack borosilicate glass fracture tensile strength ranges between 22-32 MPa and its fracture compressive strength ranges between 260-350 MPa (Granta Design Limited, 2019). These values drastically differ from one source of literature or experiment test to the other (Oikonomopoulou, 2019)

The fracture toughness–Young's modulus chart

Figure 20 plots the fracture toughness K_{1c} against modulus E with Toughness contours lines, G_c . The lower part of the chart plots brittle materials with a low fracture toughness K . These materials maintain these elastic behaviours until fractured. Just as in figure 19 above. With the Toughness logarithmic scale, glass and ceramics have a lower G_c than polymers.

Borosilicate glass⁵ Elasticity (Young's modulus): 61.4 - 64.5 GPa (Granta Design Limited, 2019)

Borosilicate glass Fracture Toughness: 0.6 - 0.62 MPa.m^{1/2}

Borosilicate glass Toughness (G) 5.68 - 6.16 J/m²

⁵ Based on CES EduPack 2019: Borosilicate - 7740 Compositional summary: 81% SiO₂/2% Al₂O₃/13% B₂O₃/4% Na₂O

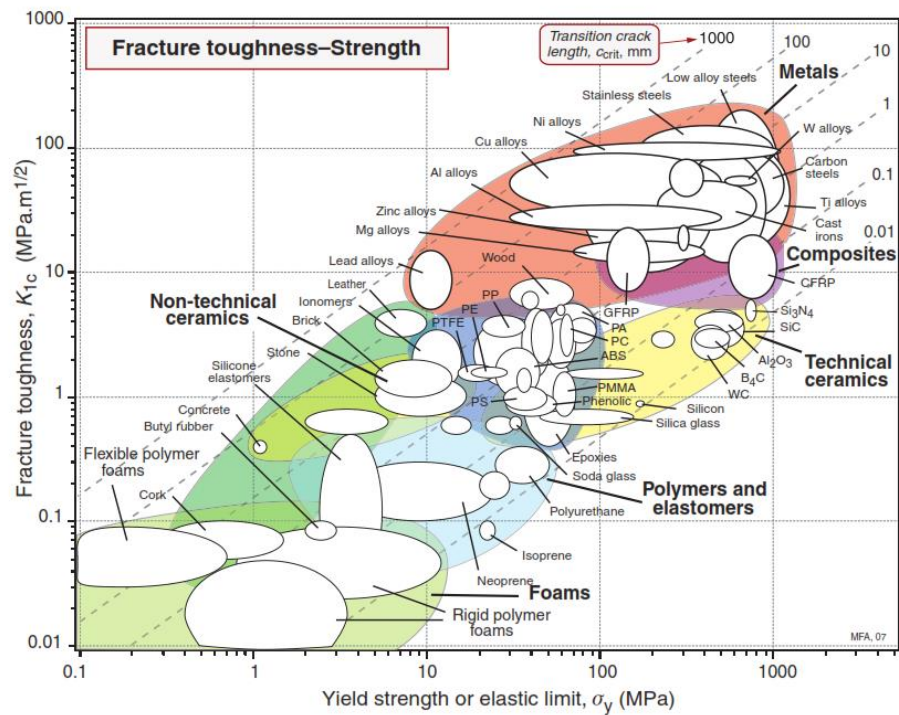


Figure 164 Fracture toughness plotted against yield strength. The transition crack size is shown, c_{crit} , is shown in by the contours (Ashby et al., 2019)

The fracture toughness– Yield strength chart

When the material is strength-limited for design, then the yield prior to fracture becomes a crucial figure to account for. Figure 21 plots fracture toughness against yield strength. Materials at the bottom right have low toughness but high strength. Hence, they fracture before they yield. Soda lime glass is in this region (bottom right), meaning that it will fracture before it yields. This can also mean that designing with glass would be a fracture-limited design, not a strength-limited design. (Ashby et al., 2019) Nevertheless, fracture cannot be measured and therefore we can only design based on tension stress and deflection. It is important to understand fracture to understand glass behaviour and then understand why fracture is not used as a design criterion.

Borosilicate glass Yield Strength: 25.2 – 27.8 MPa

Borosilicate glass Fracture Toughness: $6e5 - 6.2e5 \text{ Pa.m}^{0.5}$

Flexural strength (modulus of rupture): 32.8 - 36.2 MPa

Table 18 Summary of properties of 7740 Borosilicate glass based on CES EduPack¹ averages (Granta Design Limited, 2019) ***
 Since glass would break due to local tensile stresses before it could ever reach its allowable compressive level. That is why the real allowable compressive limit cannot be verified through tests. (Emami, 2013) Compressive Strength: 800- 1000 MPa (Saint Gobain, 2018)

Property	Units	7740 - Borosilicate glass
Composition	%molecules	81% SiO ₂ 2% Al ₂ O ₃ 13% B ₂ O ₃ 4% Na ₂ O
Density	kg/m ³	2225
Elasticity (Young's modulus)	GPa	62.95
Yield strength (elastic limit)	MPa	26.5
Yield Strength	MPa	26.8
Fracture Toughness	Pa.m ^{0.5}	6.1 e5
Tensile strength	MPa	26.5
Compressive strength	MPa	265 – 1000 ***
Toughness (G)	J/m ²	6.01
Flexural strength (modulus of rupture)	MPa	34.5
Shear modulus	GPa	26.25
Poisson's ratio	-	0.2
Thermal expansion coefficient	strain/°C	3.245 e-6
Specific thermal capacity	J/kg.°C	780

Appendix B: Dynamic relaxation of the shell using Particle-Spring form finding Method

A.1 Dynamic relaxation

Step 1: A curve is created in rhino. This curve forms the space boundary of the form yet to be relaxed.

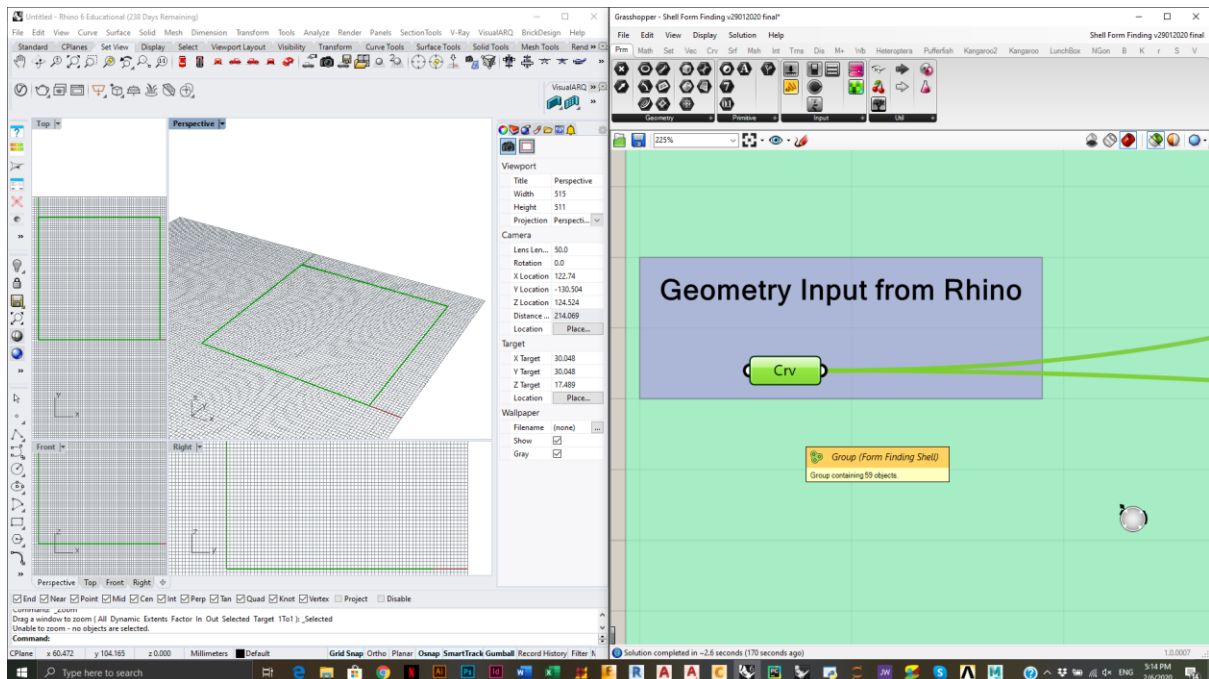
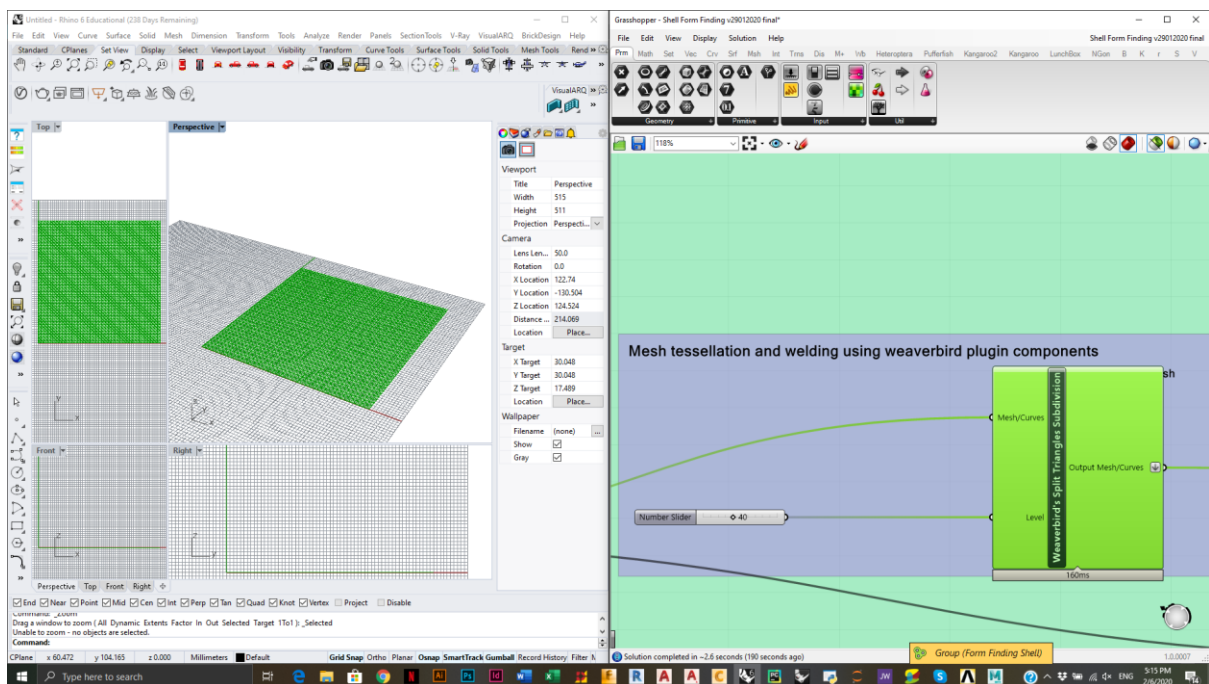
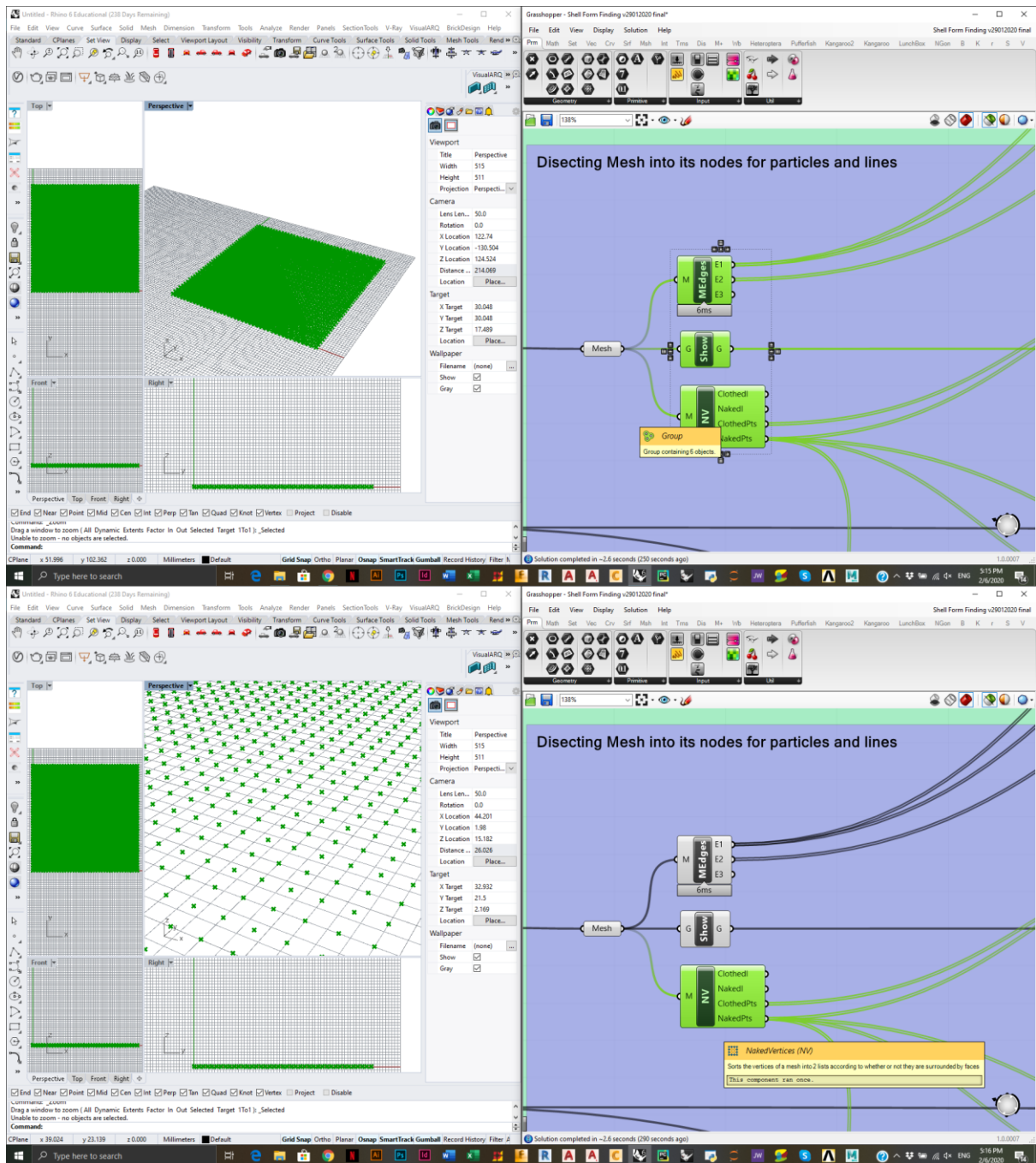


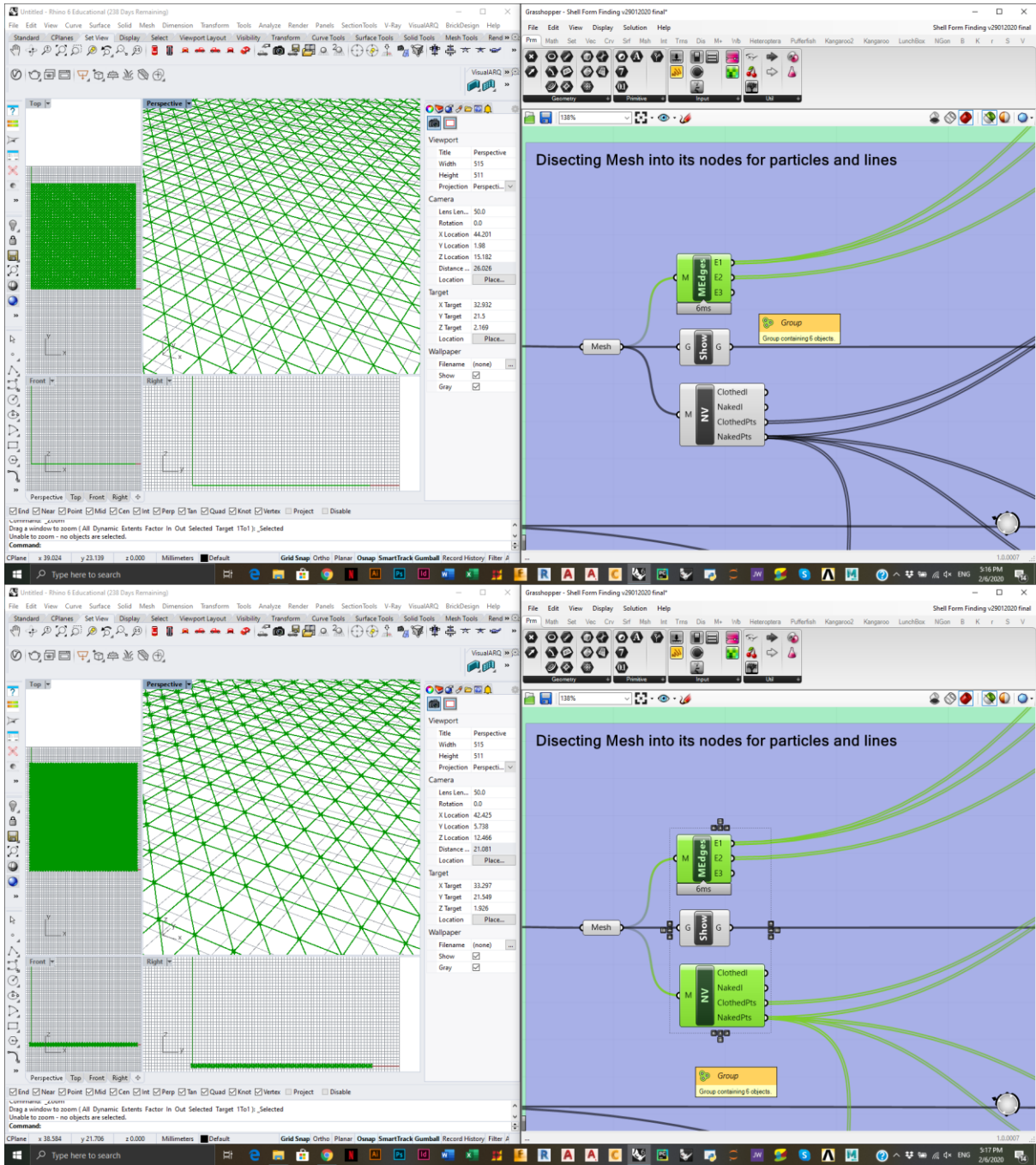
Figure 165 Steps of form finding via Rhino (left) and Grasshopper (right). Step1: Setting the space boundary. (Source: Author)

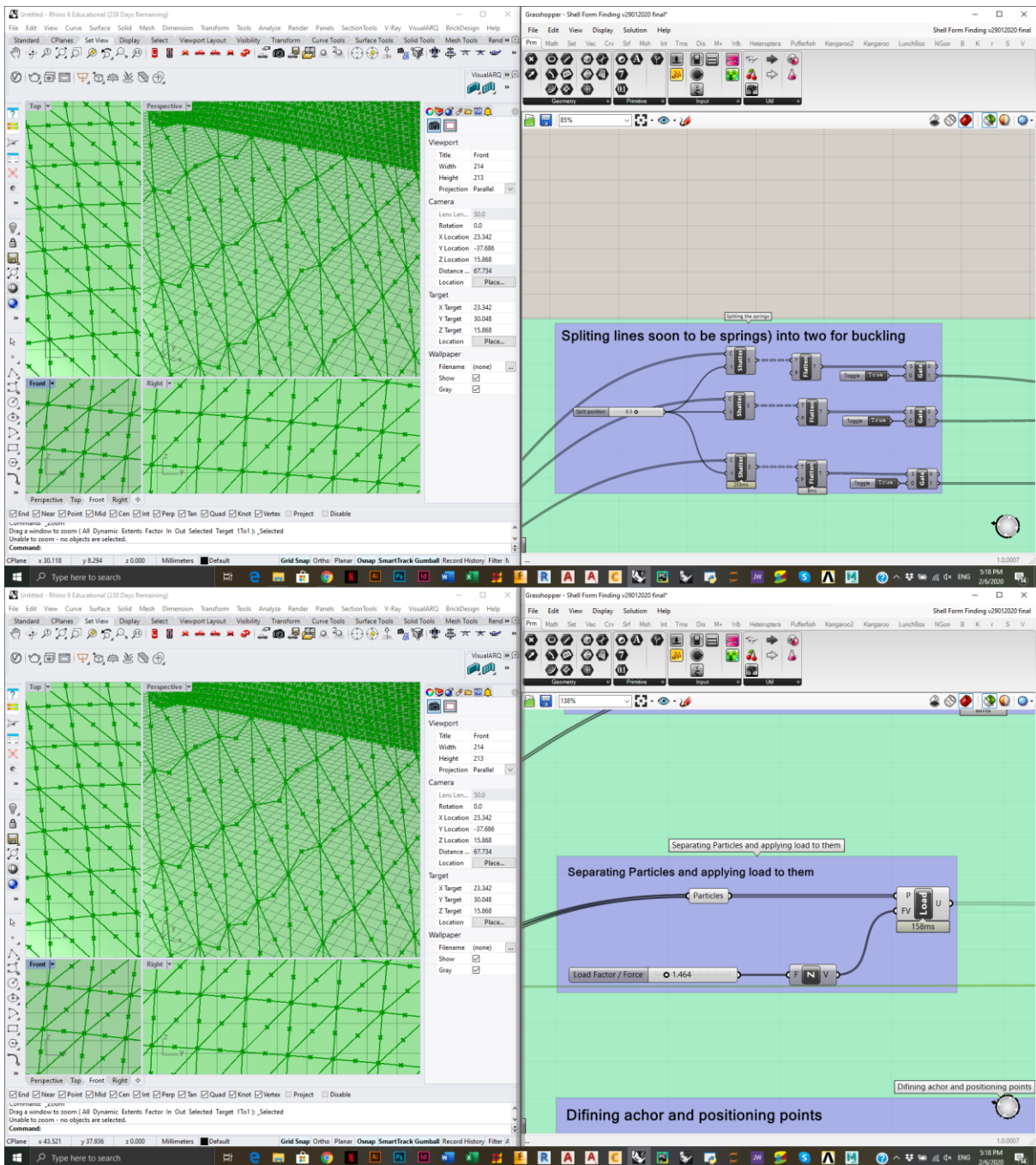


Step 2: The curve is imported into grasshopper and subdivided into U and V directional grid along with diagonal connections. This is done using a Weaverbird-plugin component called split triangles subdivision. It created a mesh from the curve then tessellates it. The pattern of tessellation (division) will have influence on form the mesh will relax into. Particle-Spring grid/network would integrate the splitting of the springs to buckle when under compression. The number of divisions and the number of particles would determine the precision, accuracy and smoothness of the surface. The load will be more

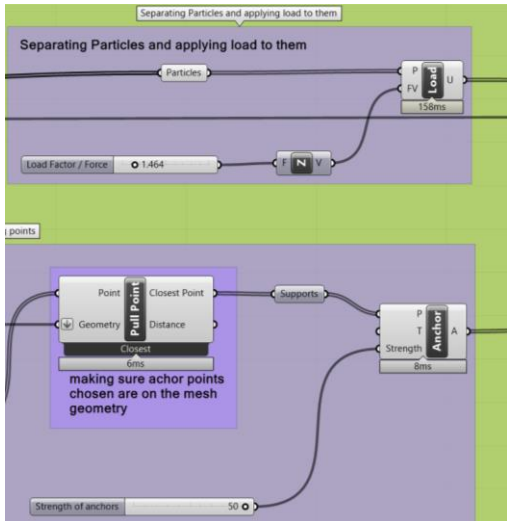
evenly distributed when the subdivision is higher. (Eigenraum, 2018).





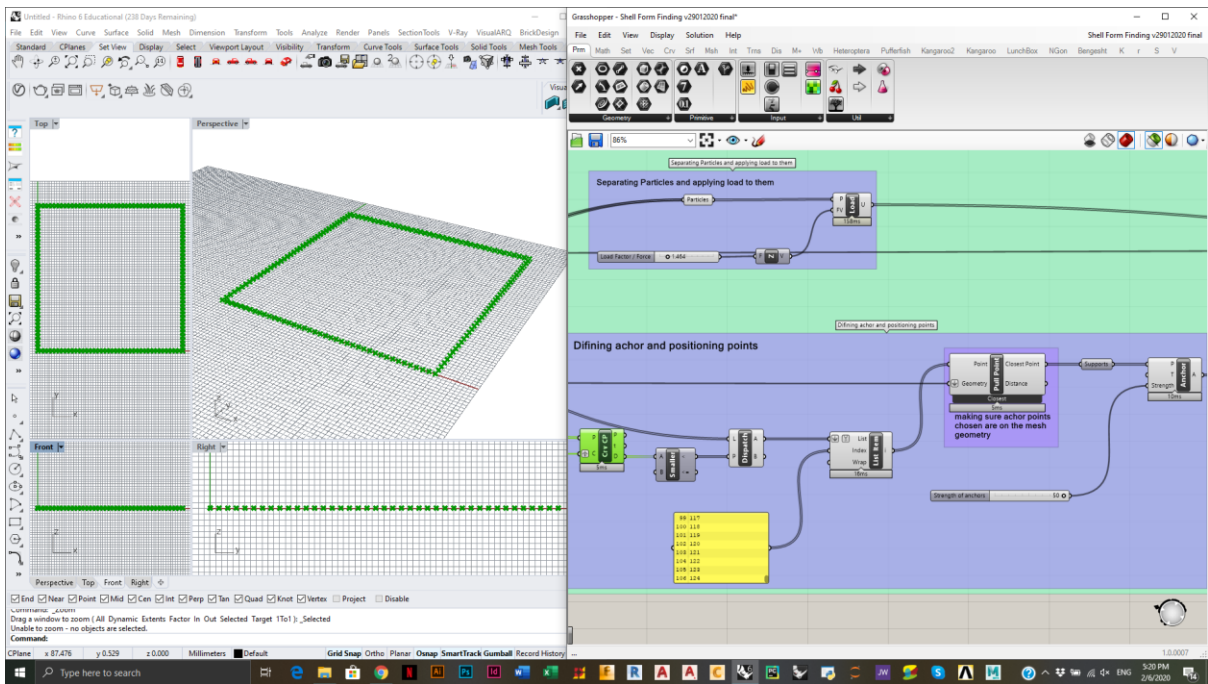


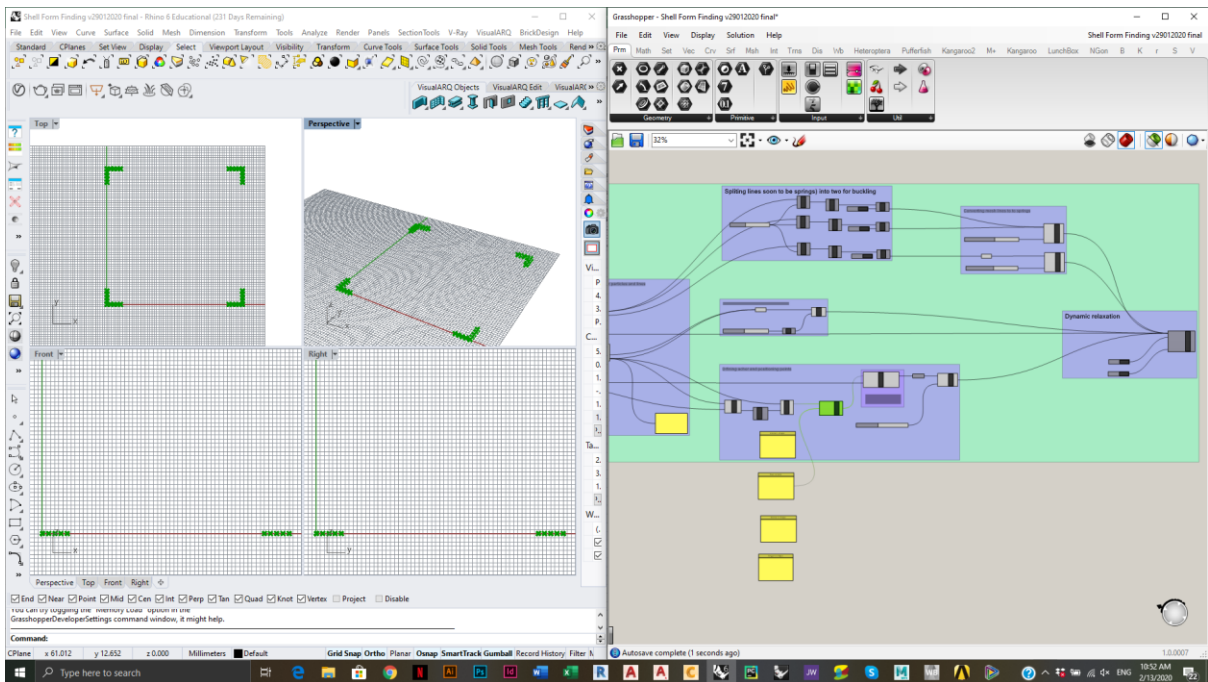
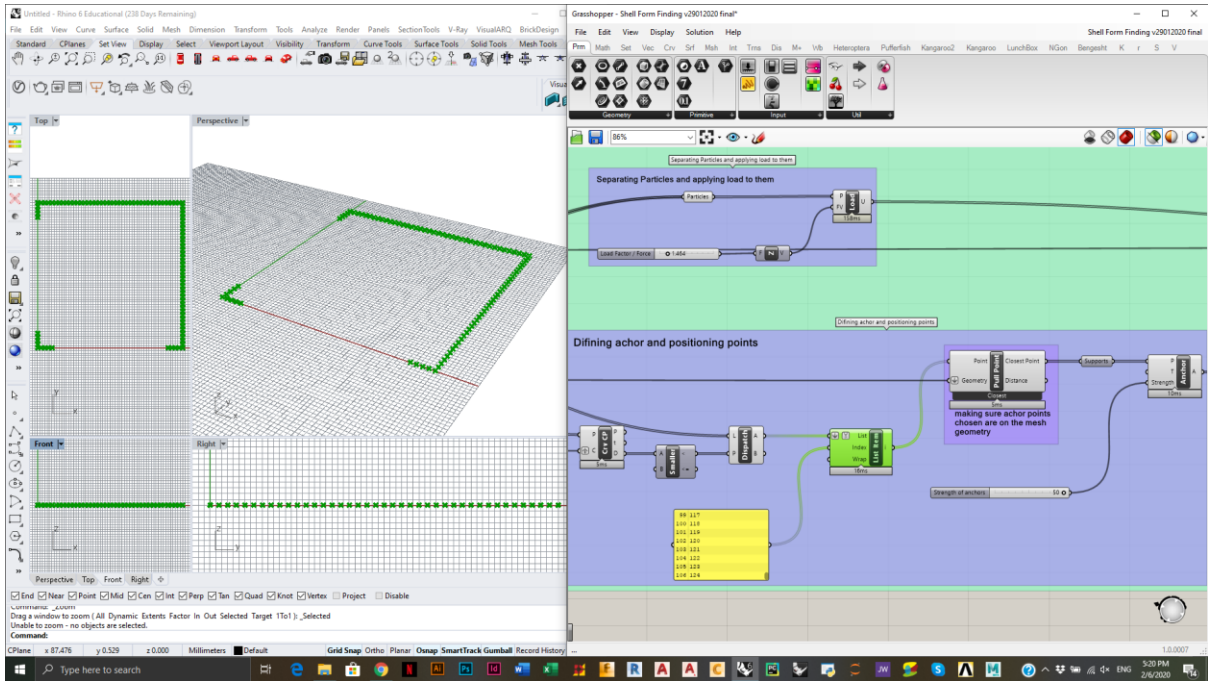
Step 3: After the mesh is subdivided into triangles each diagonal and orthogonal line is split into two using by particle in the middle using the shatter component. Then the lines are converted into springs using the length line component. A spring behaves differently as explained above.

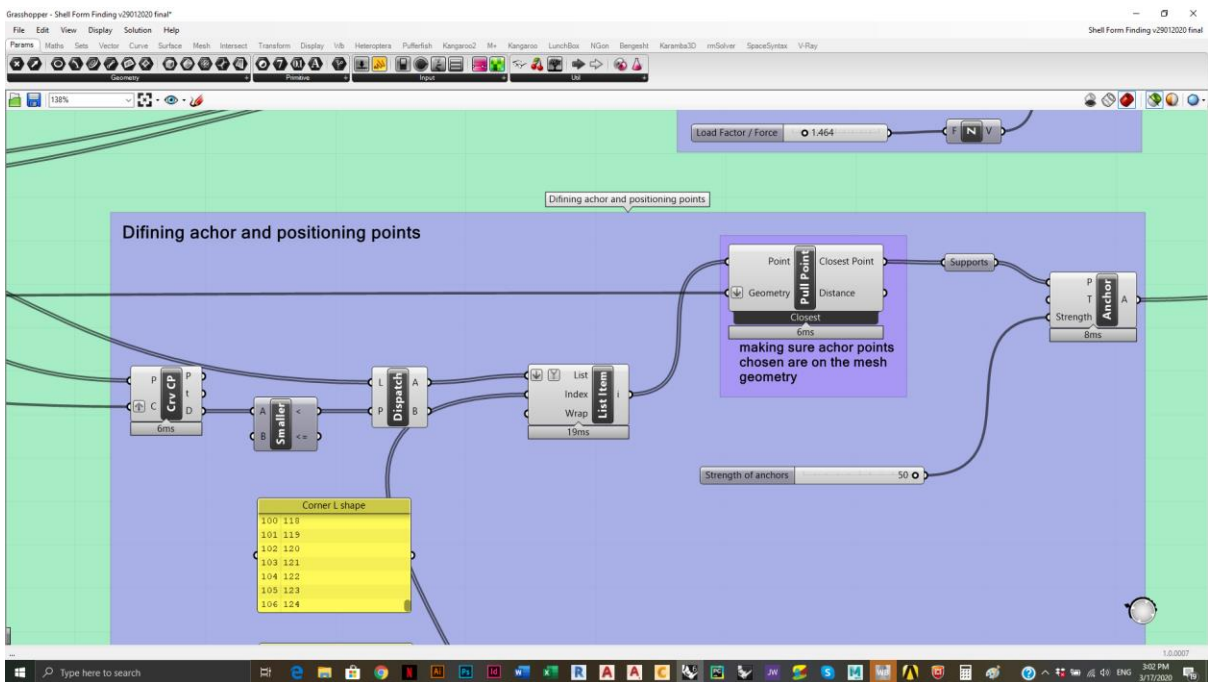
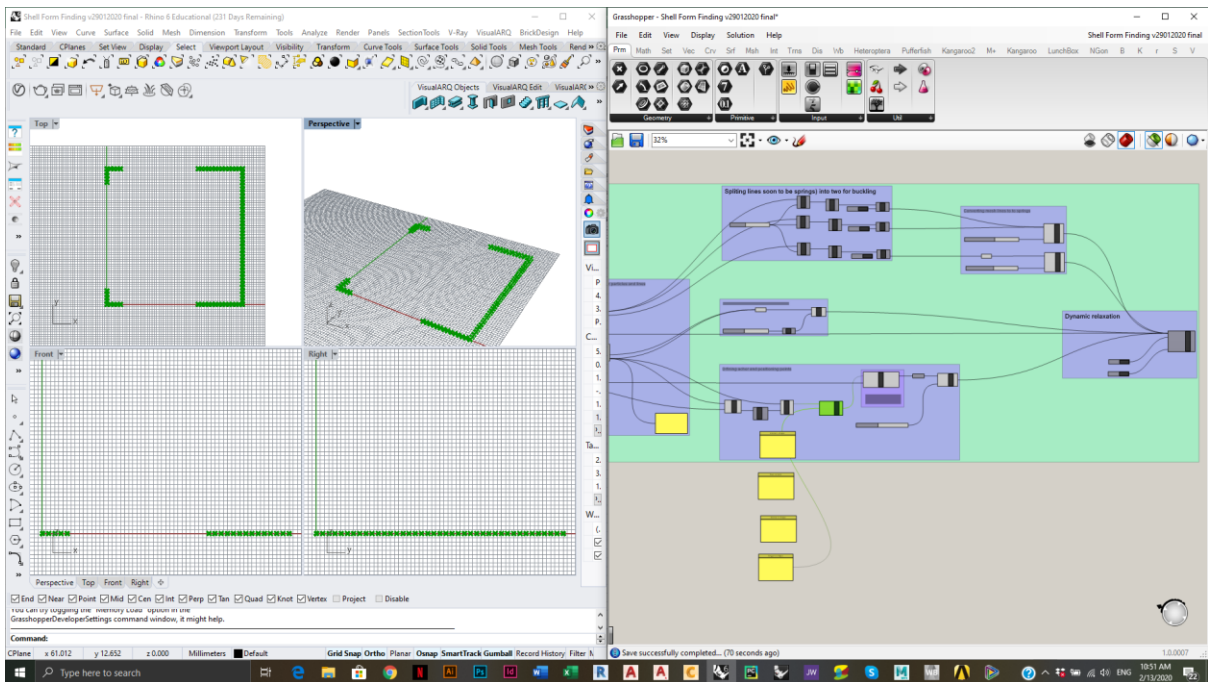


Step 4: A flipped gravitational force is applied to the particles. The anchors resistivity is controlled.

Step 5: The anchors are defined by choosing the intended particles by means of indexing a list Item of all circumference particles (“naked points”). The points were chosen based on the booth shape required by the Material District exhibition.

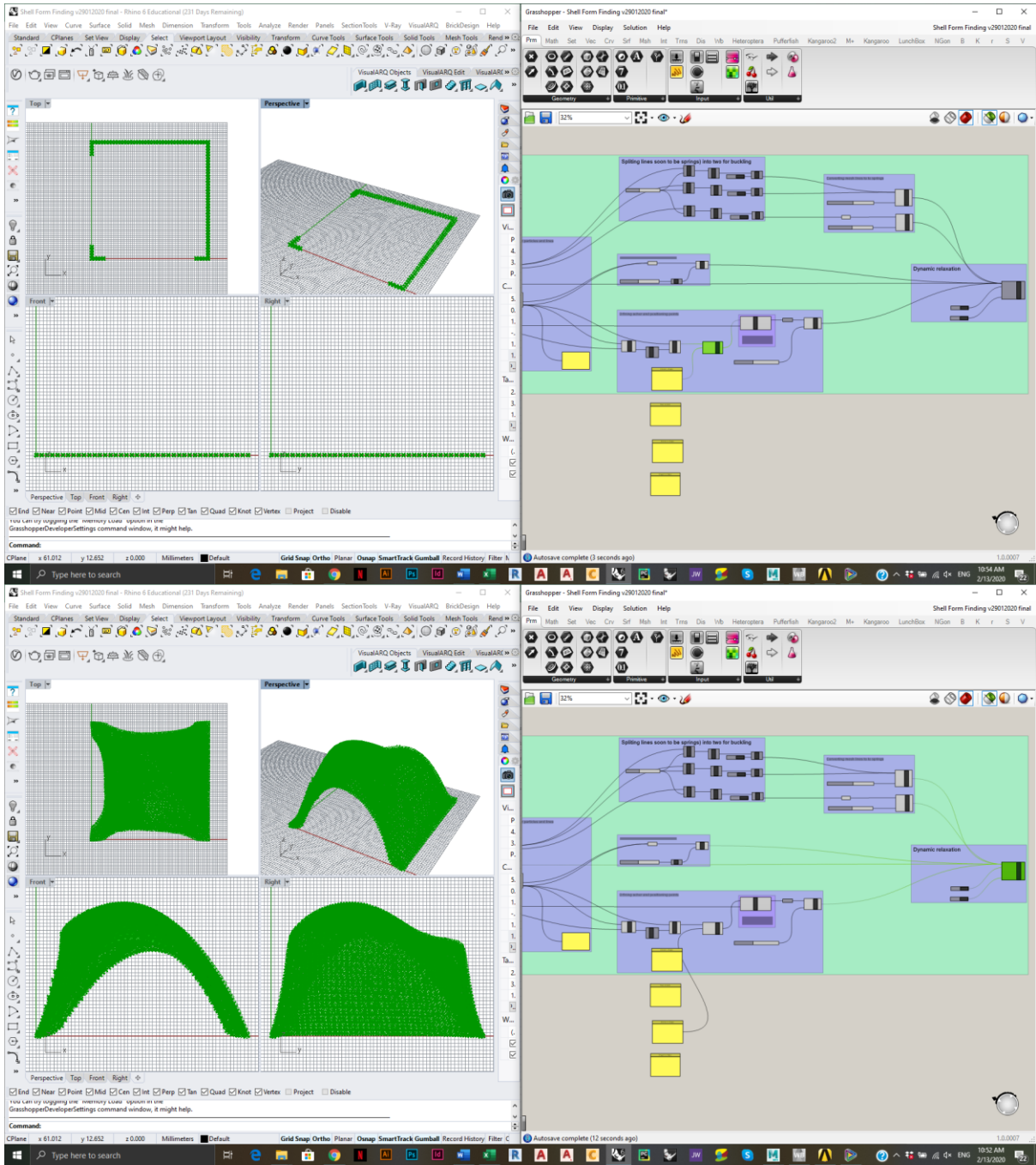


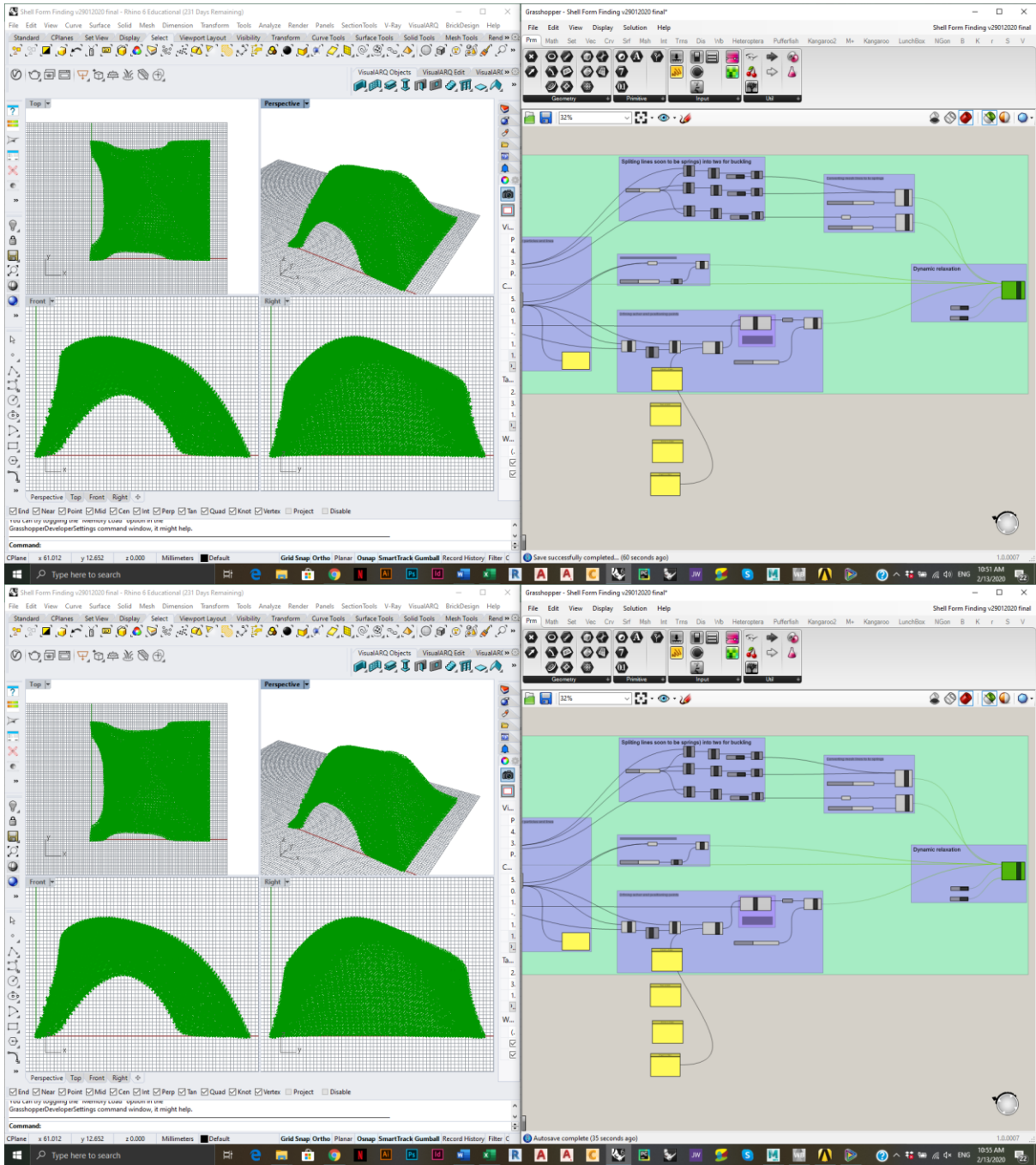


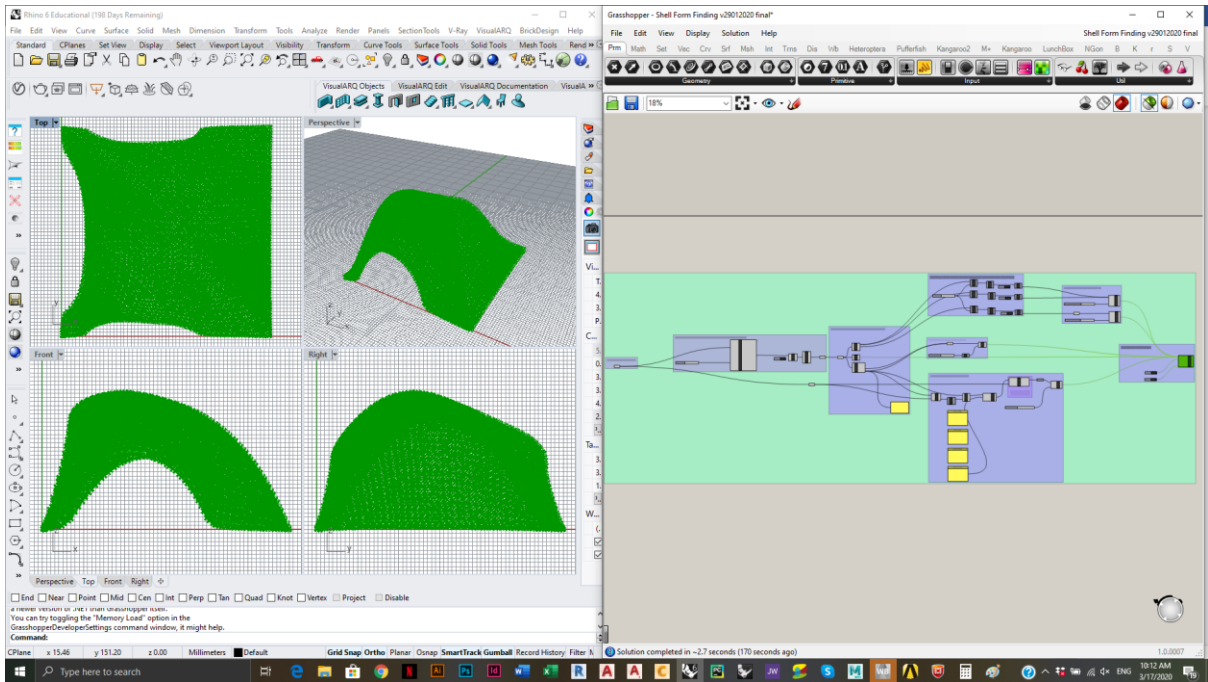
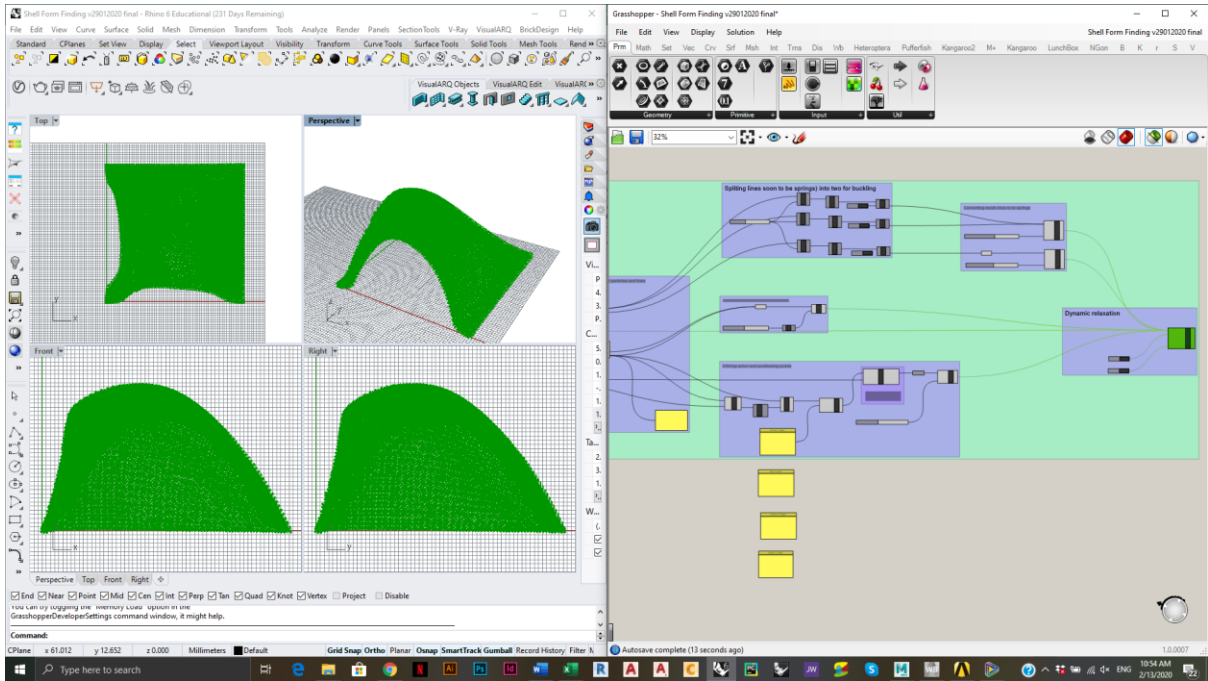


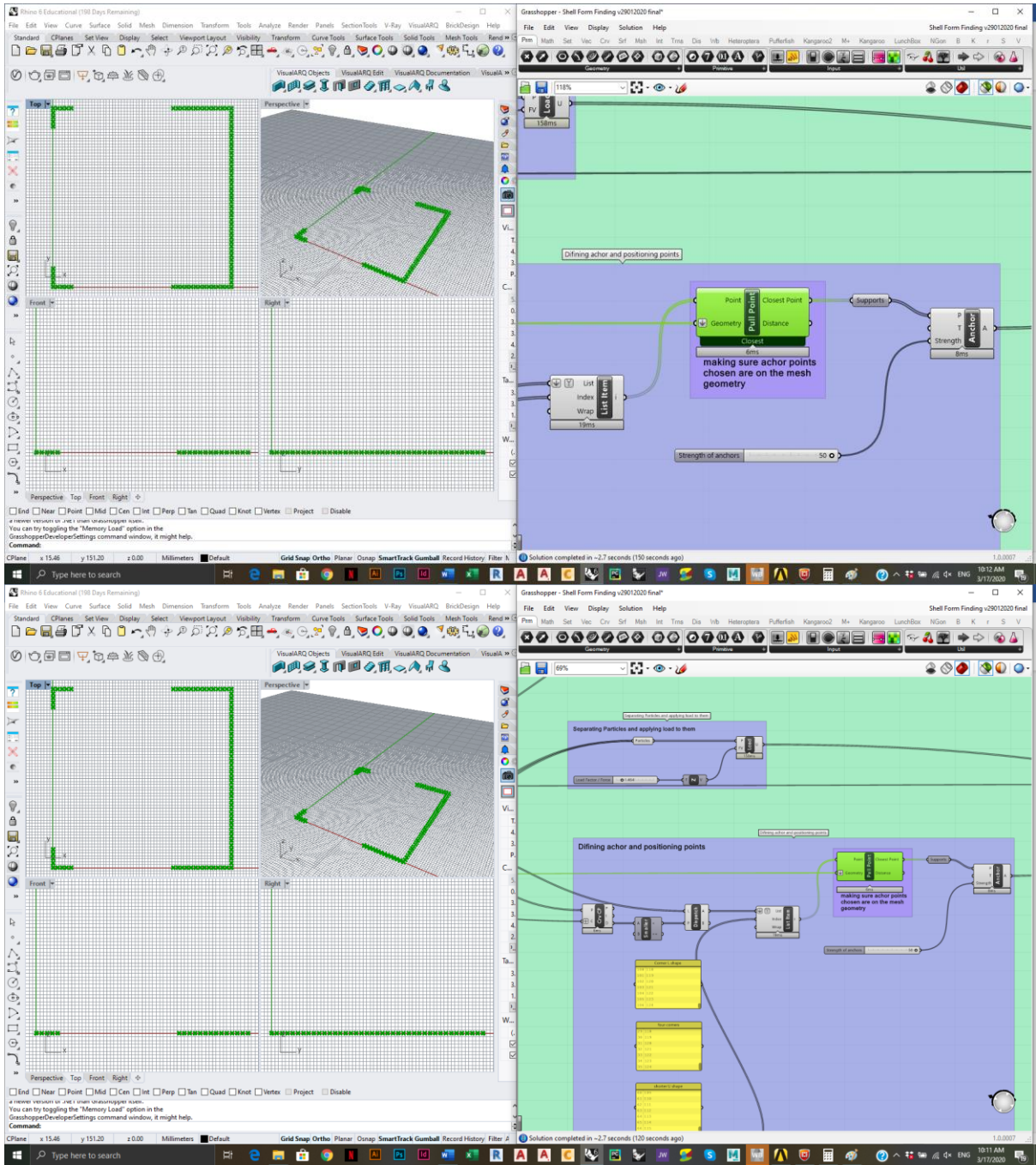
Step 6: The form is lofted and relaxed by means the component: “Kangaroo Bouncy Solver”. The springs’ resistivity (damping level) and force-controlled parameters in this phase are unitless. Nevertheless, the relative relationship between the parameters is sufficient for achieving the relaxed shape intended.

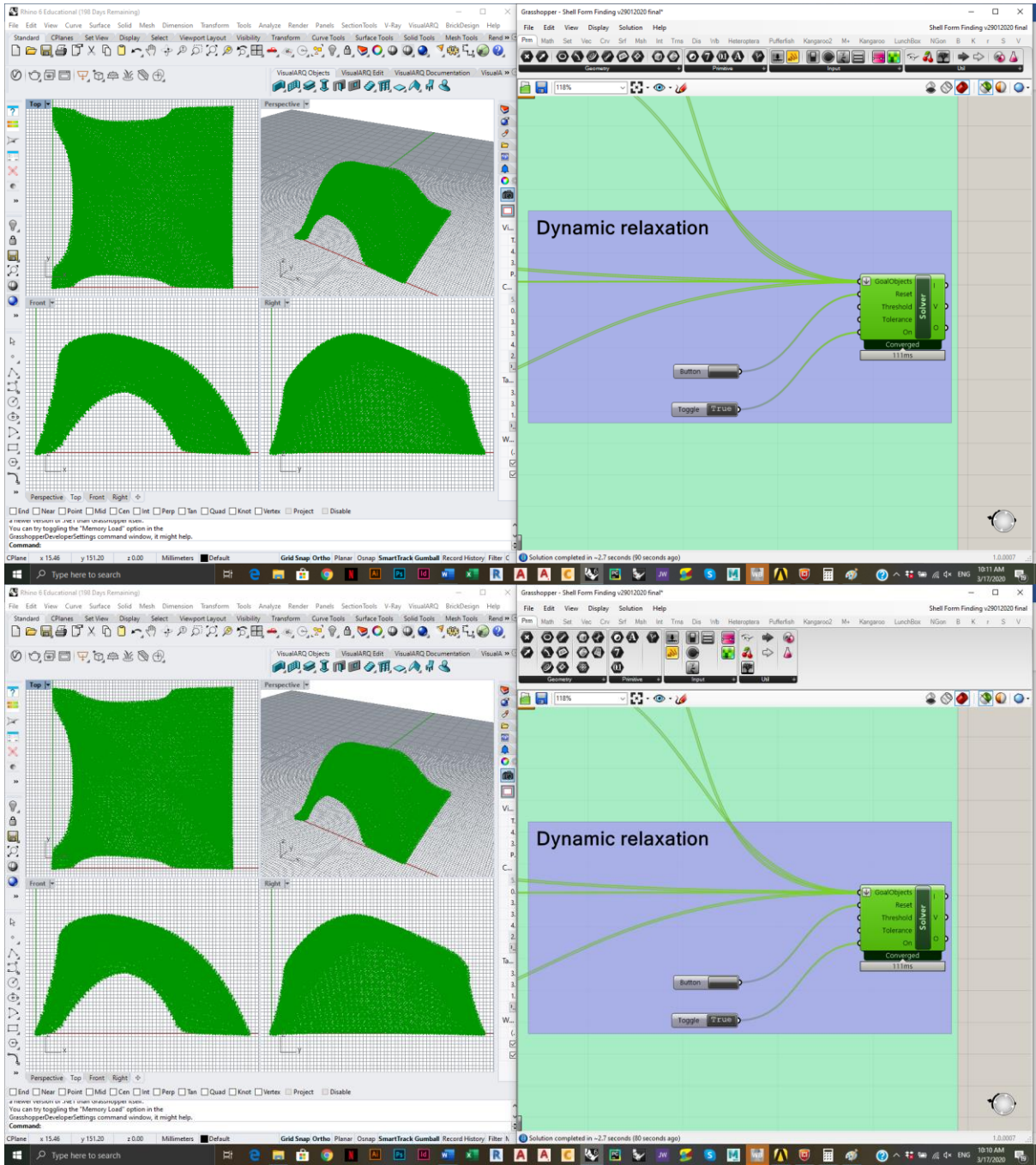
Step 7: result can either be baked for post-processing and analyses using other TO and FEA software or plugged into Kangaroo (grasshopper plugin) for structural verification. It should be noted that Kangaroo is not a certified structural verification plug in, but through practice considered accurate for instant feedback on the structural integrity of the design.

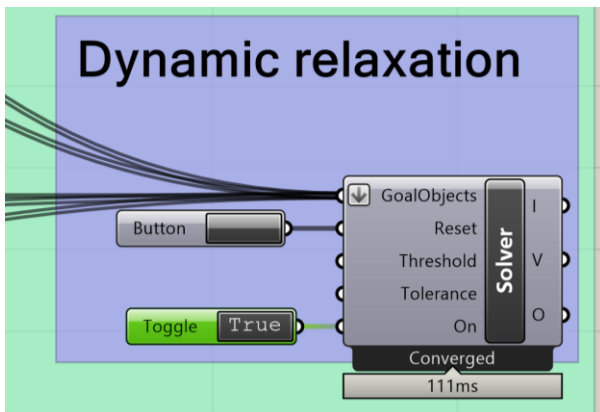
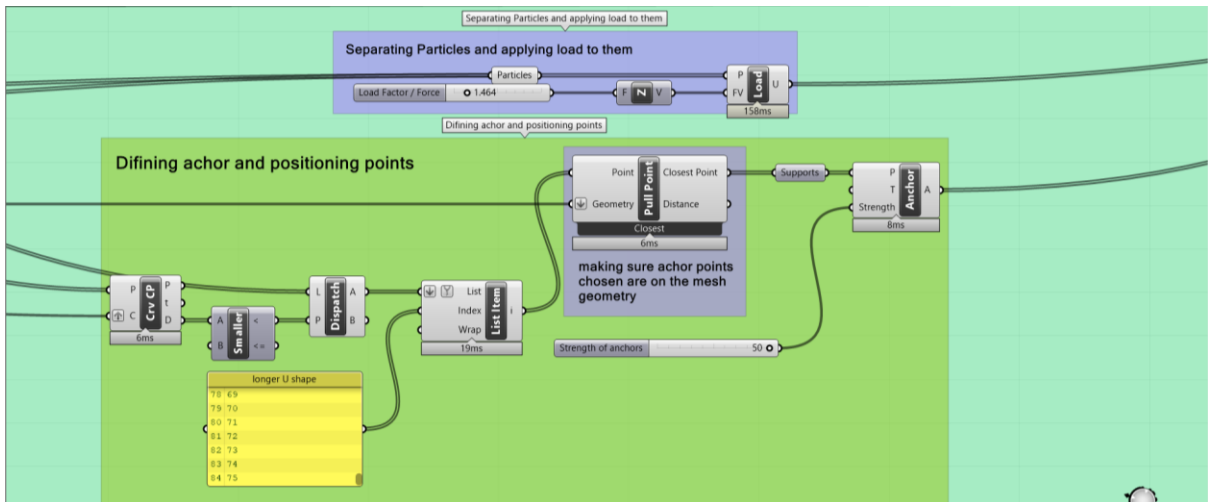
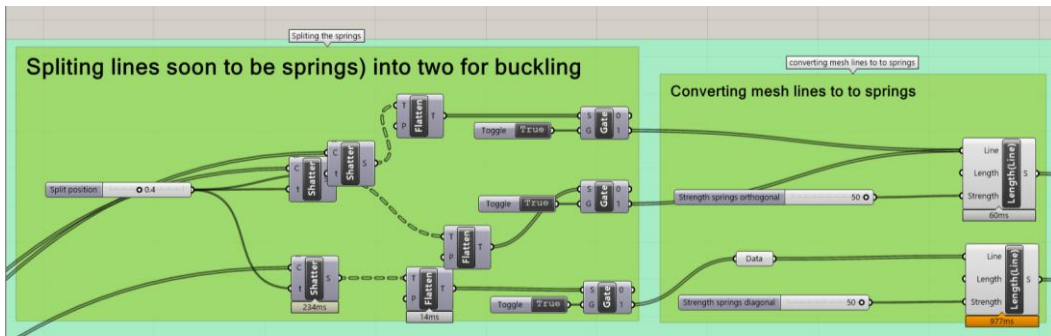
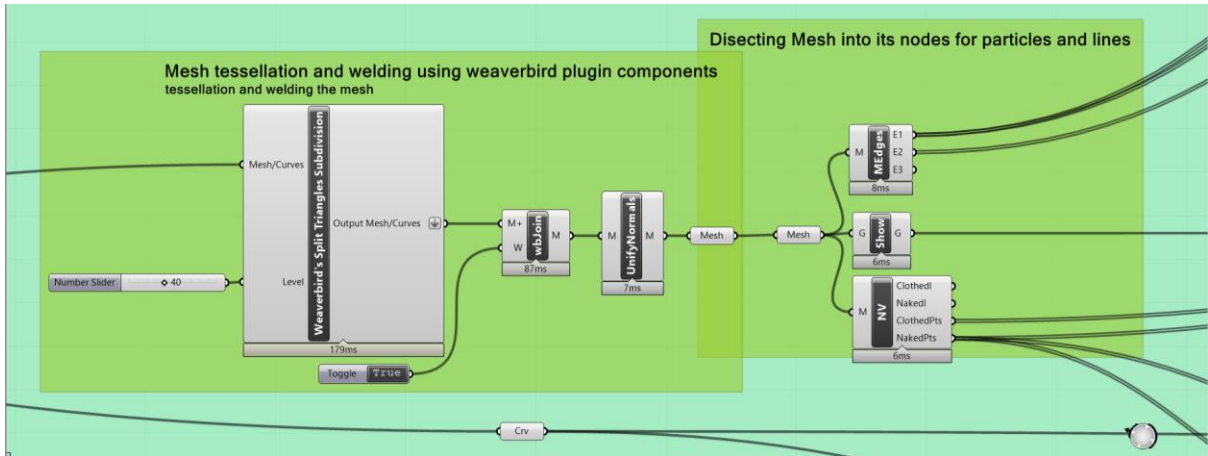








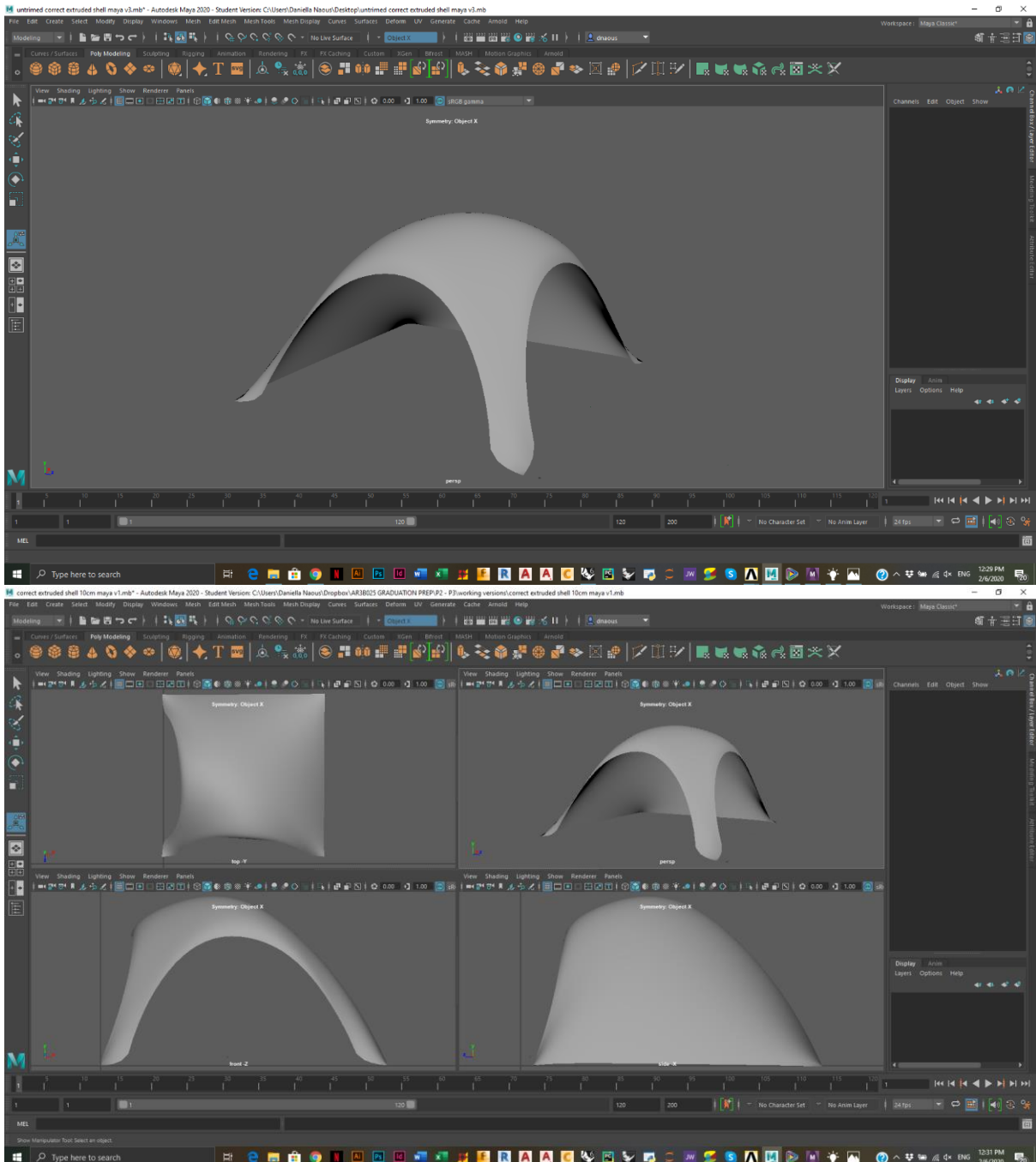


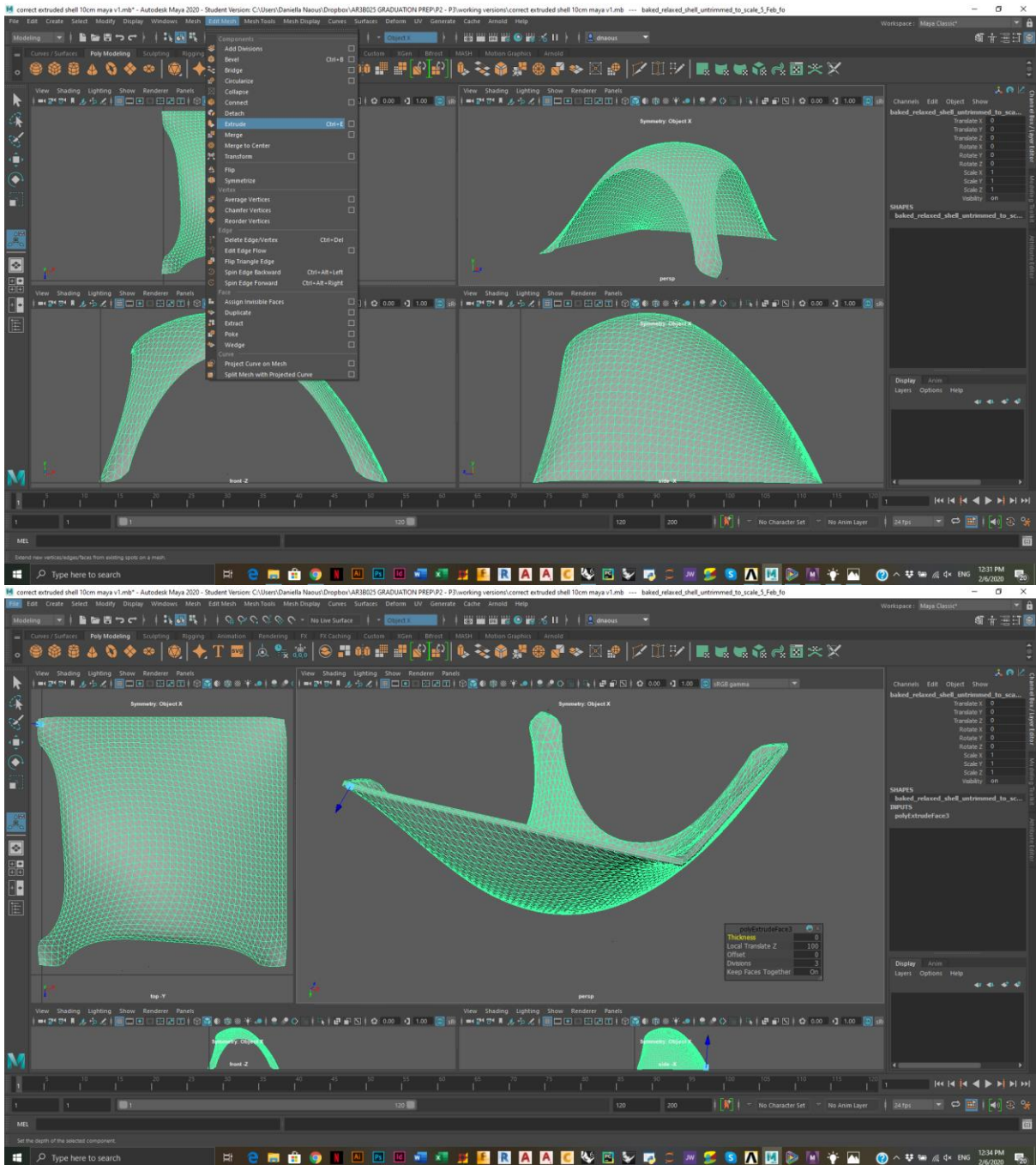


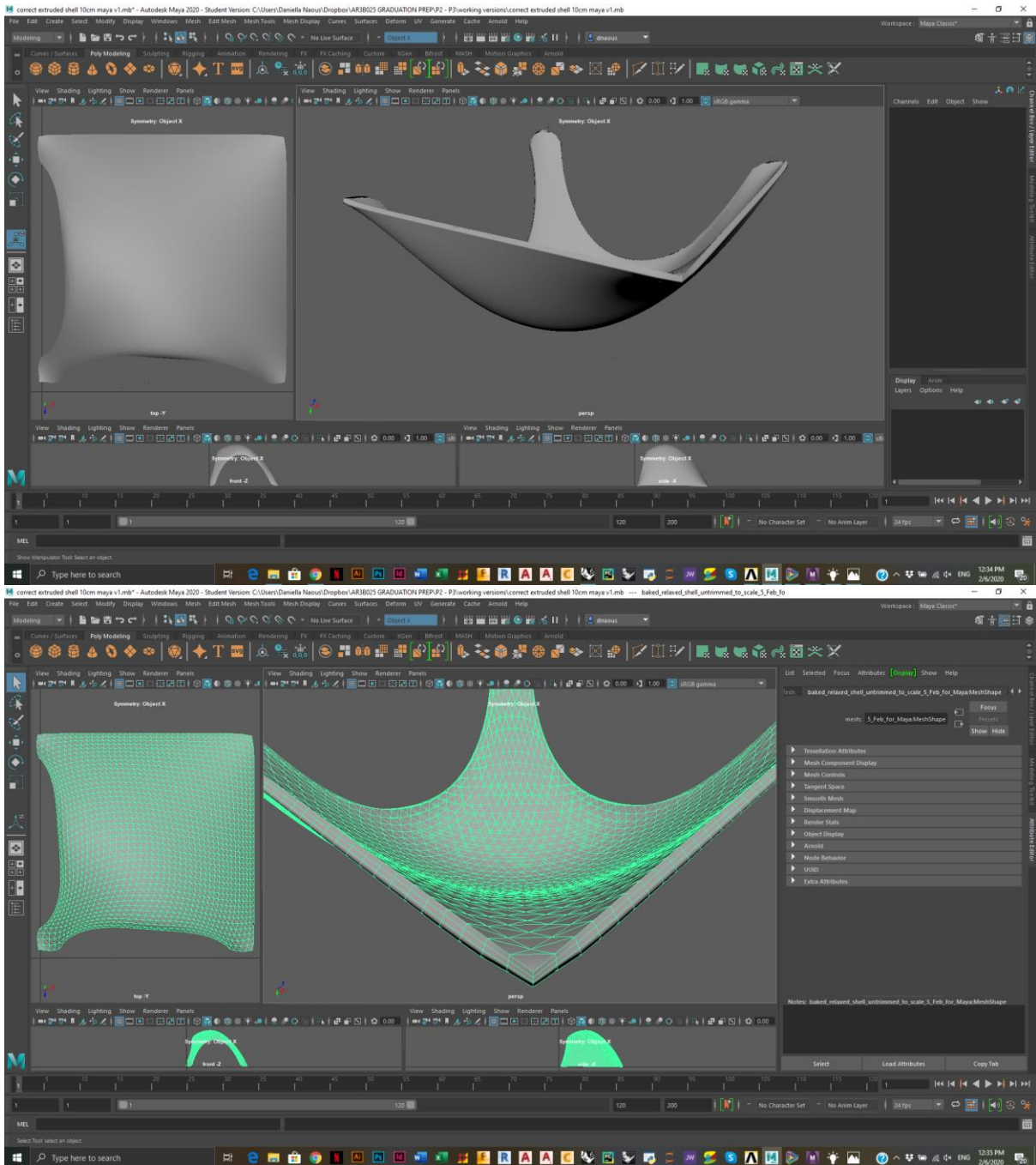
A.2 Meshing

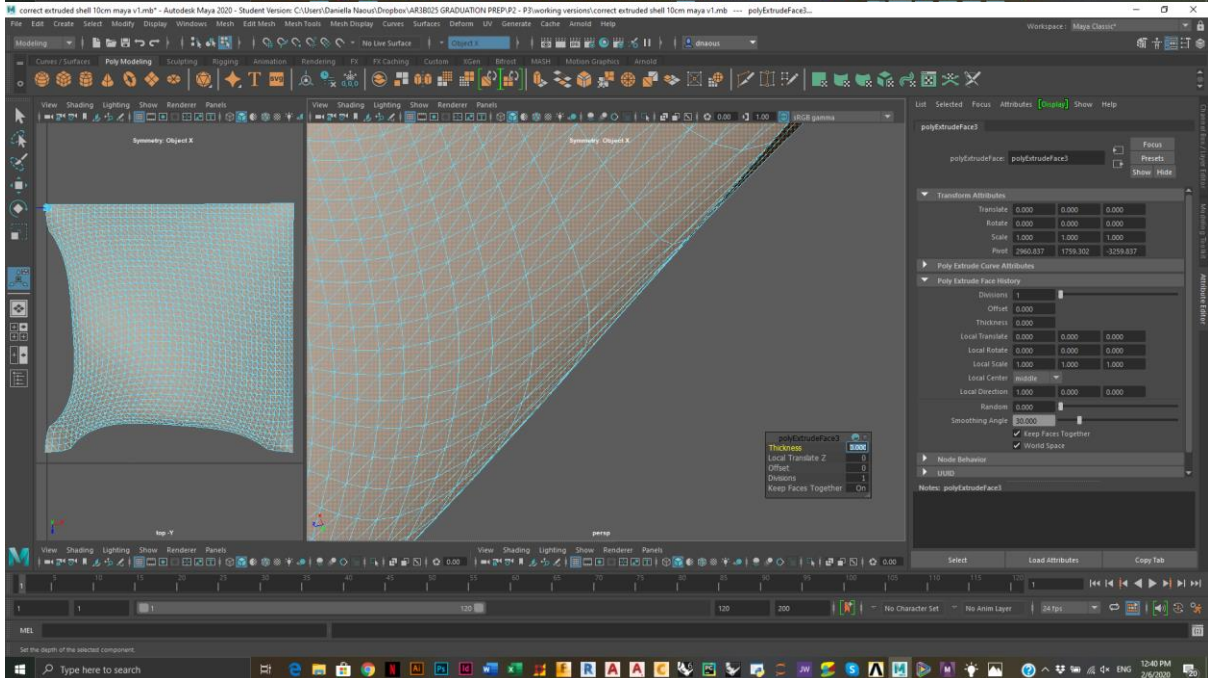
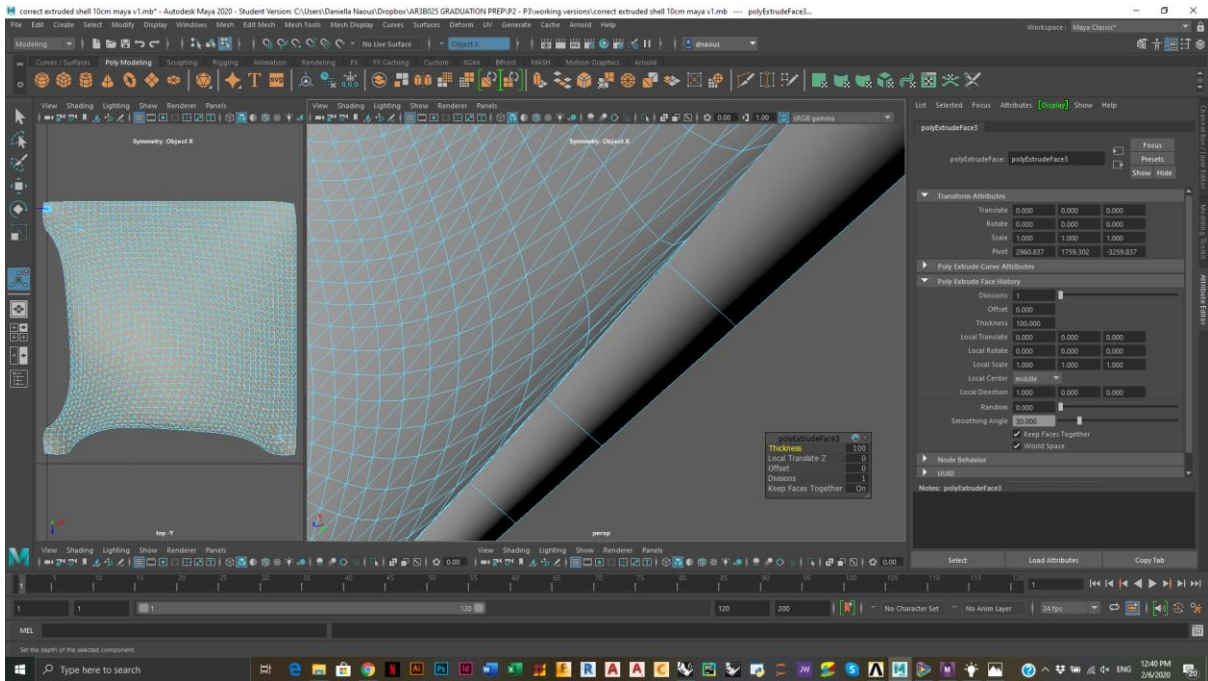
Procedure:

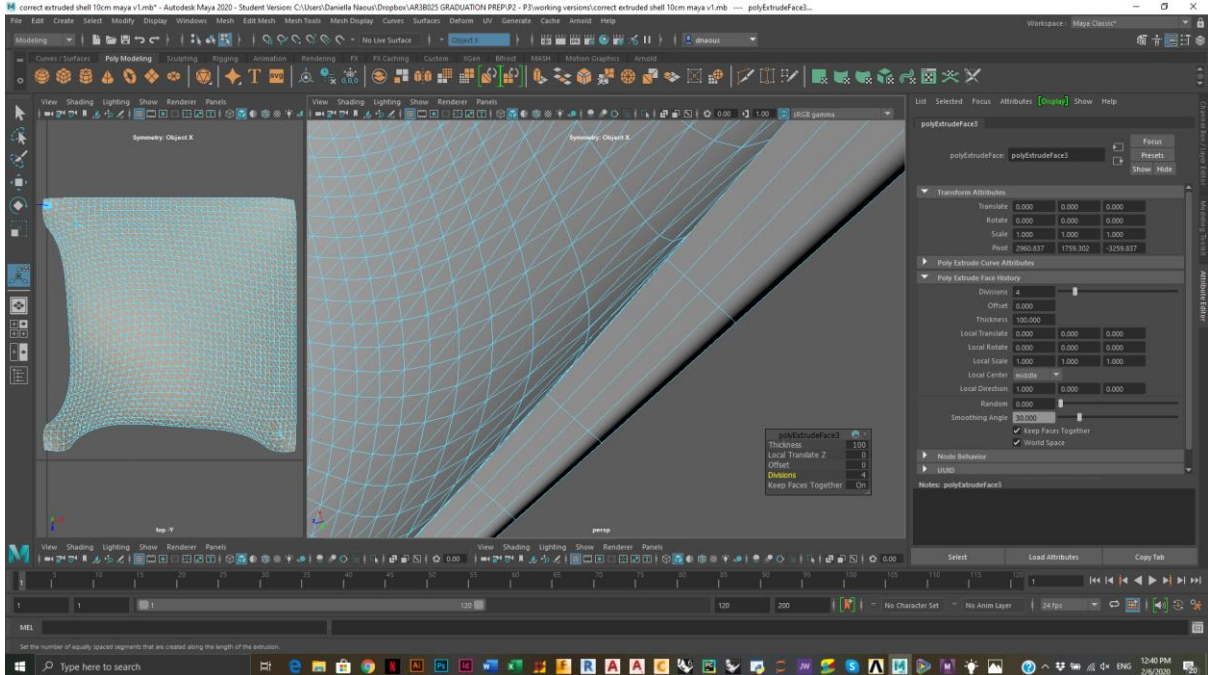
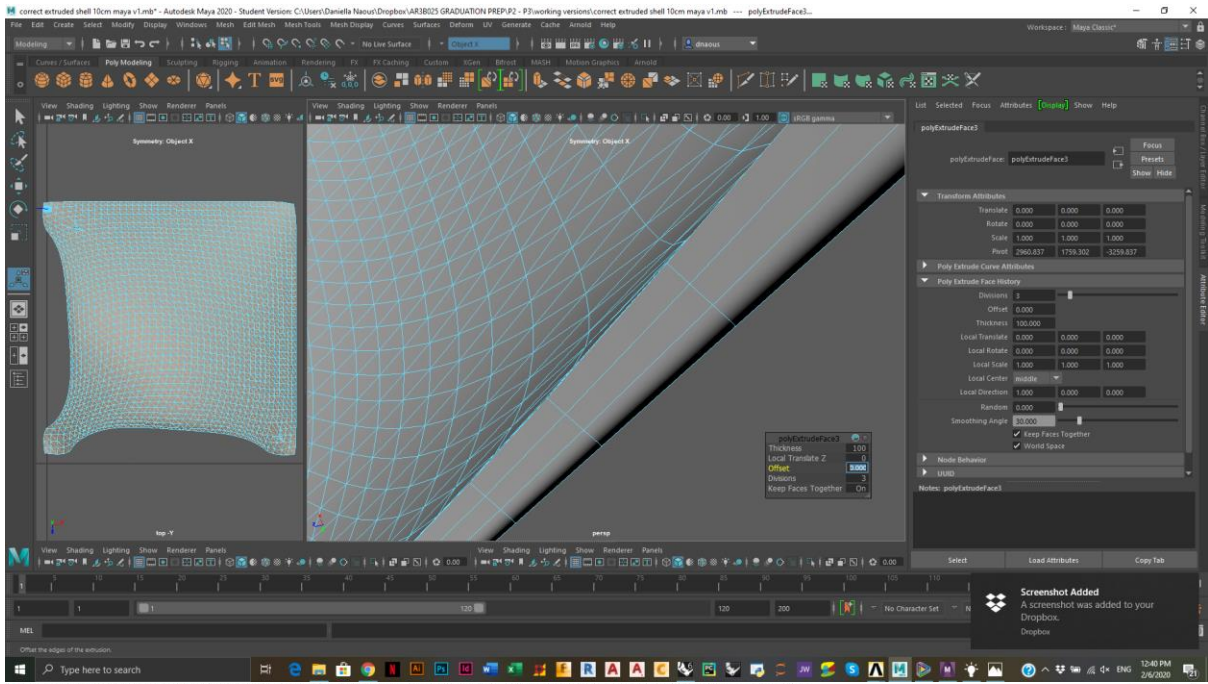
1. Give thickness in Maya through exclusion in z direction
2. Then trim the shell for clean foundation
3. Import to Ansys
4. Make solid using Ansys solid claim (Ansys)
5. Then mesh using mechanical Ansys

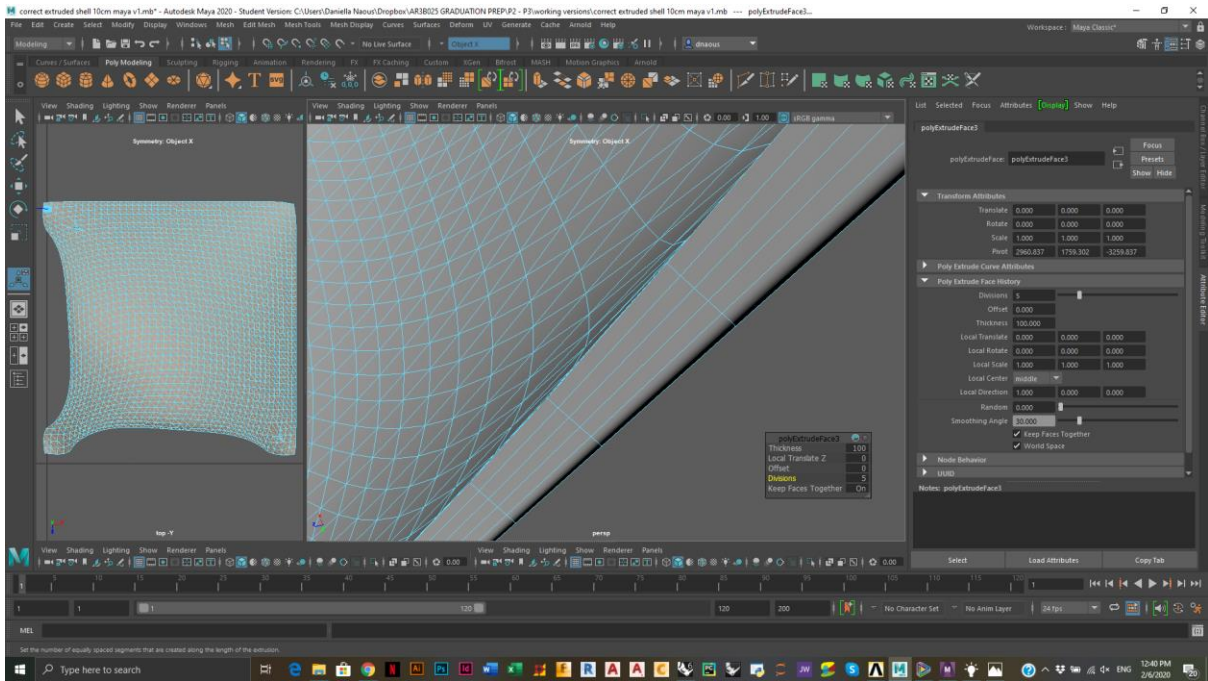




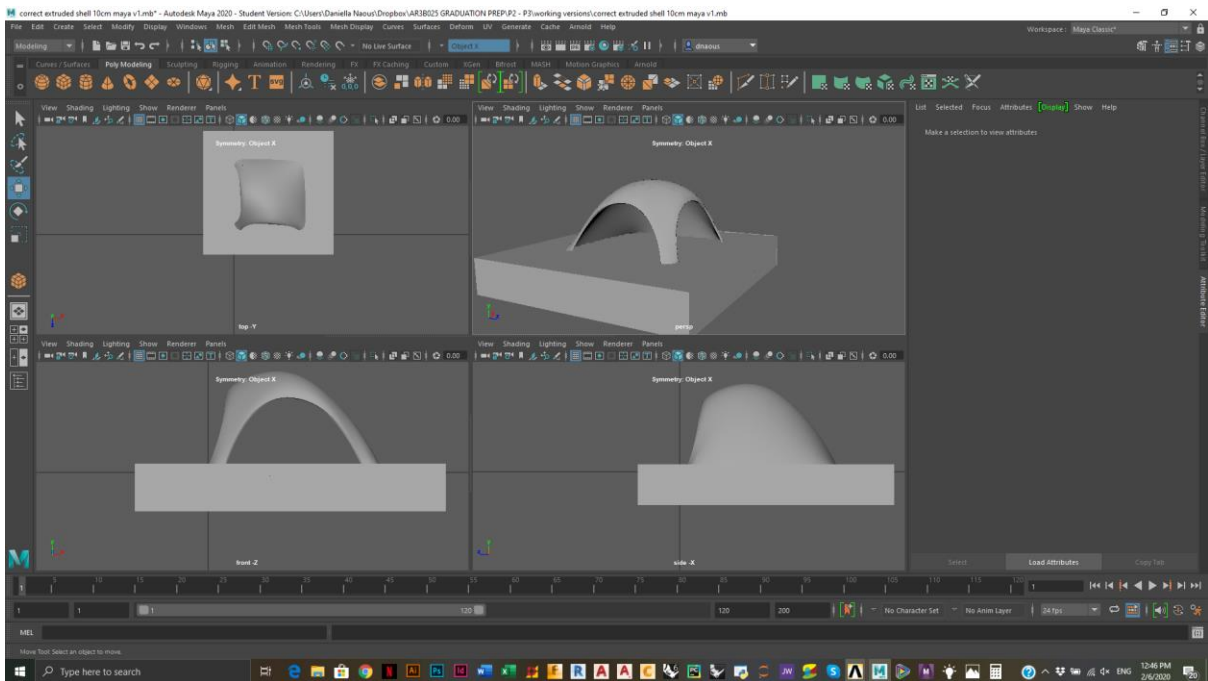


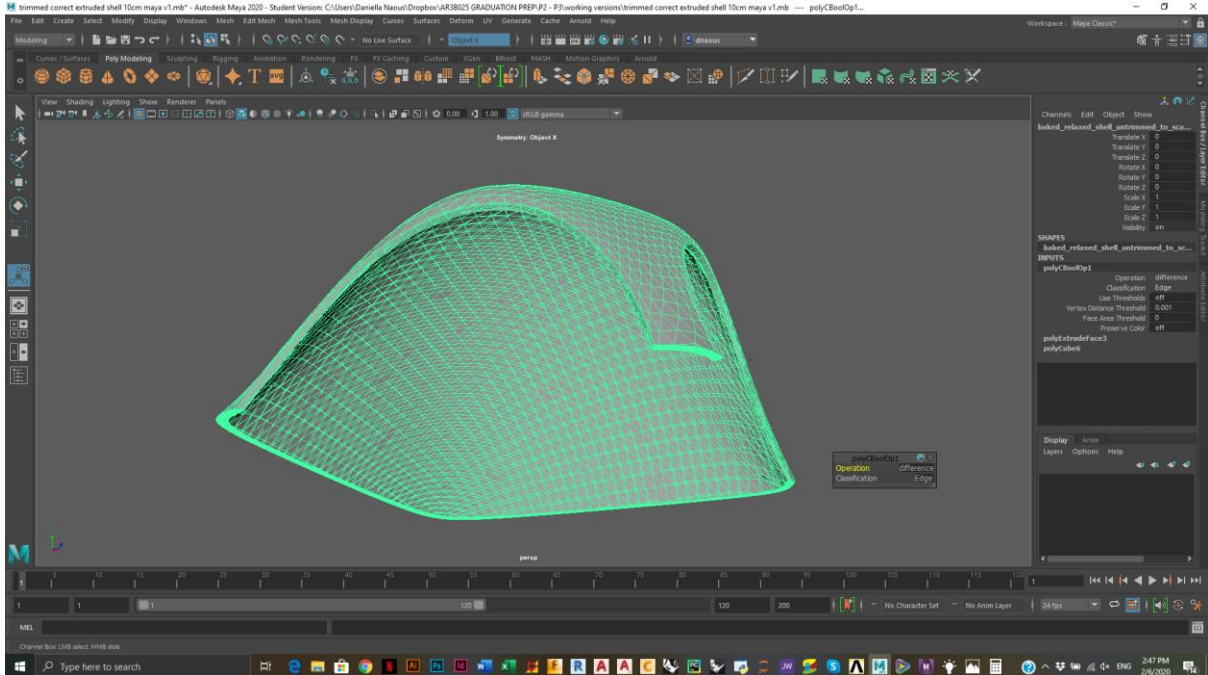
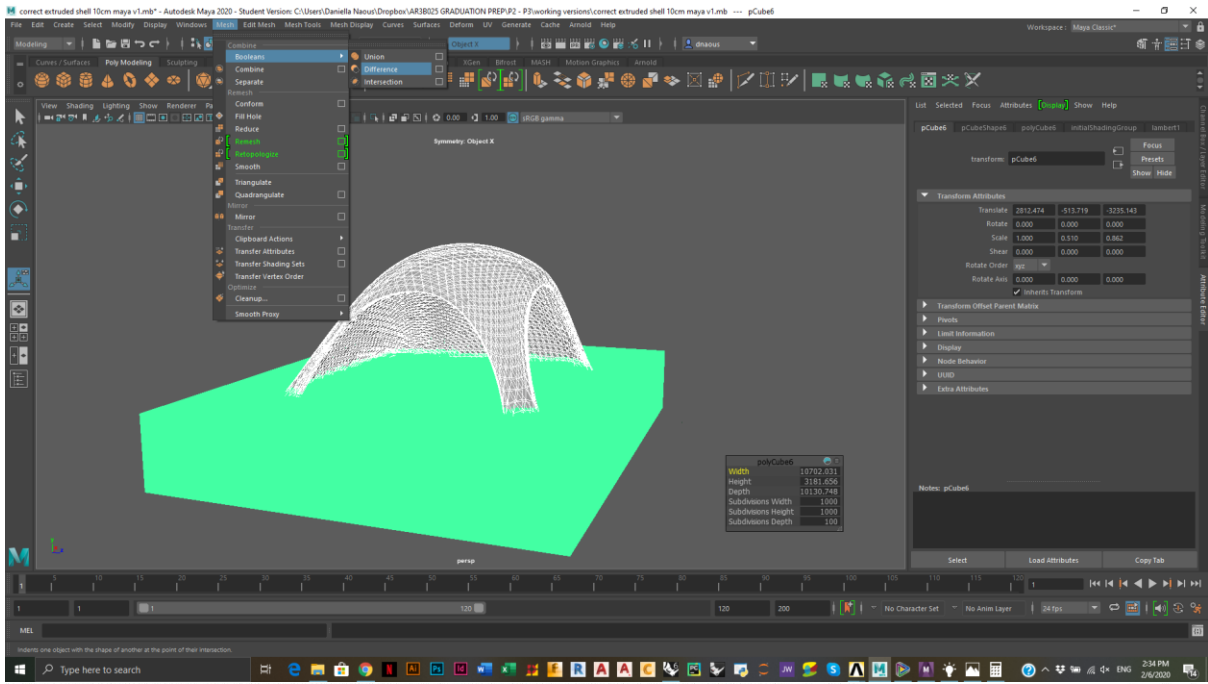


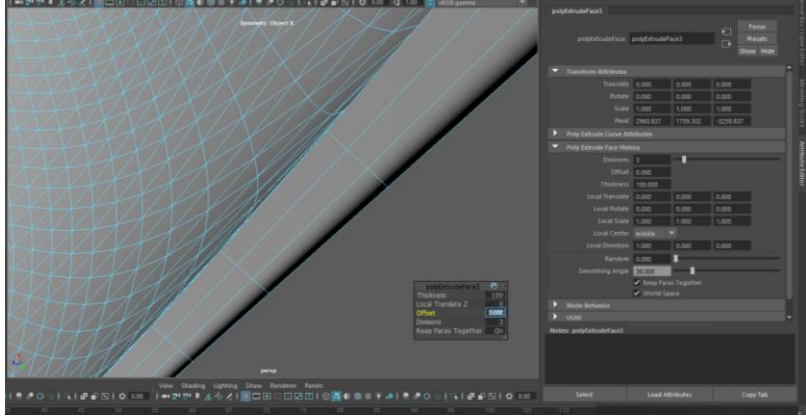
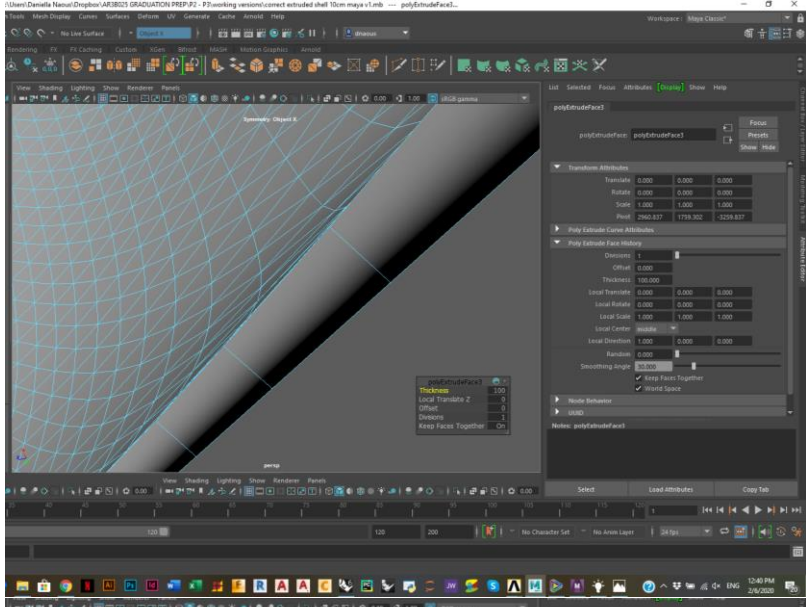
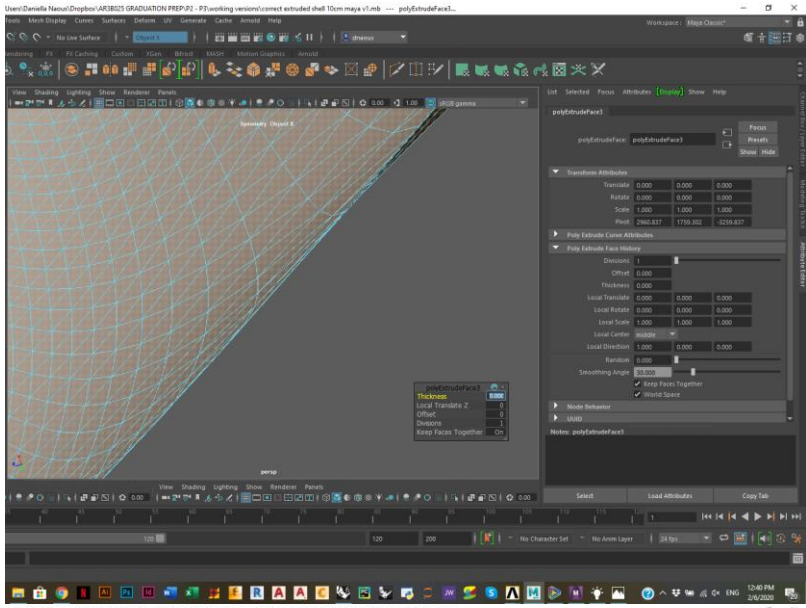


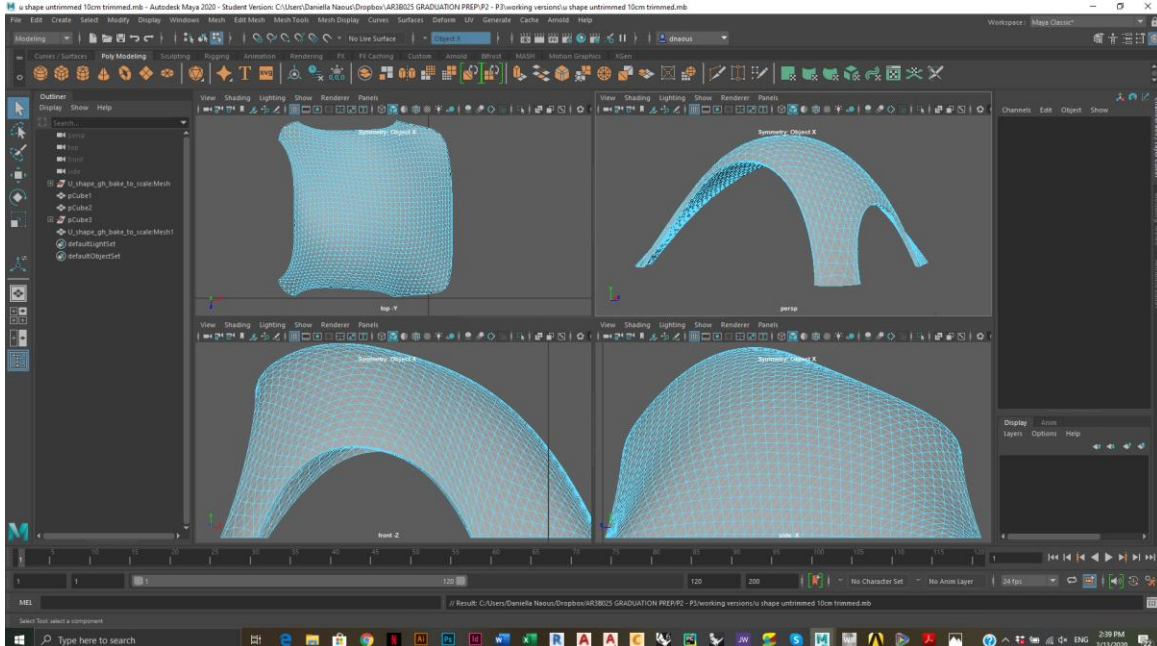
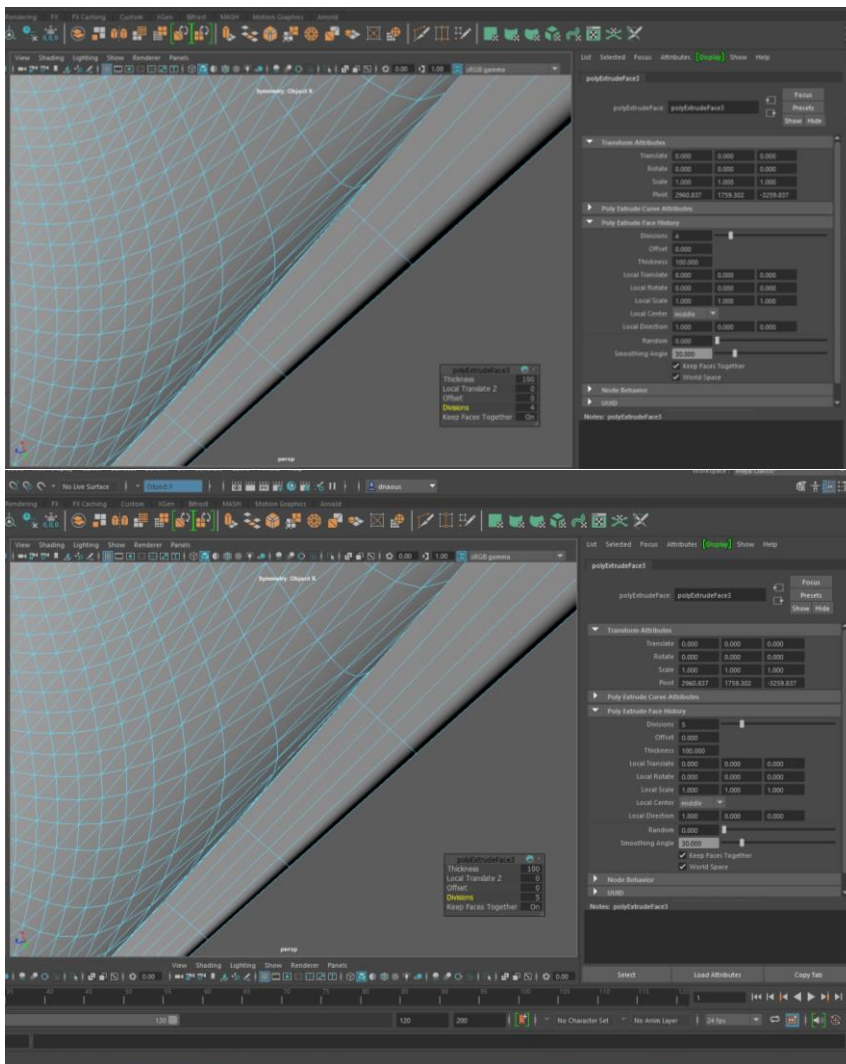


Adding subdivisions in the thickness adds layers for the thickness to be optimised. Instead of having one voxel throughout the entire thickness. Topology optimisation can also now decide how many voxels are there needed within the thickness





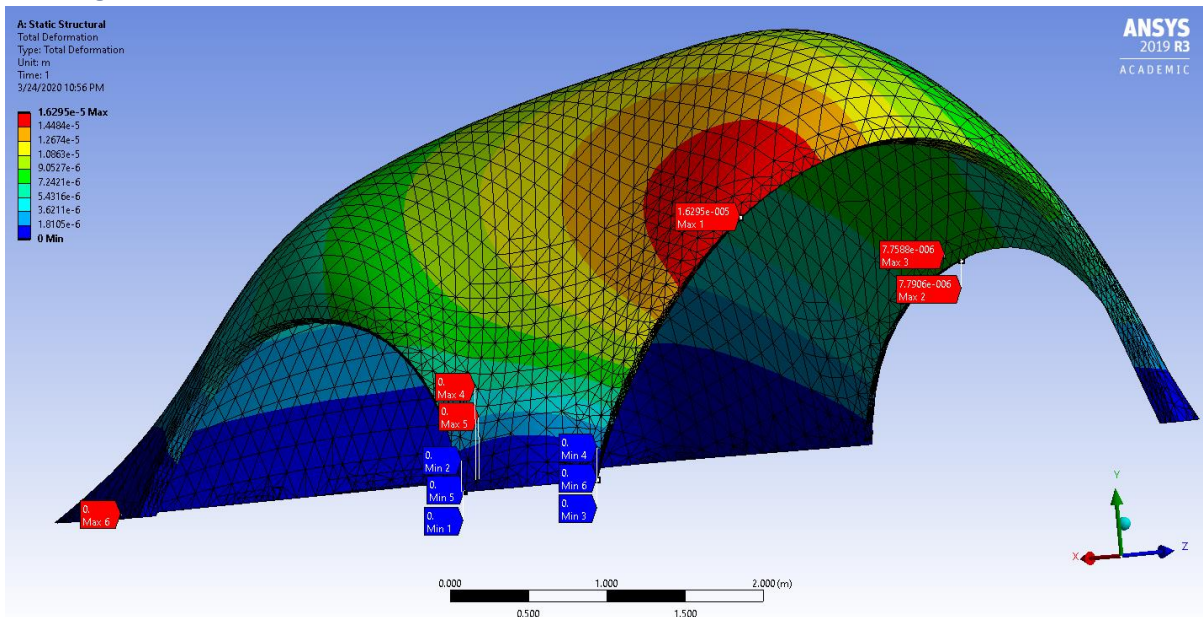


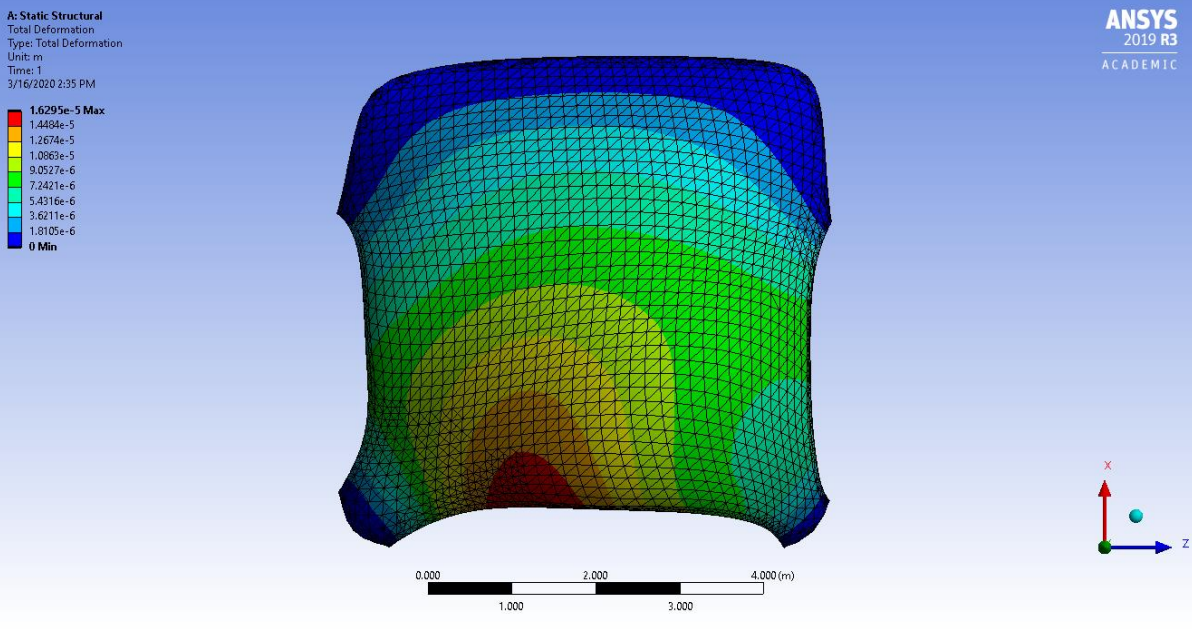
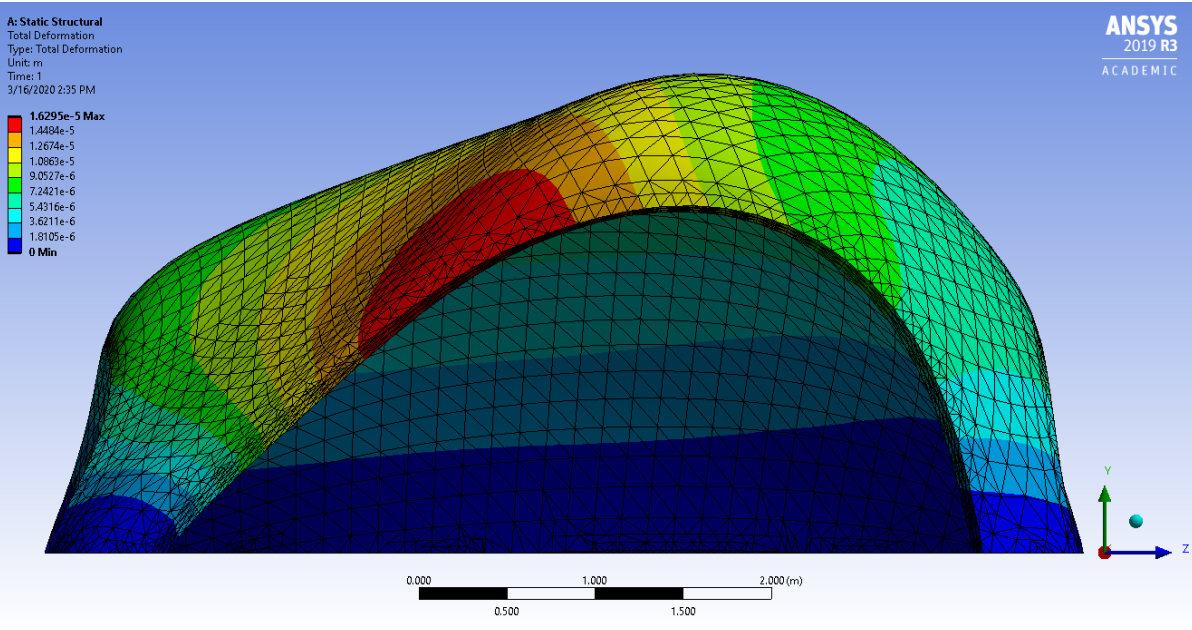


Extruding the thickness could only be done properly using Maya. Rhino is a more suitable for NURBS, Maya is more powerful when editing meshes. The thickness has been divided into several layers (5) this allows TO to choose whether the same thickness is needed everywhere or not. If it was not divided into divisions of

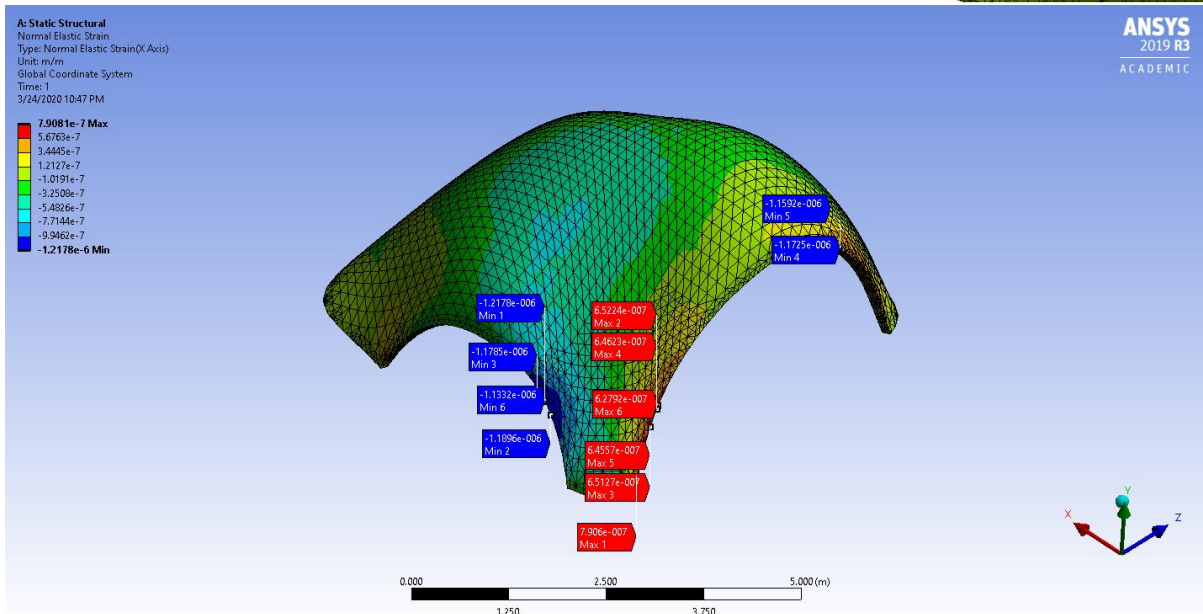
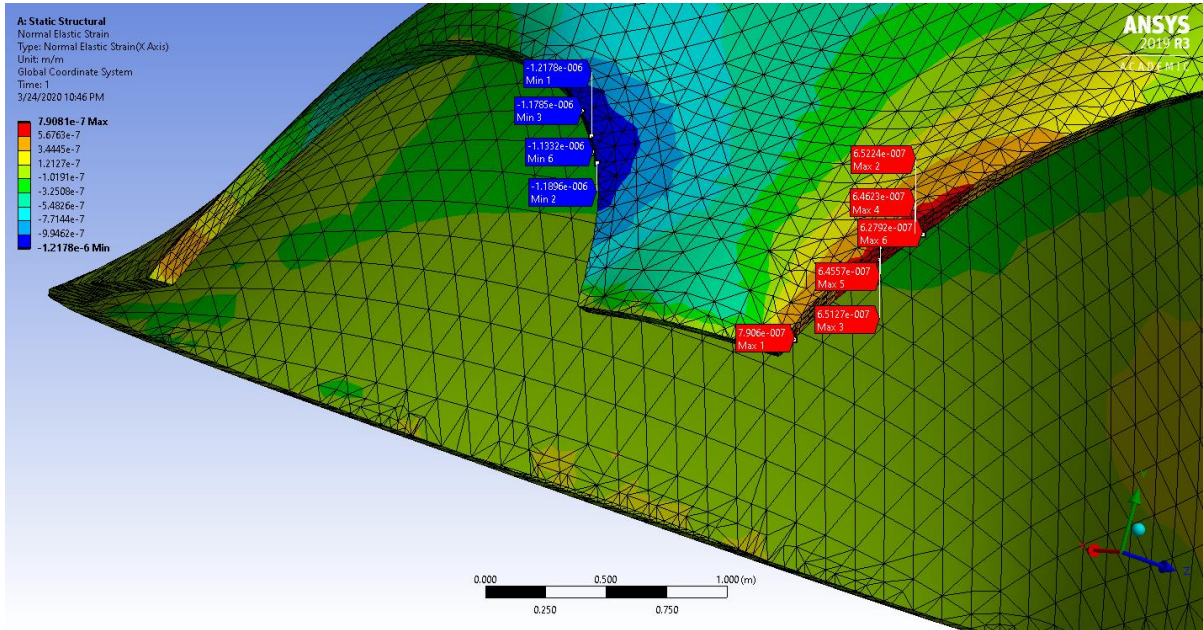
Appendix C: FEA Results from Ansys

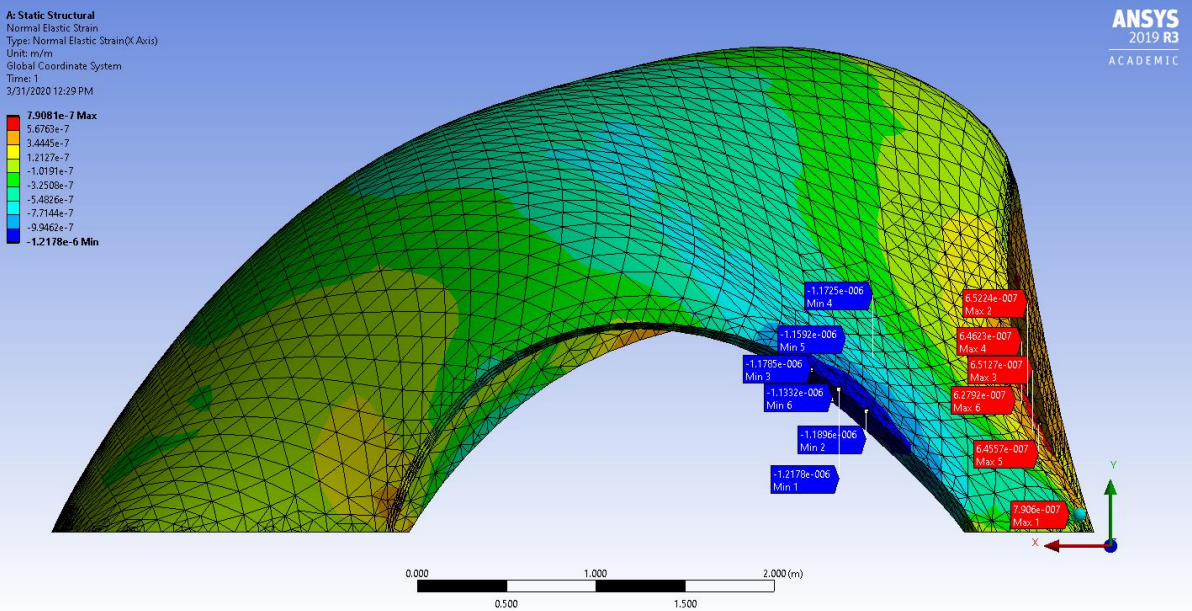
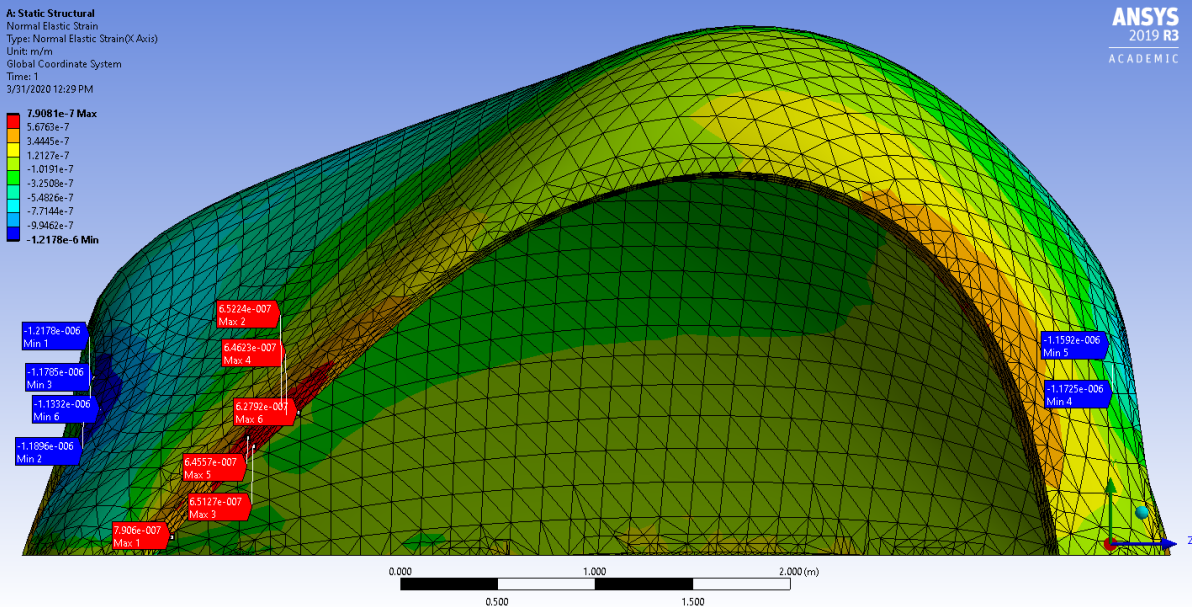
C.1 Original 10cm thick shell – Deformations





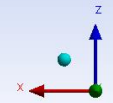
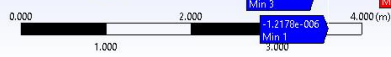
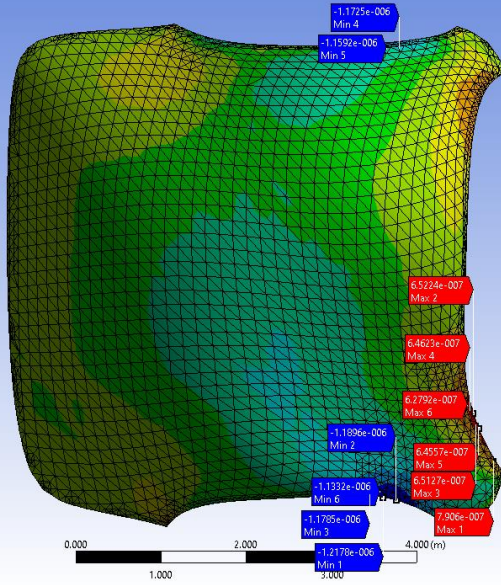
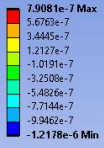
C.2 Original 10 cm shell – Normal Elastic Strain



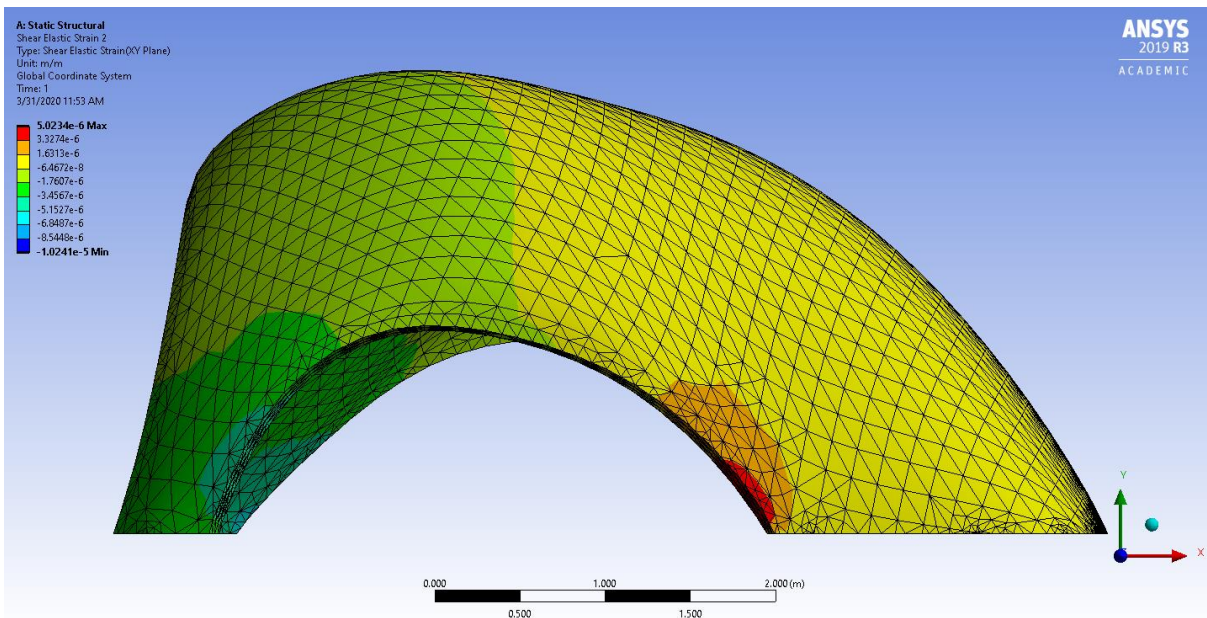
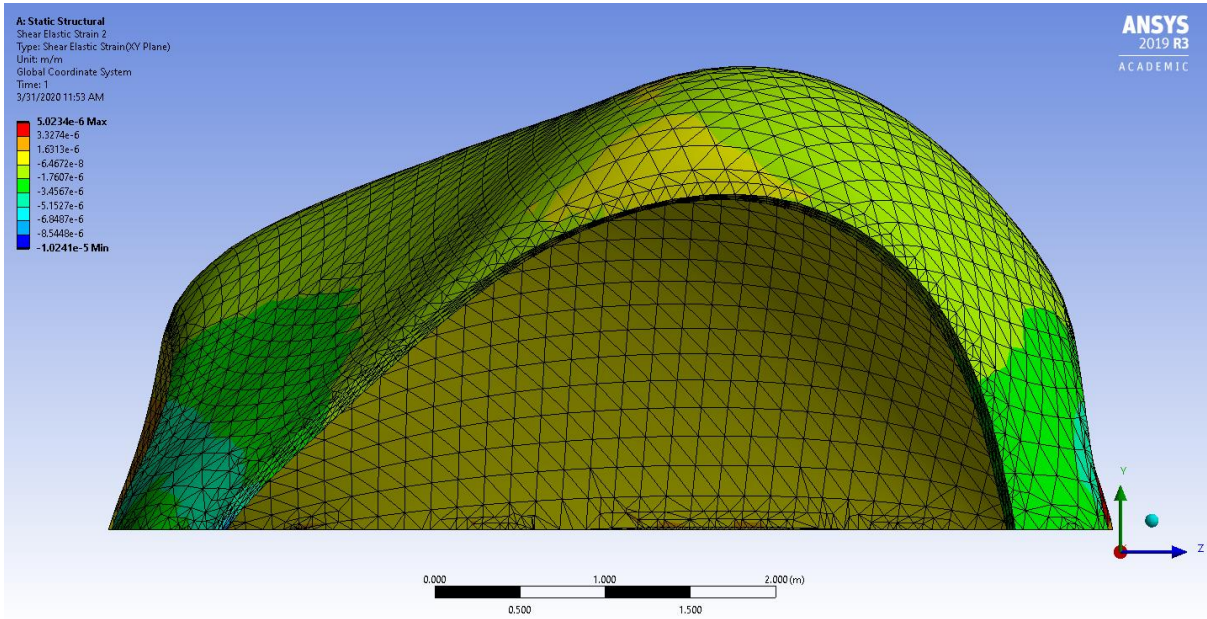


A: Static Structural
Normal Elastic Strain
Type: Normal Elastic Strain(X Axis)
Unit: m/m
Global Coordinate System
Time: 1
3/31/2020 12:29 PM

ANSYS
2019 R3
ACADEMIC



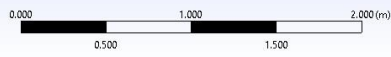
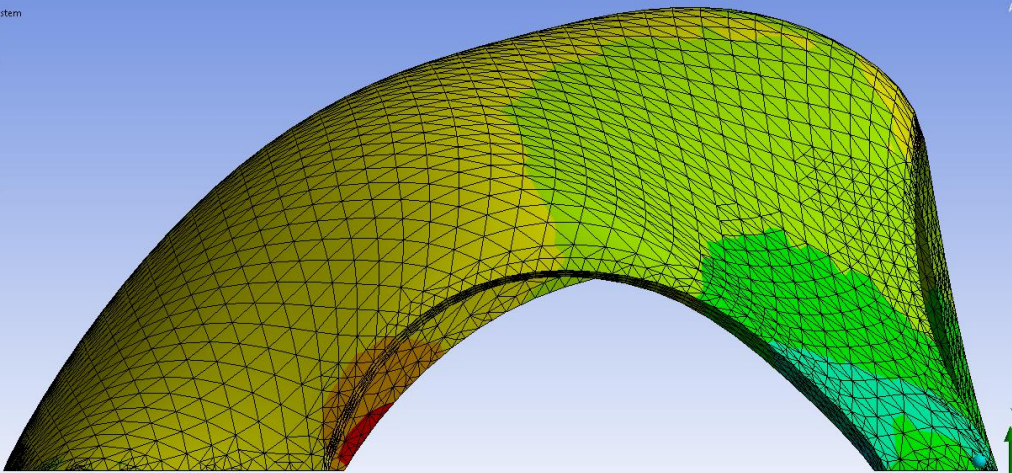
C.3 Original 10 thick shell – Shear elastic strain



A: Static Structural
Shear Elastic Strain 2
Type: Shear Elastic Strain(OY Plane)
Unit: m/m
Global Coordinate System
Time: 1
3/31/2020 11:53 AM

ANSYS
2019 R3
ACADEMIC

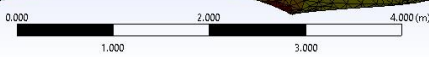
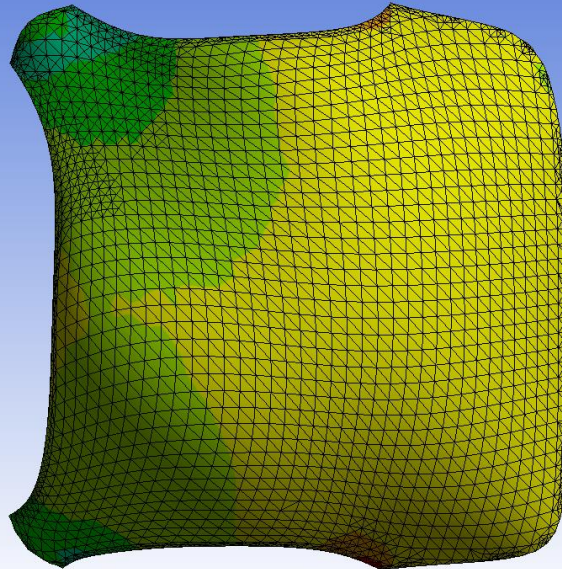
5.0234e-6 Max
3.3274e-6
1.6313e-6
-6.4672e-8
-1.7607e-6
-3.4567e-6
-5.1527e-6
-6.9487e-6
-8.5448e-6
-1.0241e-5 Min

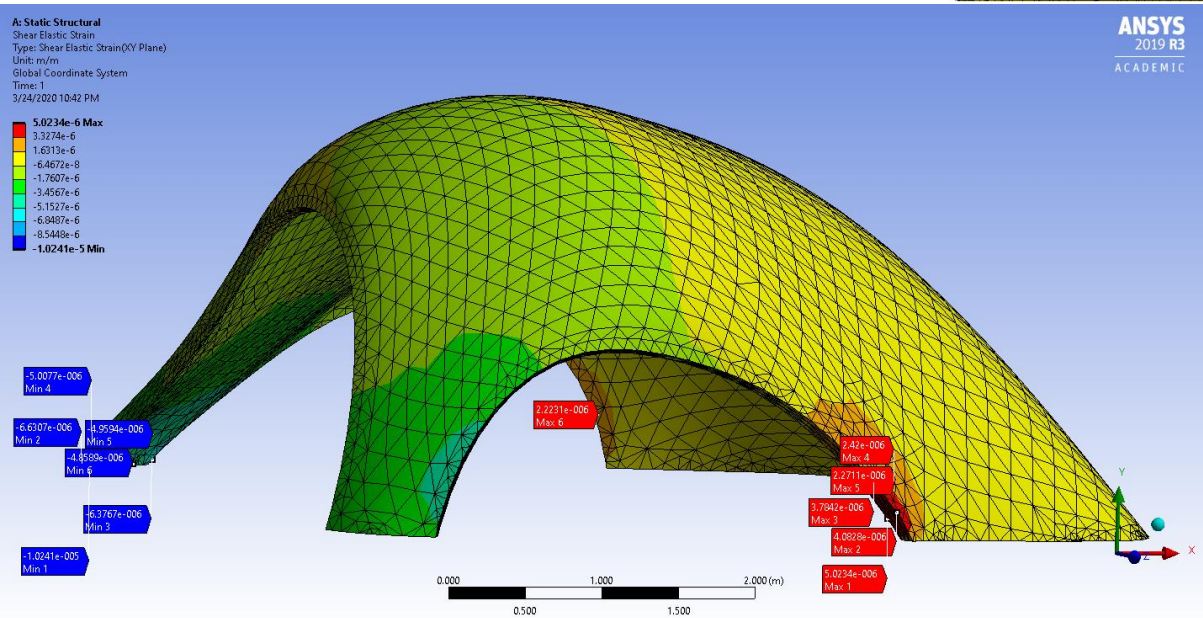
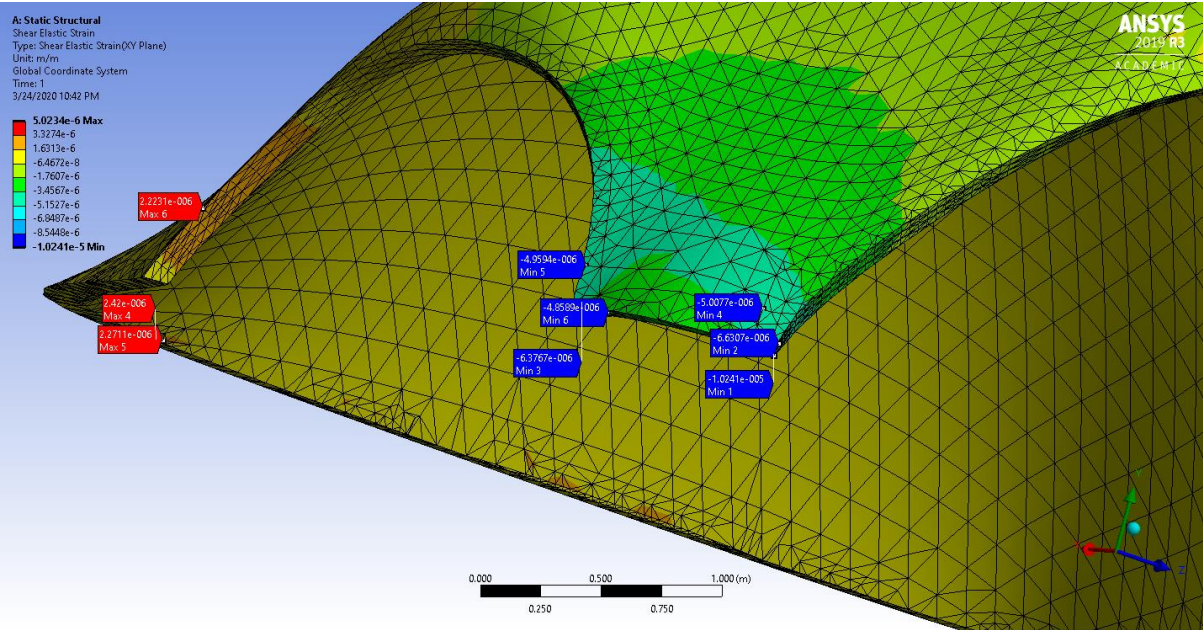


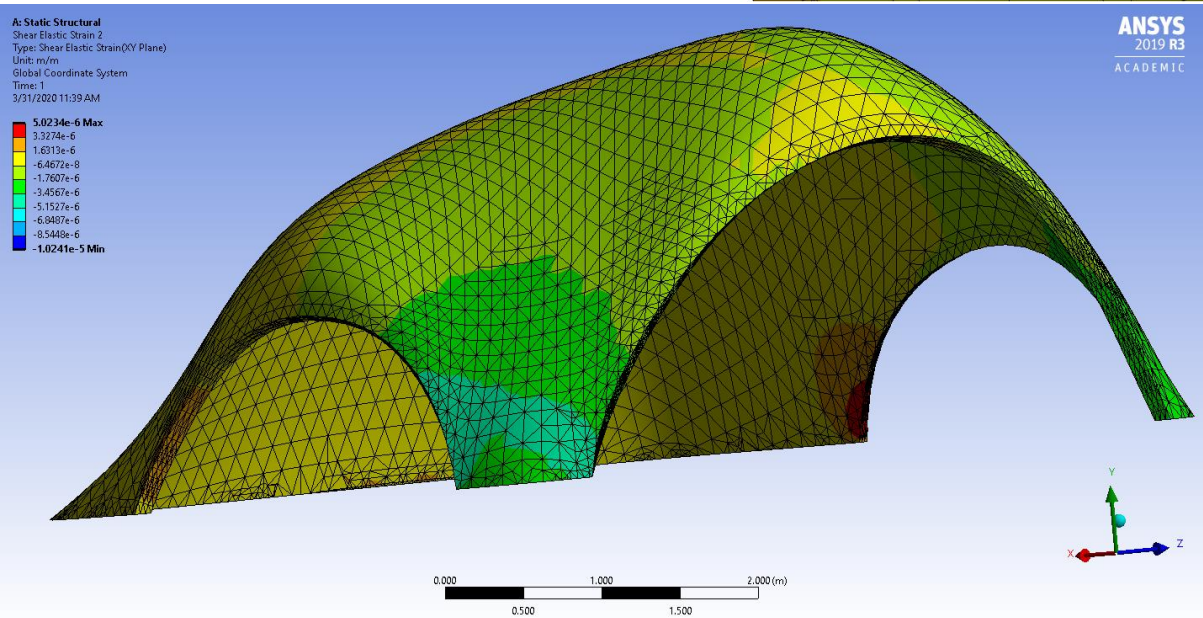
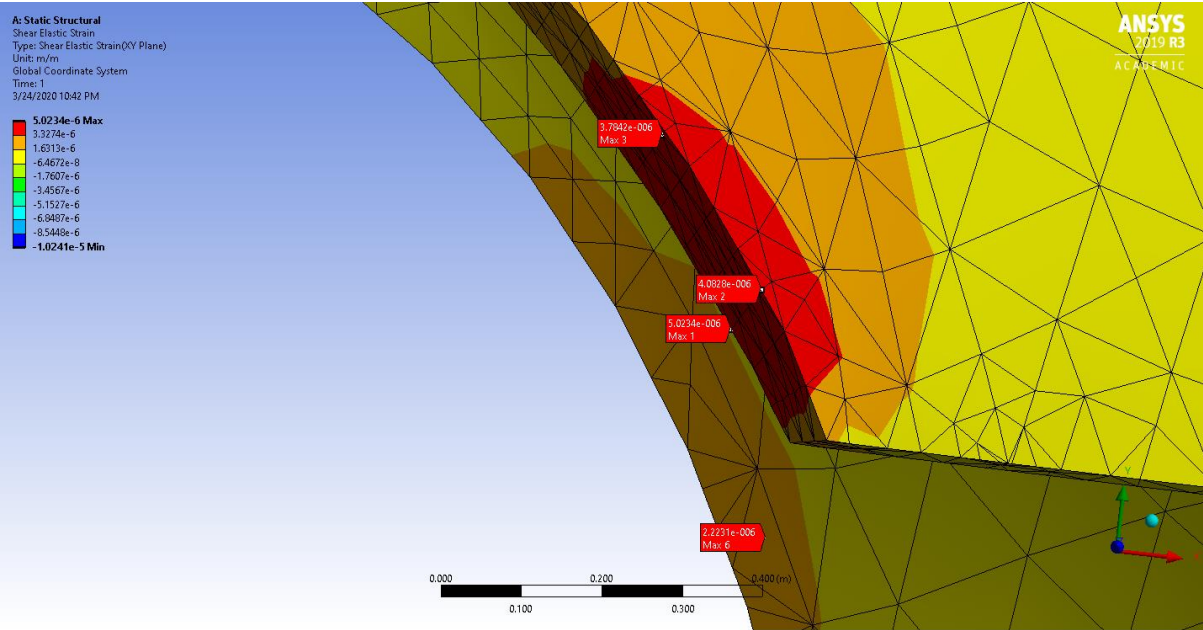
A: Static Structural
Shear Elastic Strain 2
Type: Shear Elastic Strain(OY Plane)
Unit: m/m
Global Coordinate System
Time: 1
3/31/2020 11:53 AM

ANSYS
2019 R3
ACADEMIC

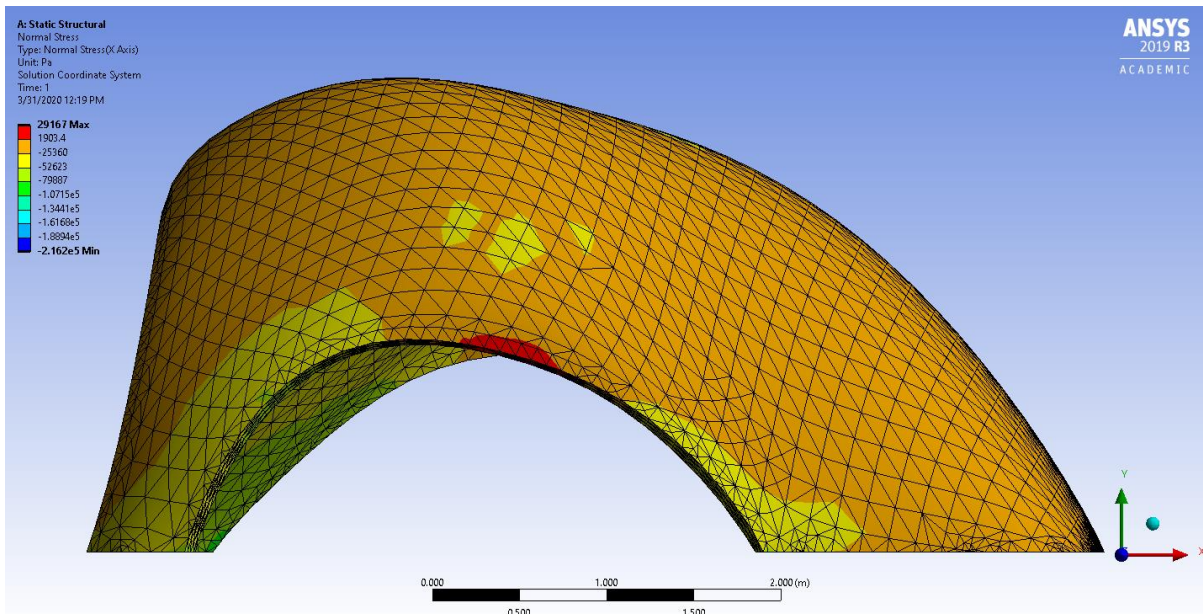
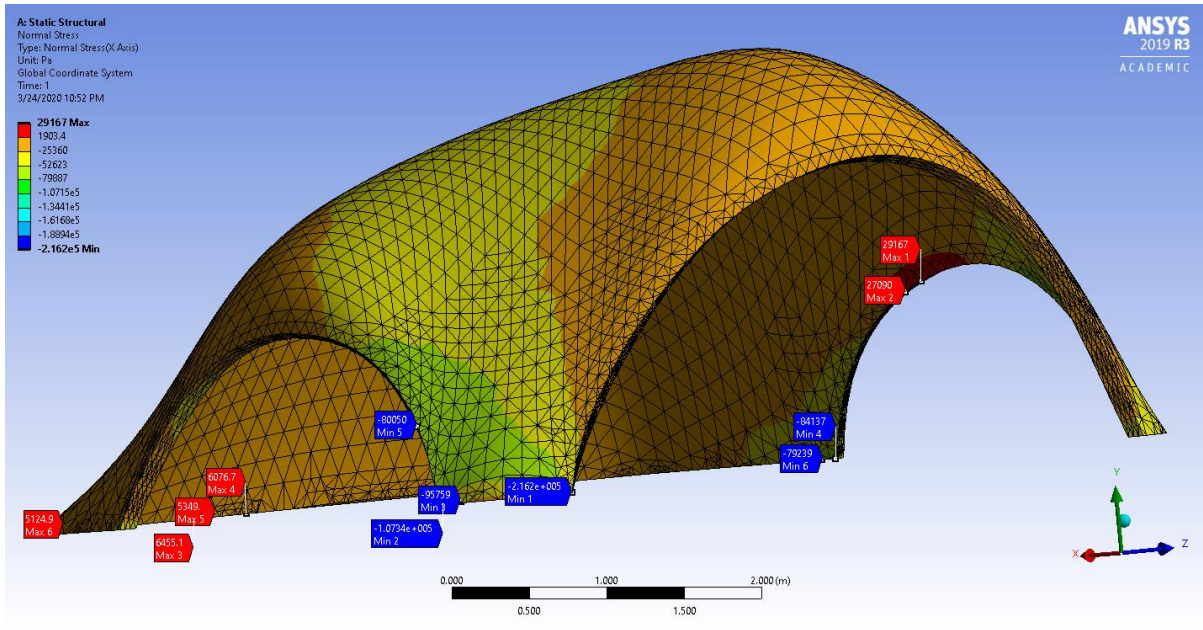
5.0234e-6 Max
3.3274e-6
1.6313e-6
-6.4672e-8
-1.7607e-6
-3.4567e-6
-5.1527e-6
-6.9487e-6
-8.5448e-6
-1.0241e-5 Min

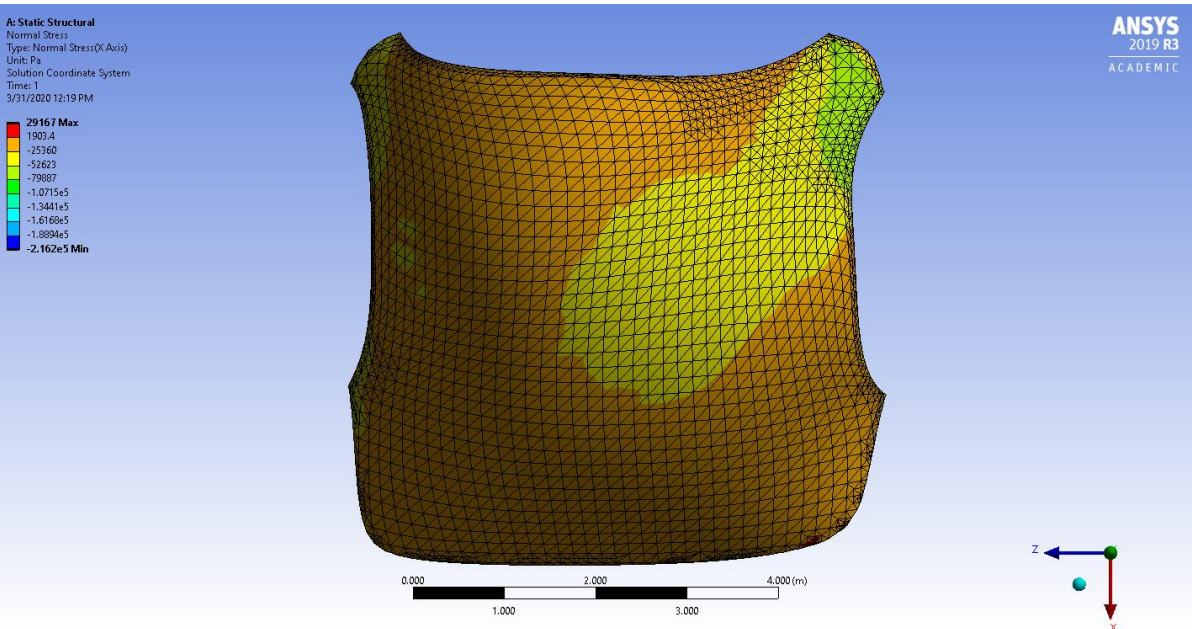
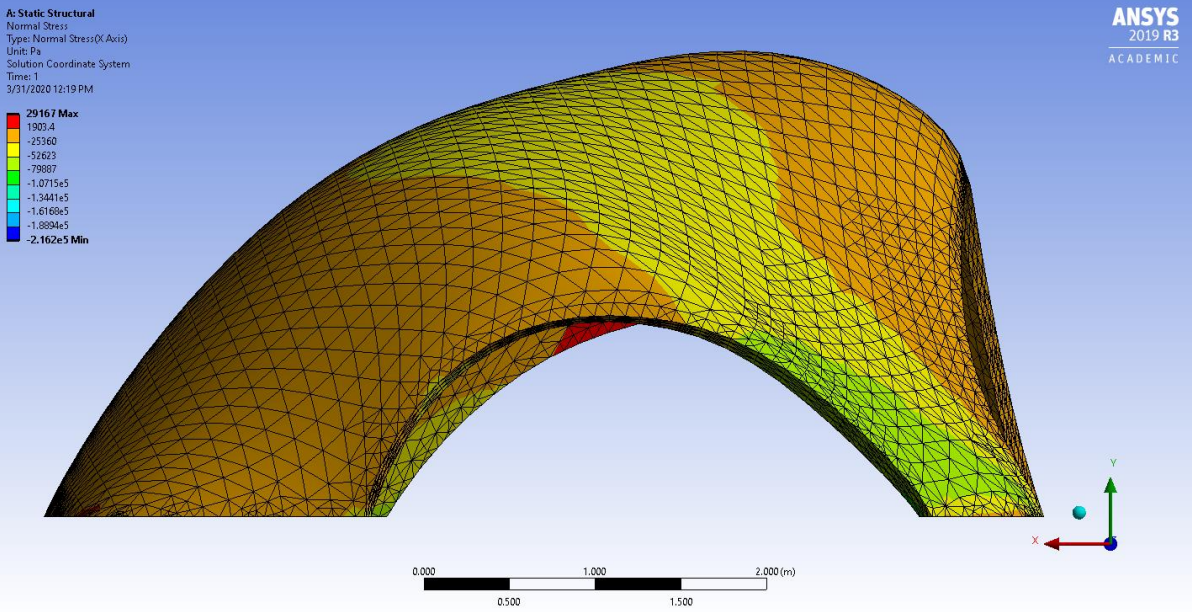




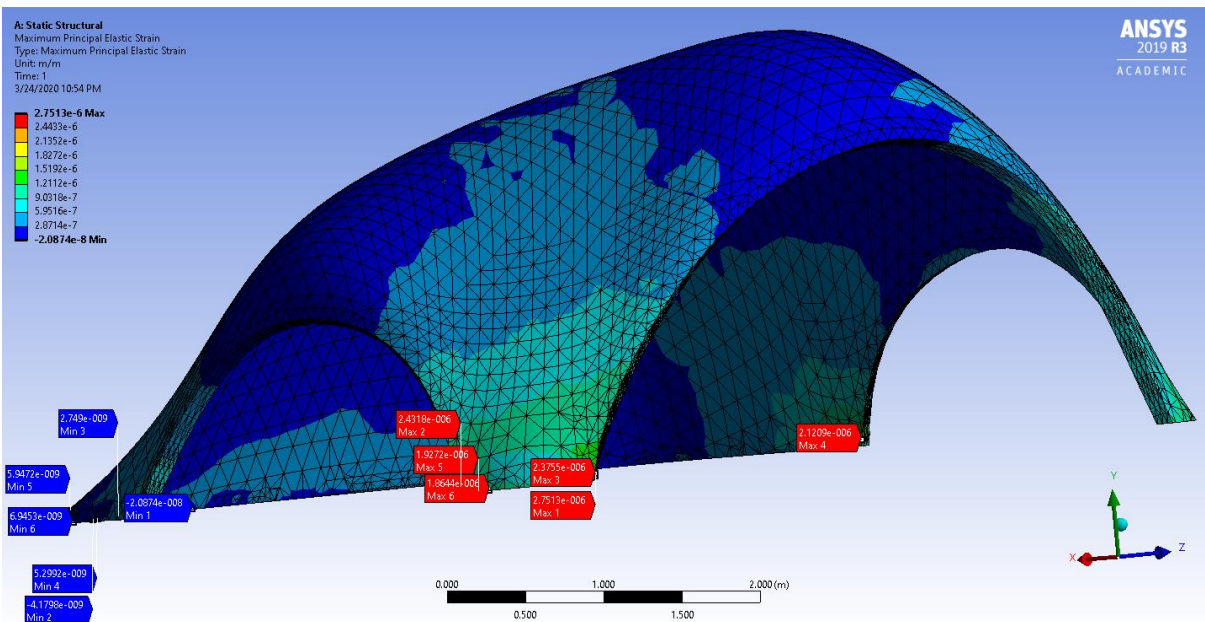
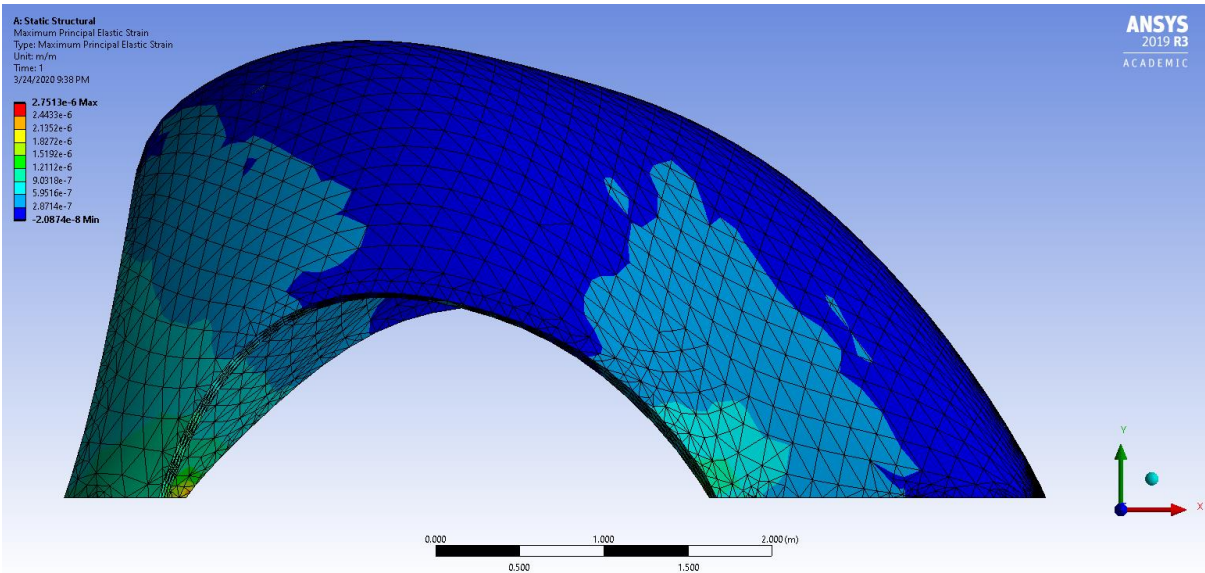
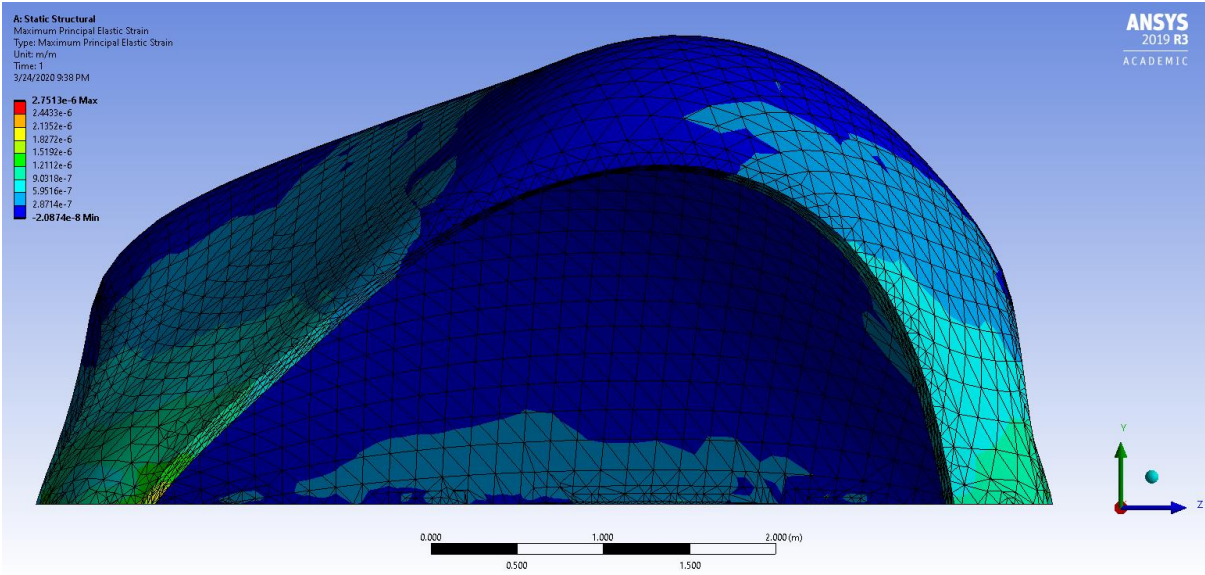


C.4 Original 10 cm shell – Normal stress

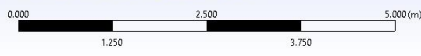
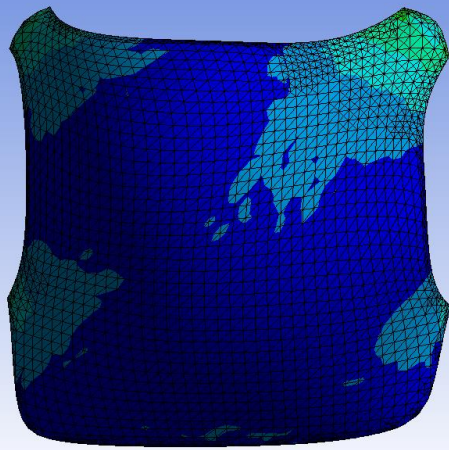
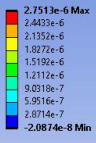




C.5 Original 10 cm shell – Maximum Principal Elastic Strain

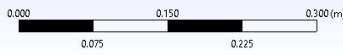
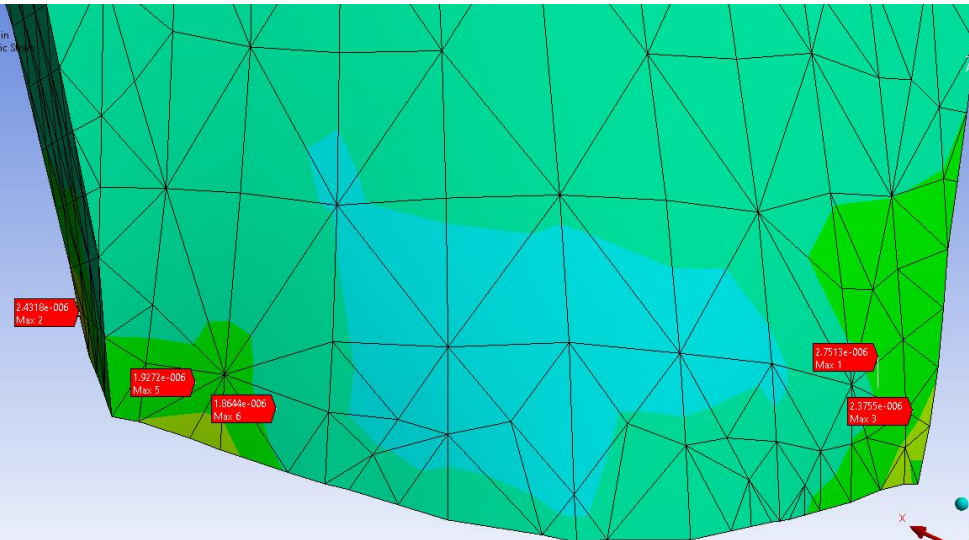
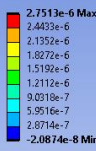


A: Static Structural
Maximum Principal Elastic Strain
Type: Maximum Principal Elastic Strain
Unit: m/m
Time: 1
3/24/2020 9:38 PM



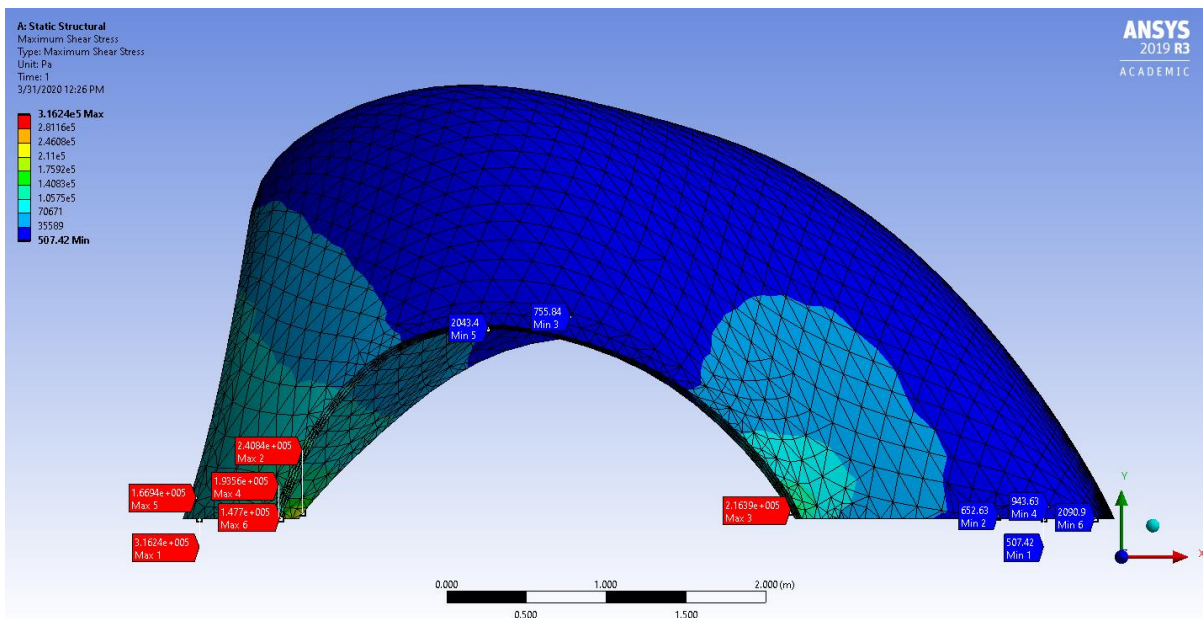
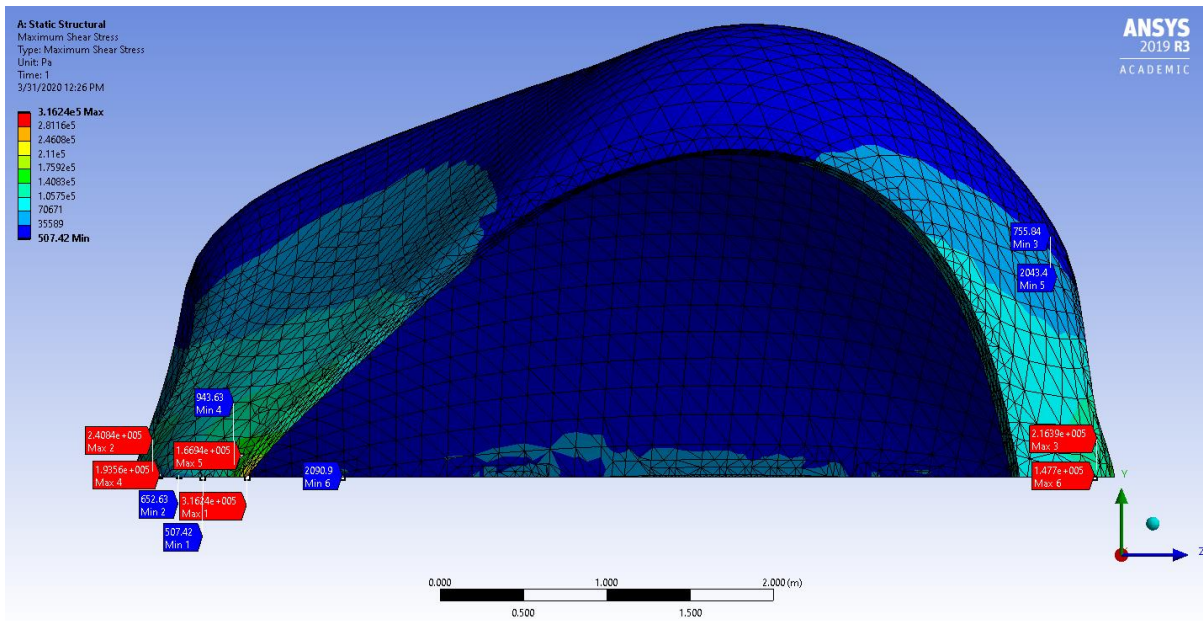
ANSYS
2019 R3
ACADEMIC

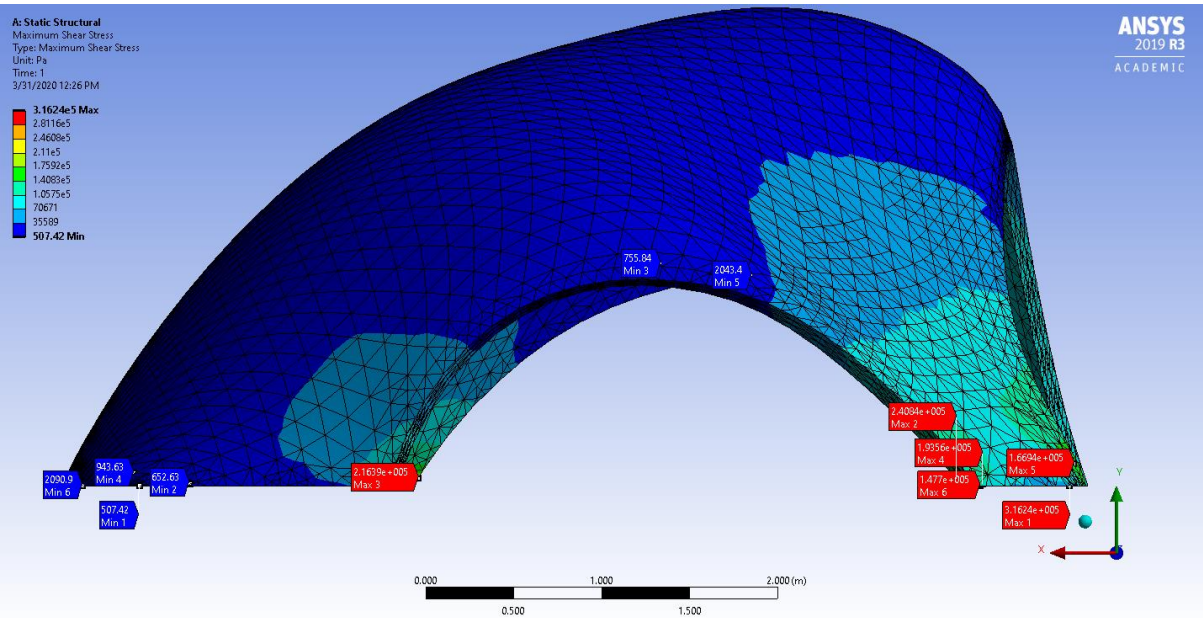
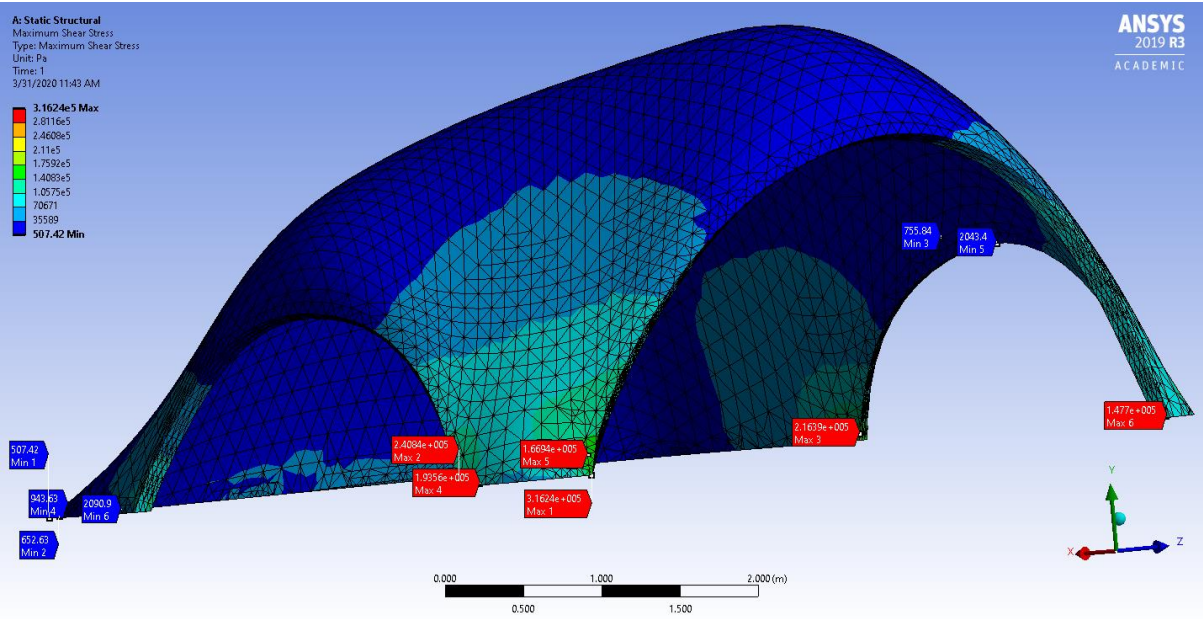
A: Static Structural
Maximum Principal Elastic Strain
Type: Maximum Principal Elastic Strain
Unit: m/m
Time: 1
3/24/2020 9:42 PM



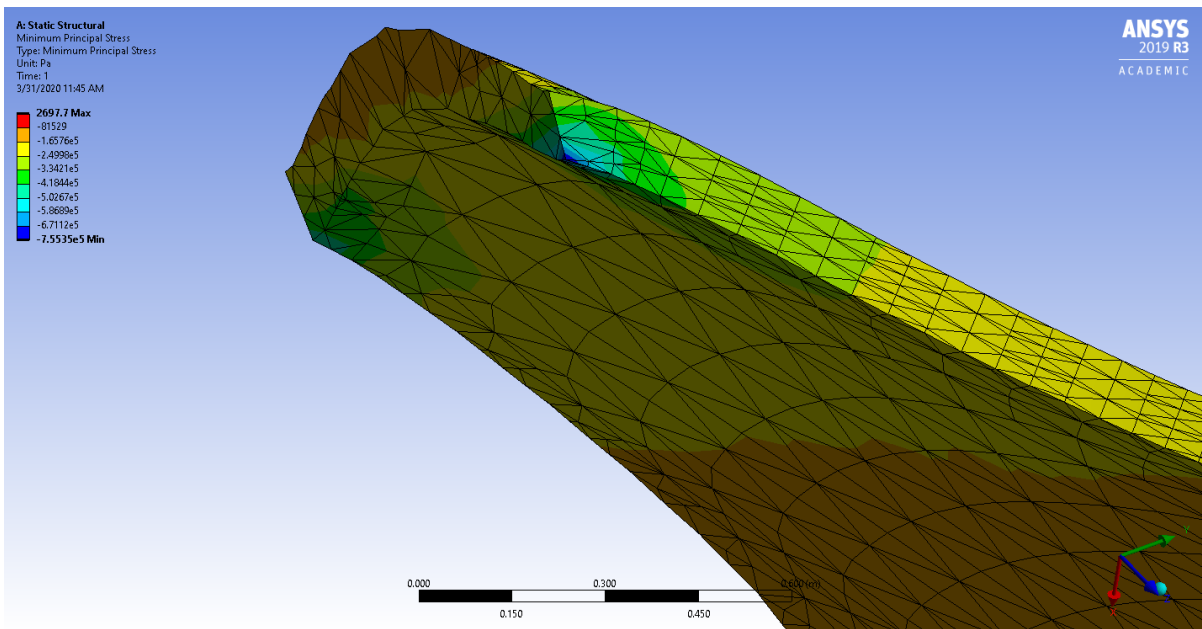
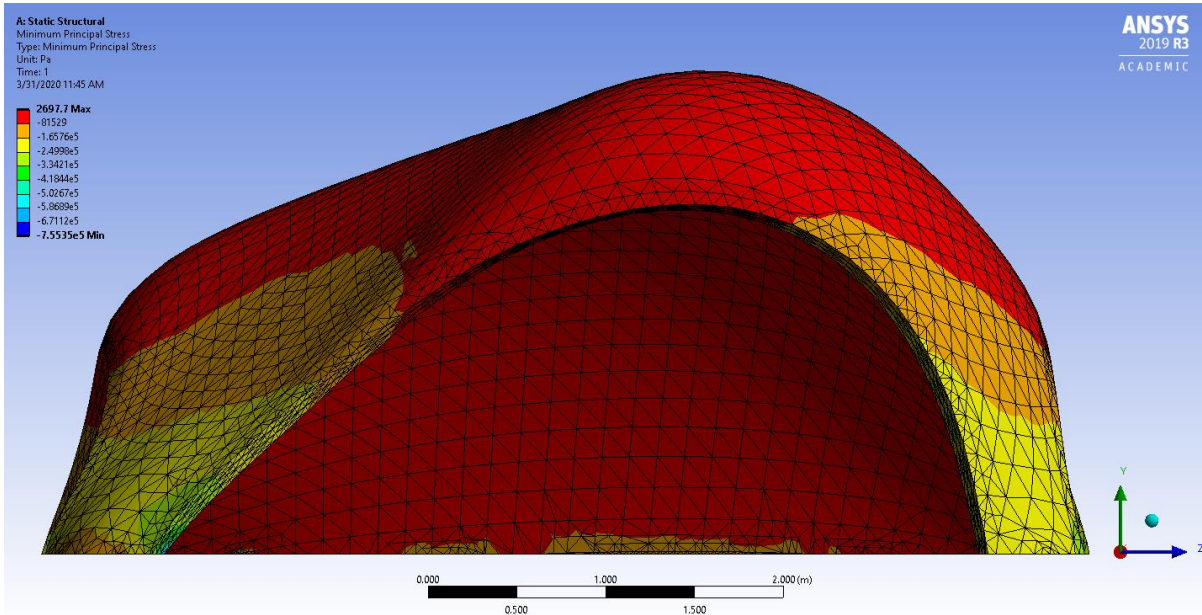
ANSYS
2019 R3
ACADEMIC

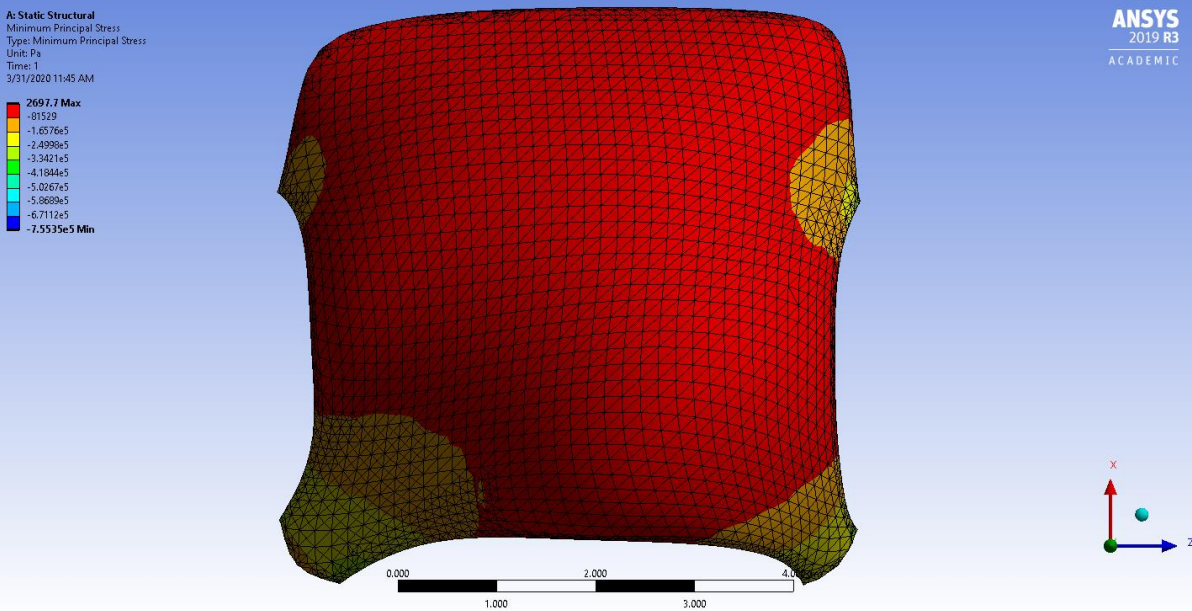
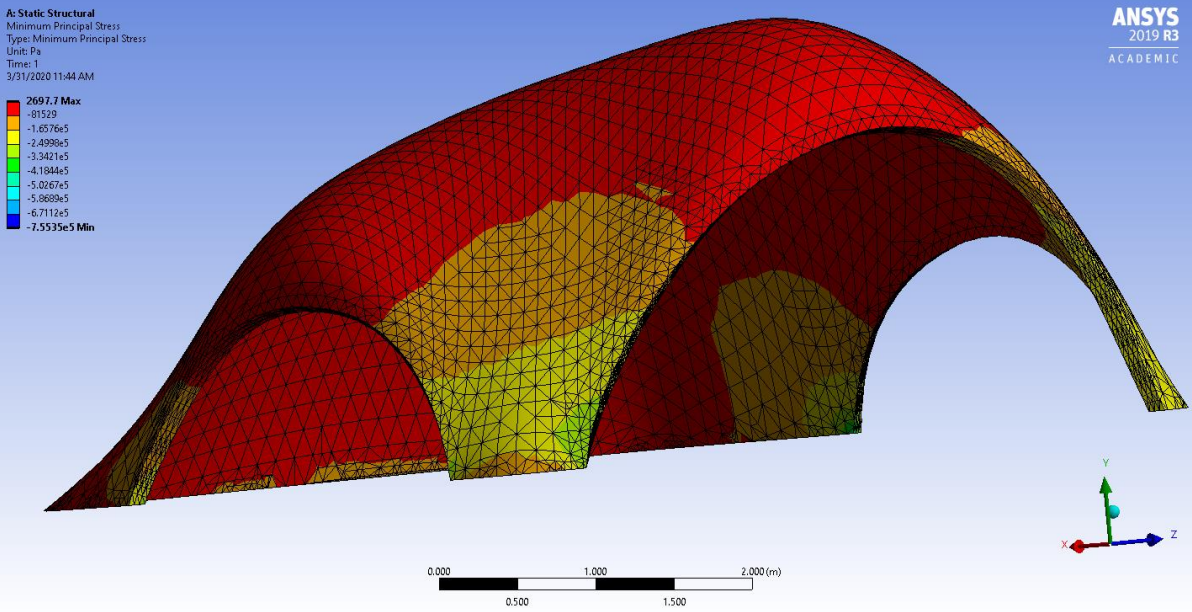
C.6 Original 10 cm shell - Maximum shear stress



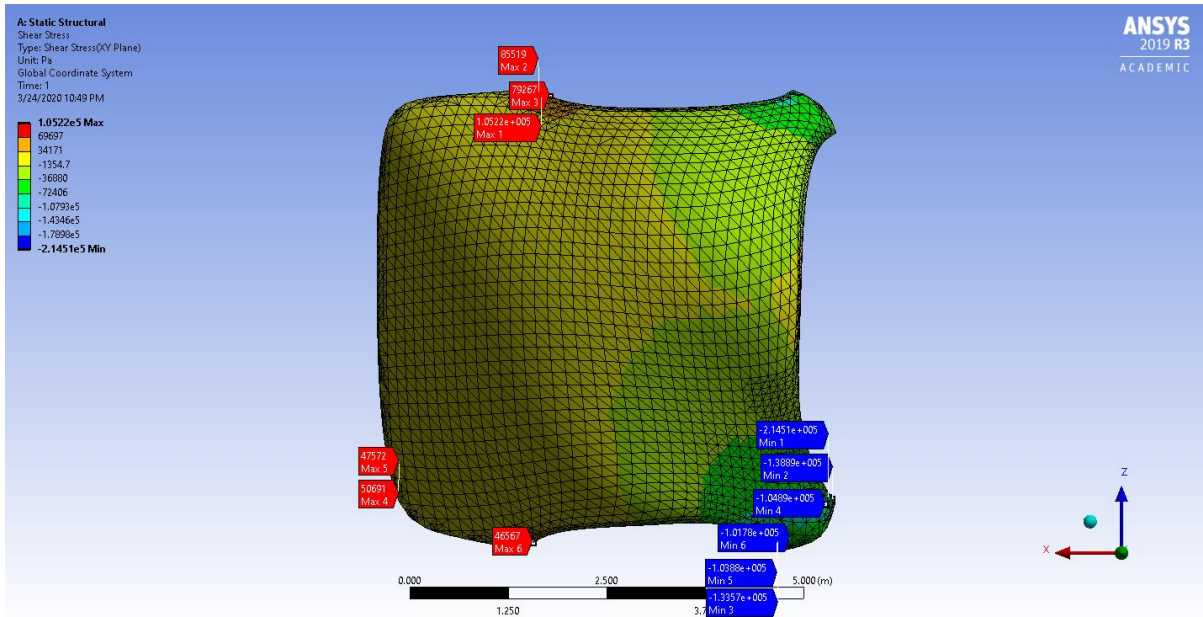


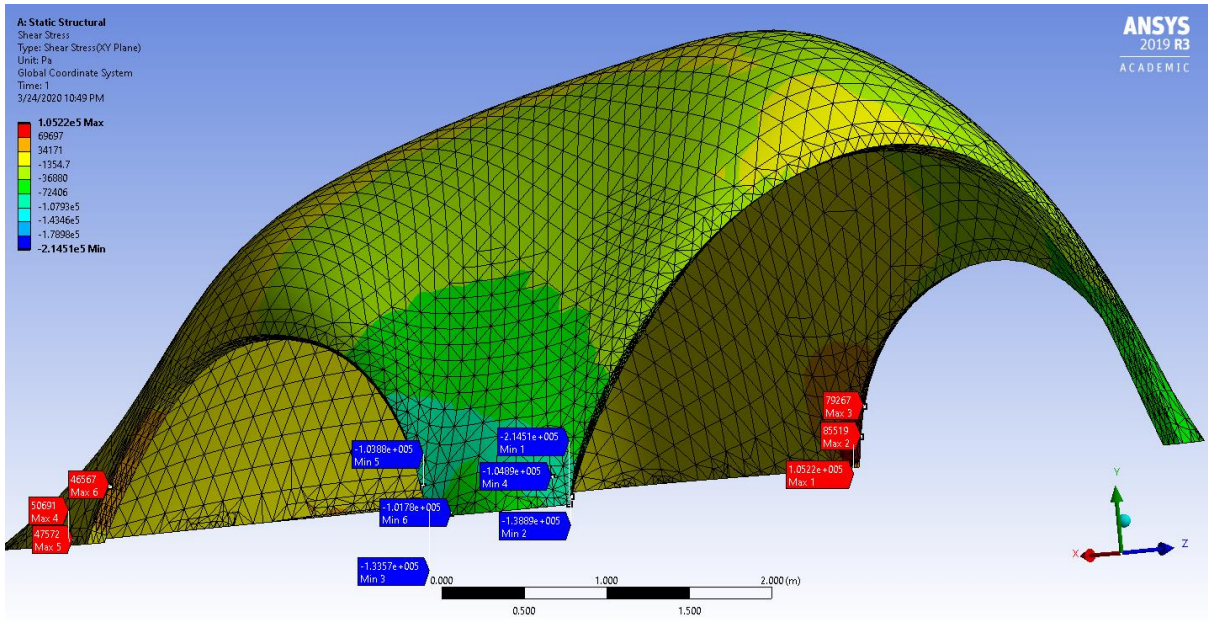
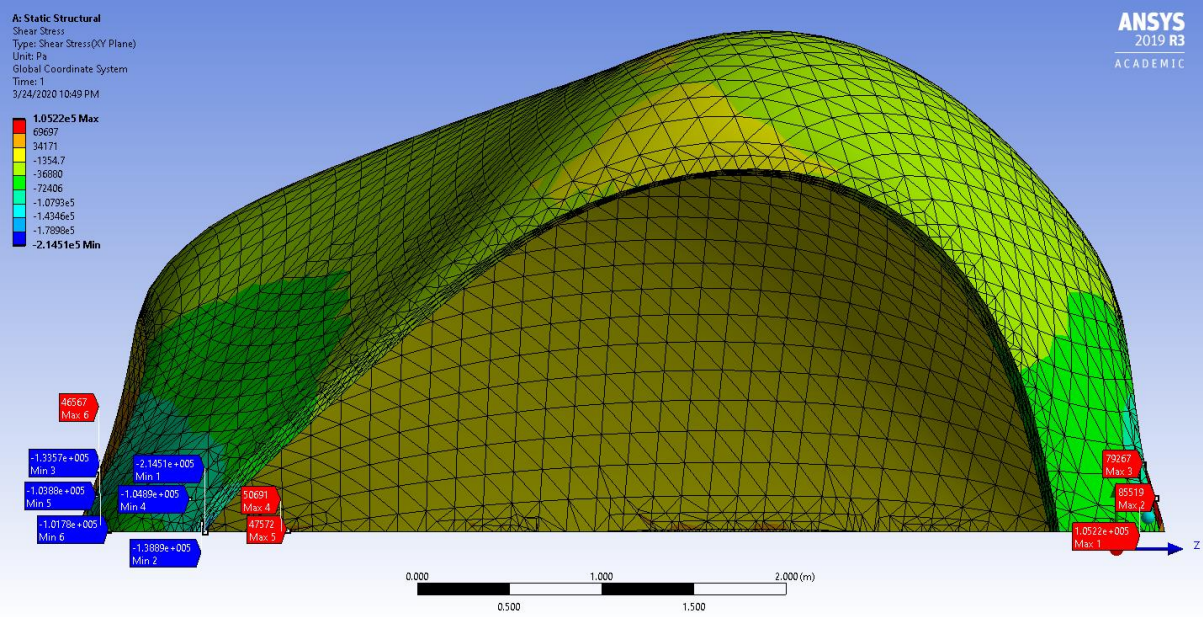
C.7 Original 10 cm shell – Minimum Principal Stress



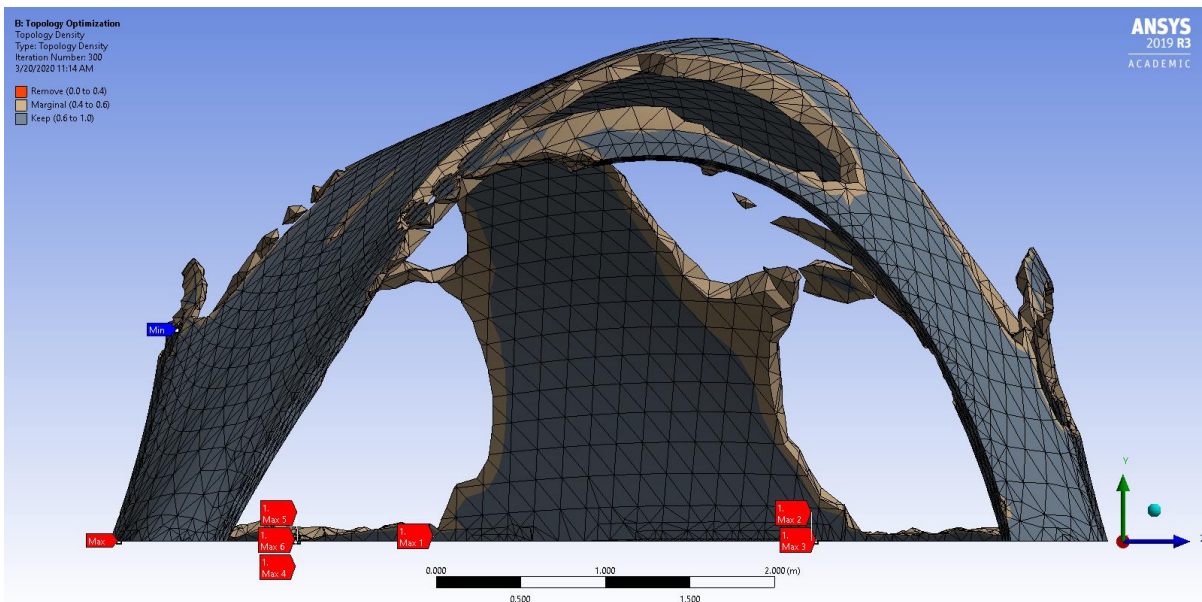
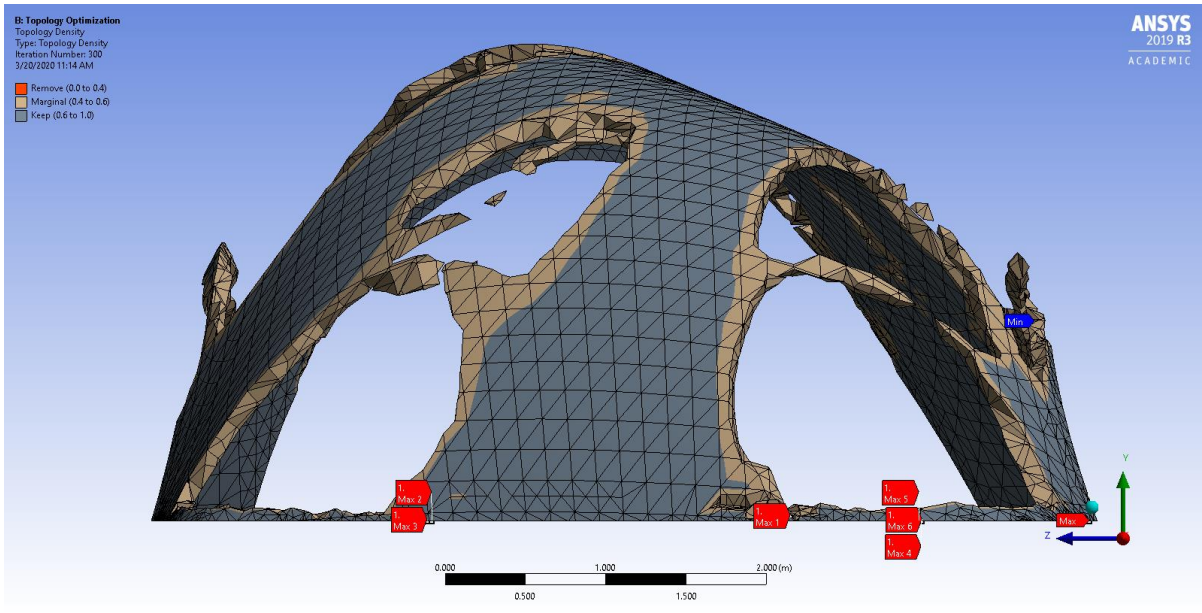


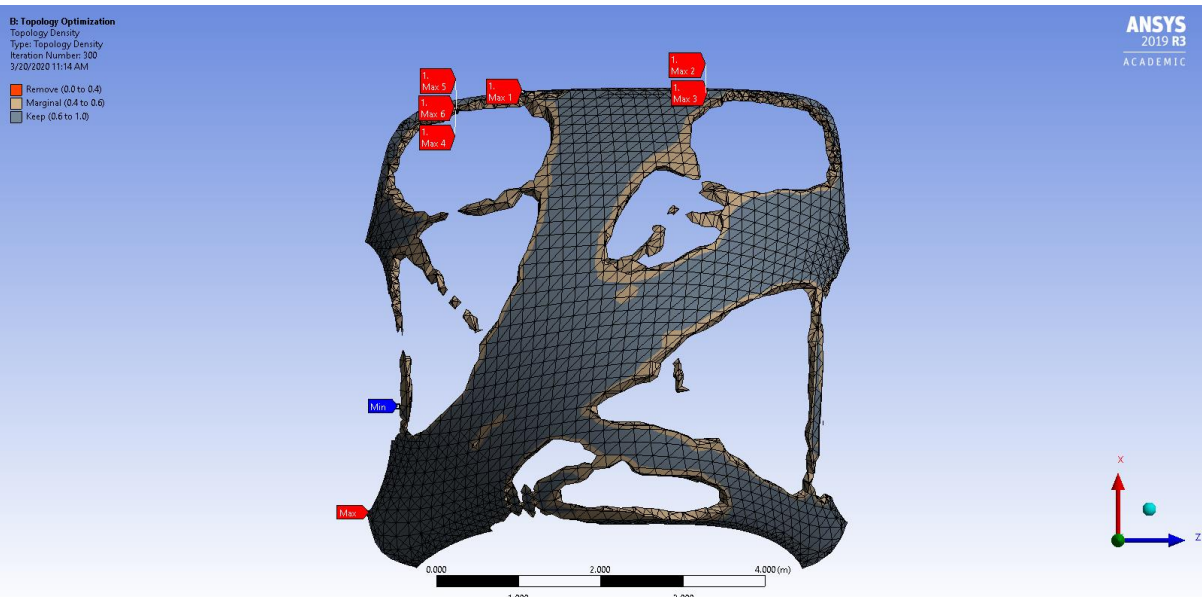
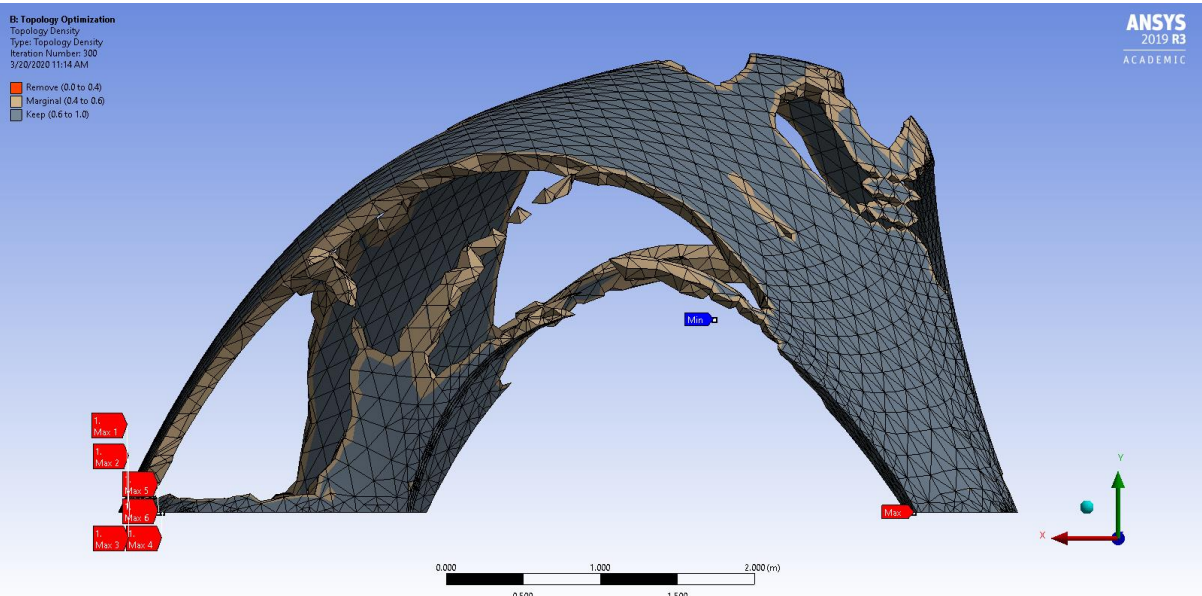
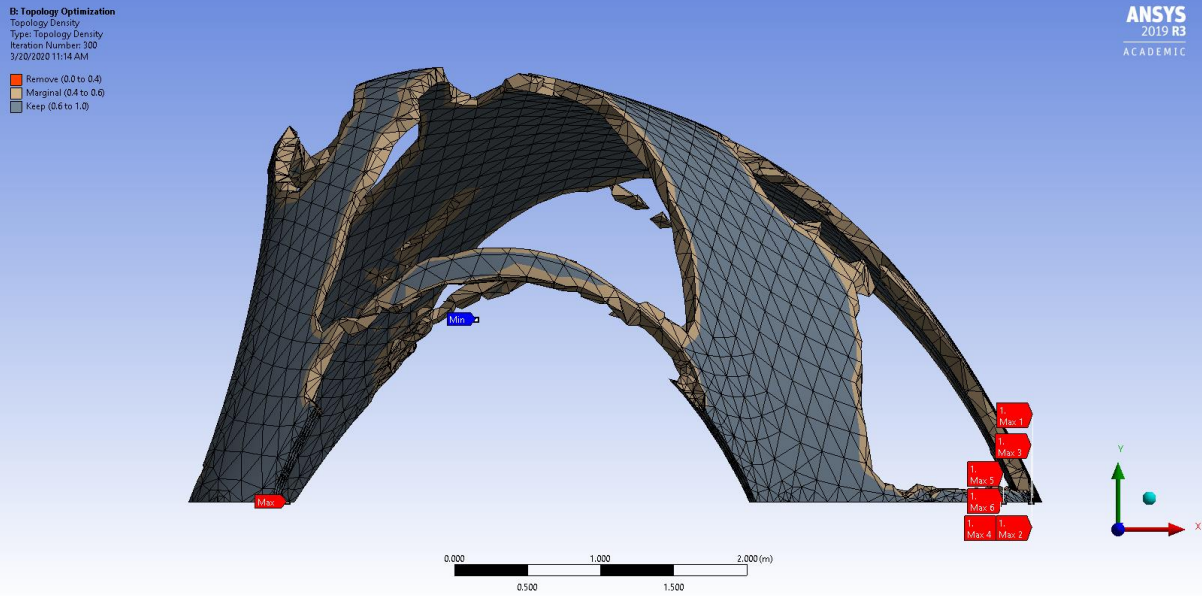
C.8 Original 10 cm shell – Shear Stress



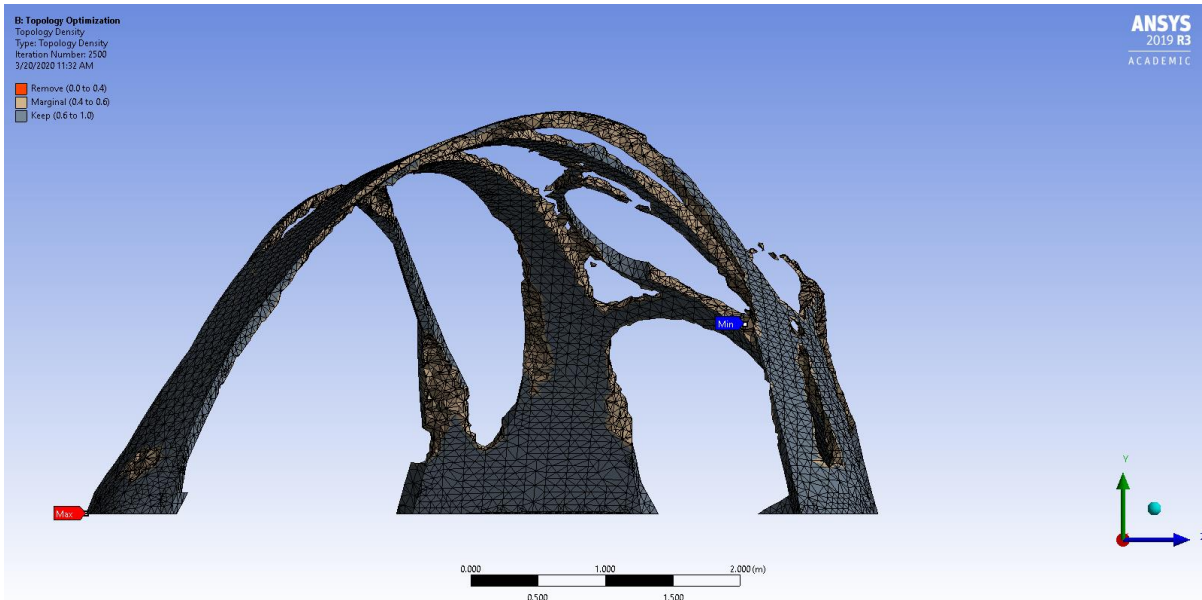
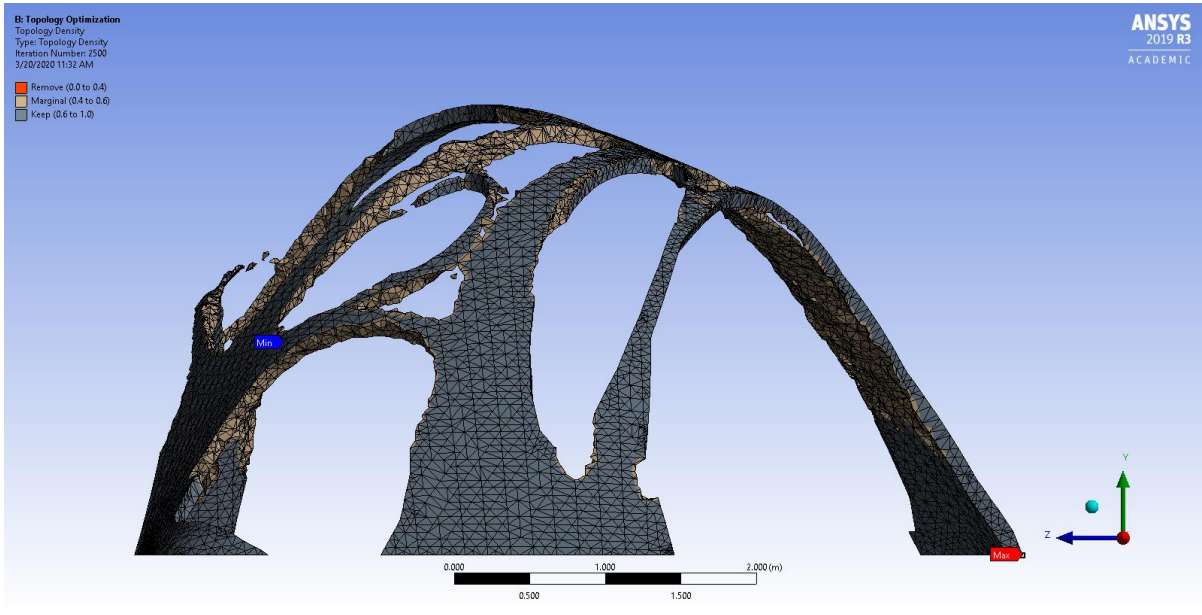


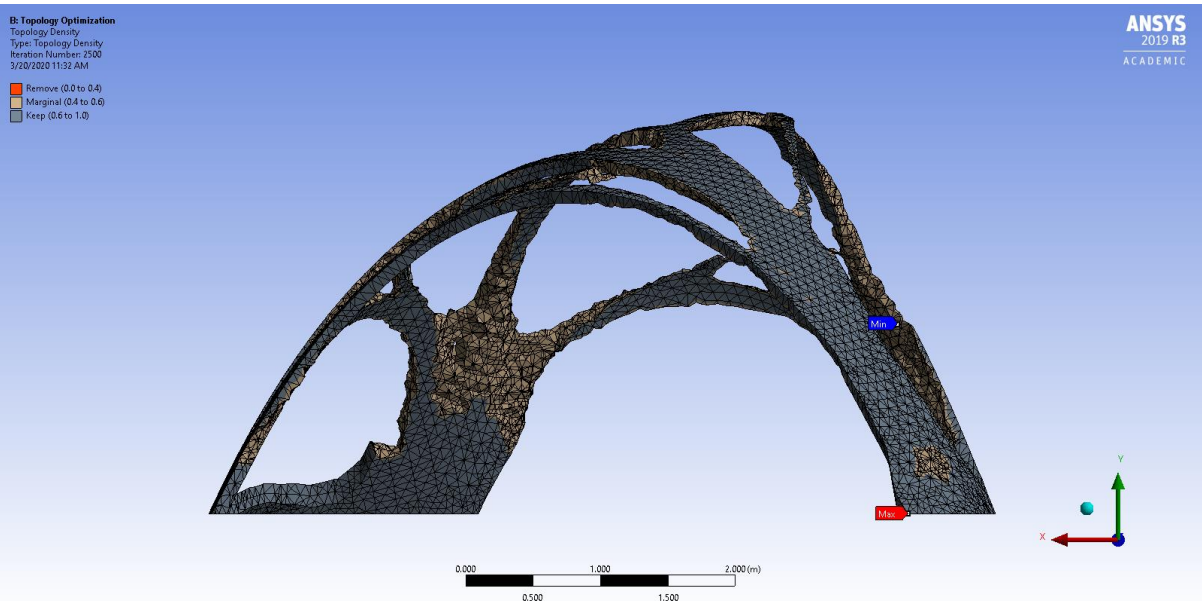
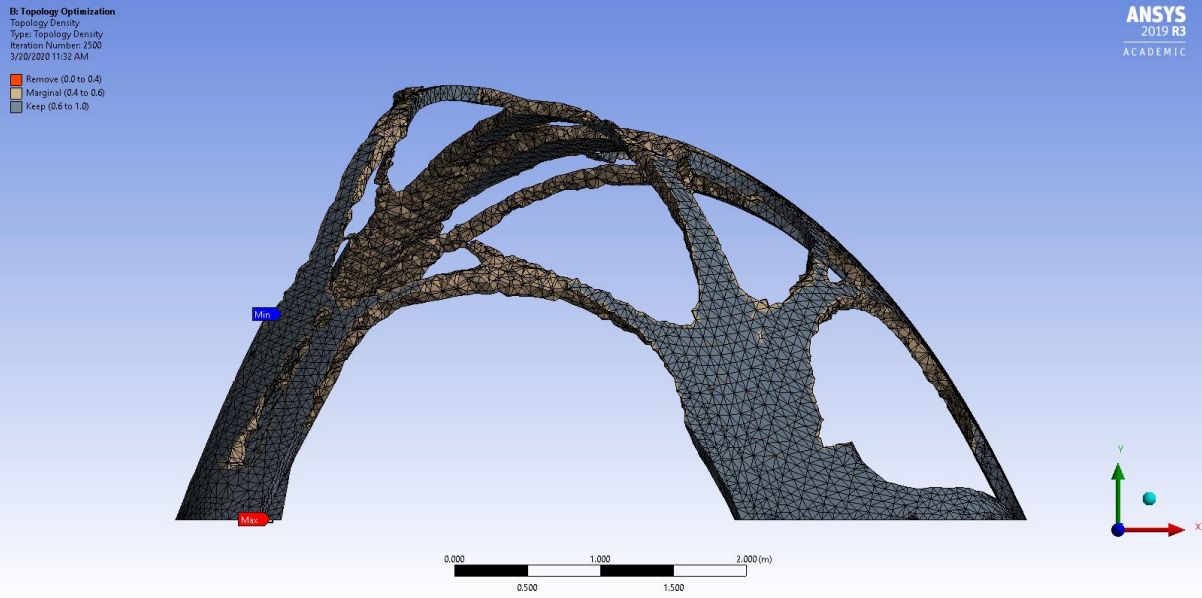
C.9 First Topology optimisation – Results



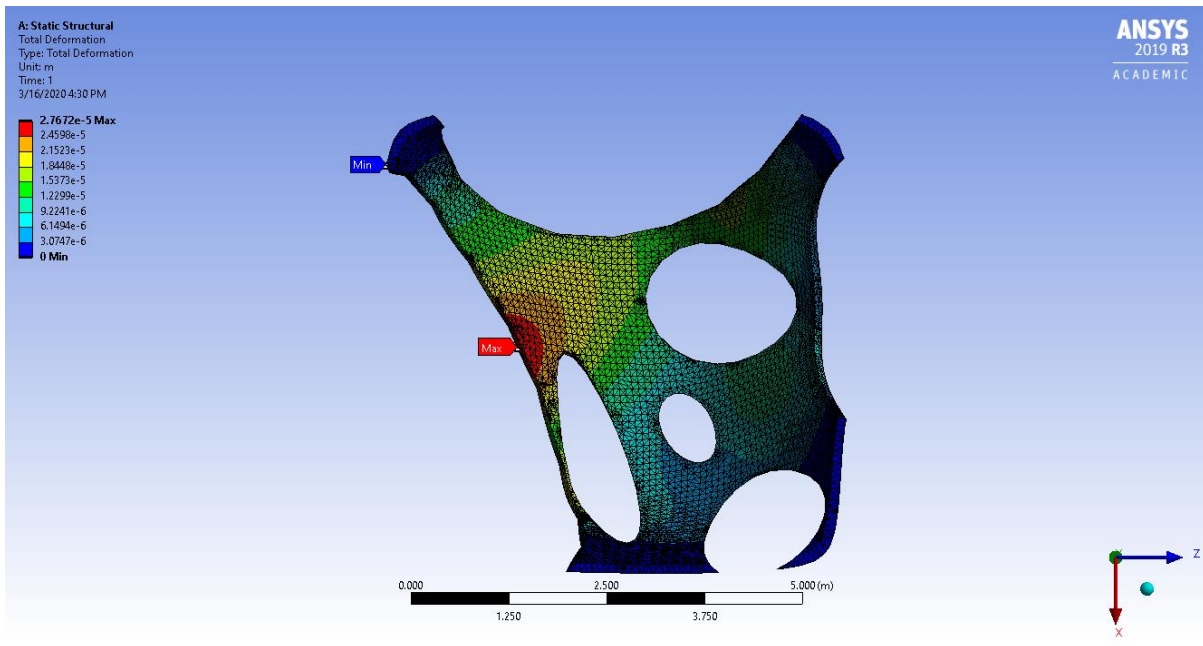
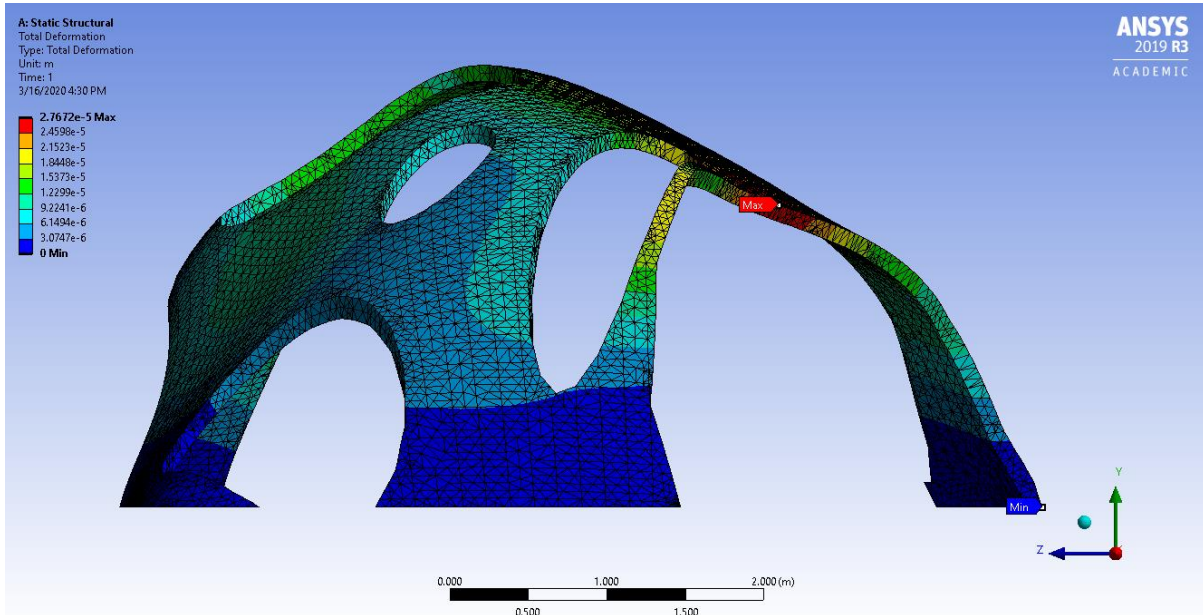


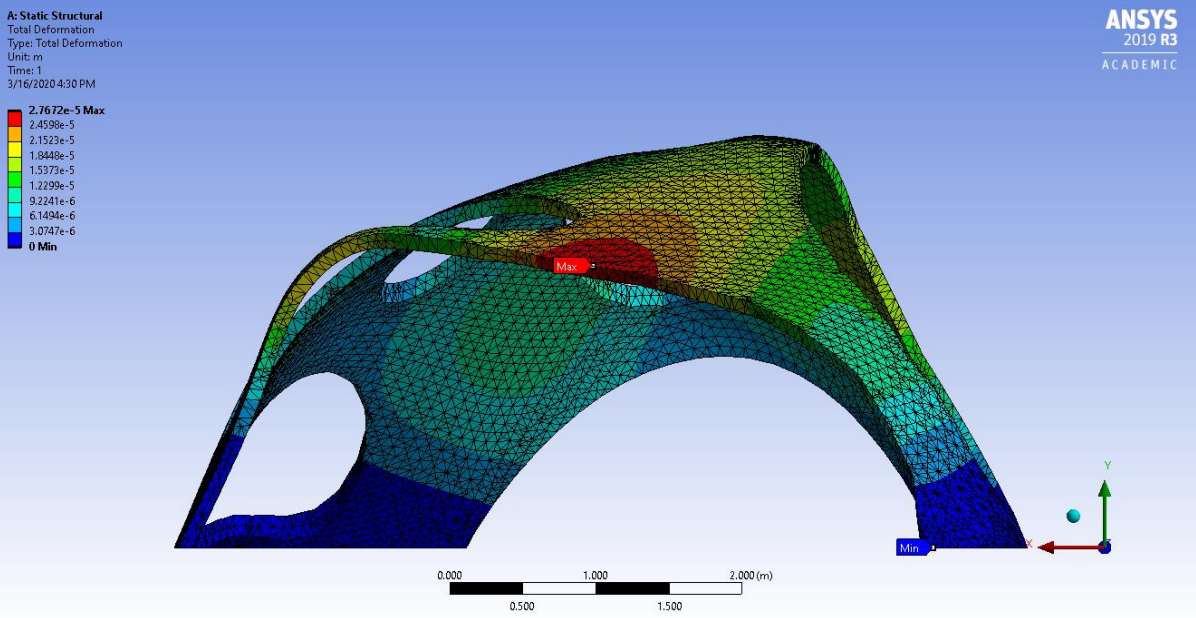
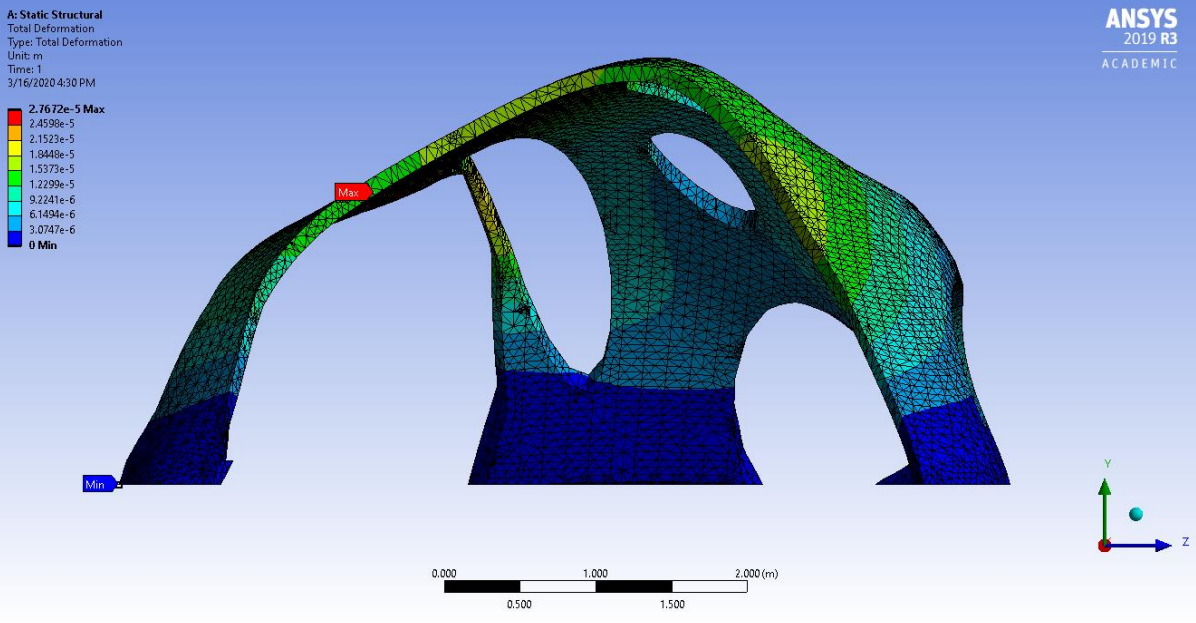
C.10 Second Topology optimisation – Results

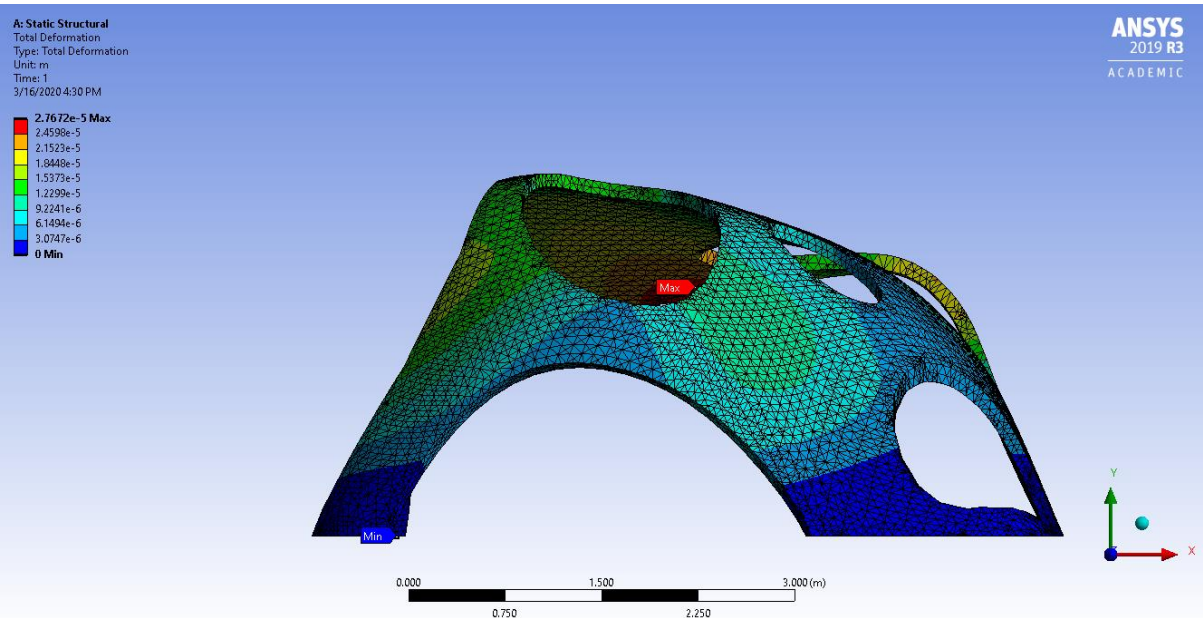
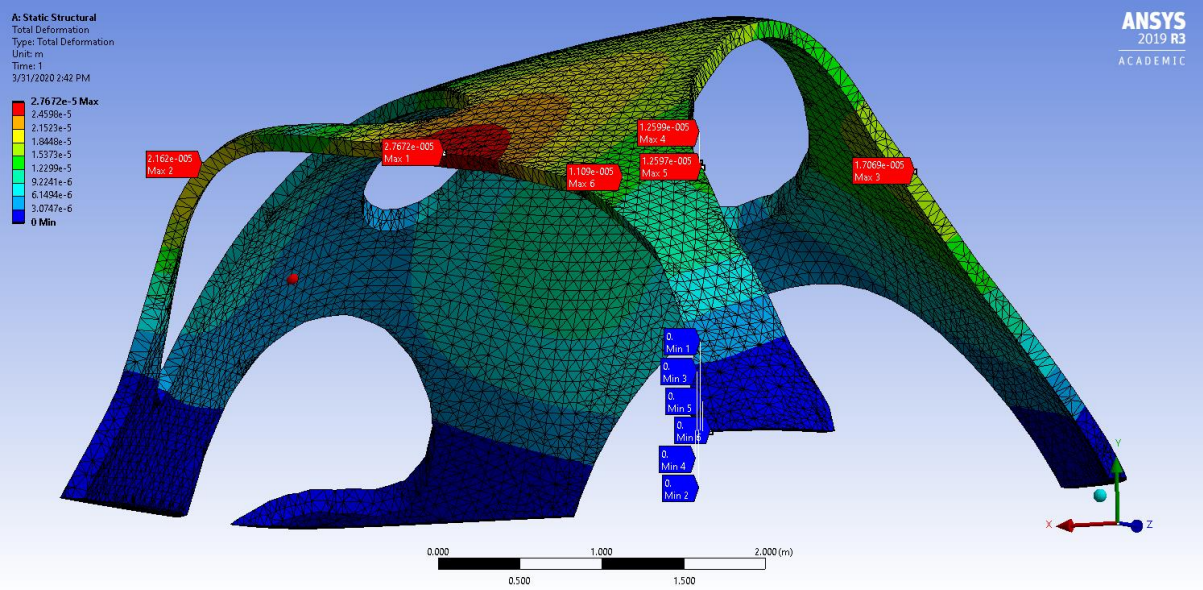


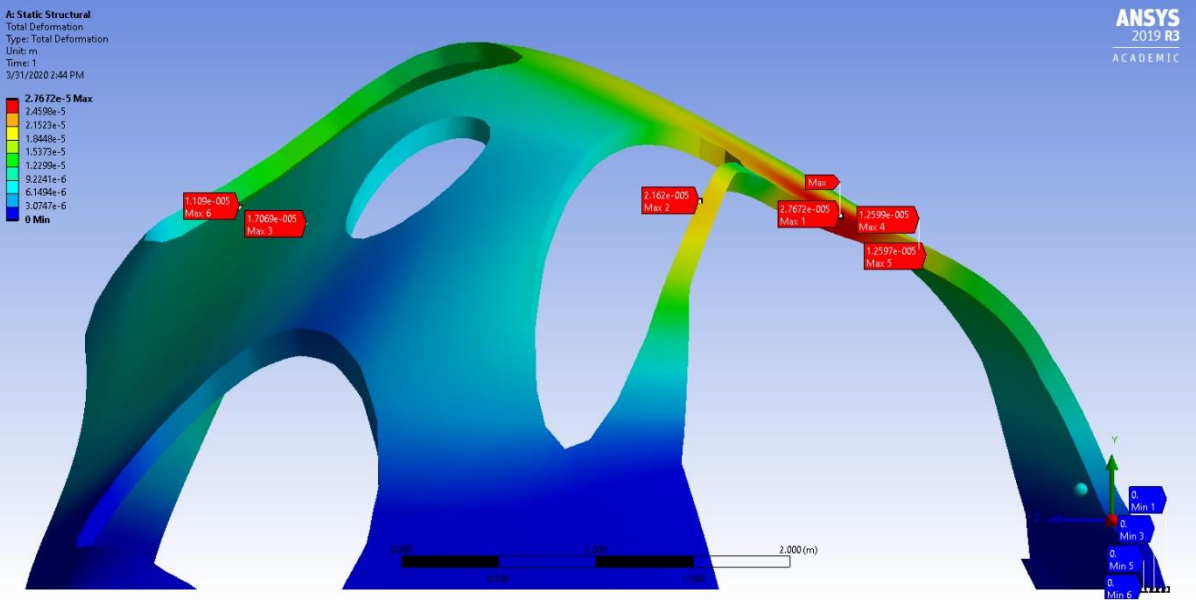
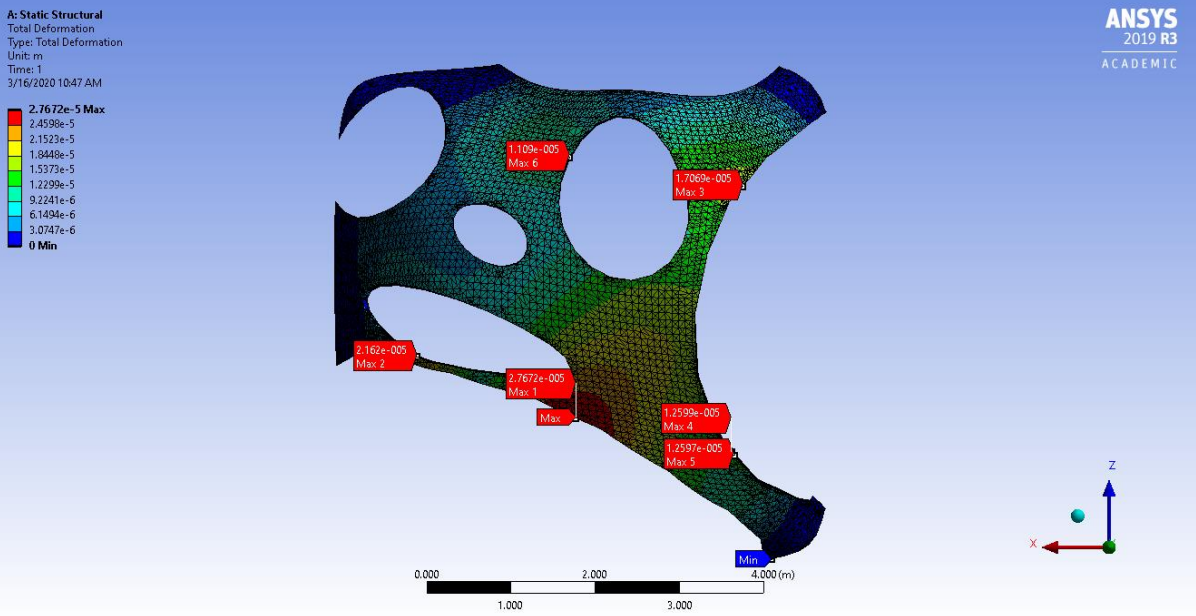


C.11 First Simplified Topology optimisation – Deformations

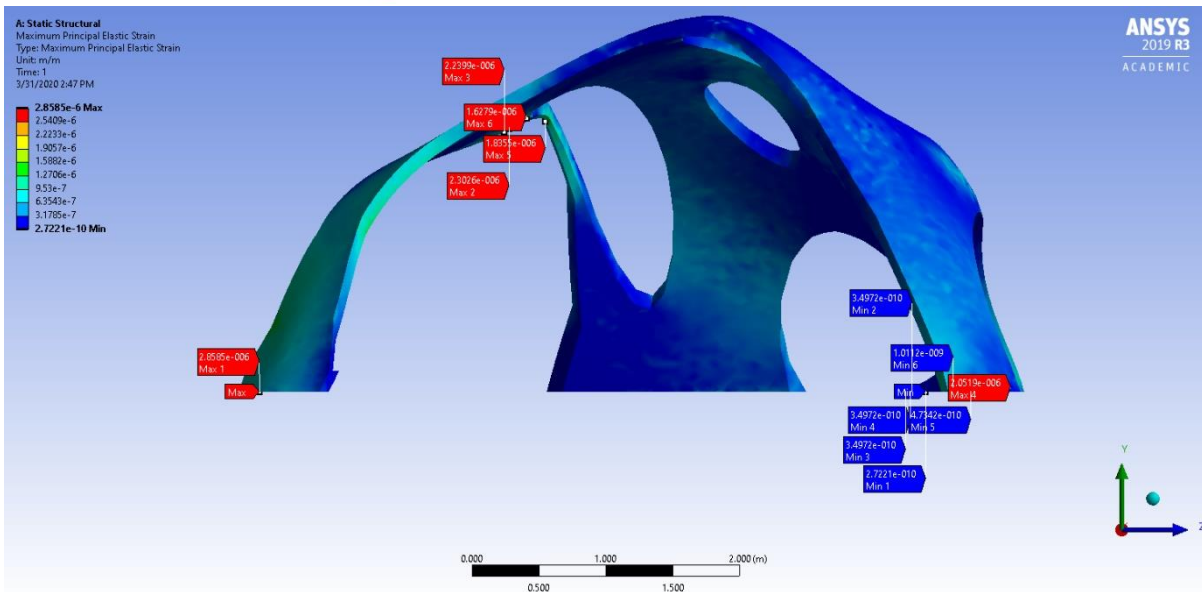
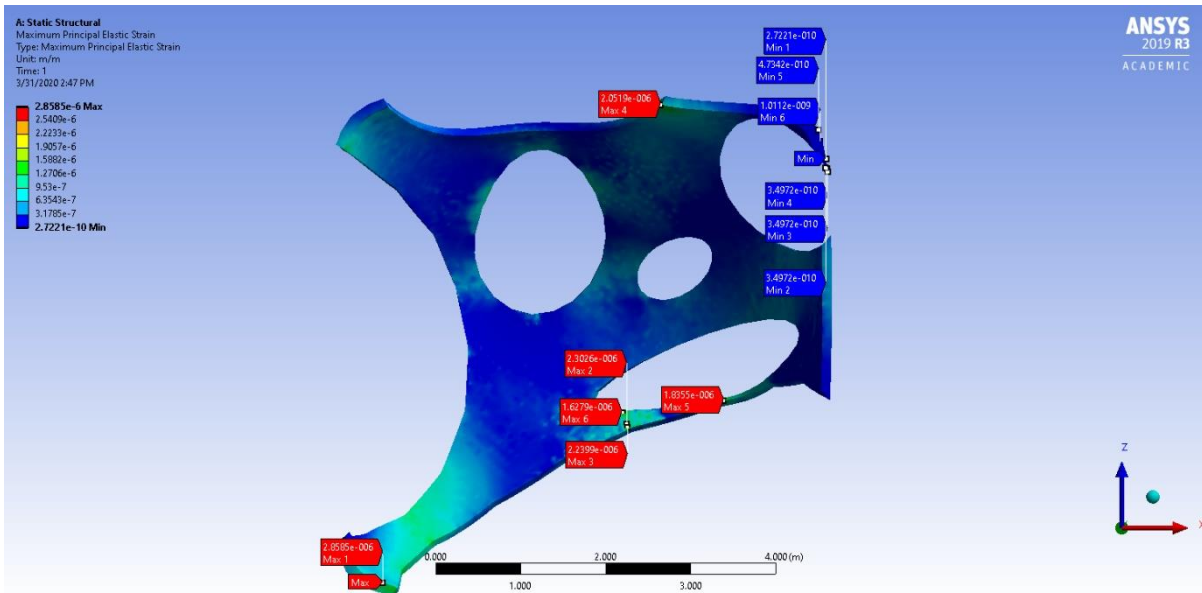
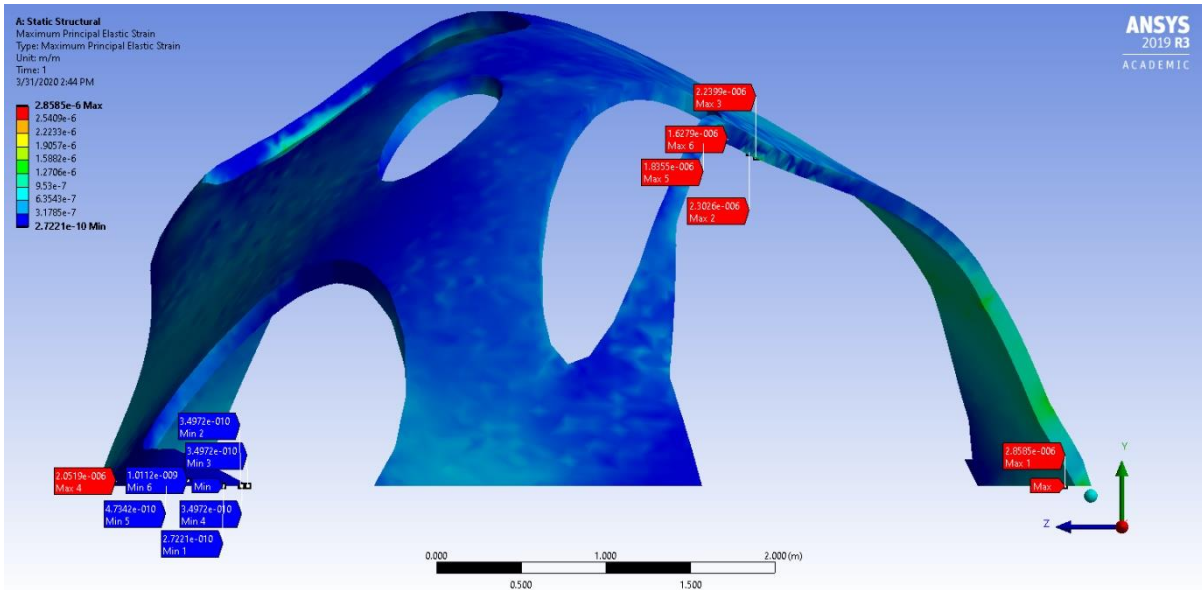


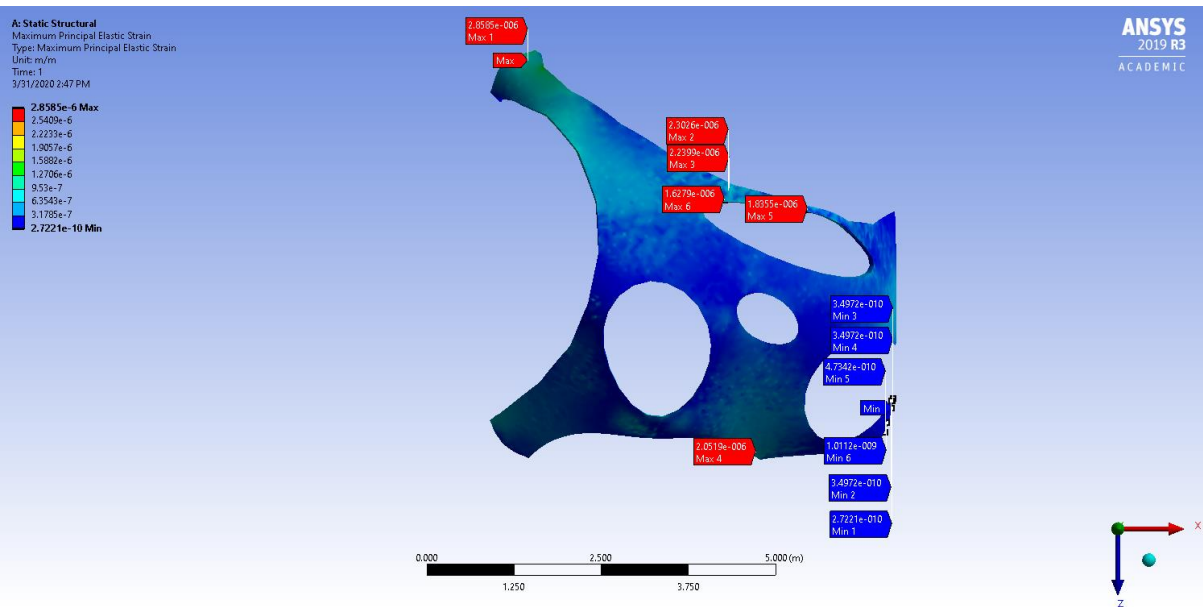
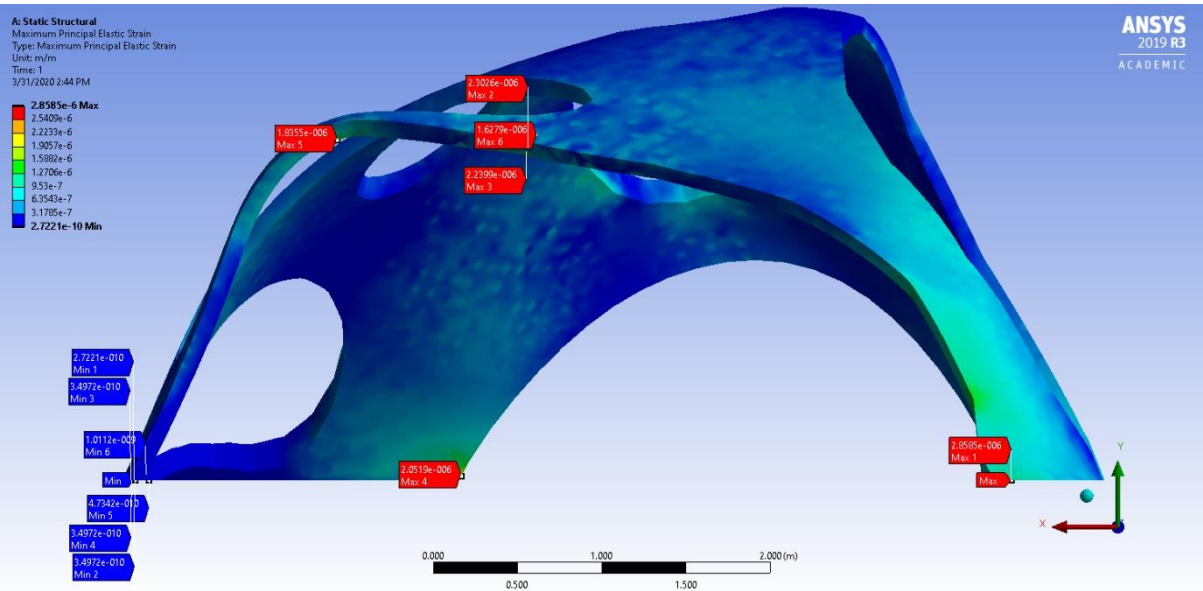
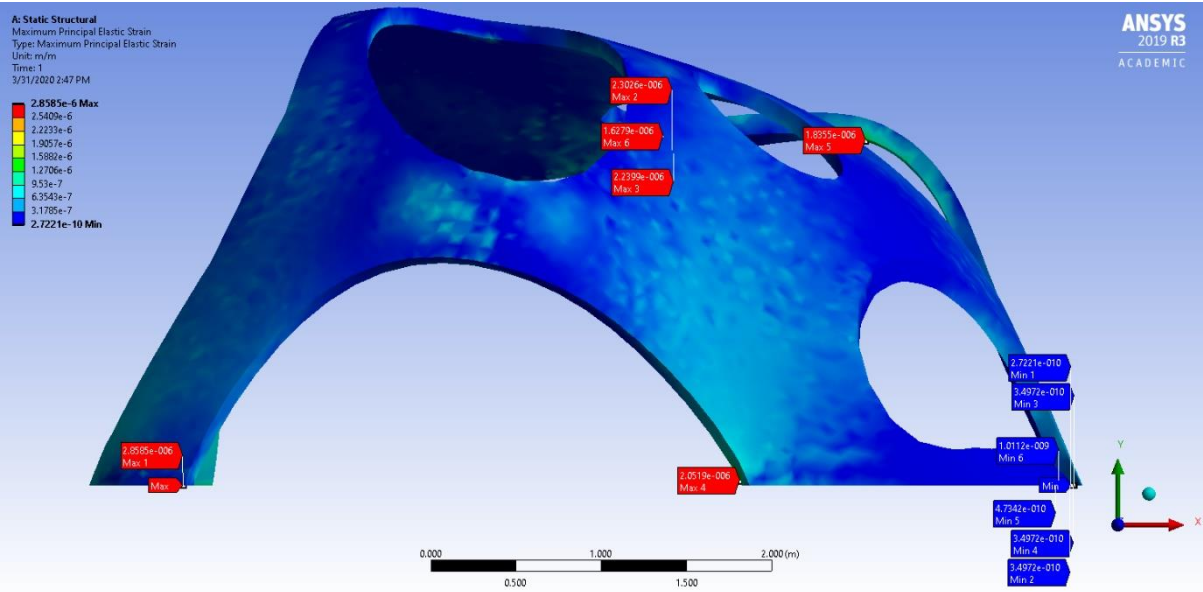




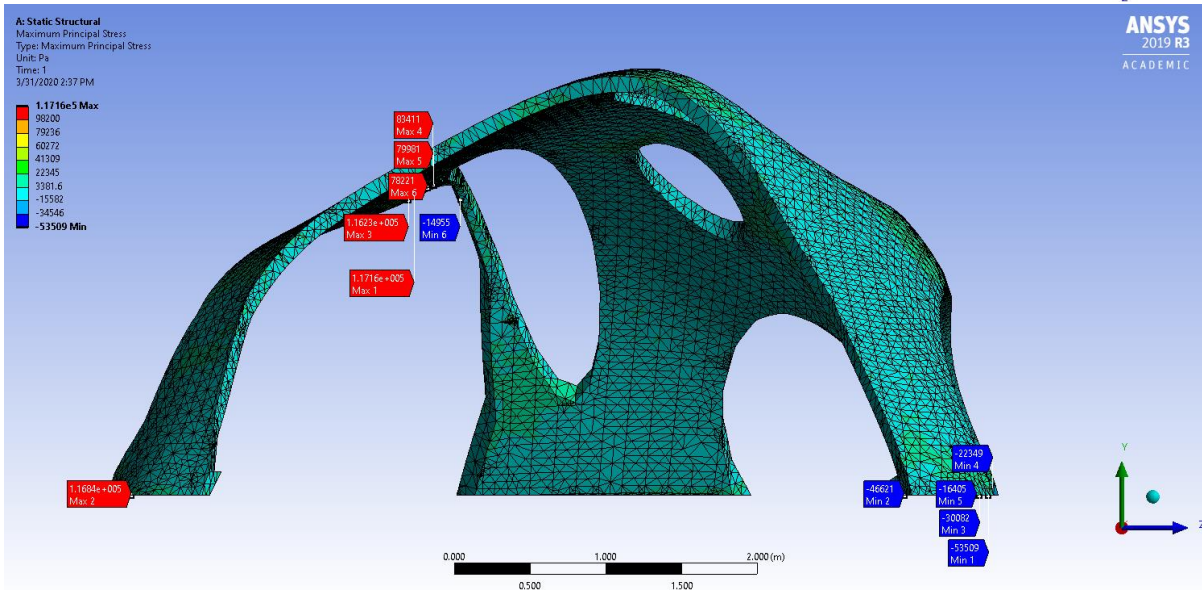
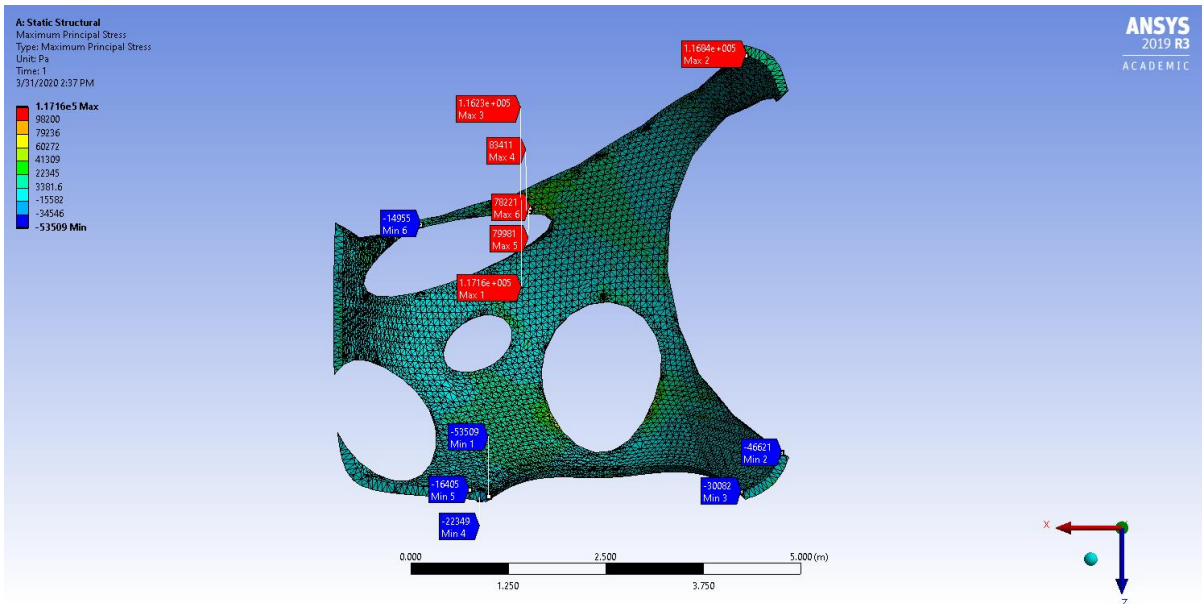
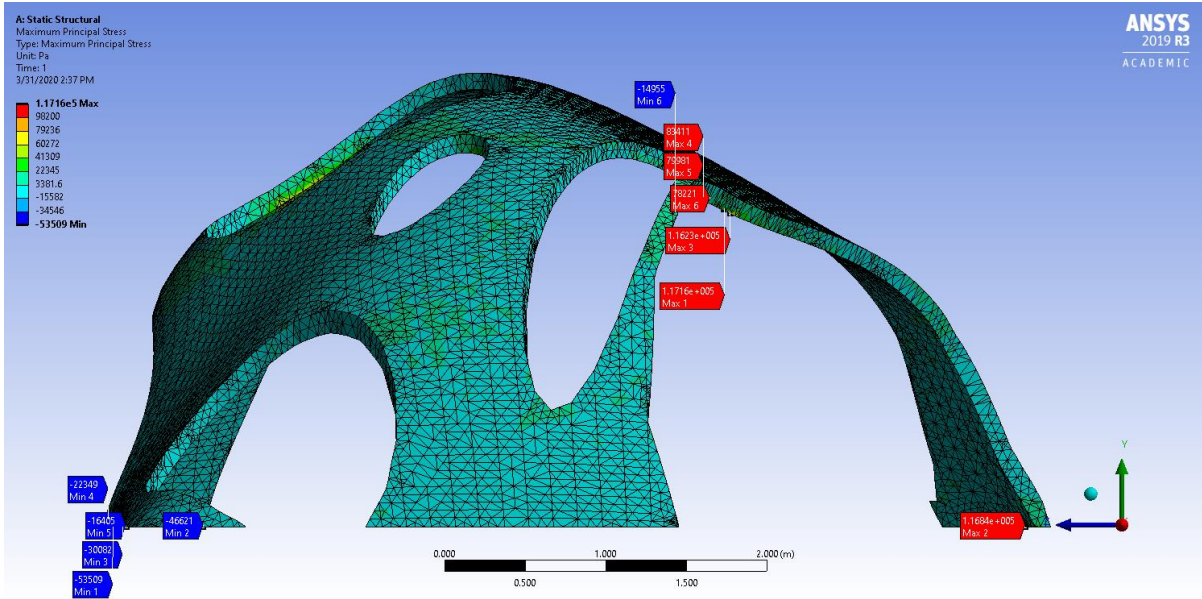


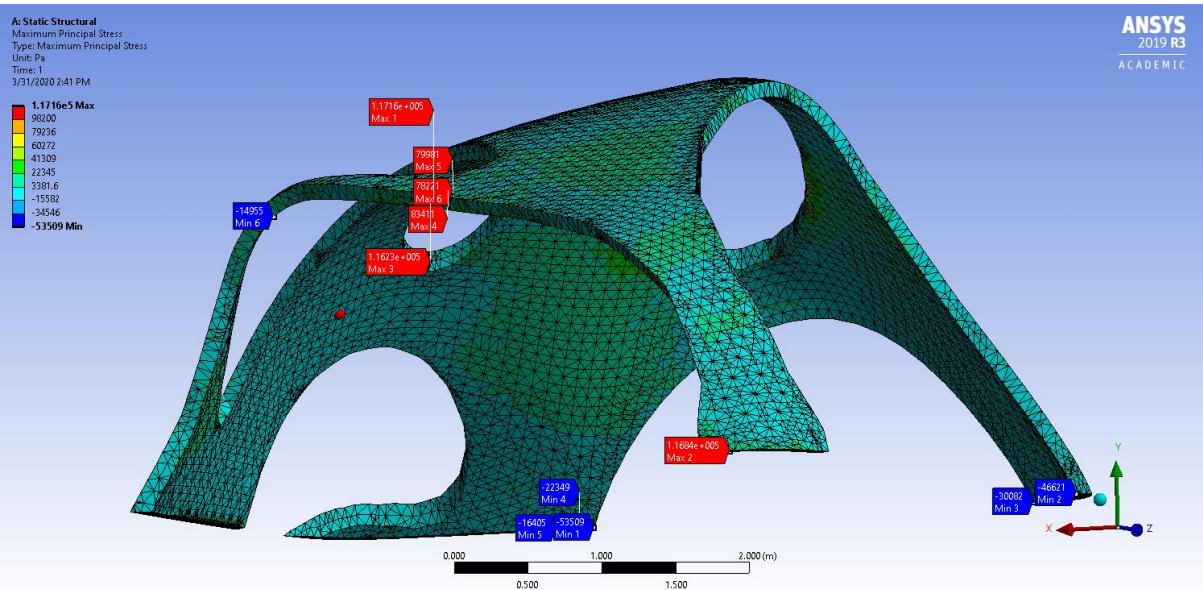
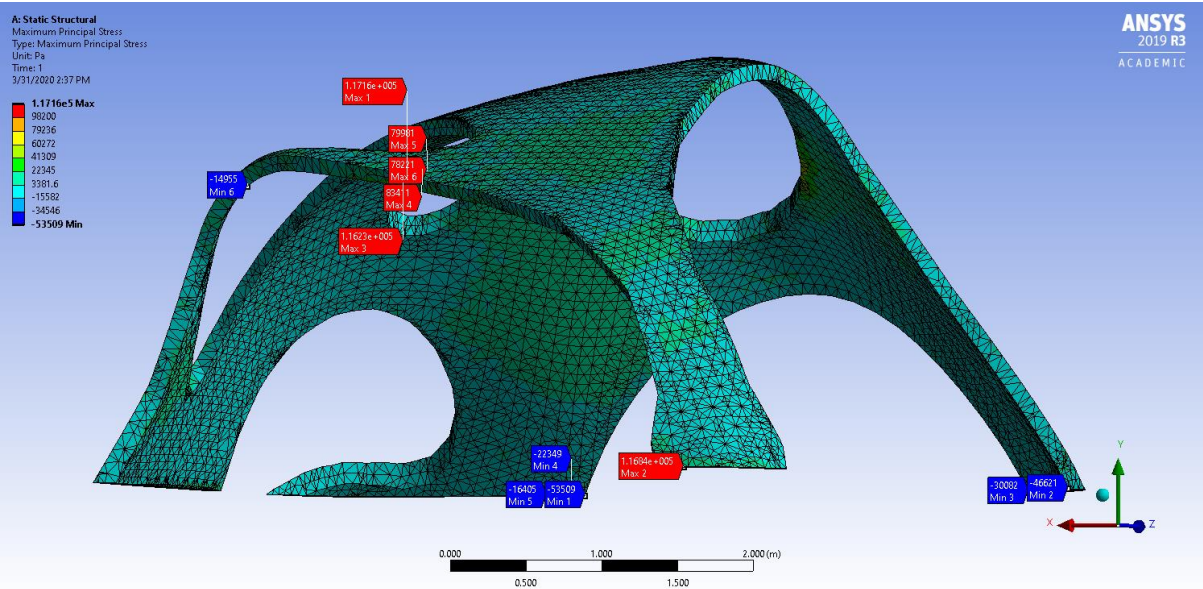
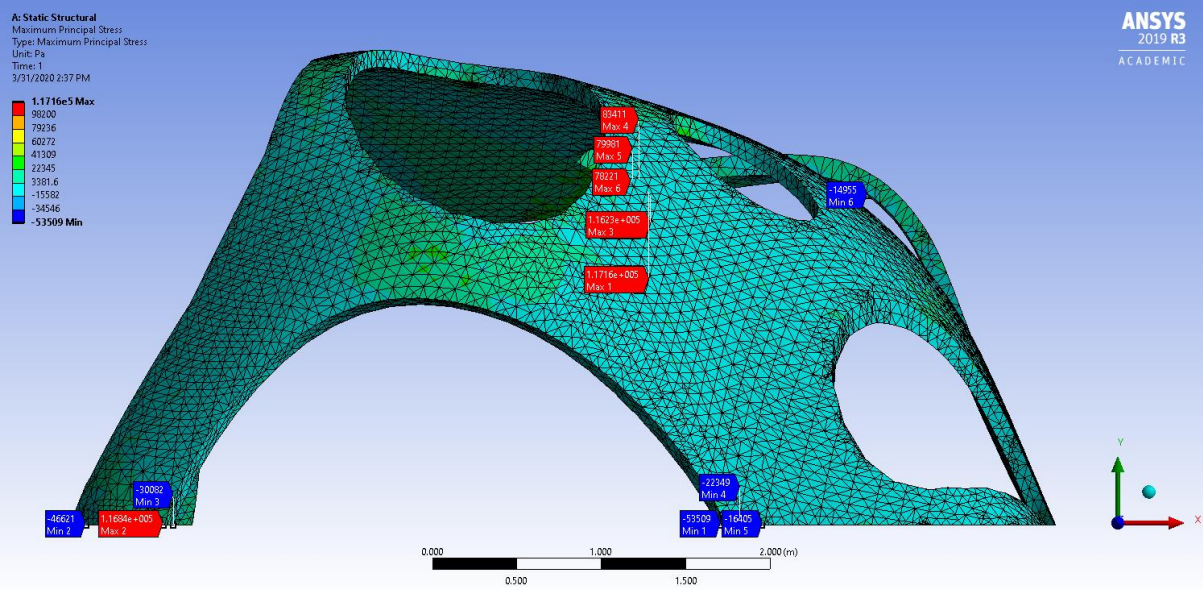
C.12 First Simplified Topology optimisation - Max Principle Elastic Strain

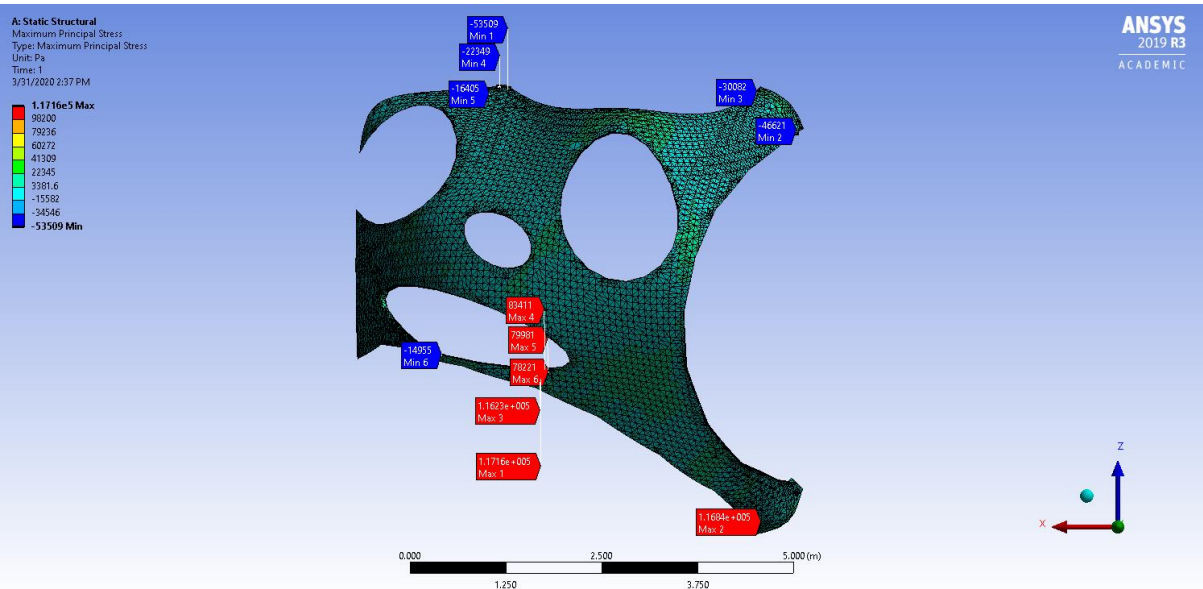
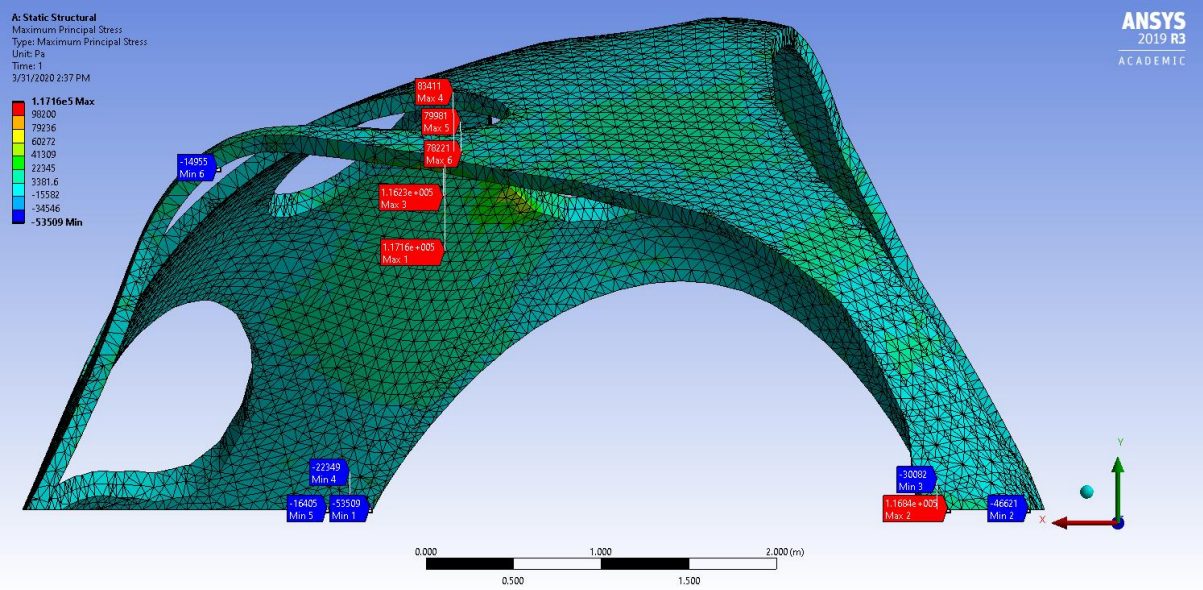




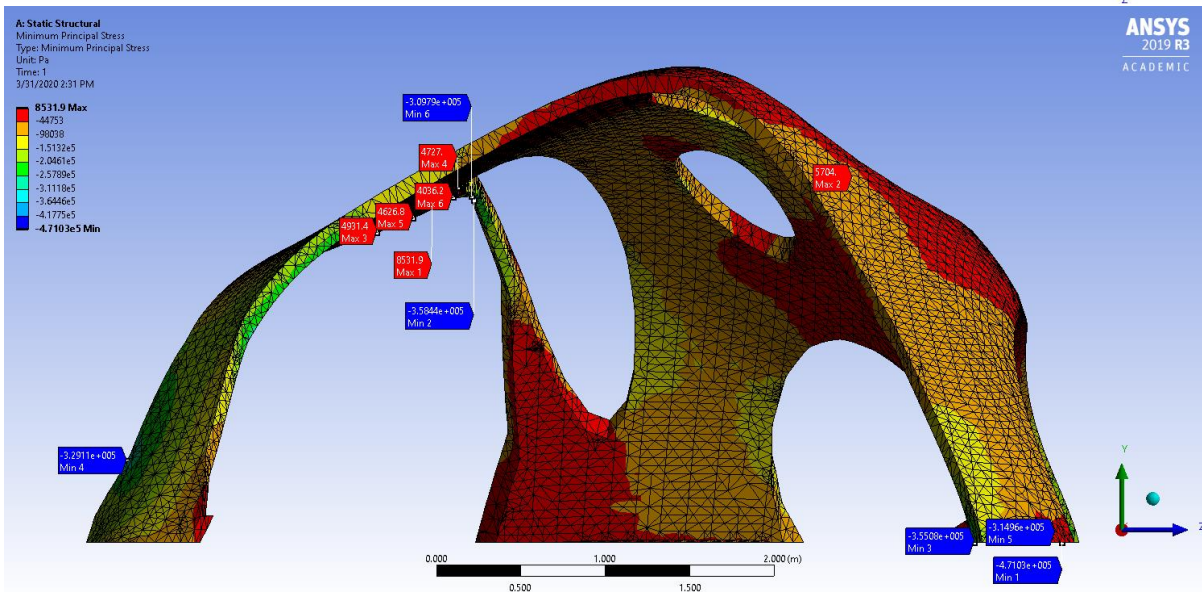
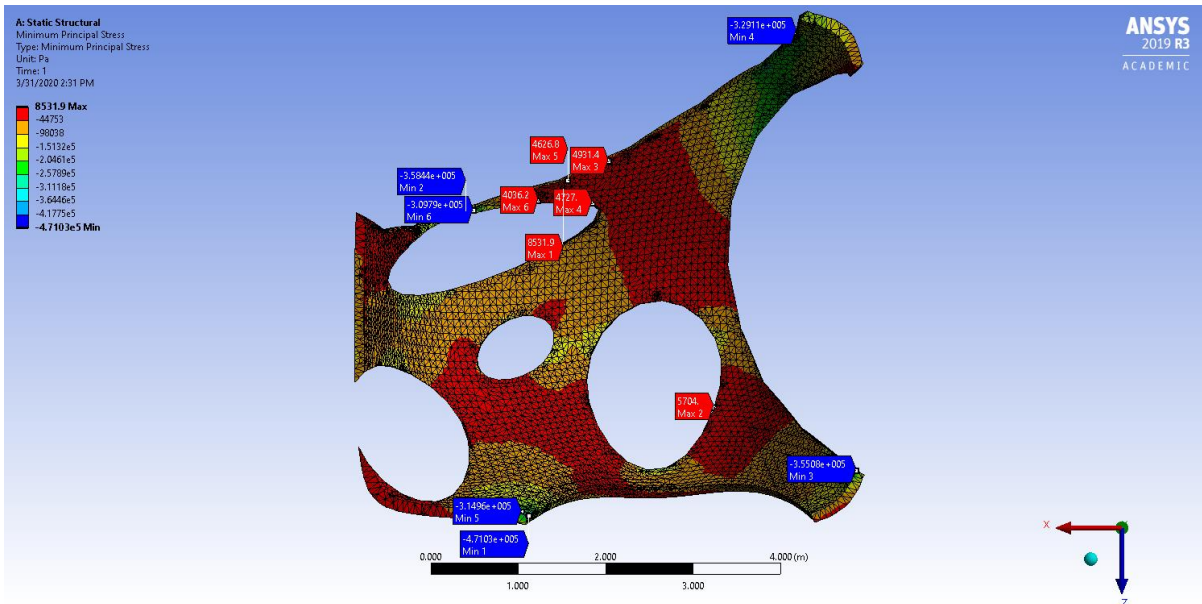
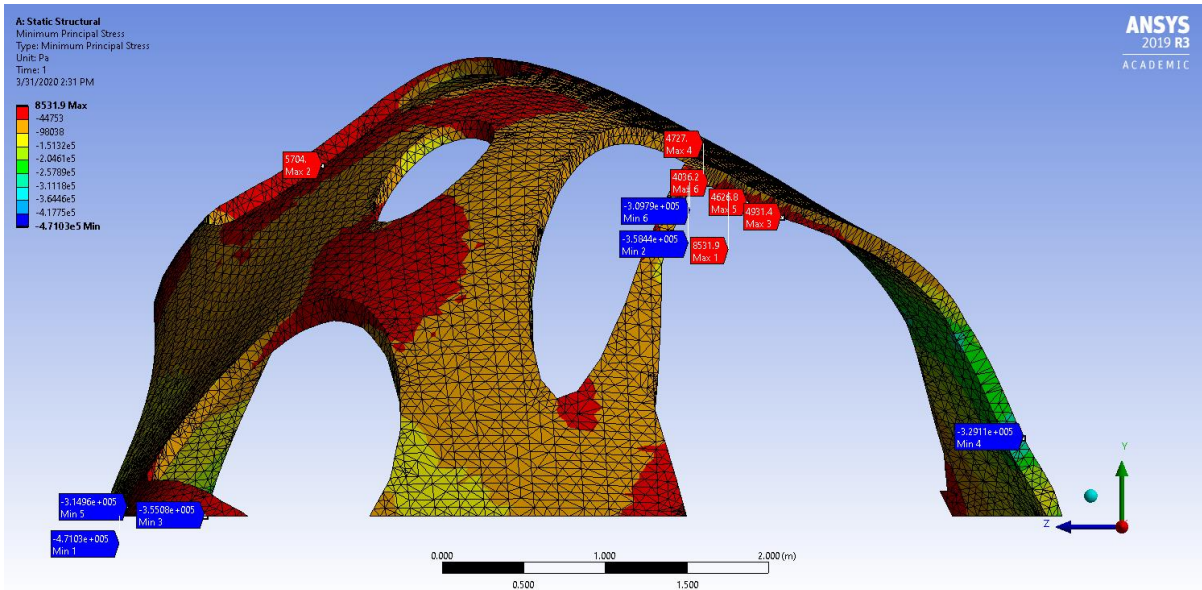
C.13 First Simplified Topology optimisation – Max Principal stress

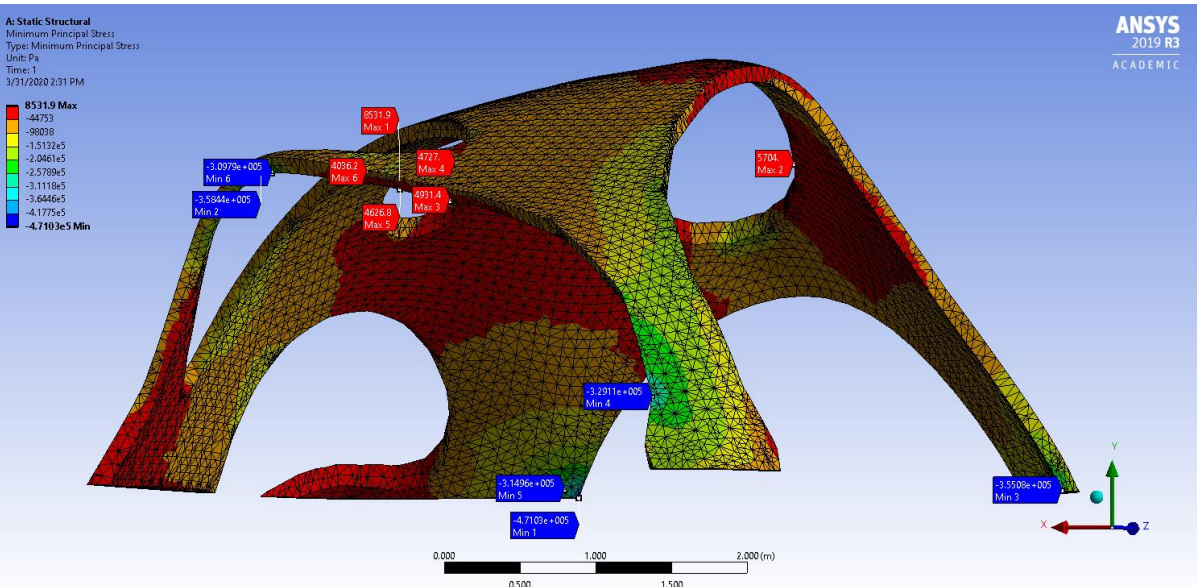
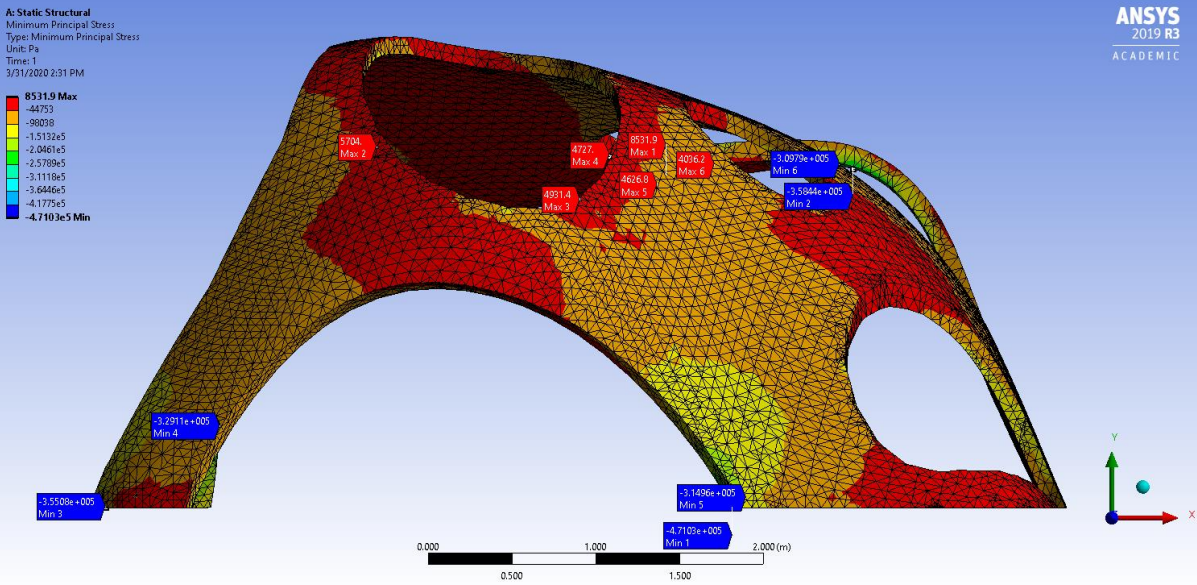


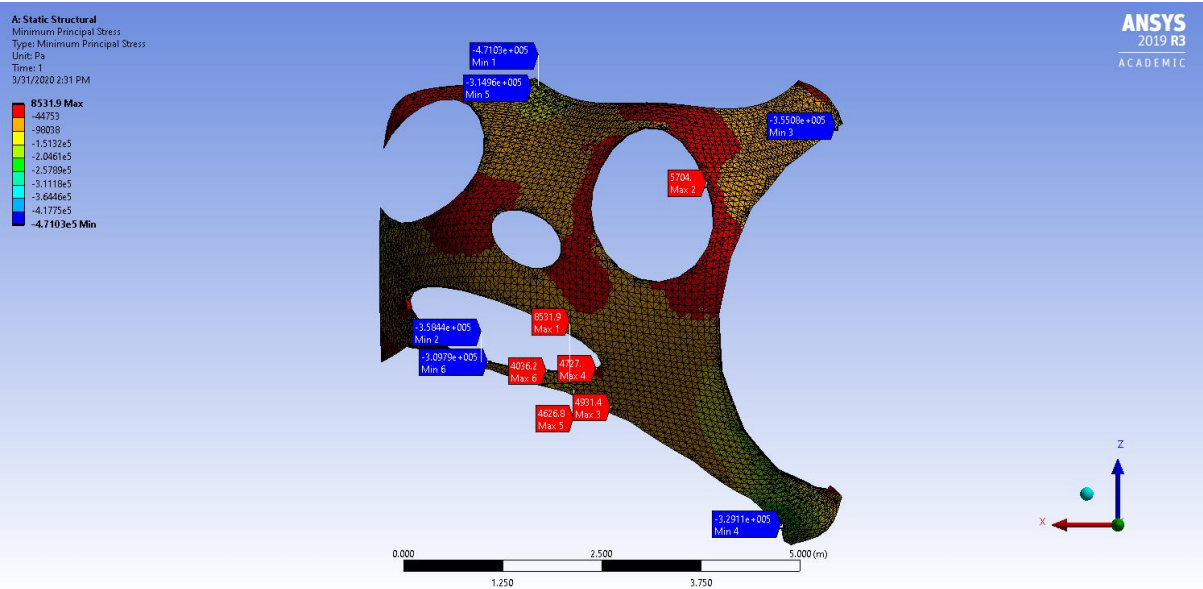
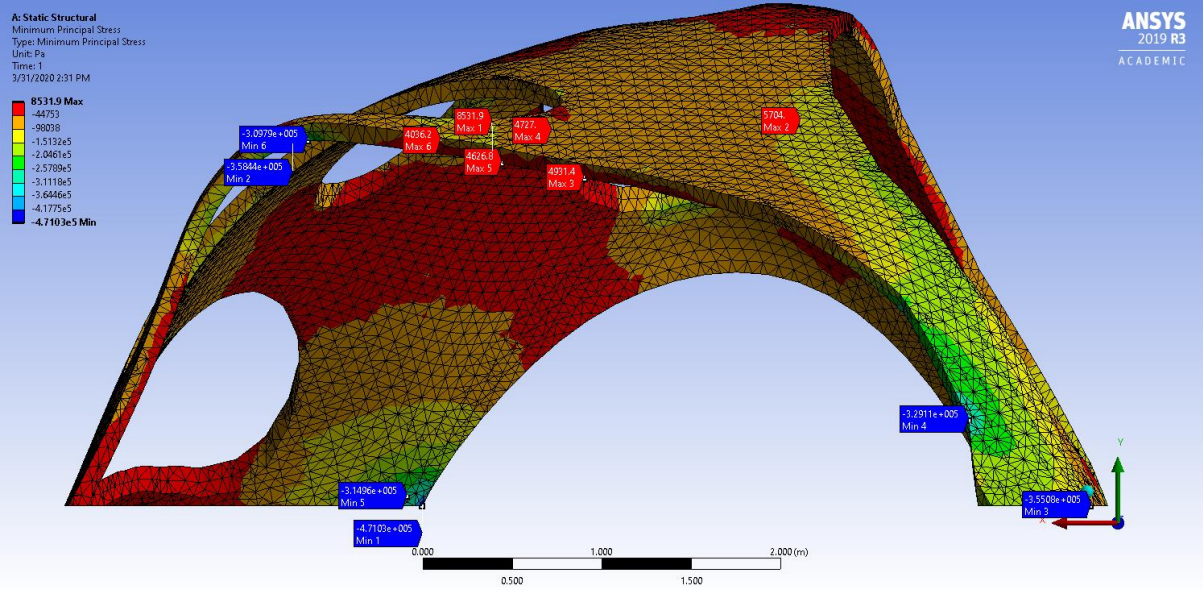




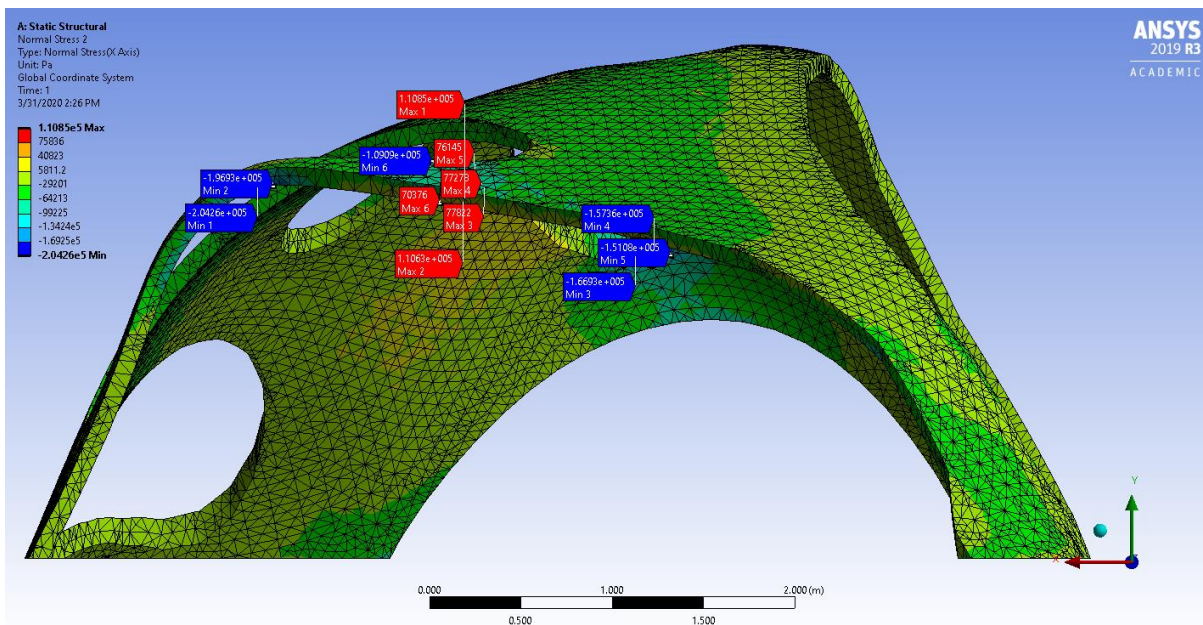
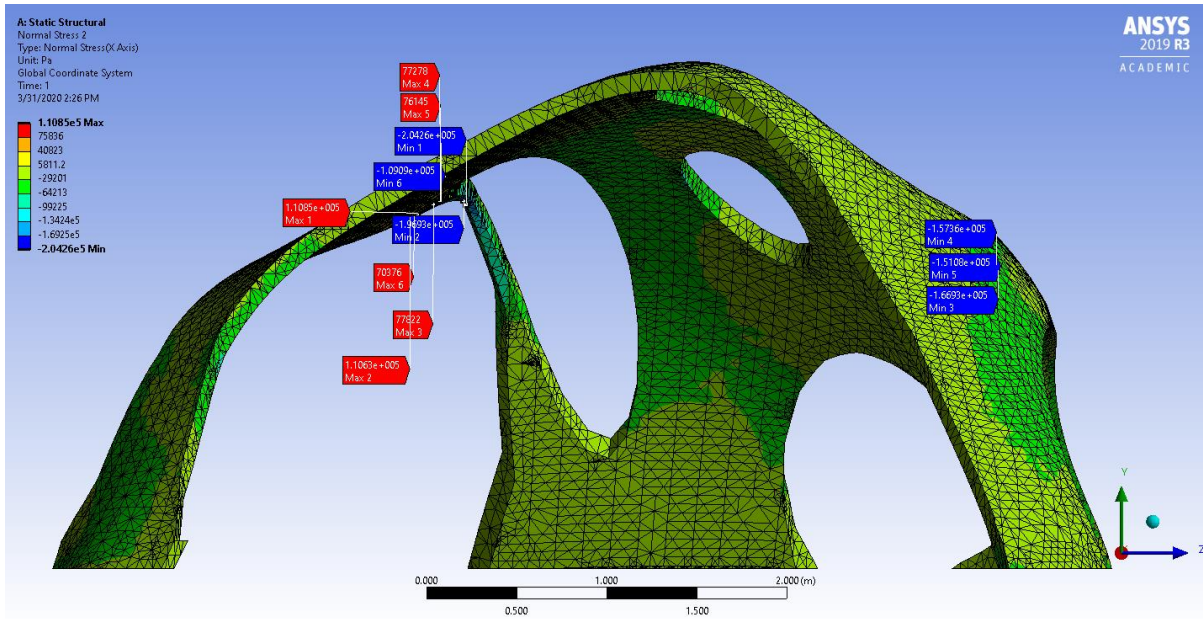
C.14 First Simplified Topology optimisation – Minimum Principal Stress

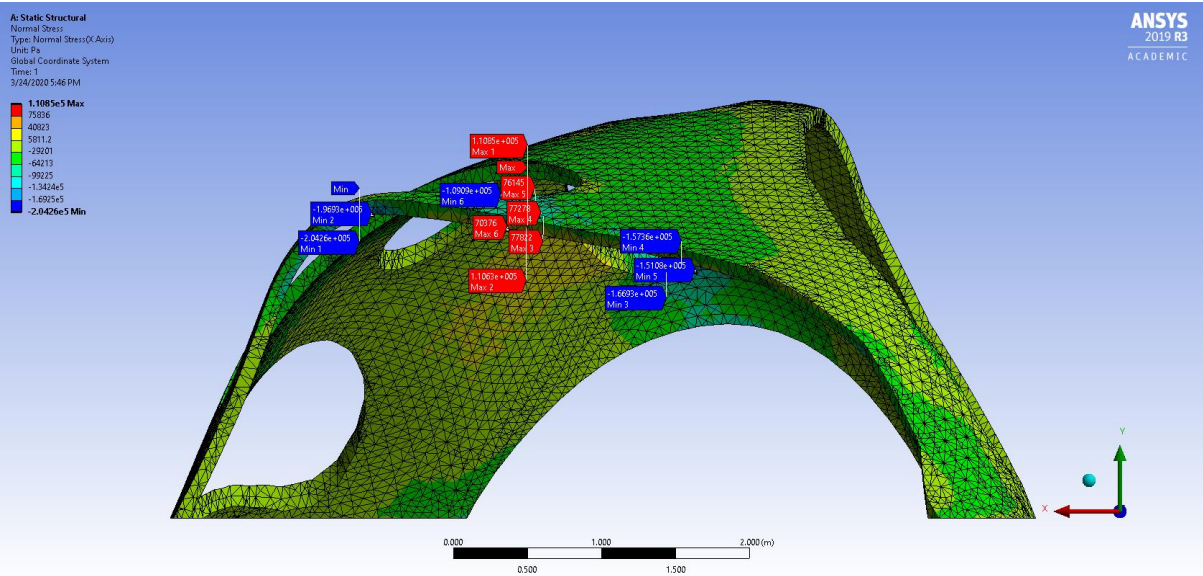
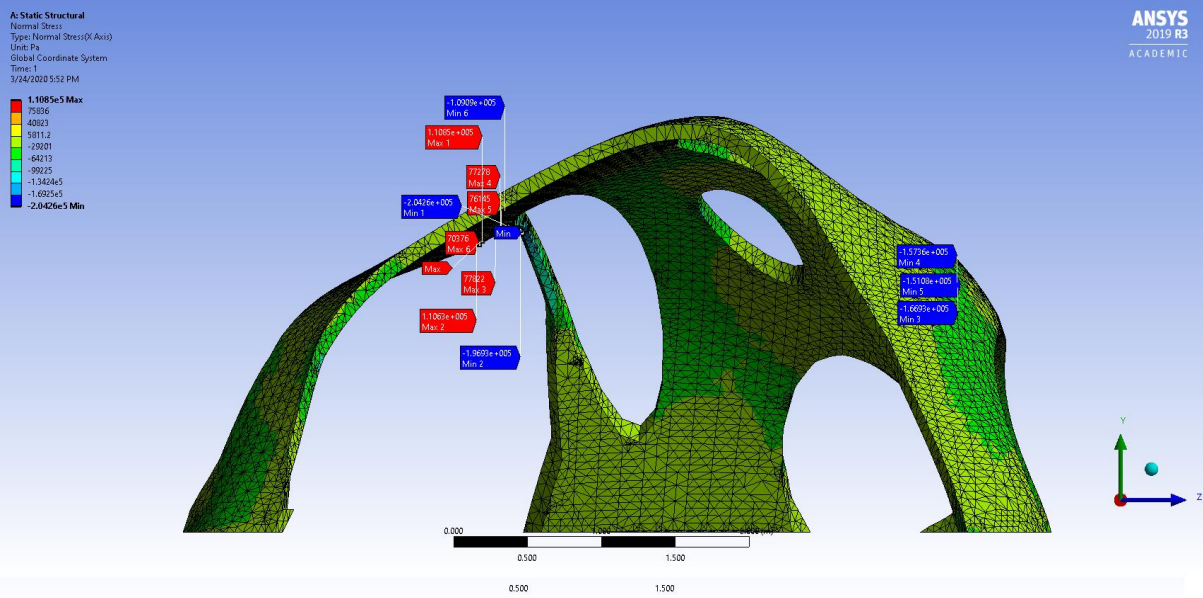
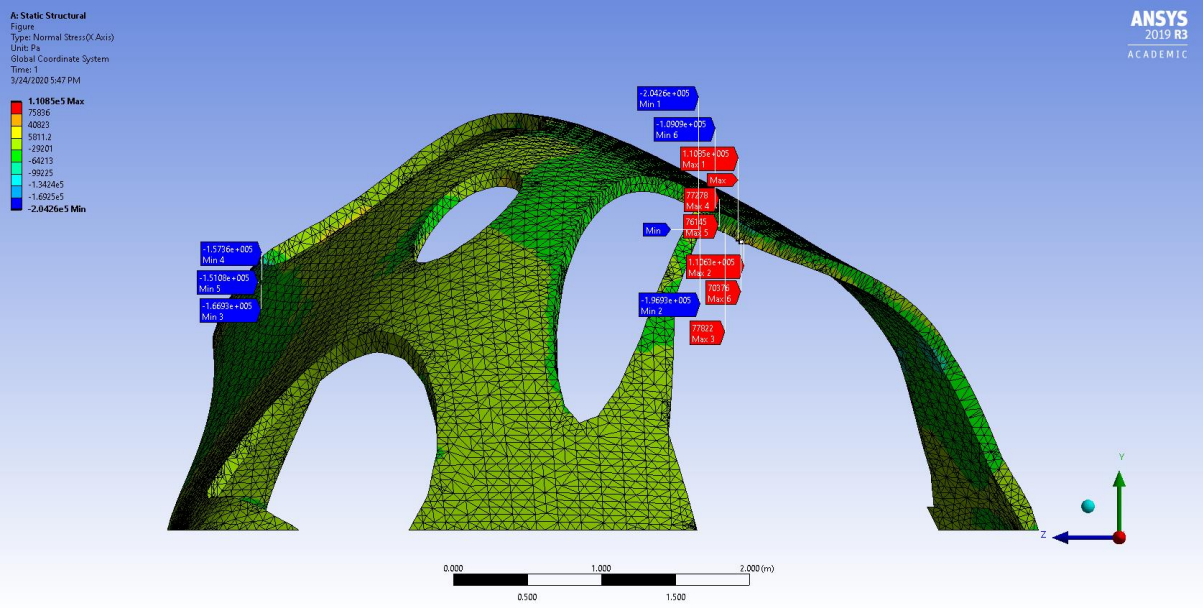


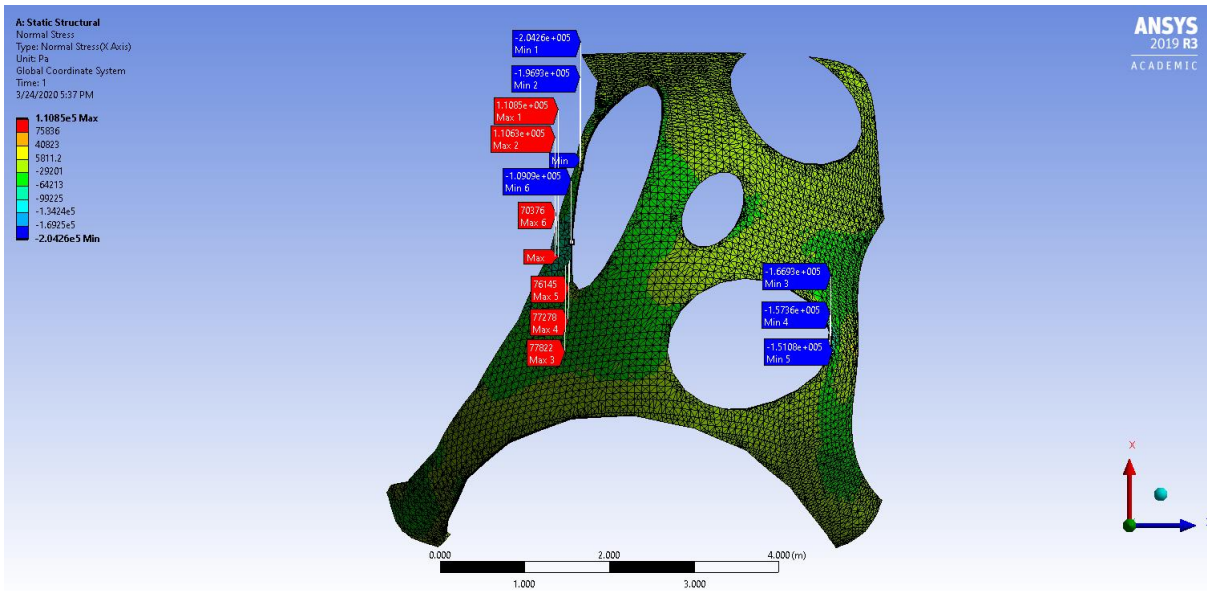
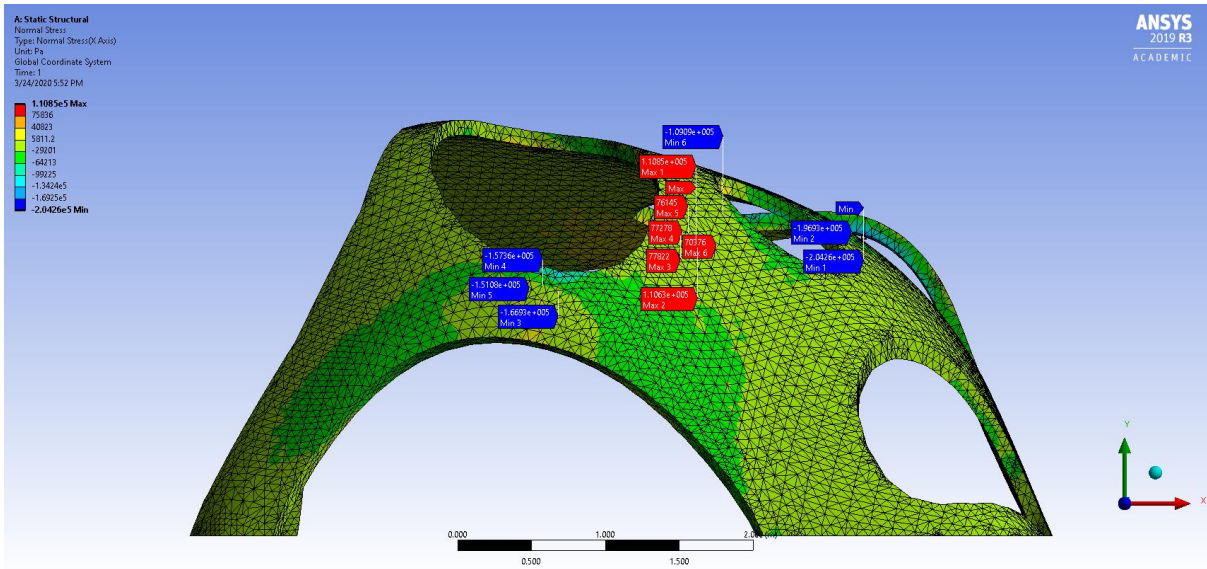




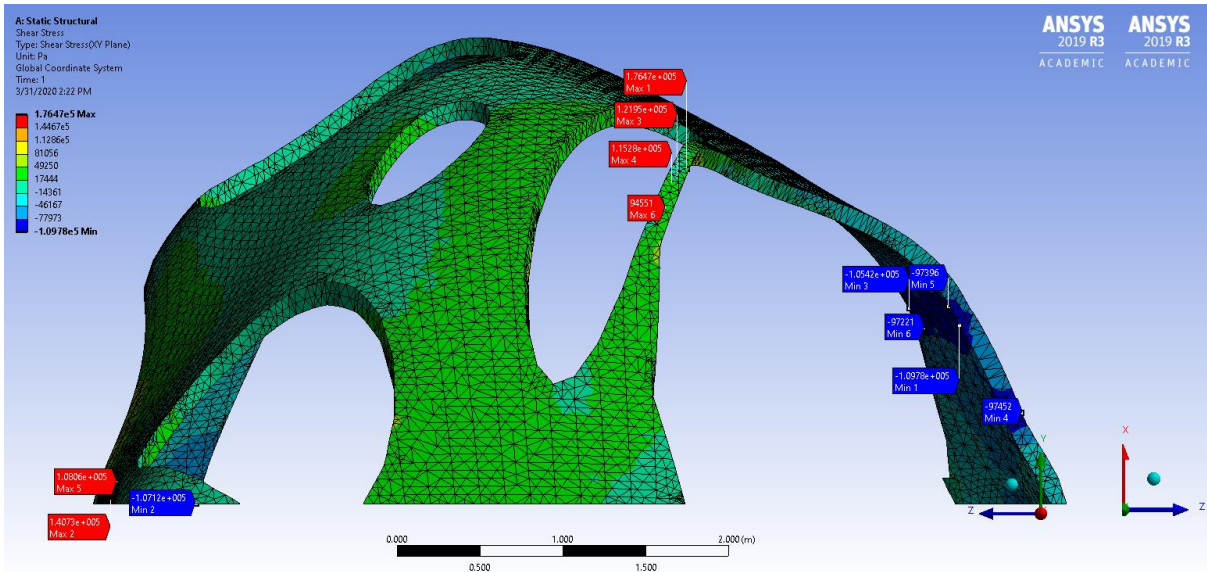
C.15 First Simplified Topology optimisation – Normal Stress

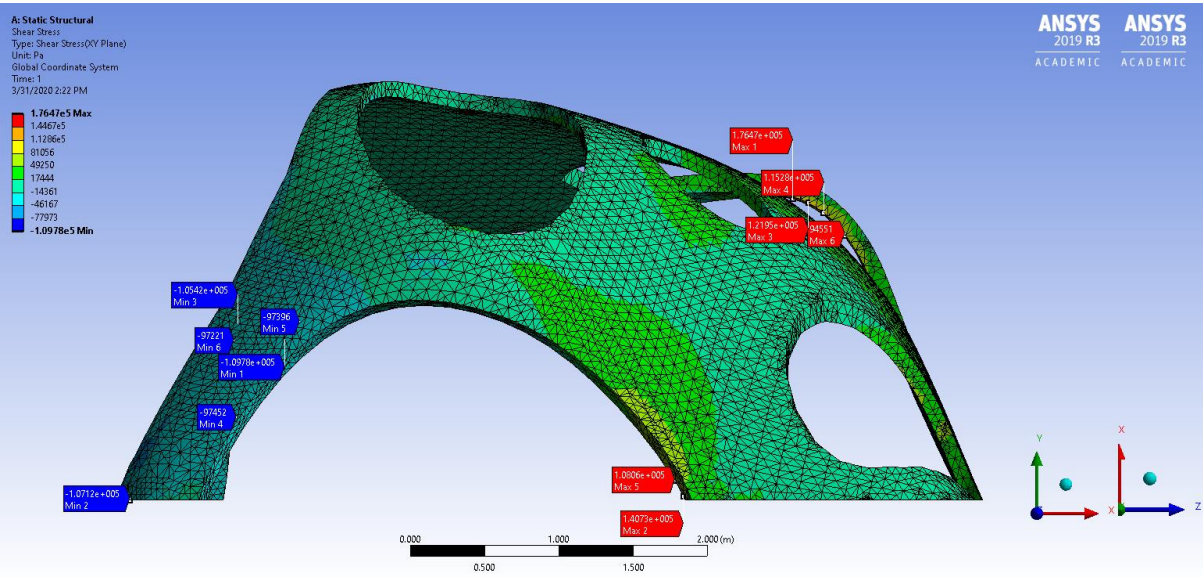
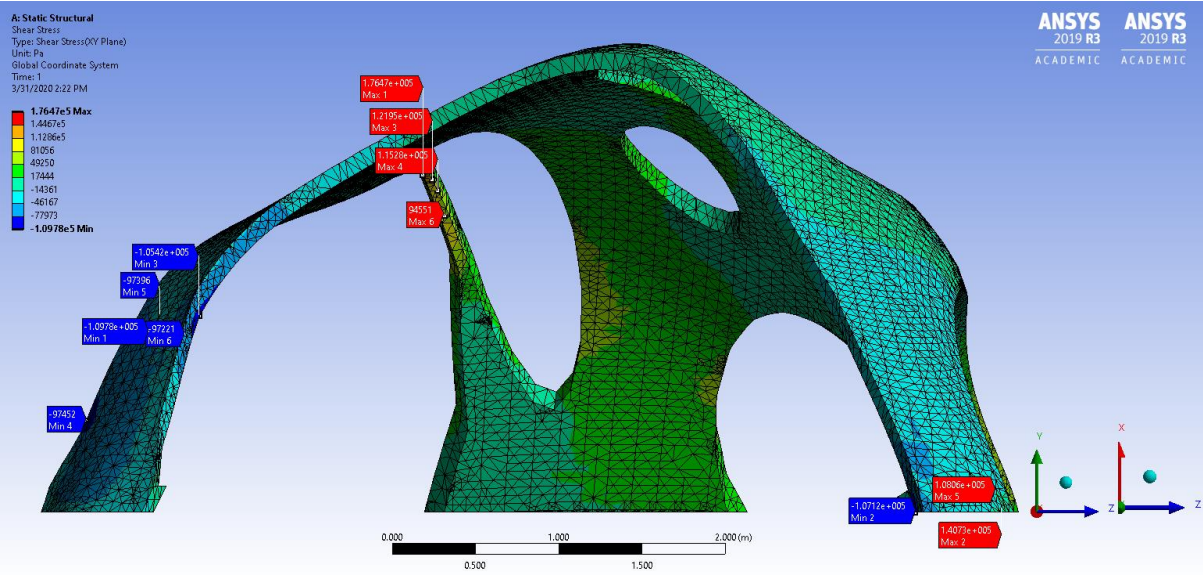
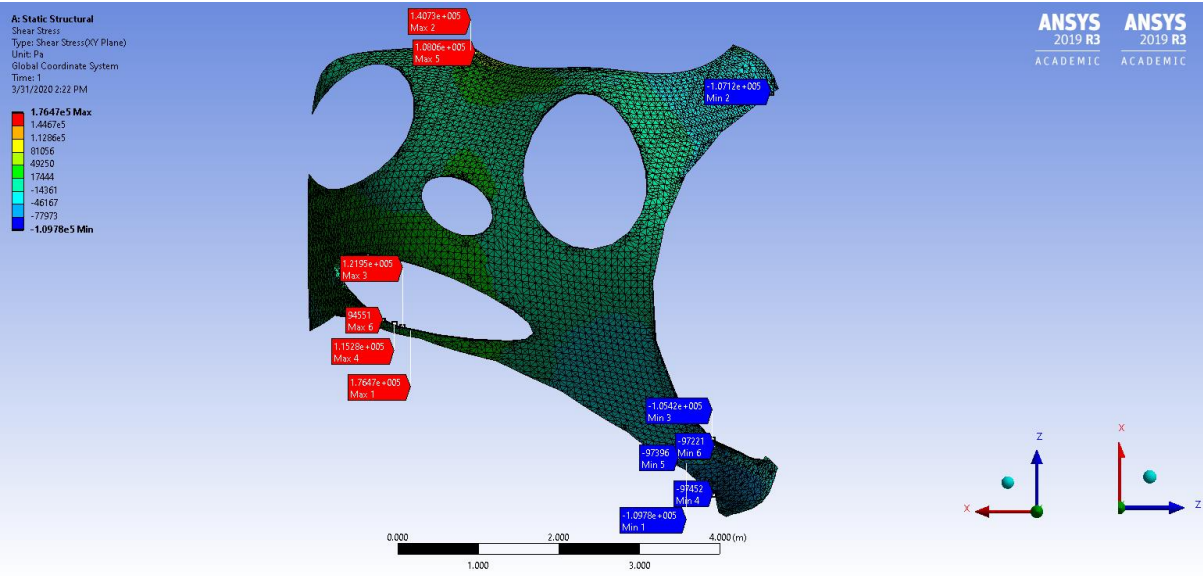


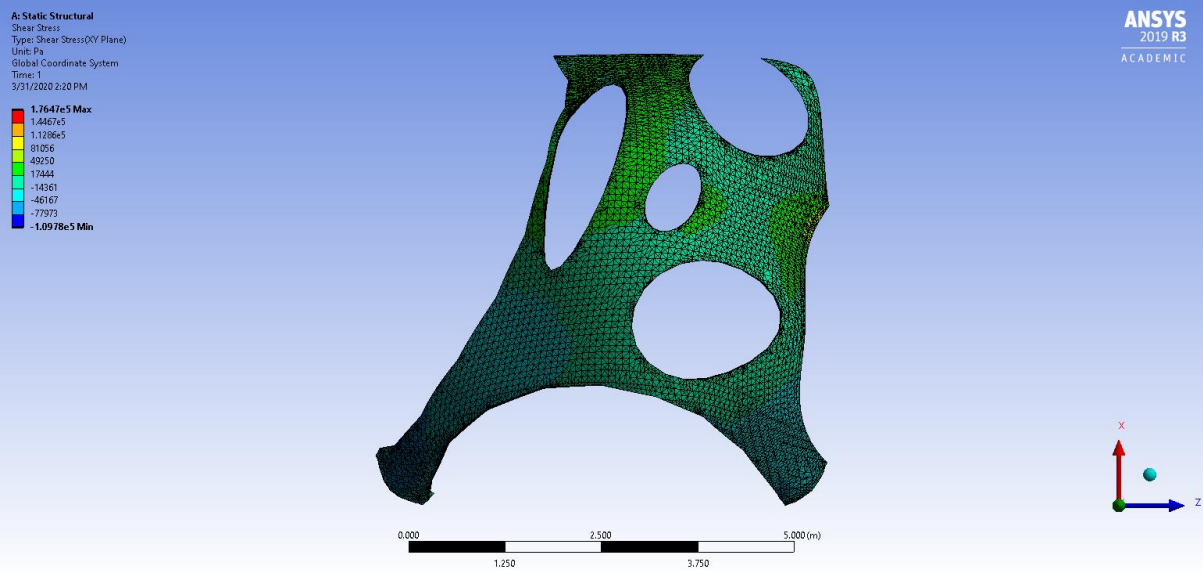
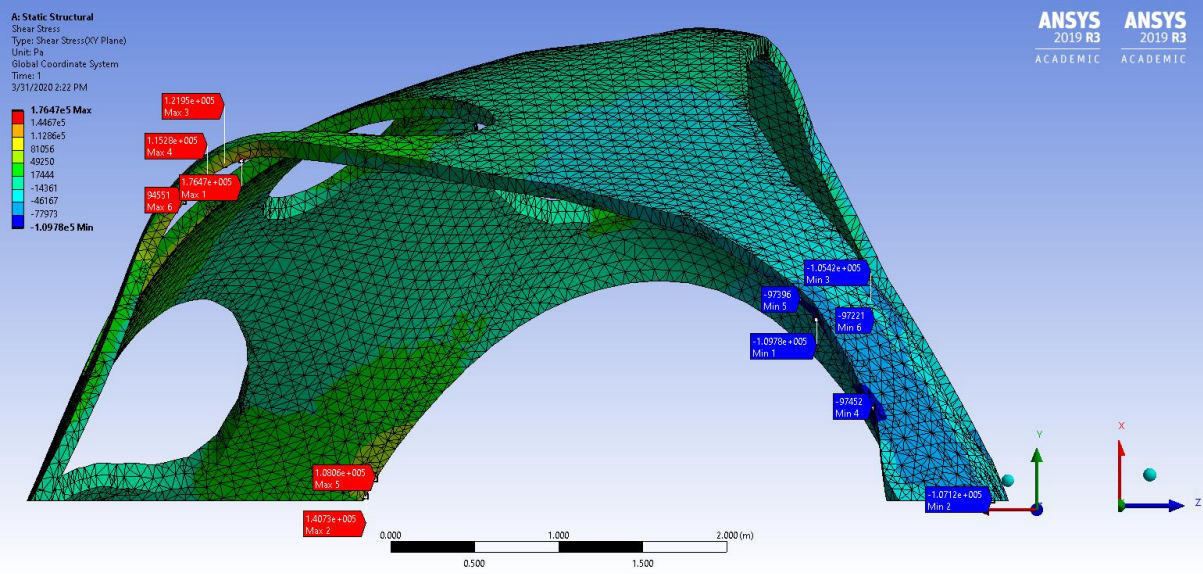




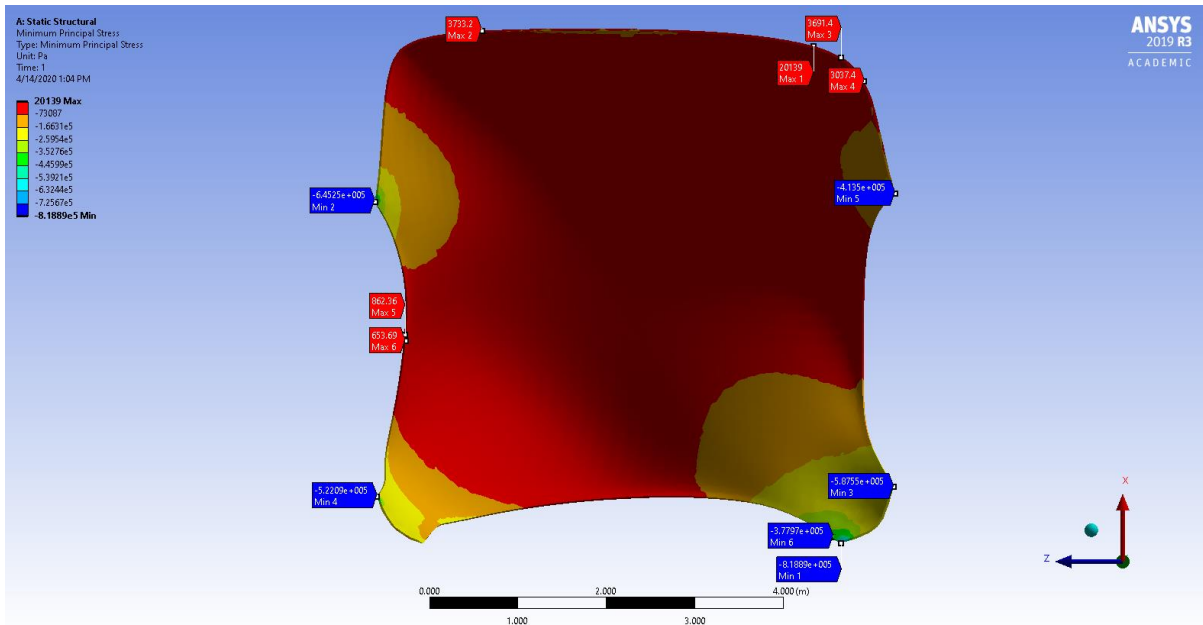
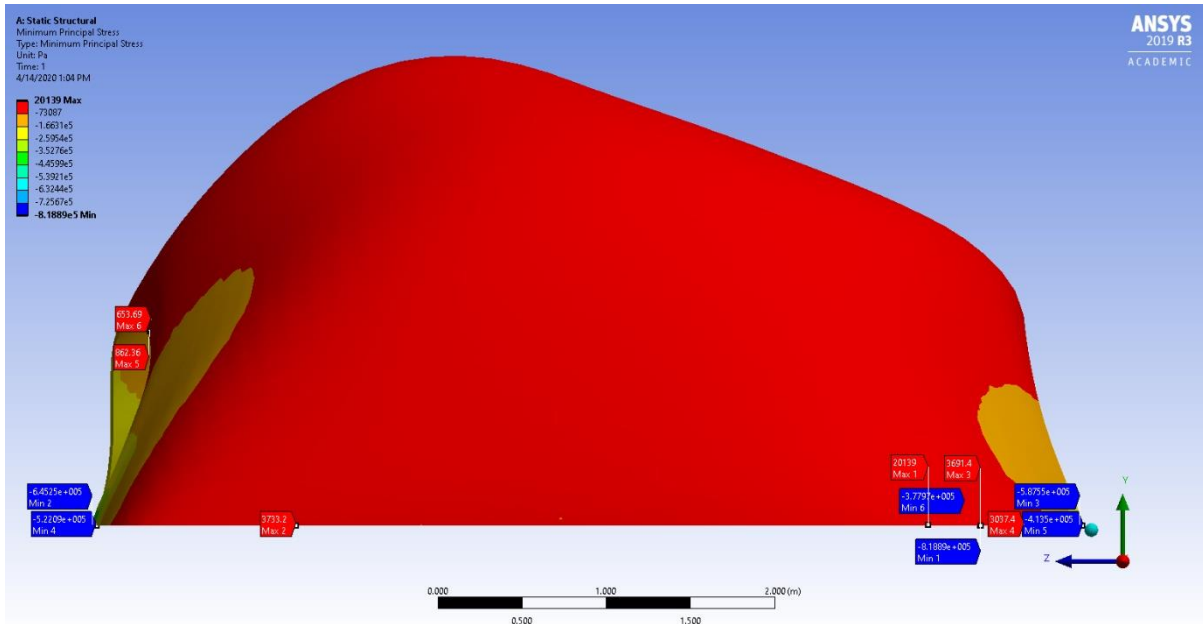
C.16 First Simplified Topology optimisation – Shear Stress

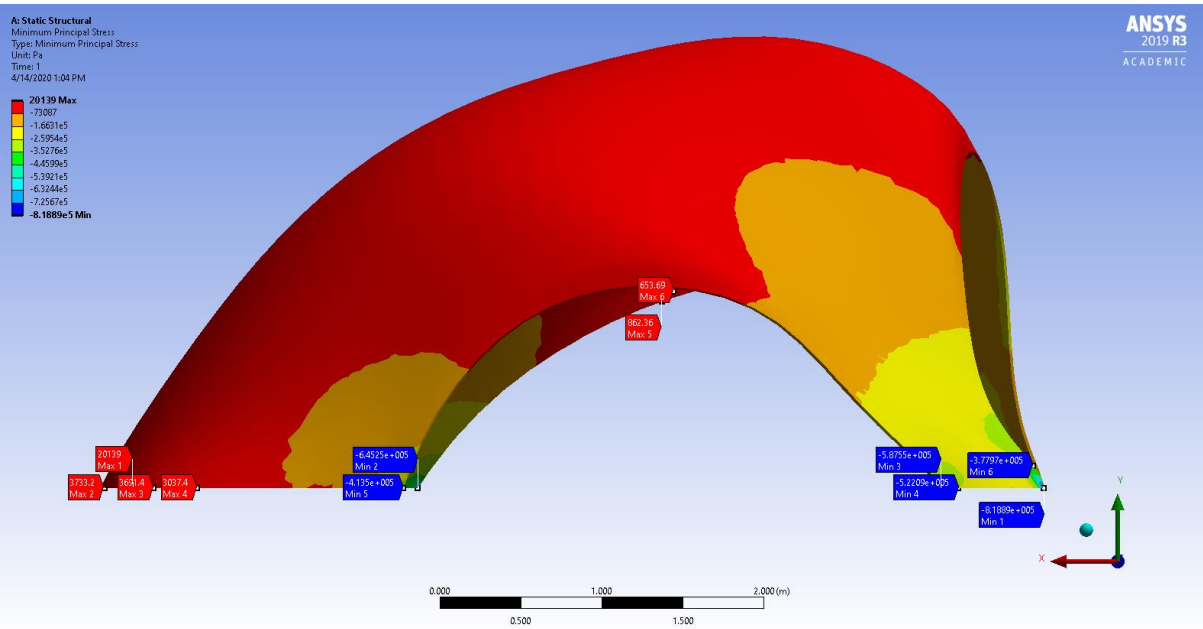
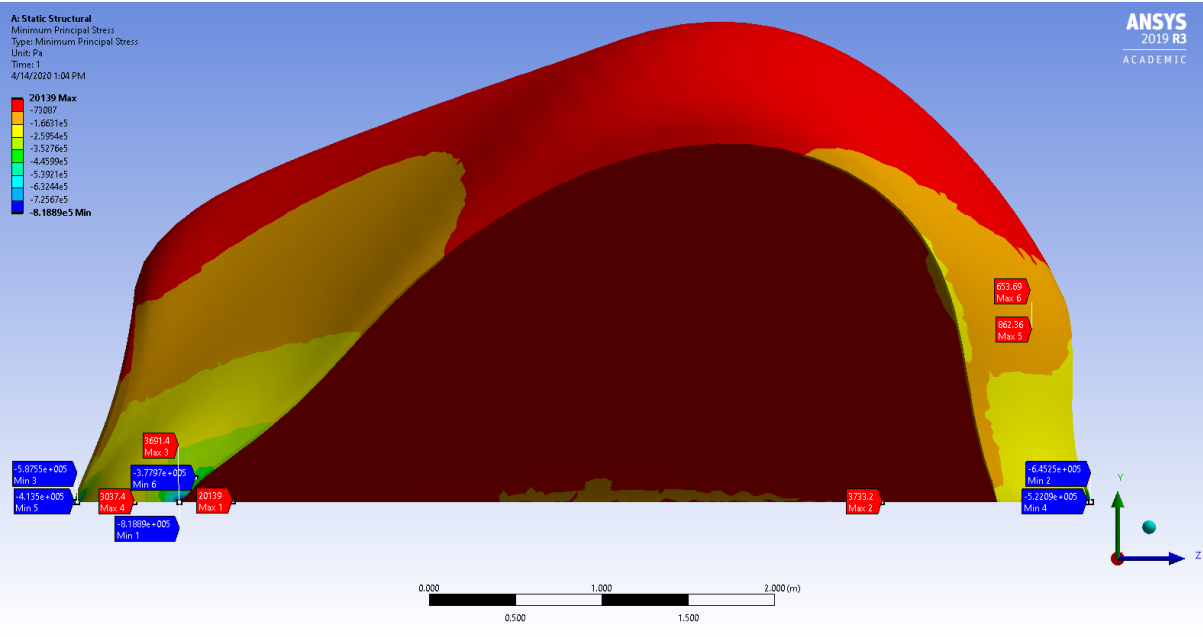


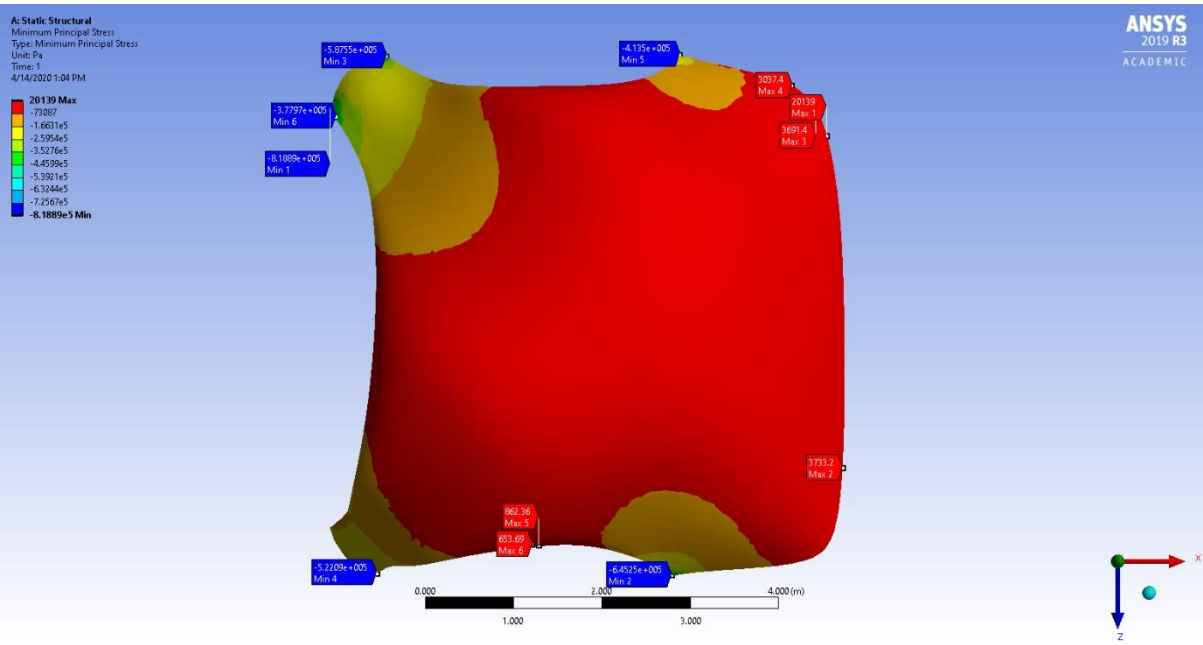
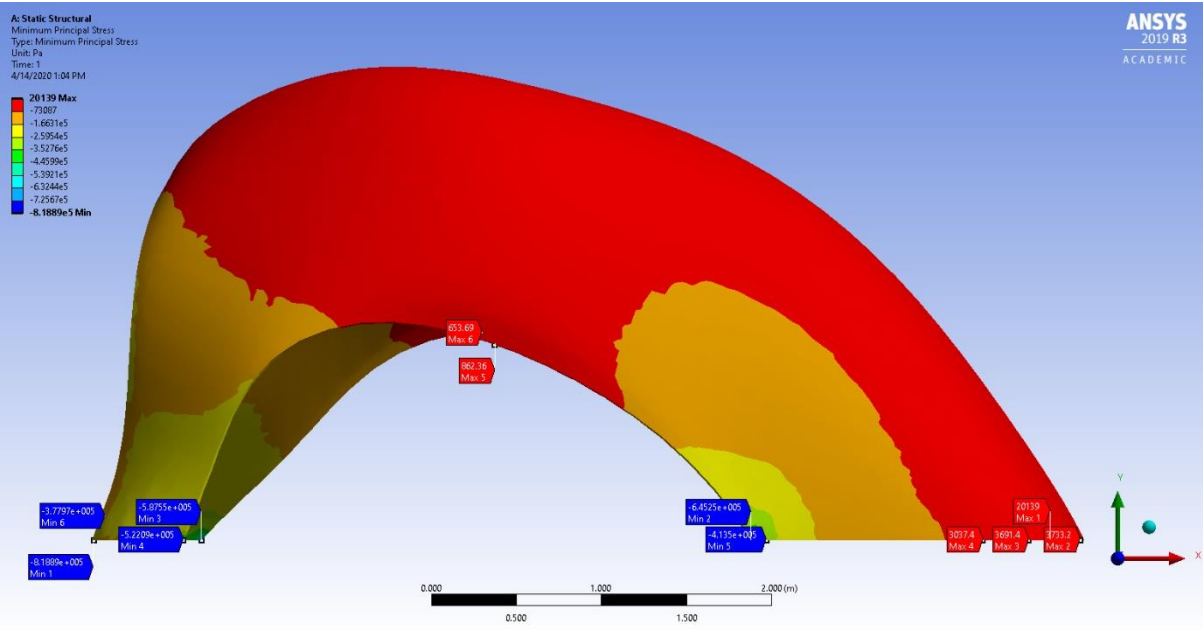




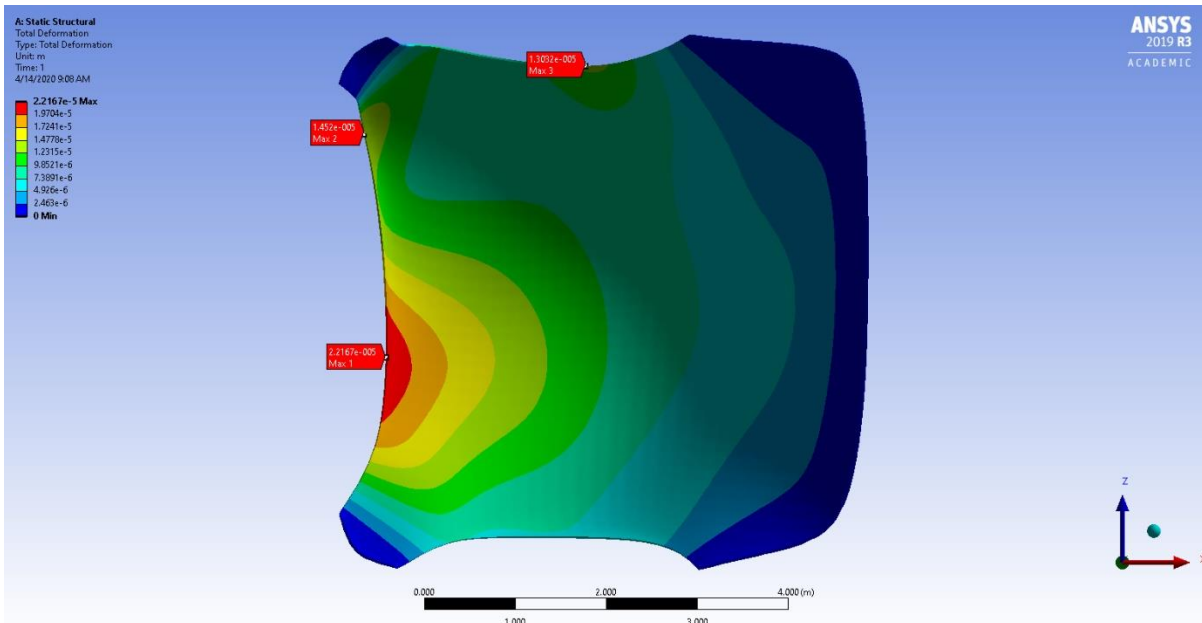
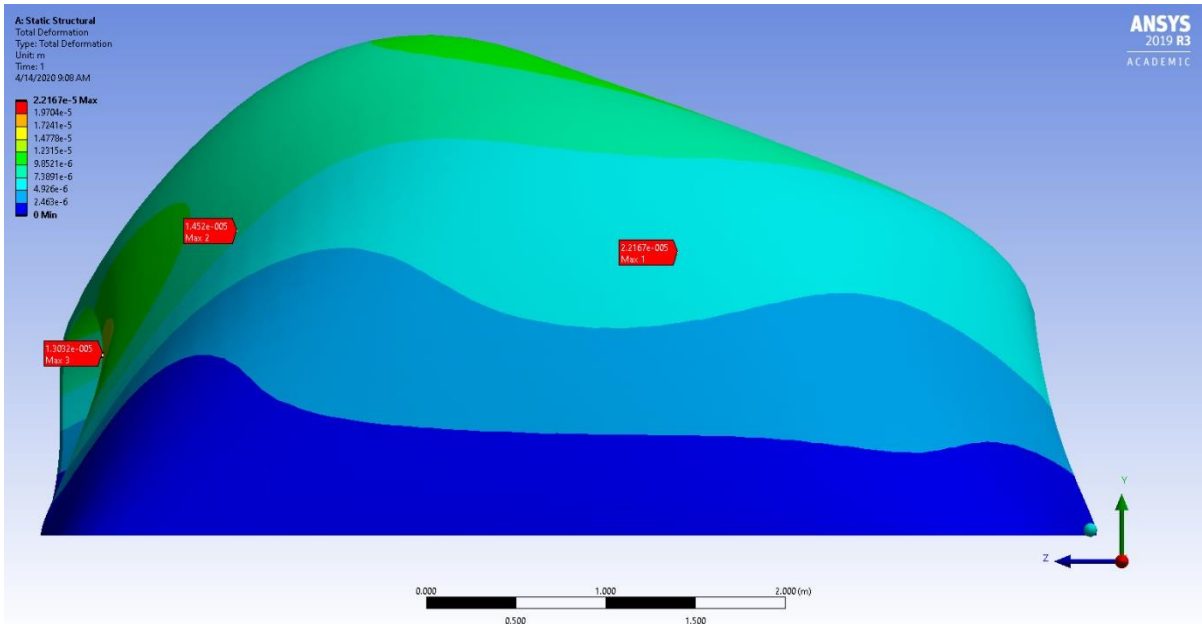
C.17 The 2 cm shell – Minimum Principal Stress

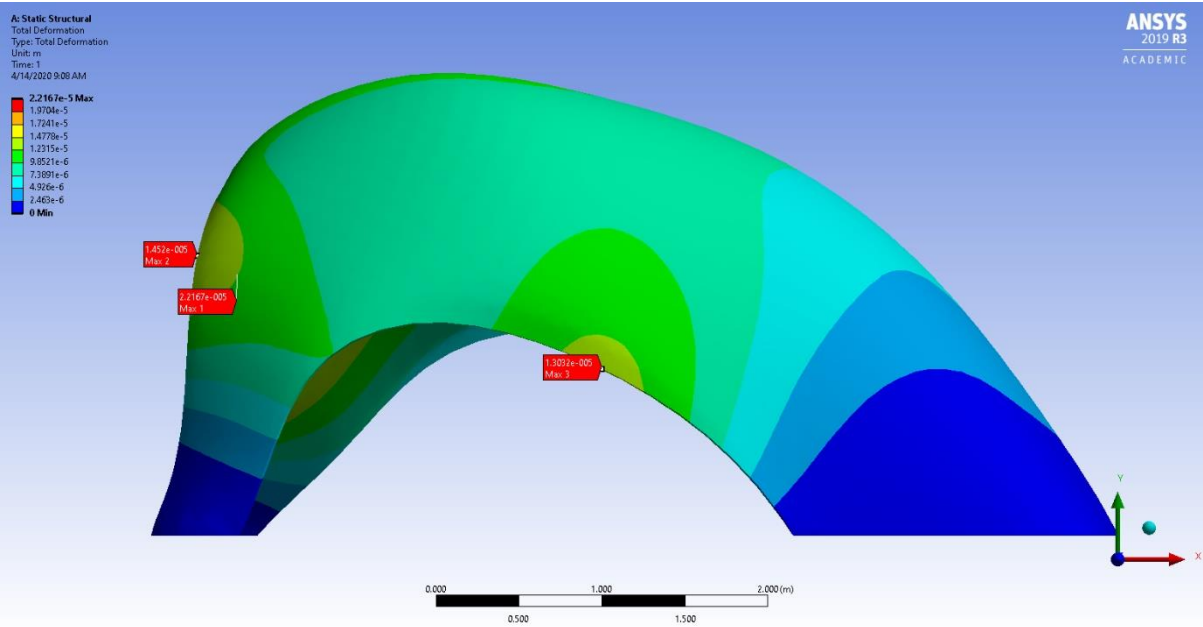
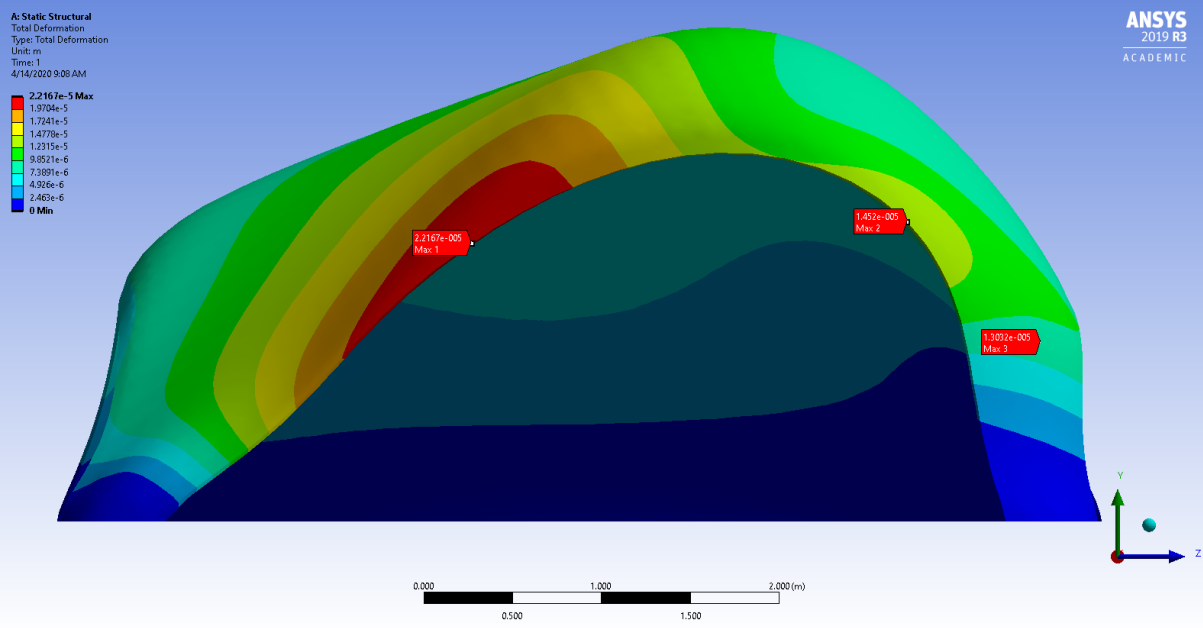


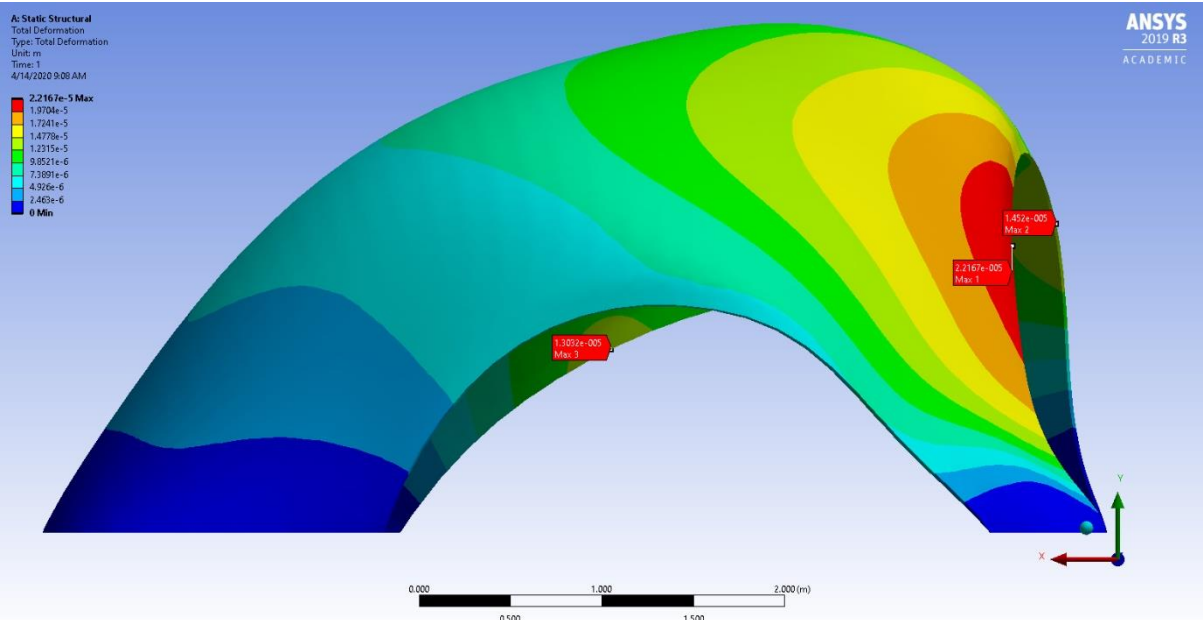
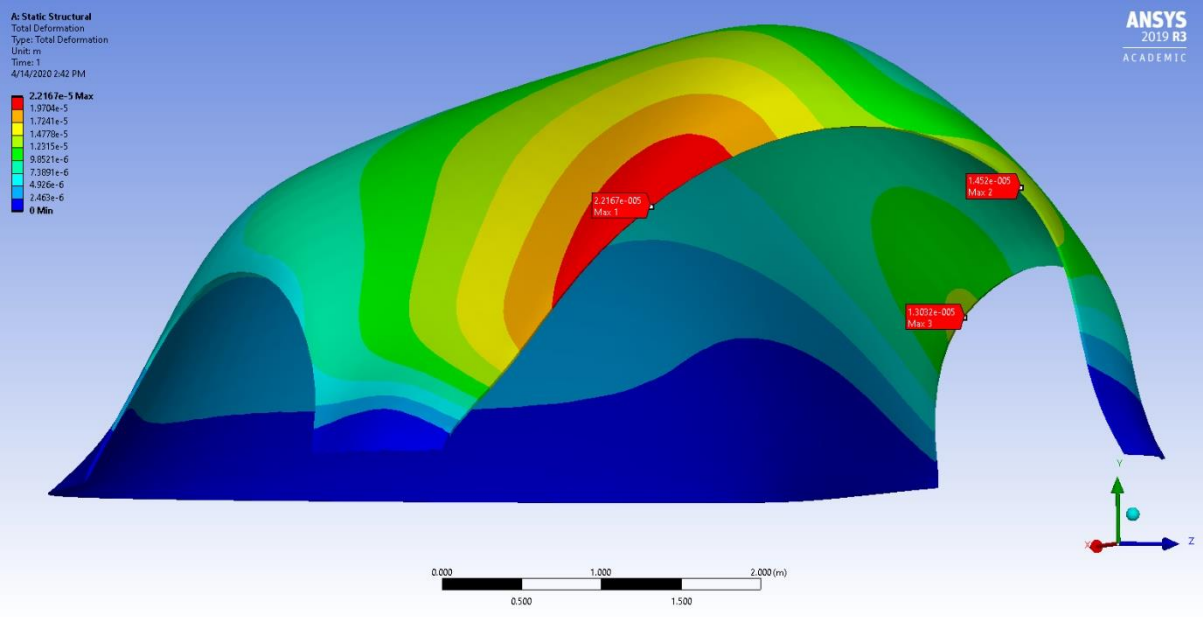


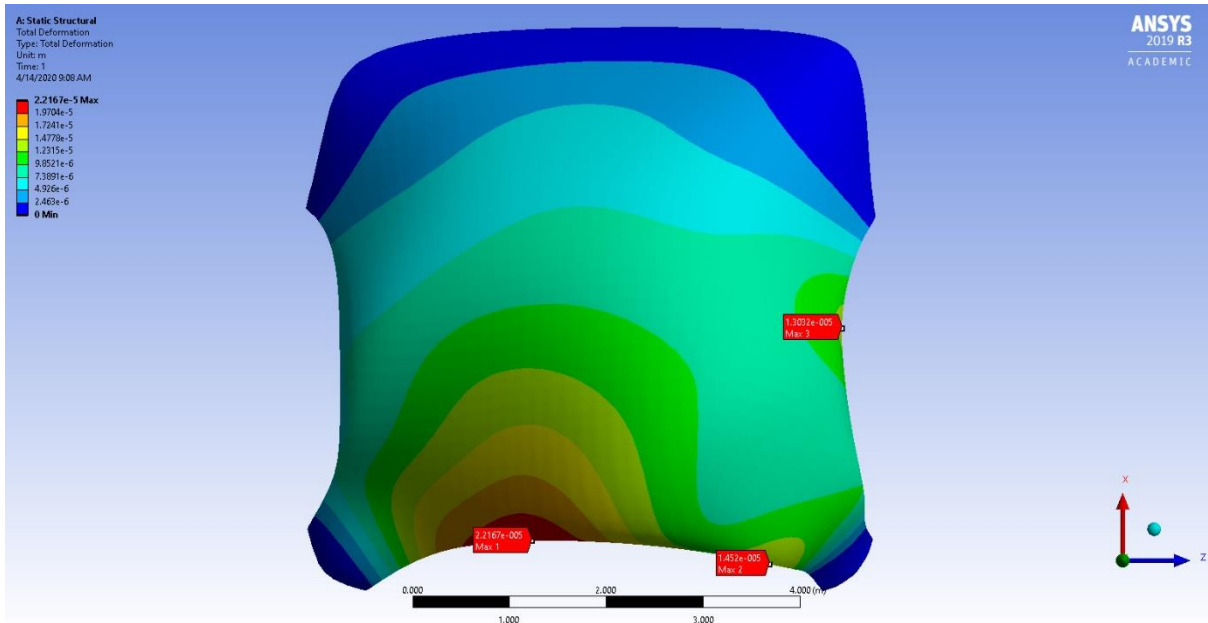


C.18 The 2 cm shell – Deformation

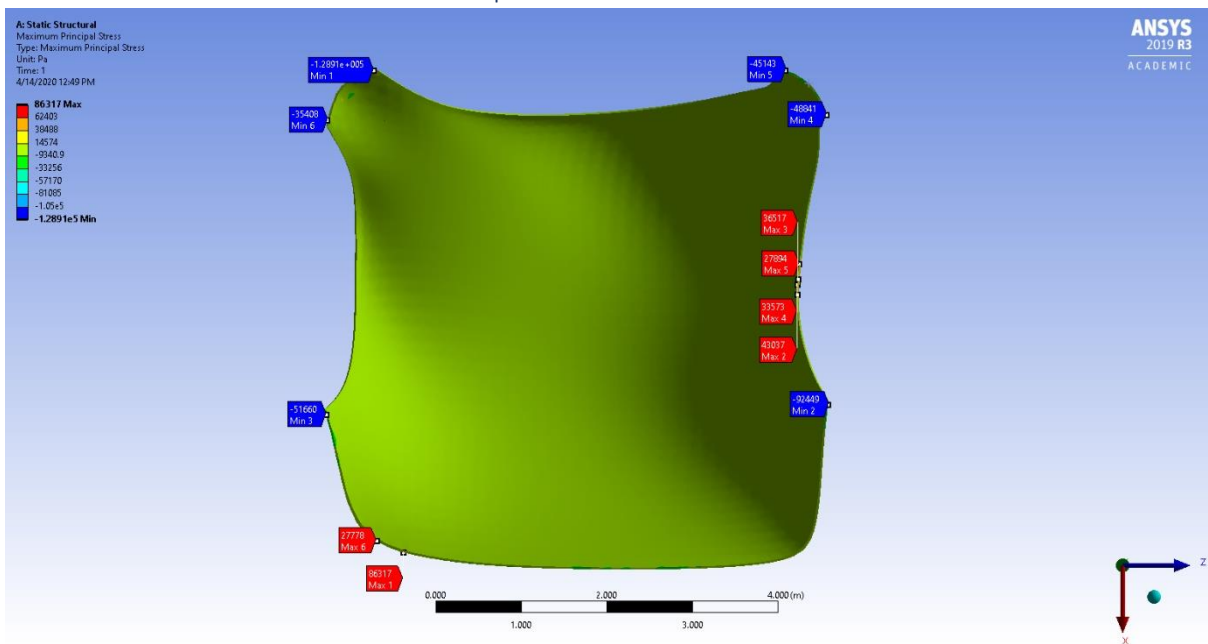


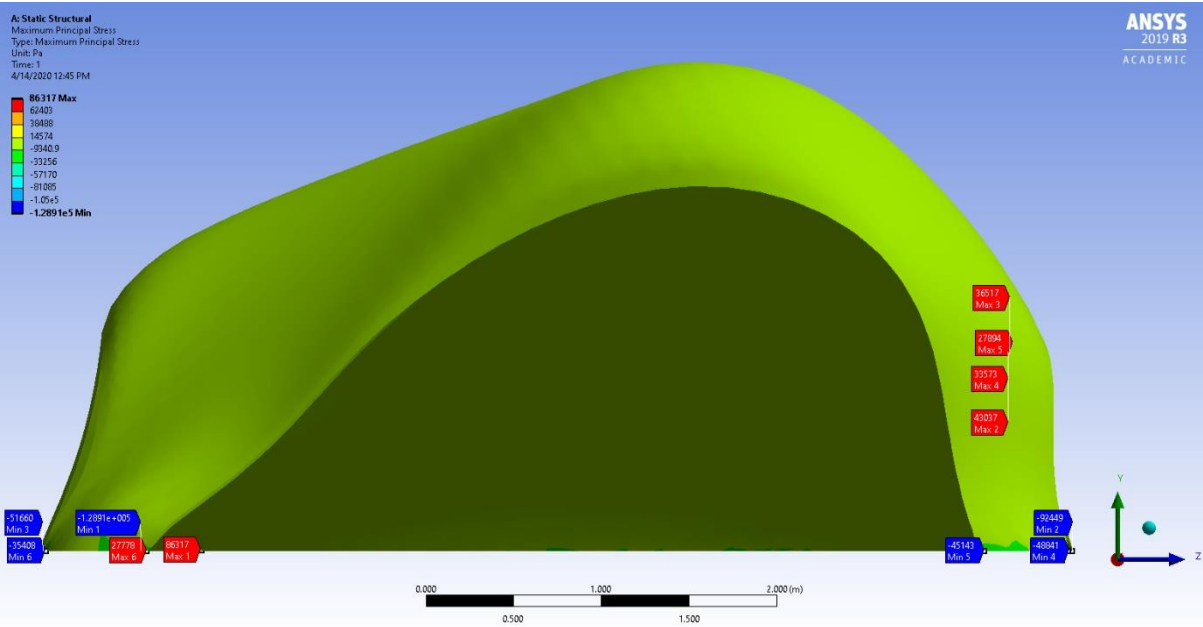
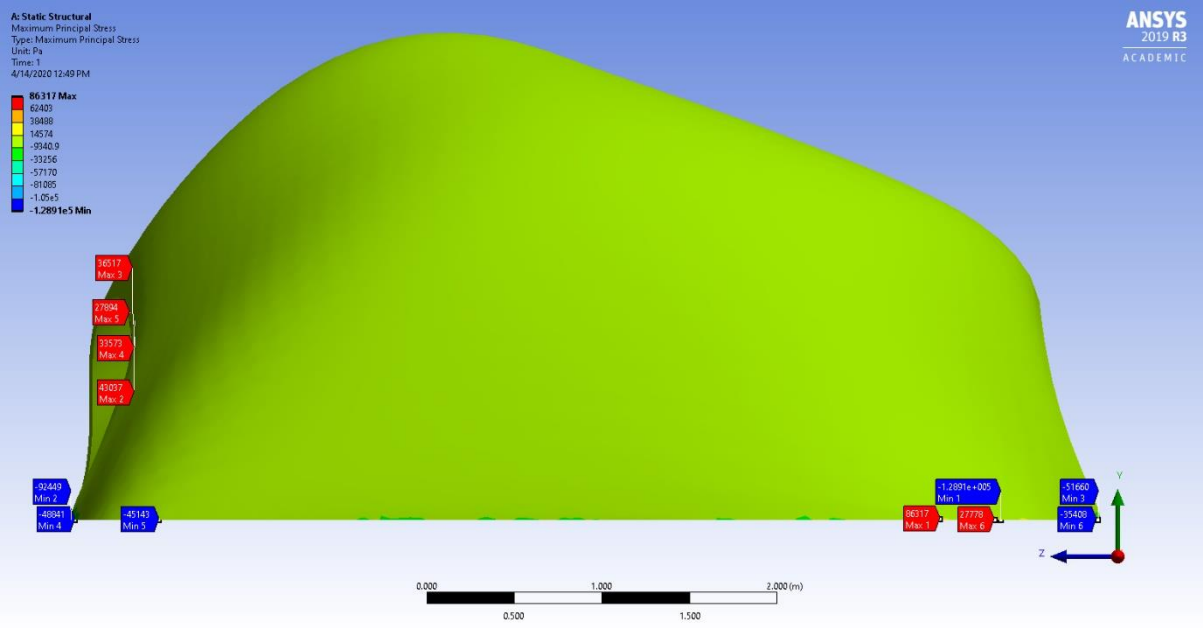


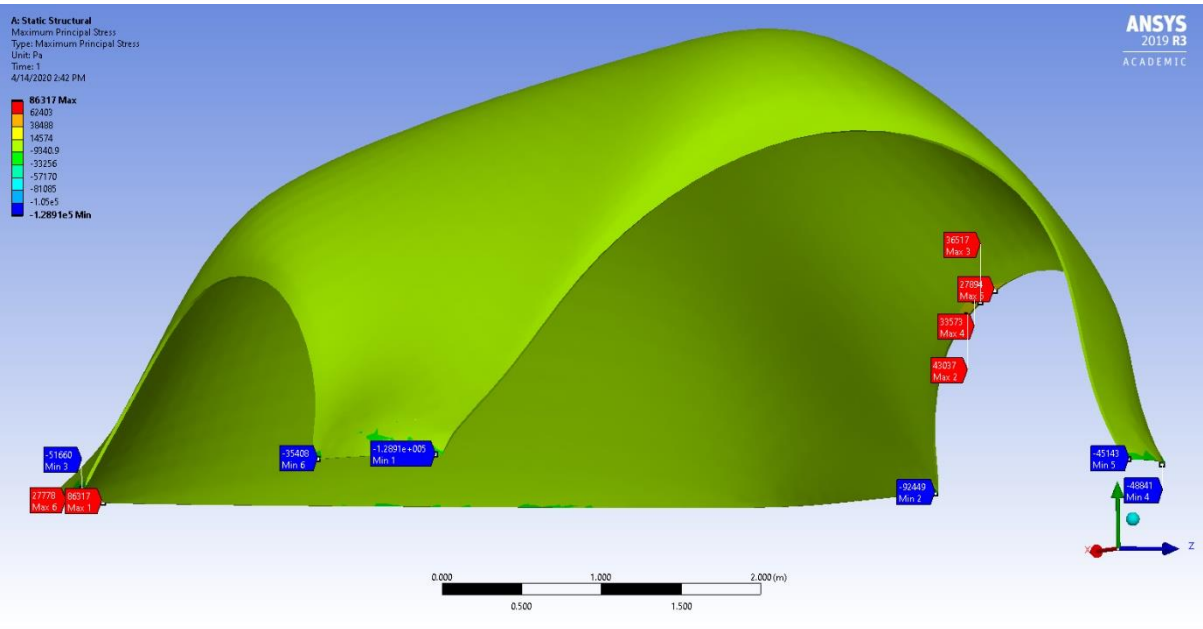
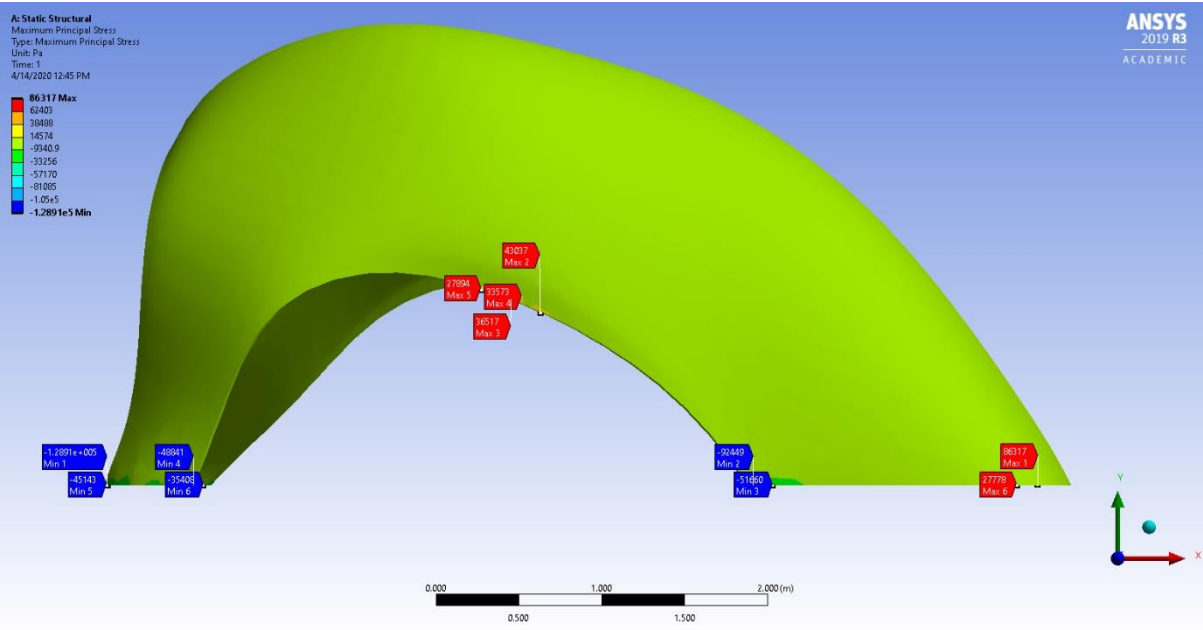


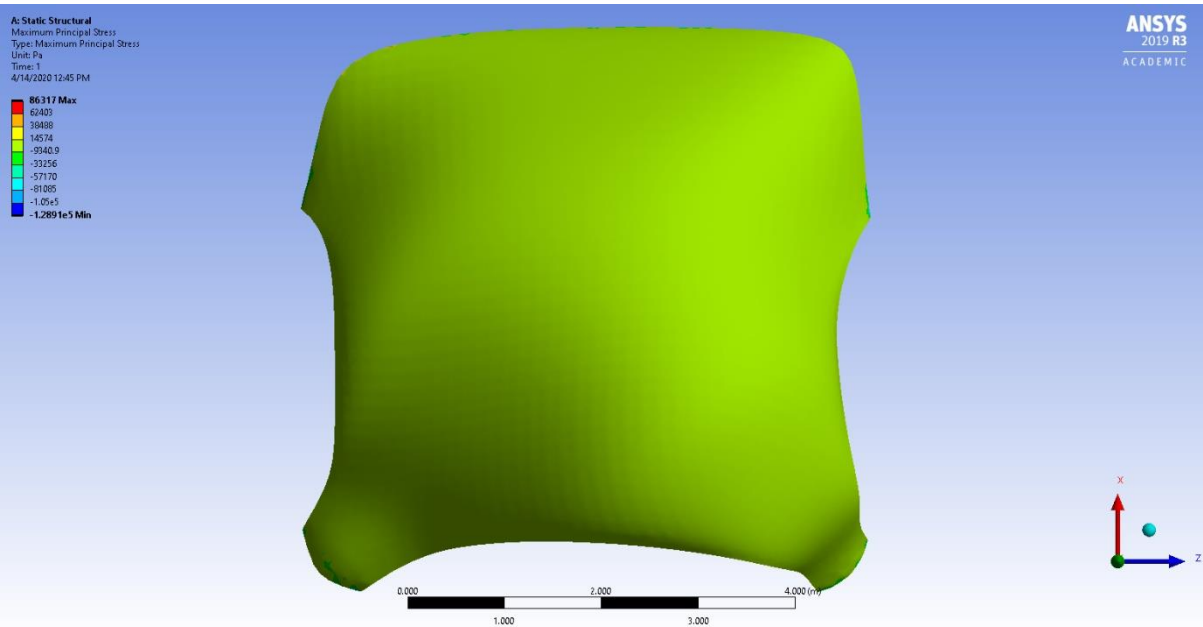
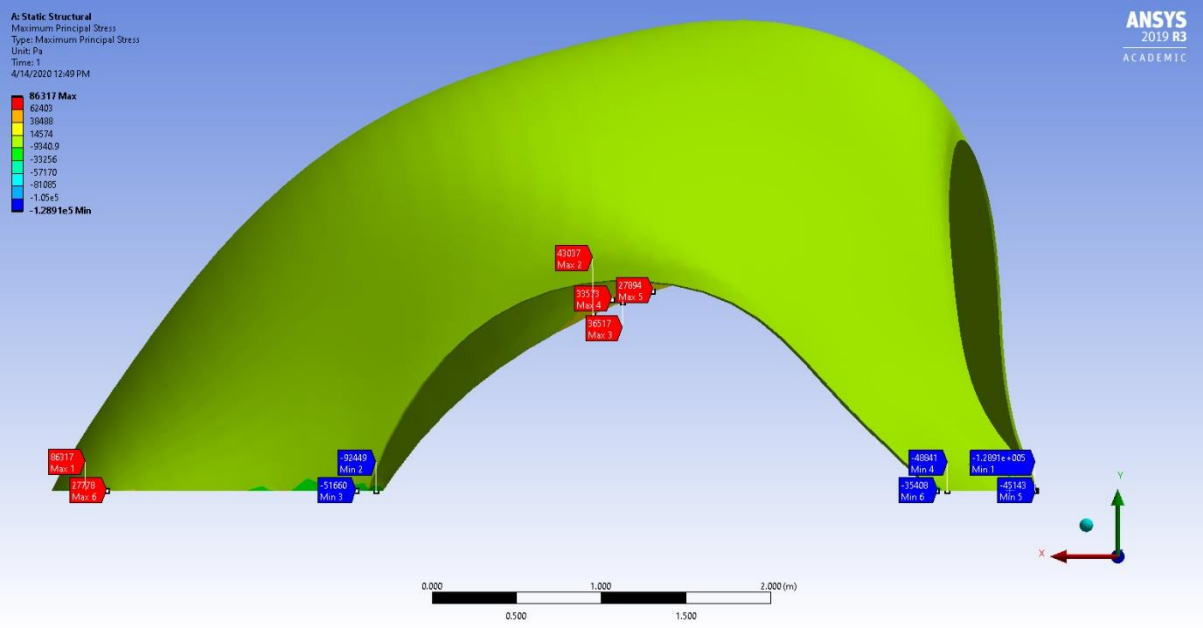


C.18 The 2 cm shell – Maximum Principal Stress

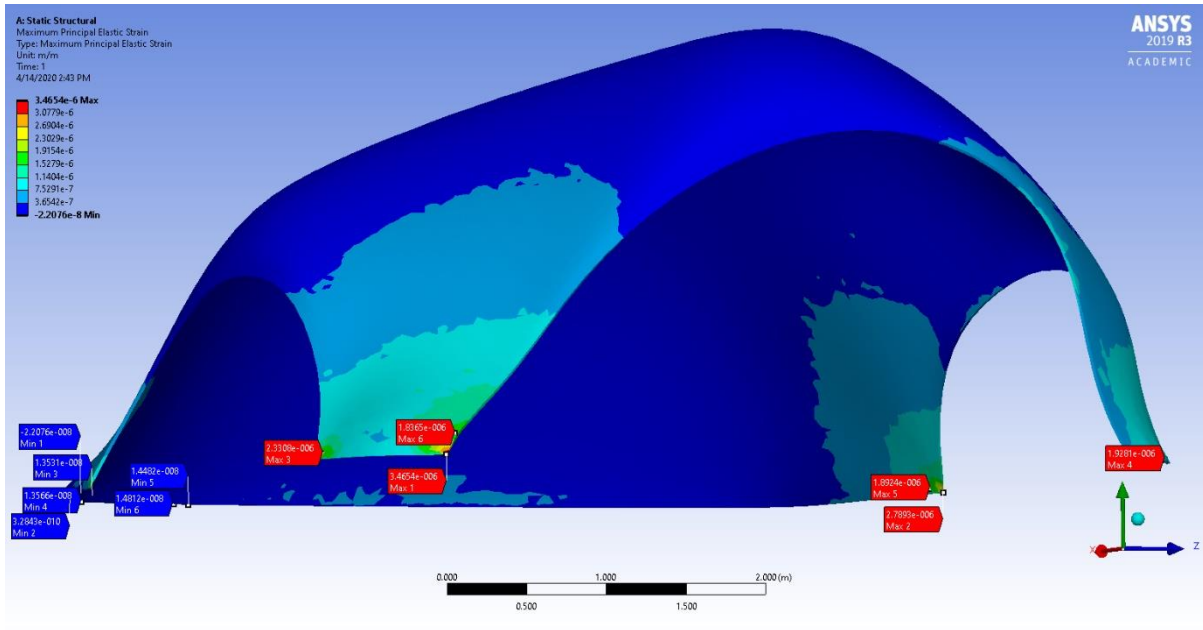




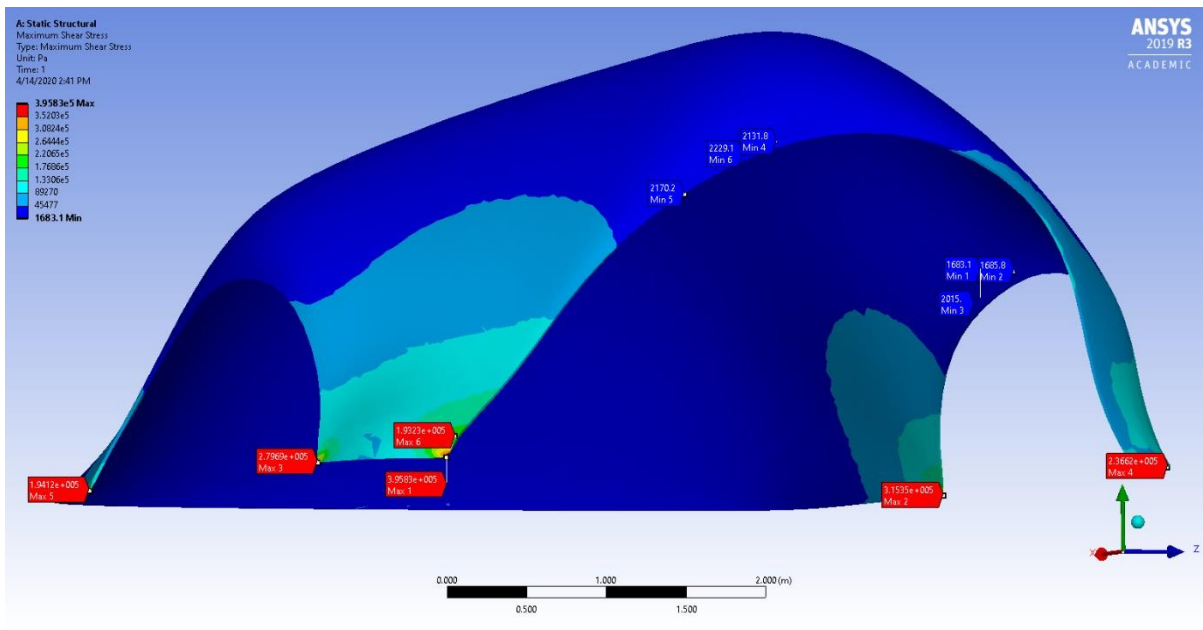




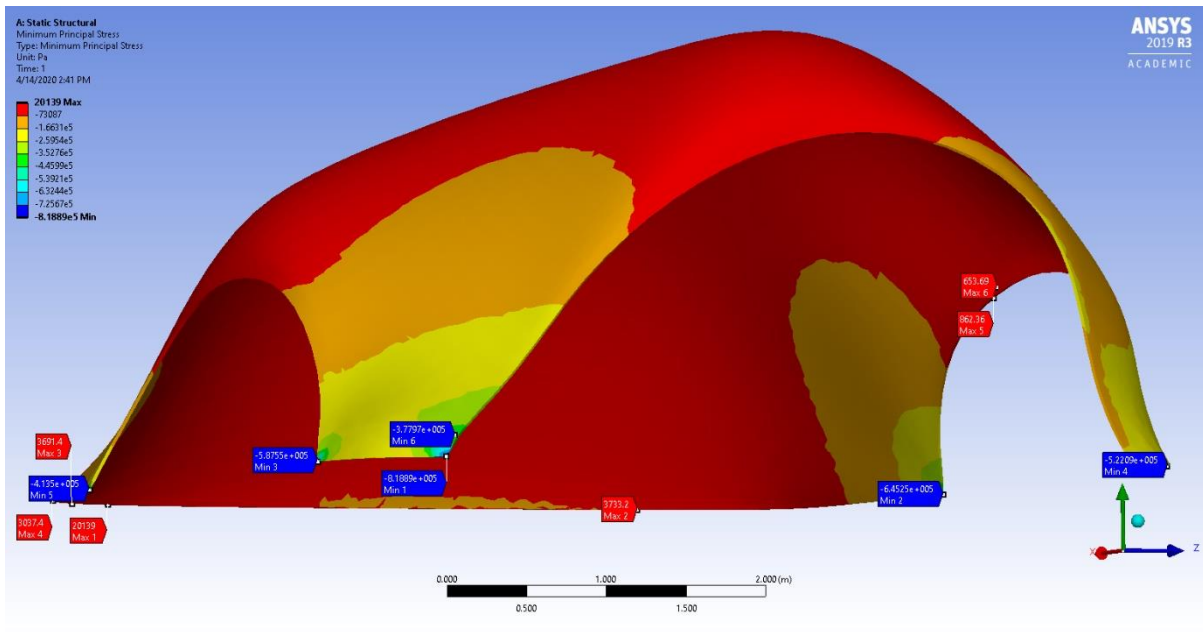
C.19 The 2 cm shell – Maximum Principal Elastic Strain



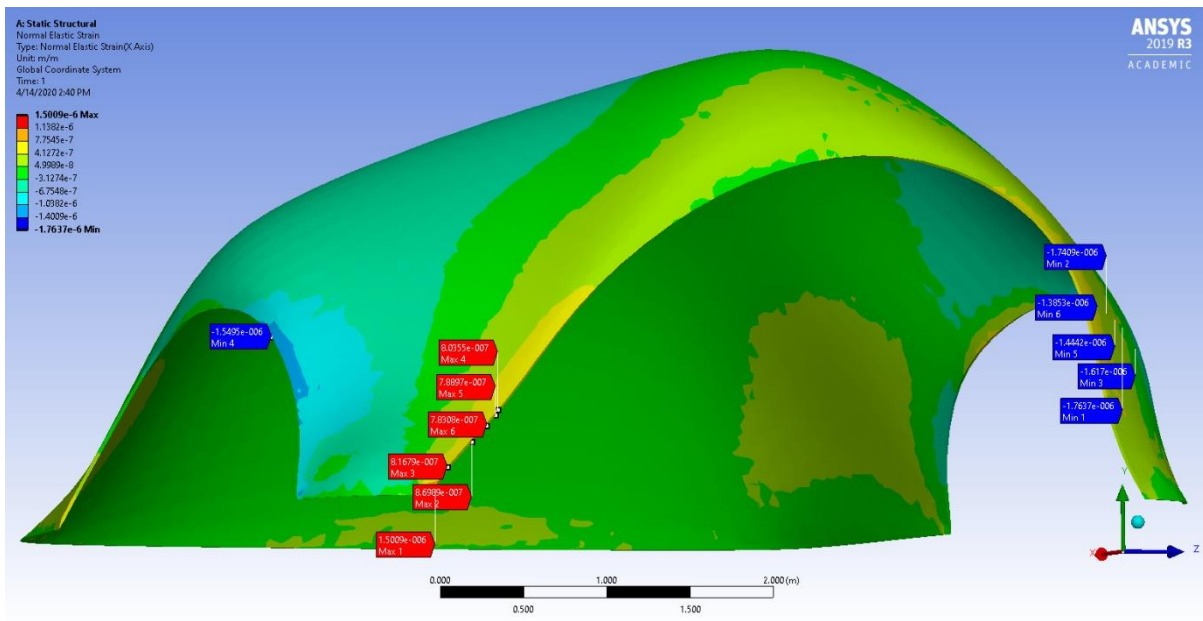
C.20 The 2 cm shell – Maximum Shear stress



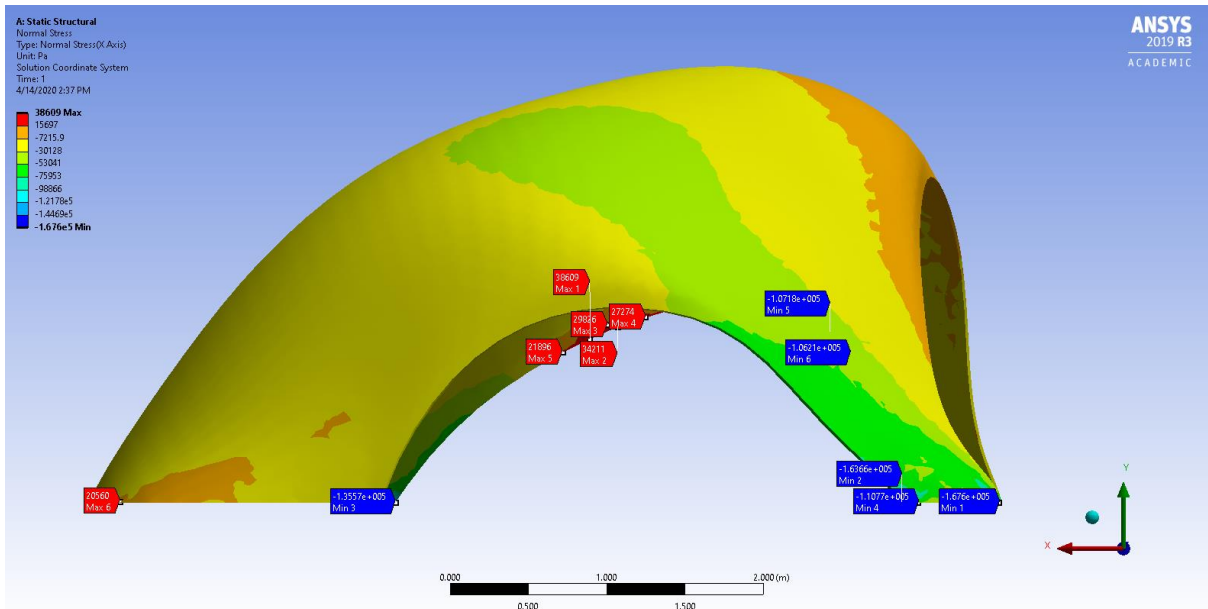
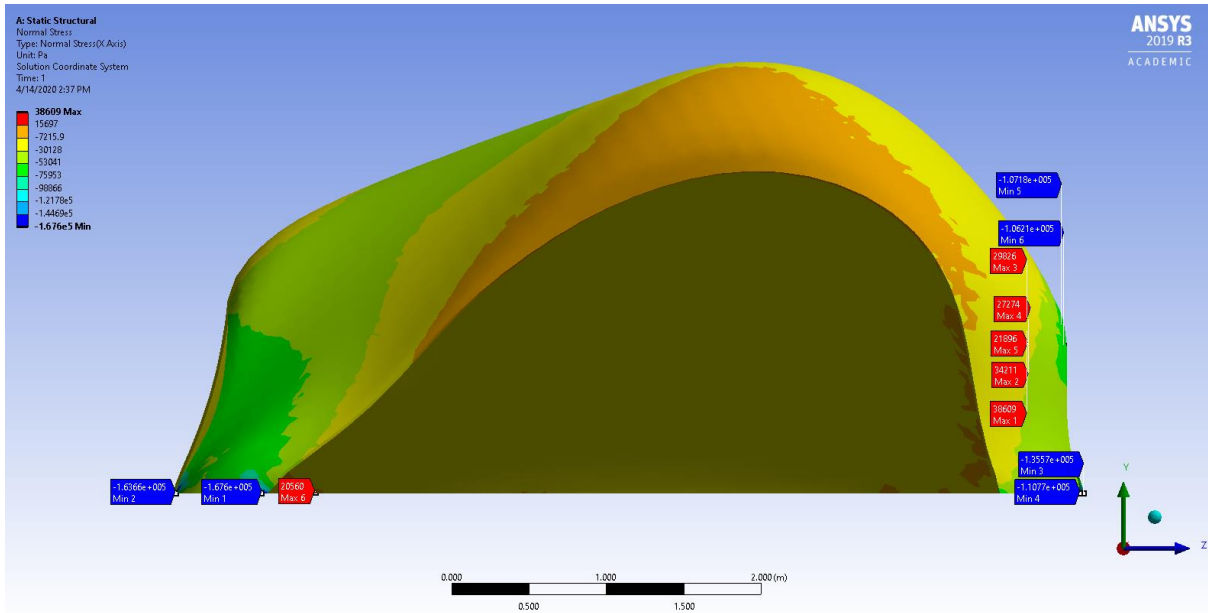
C.21 The 2 cm shell – Minimum Principal Stress



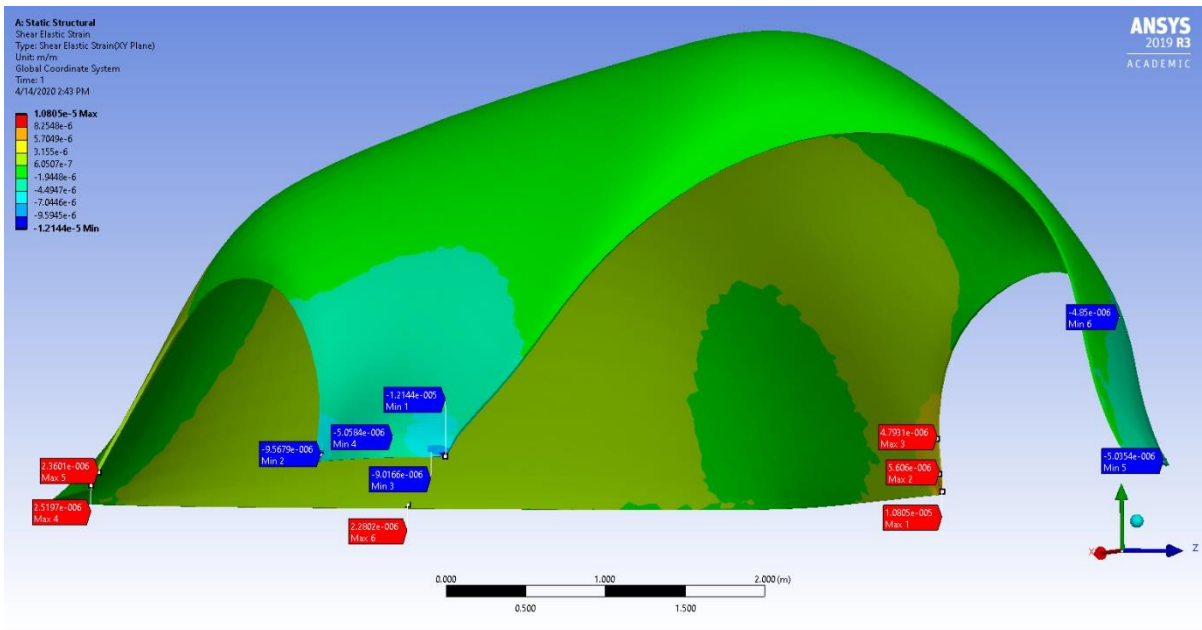
C.22 The 2 cm shell – Normal Elastic Strain



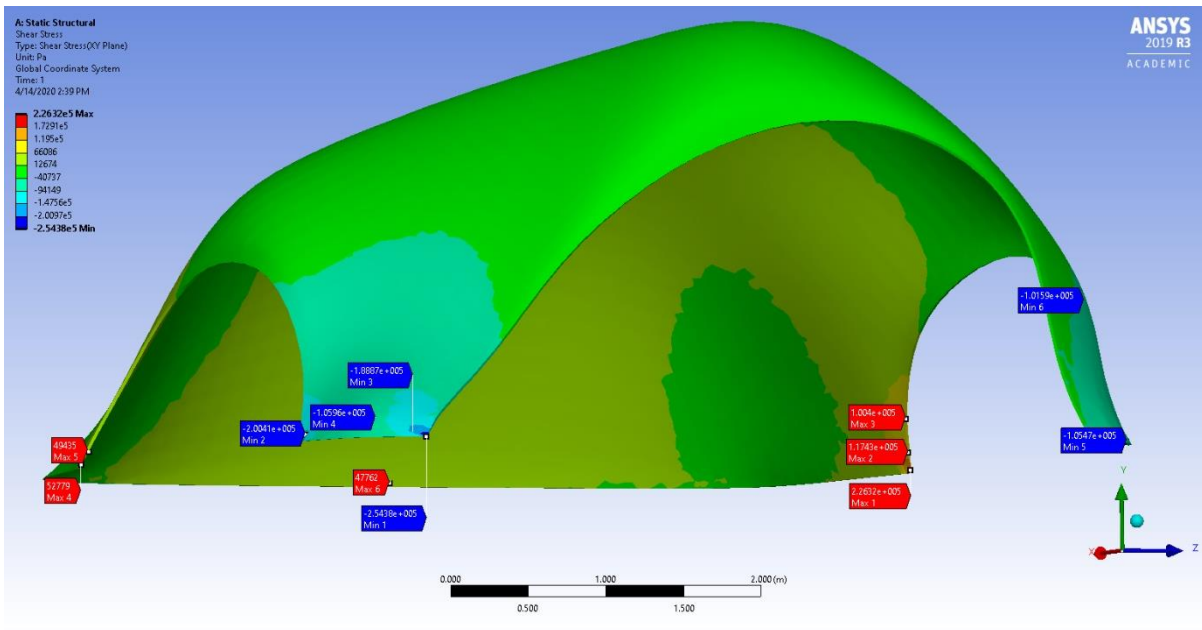
C.23 The 2 cm shell – Normal Stress



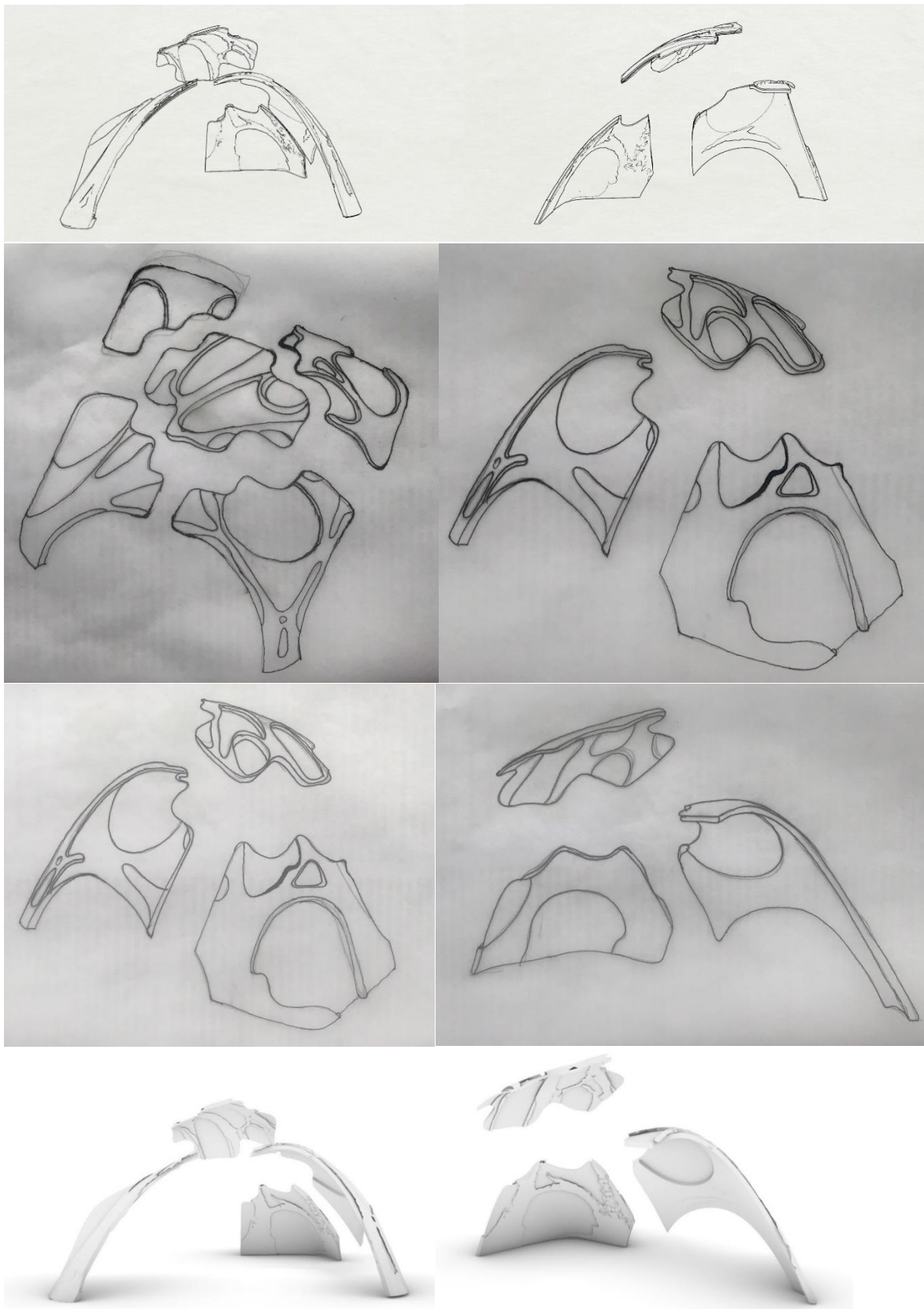
C.24 The 2 cm shell – Shear Elastic Strain

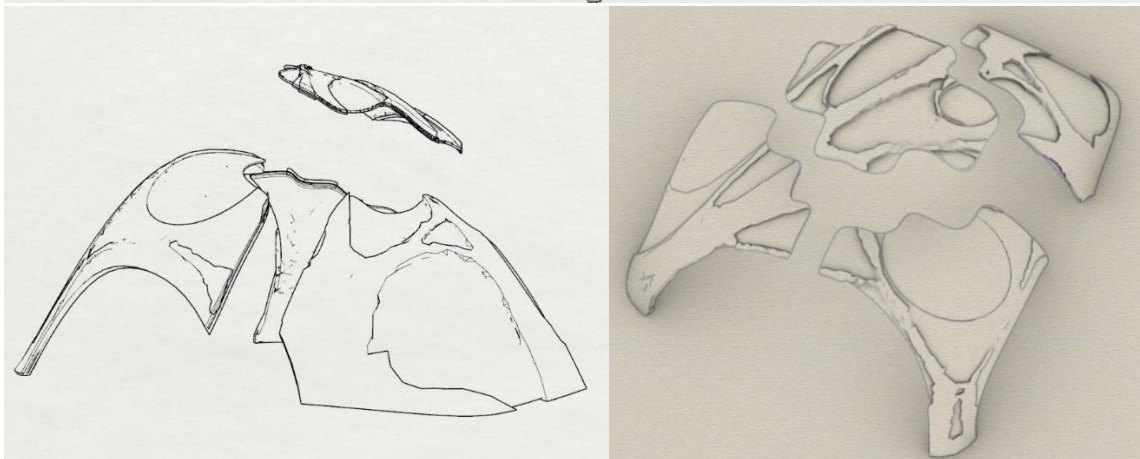
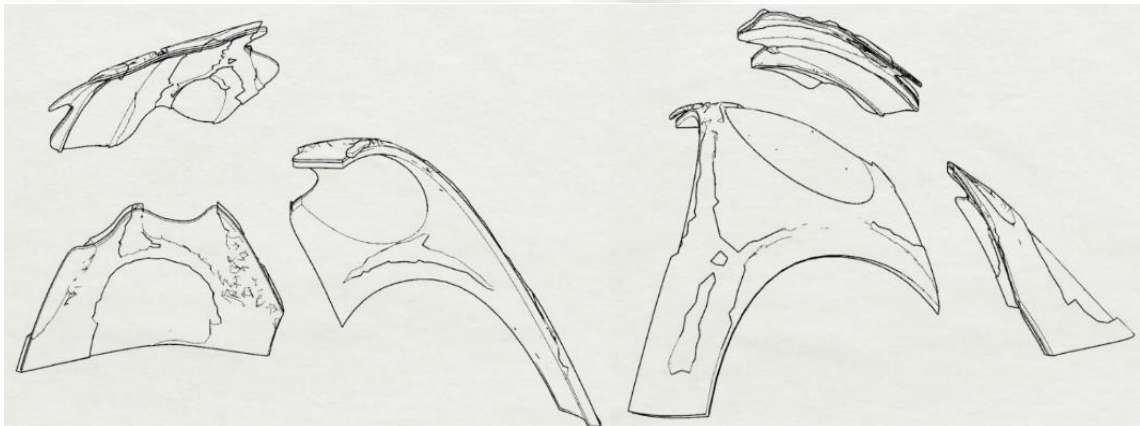
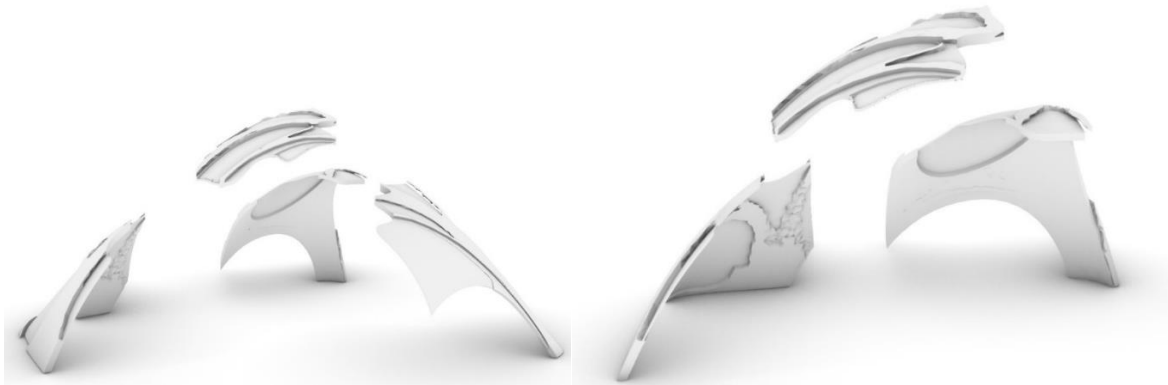


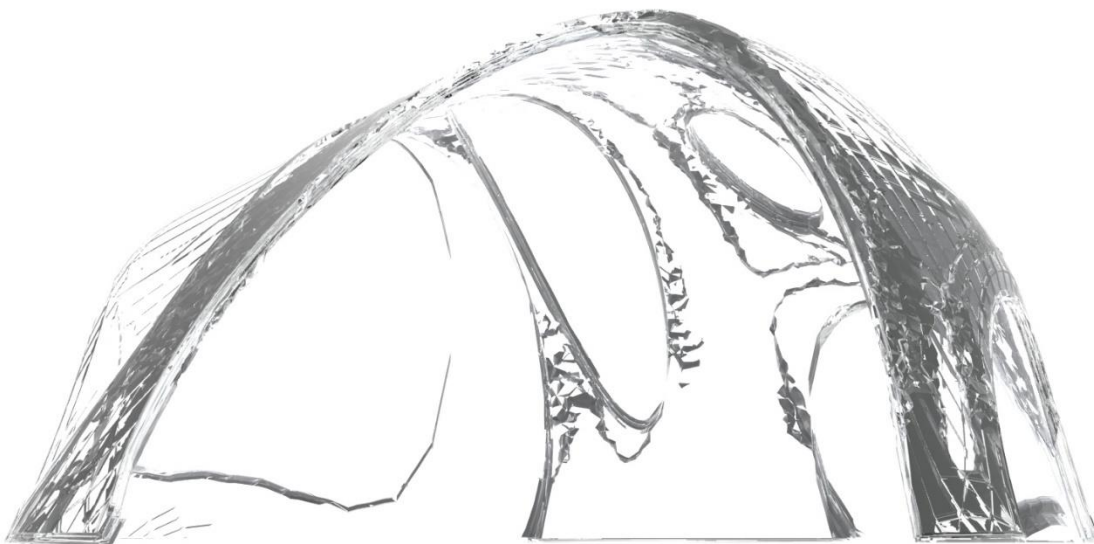
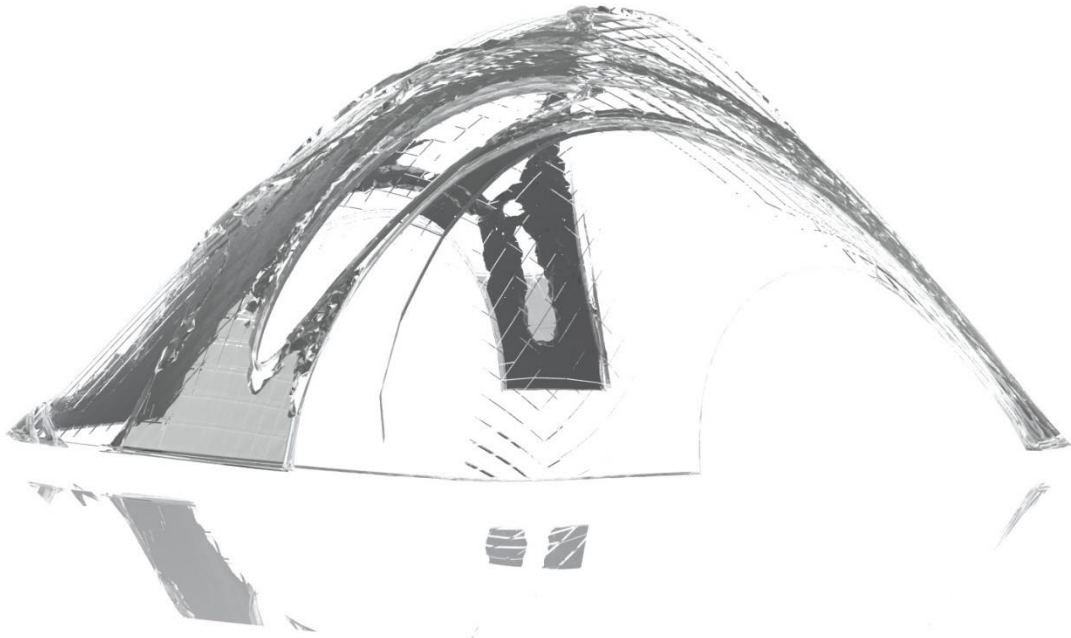
C.25 The 2 cm shell – Shear Stress

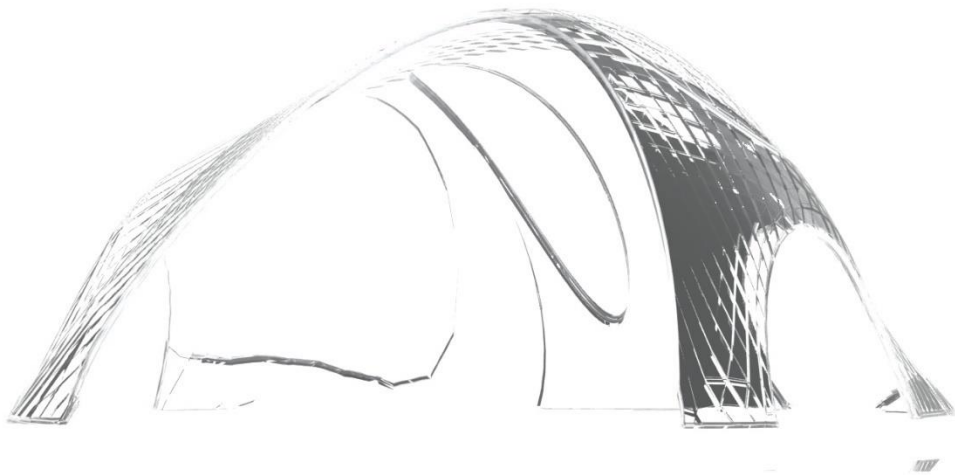
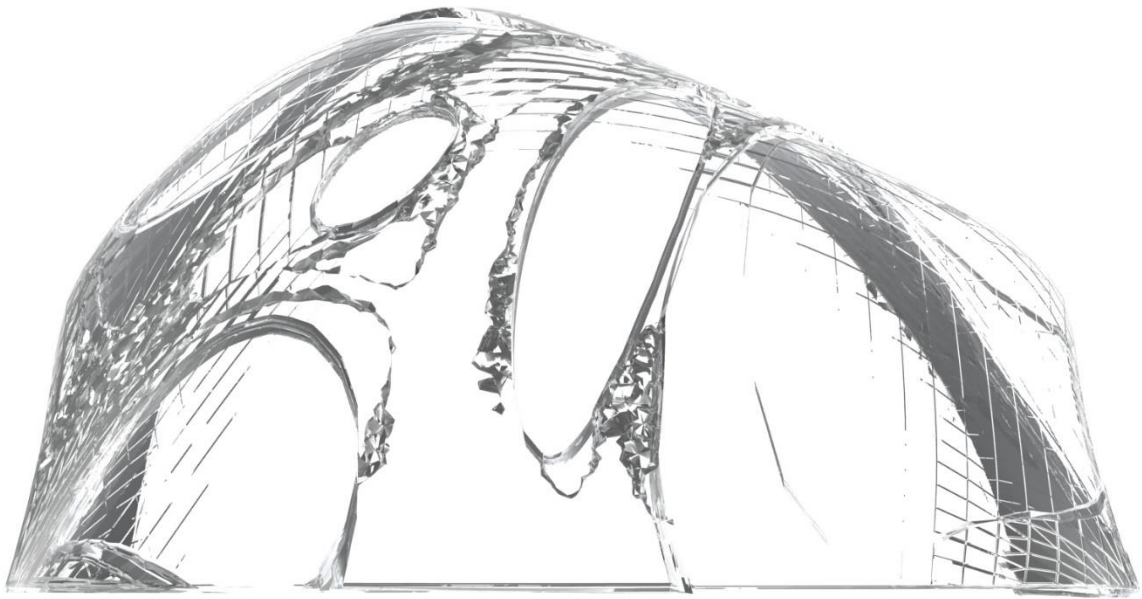


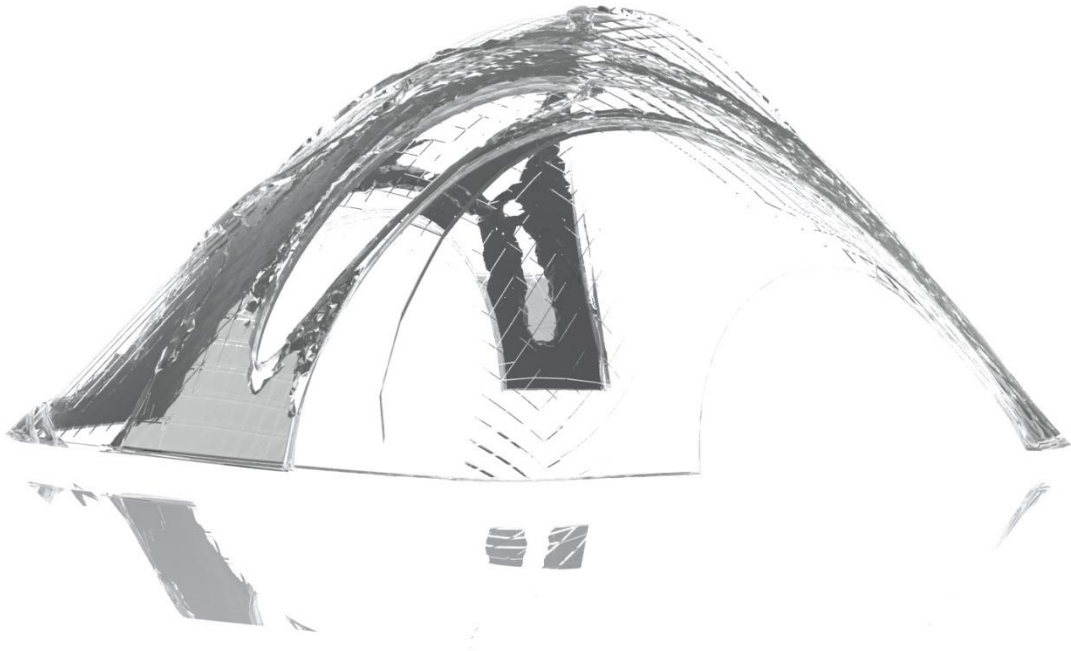
Appendix D Extra pictures from during the design process

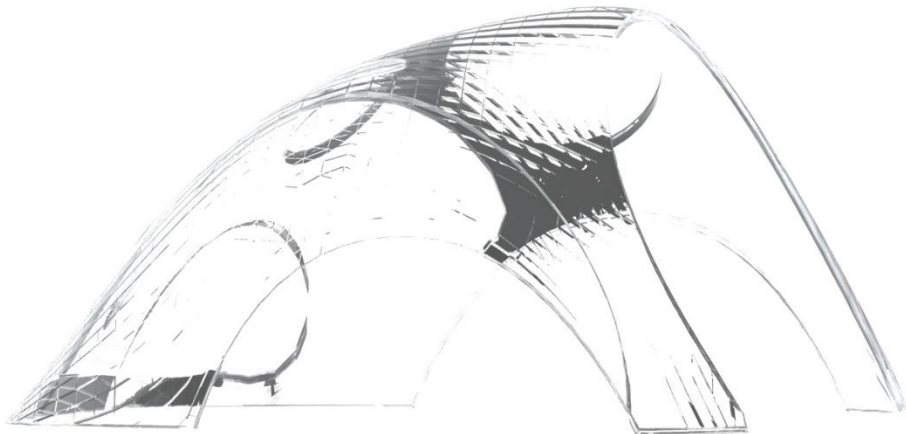
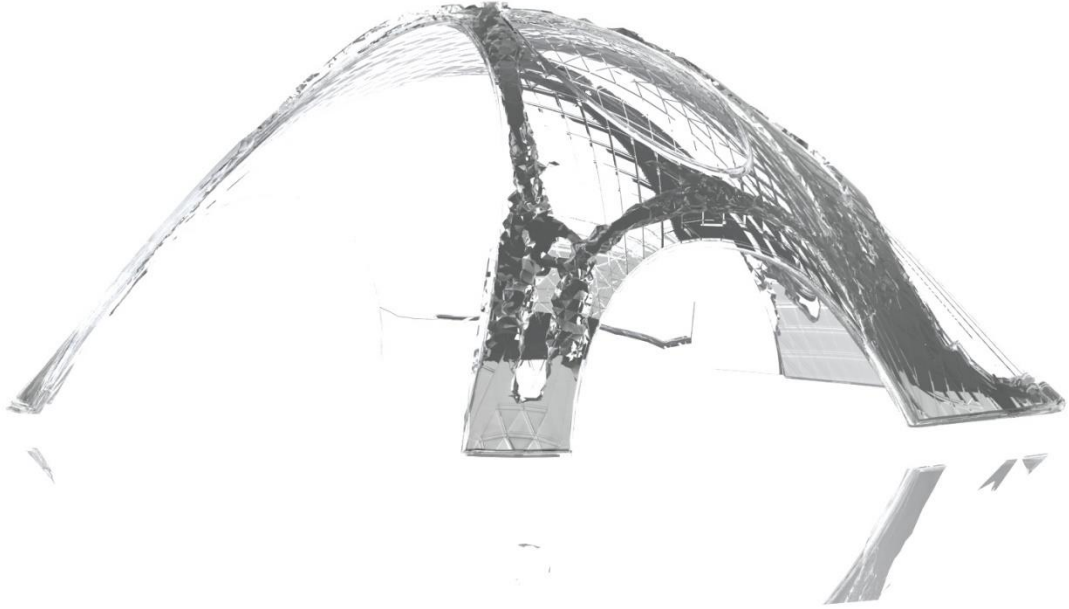


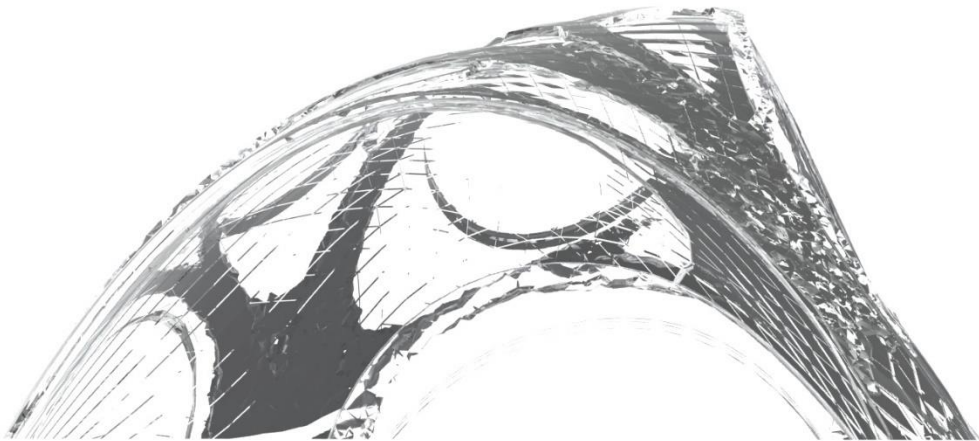
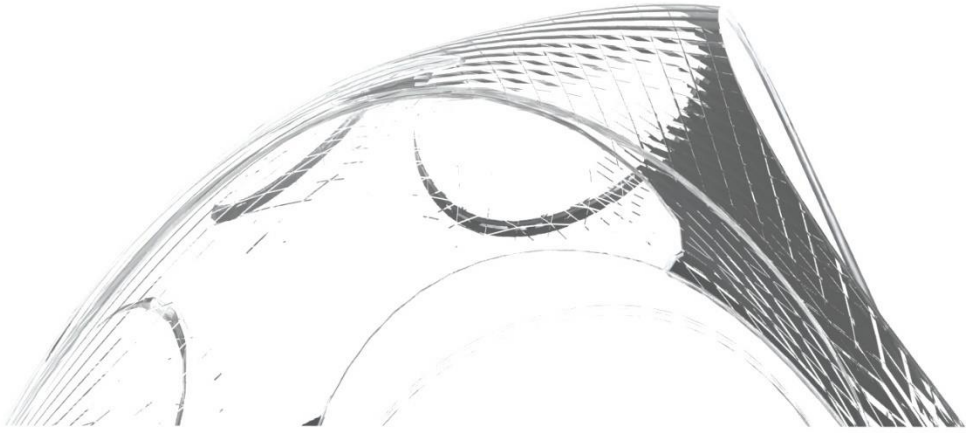


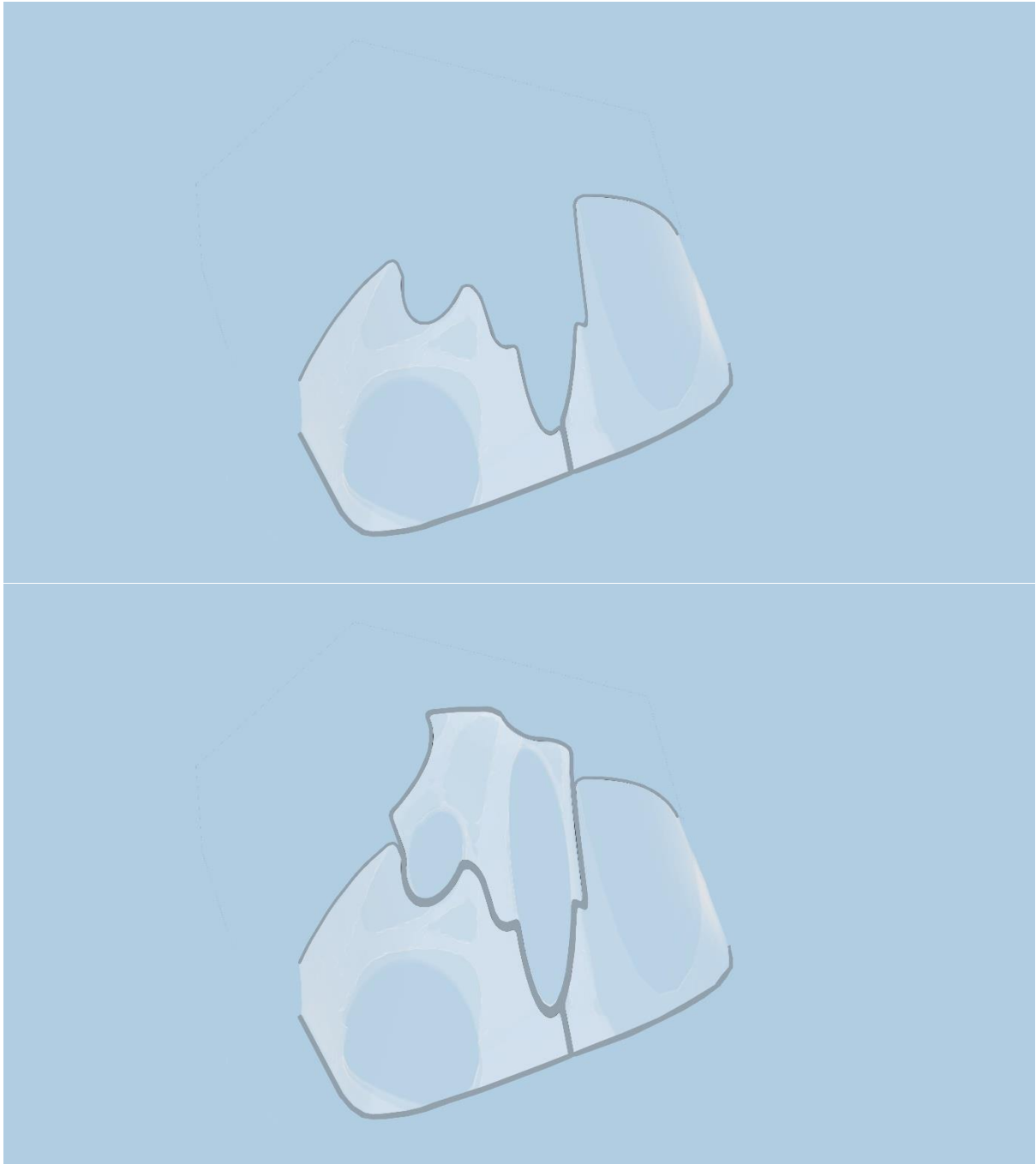


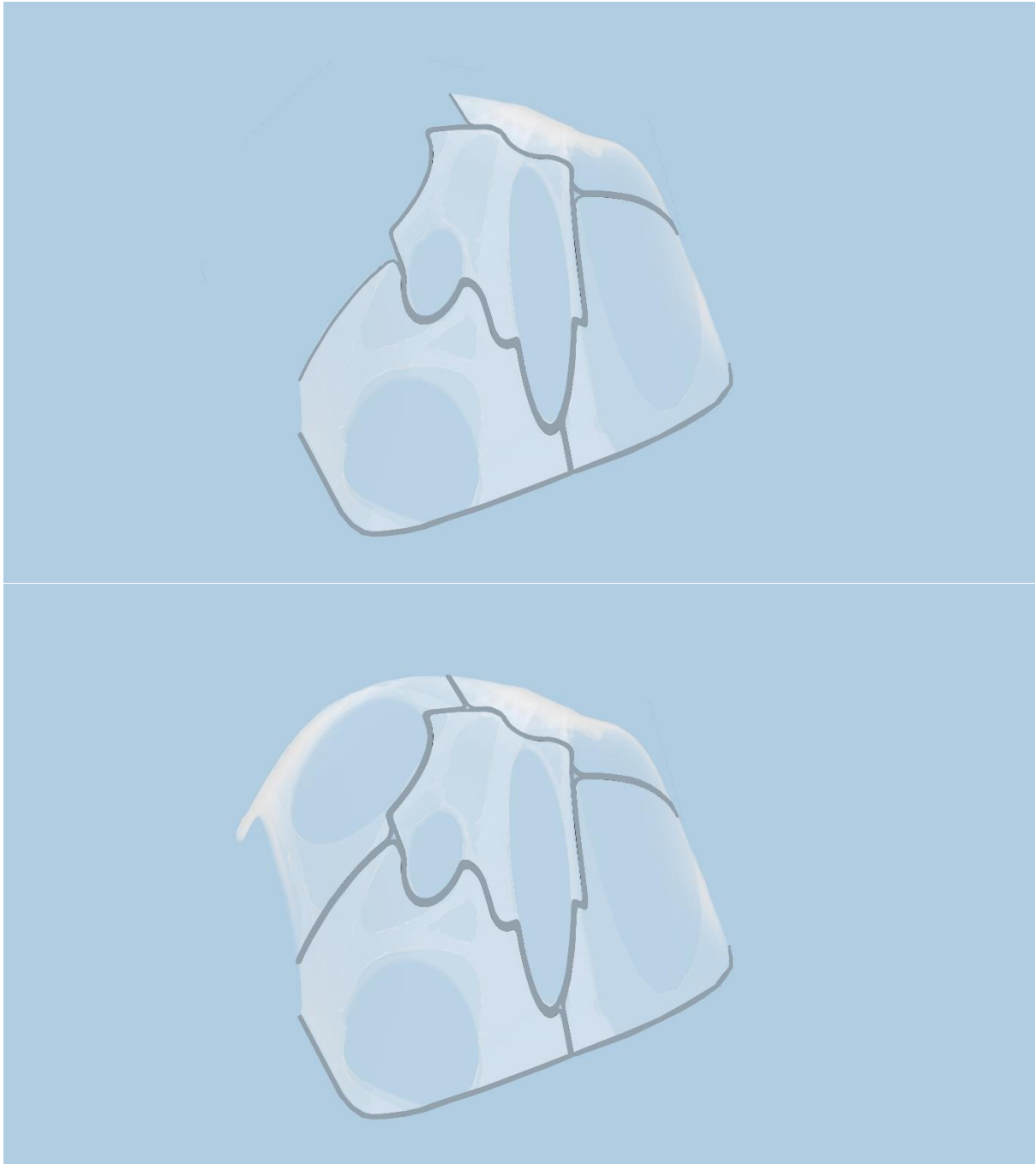




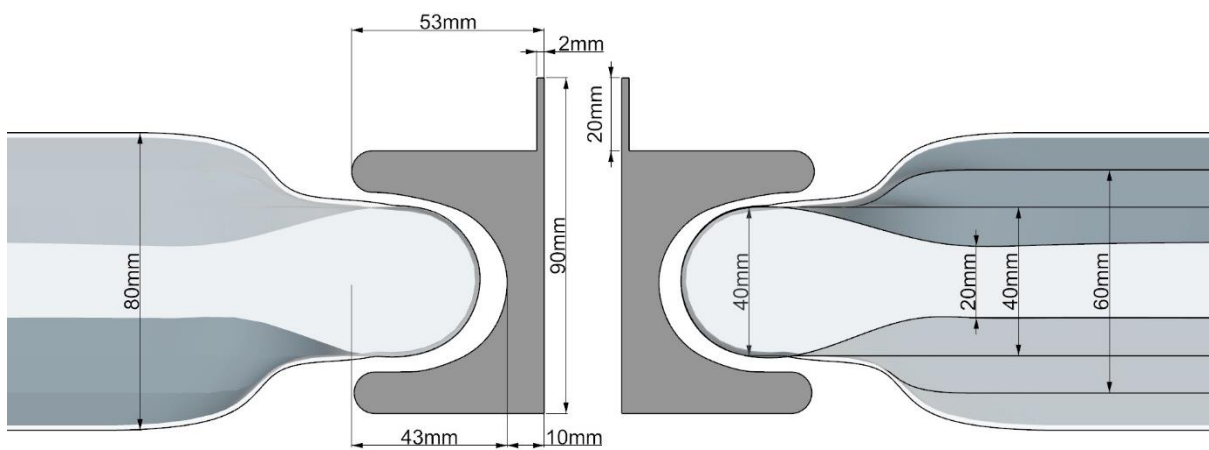
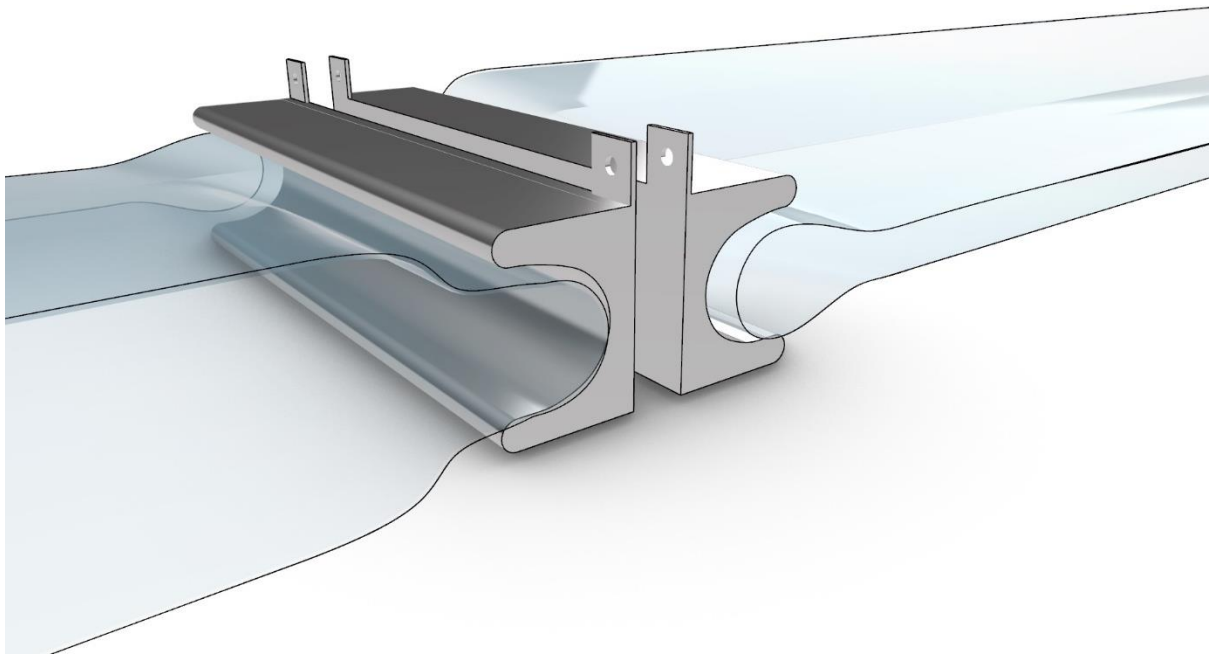




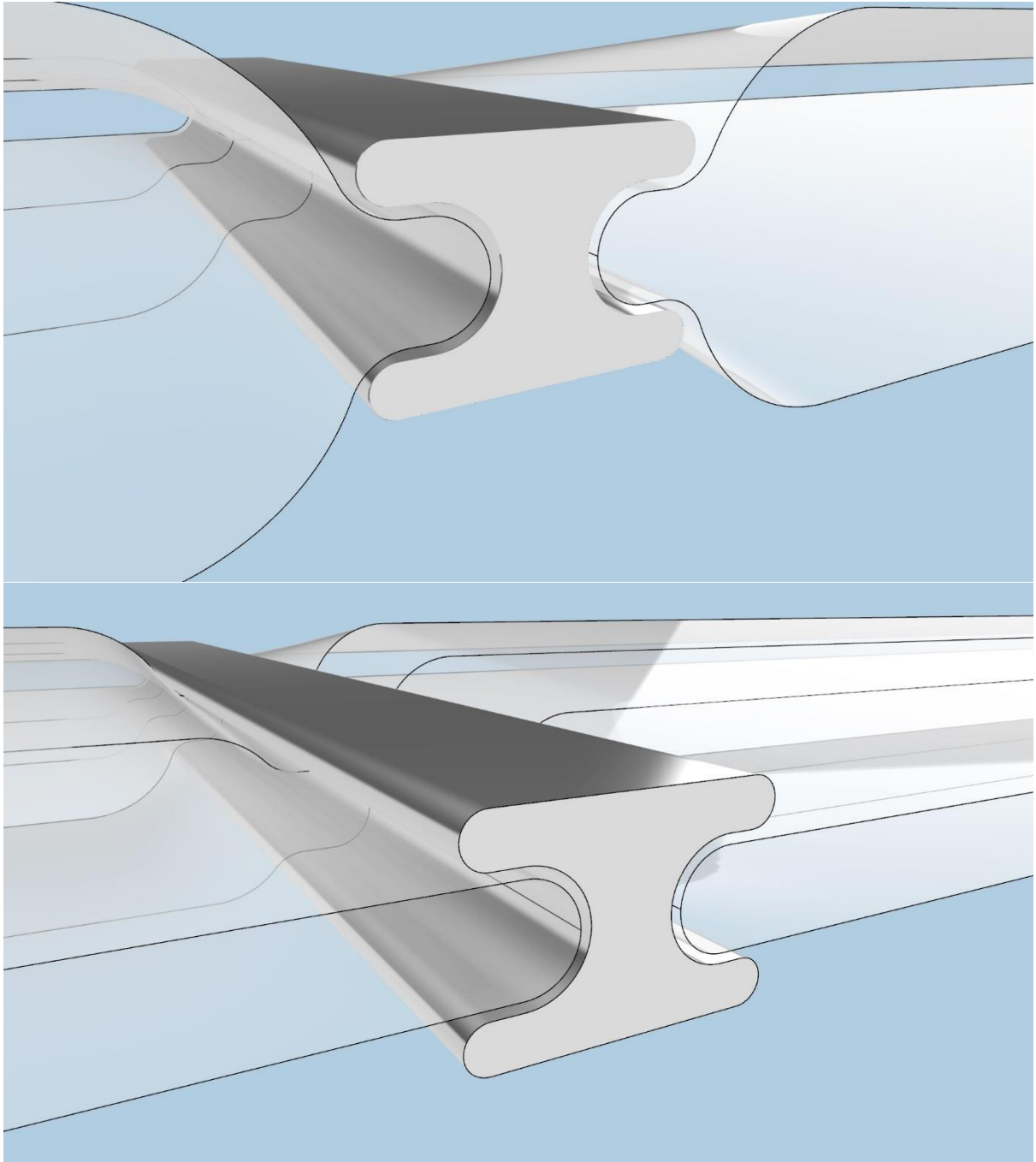


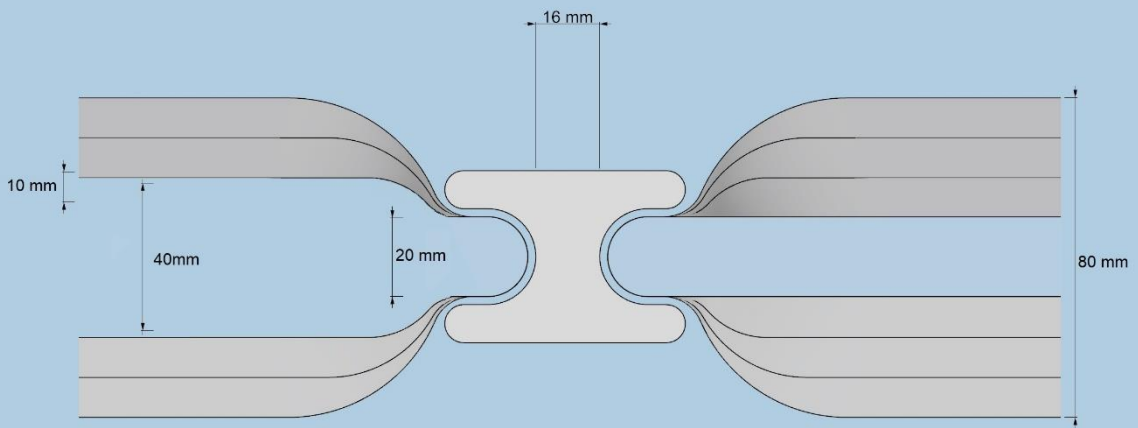
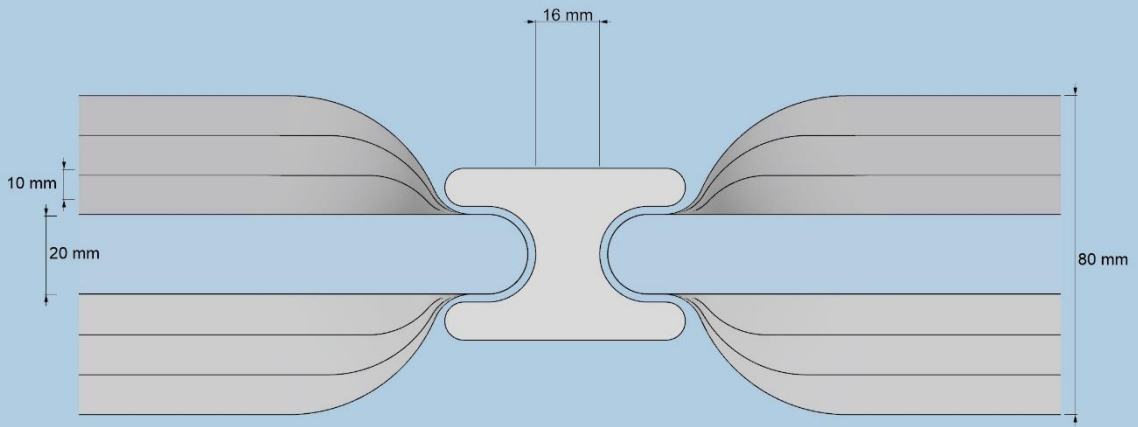


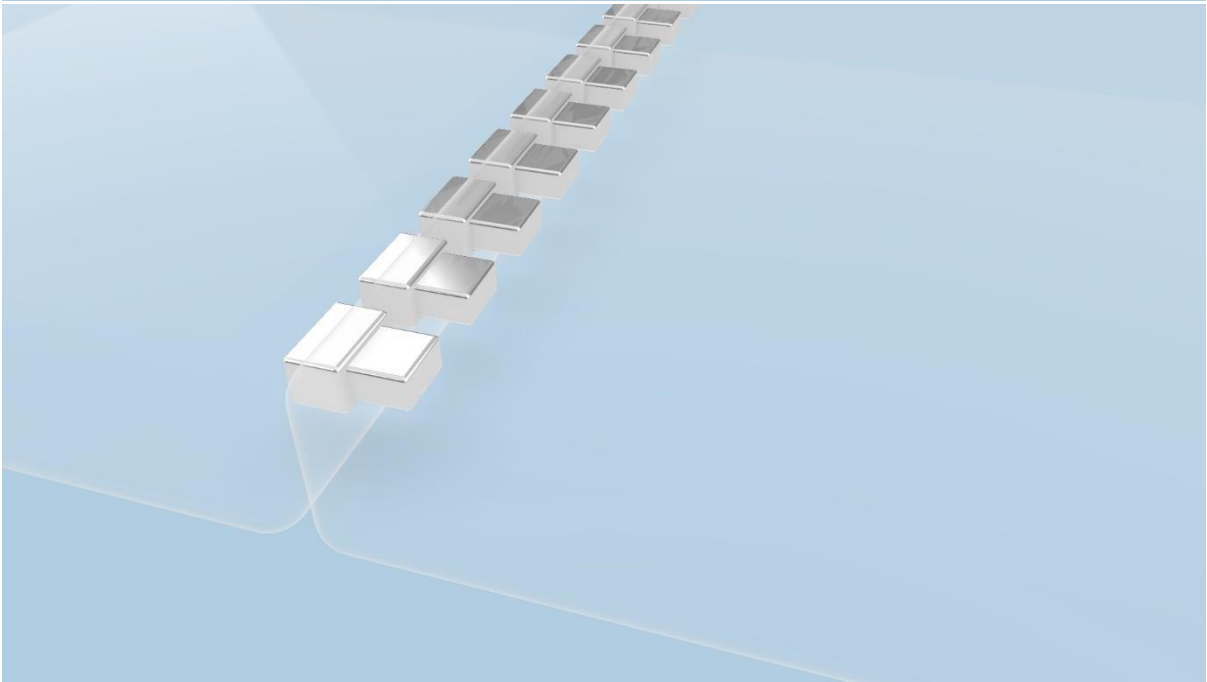
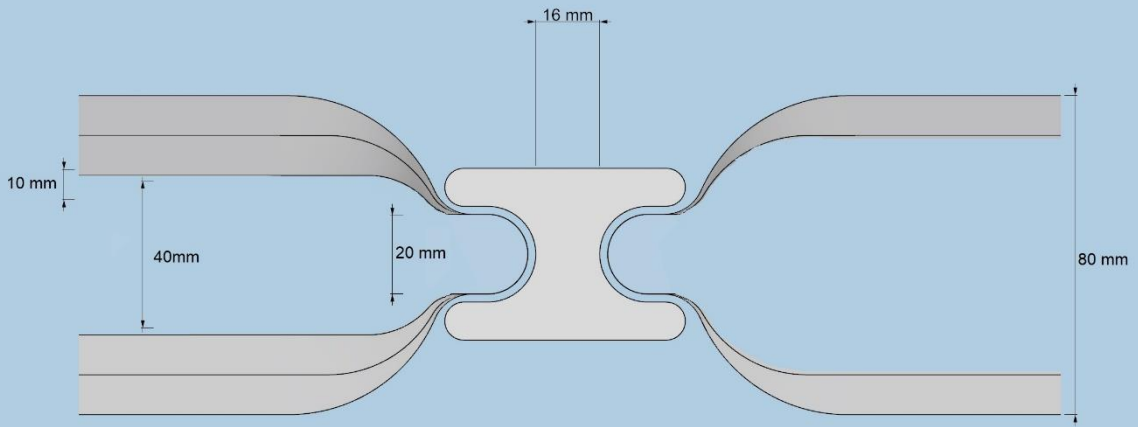
Appendix E Connections archive

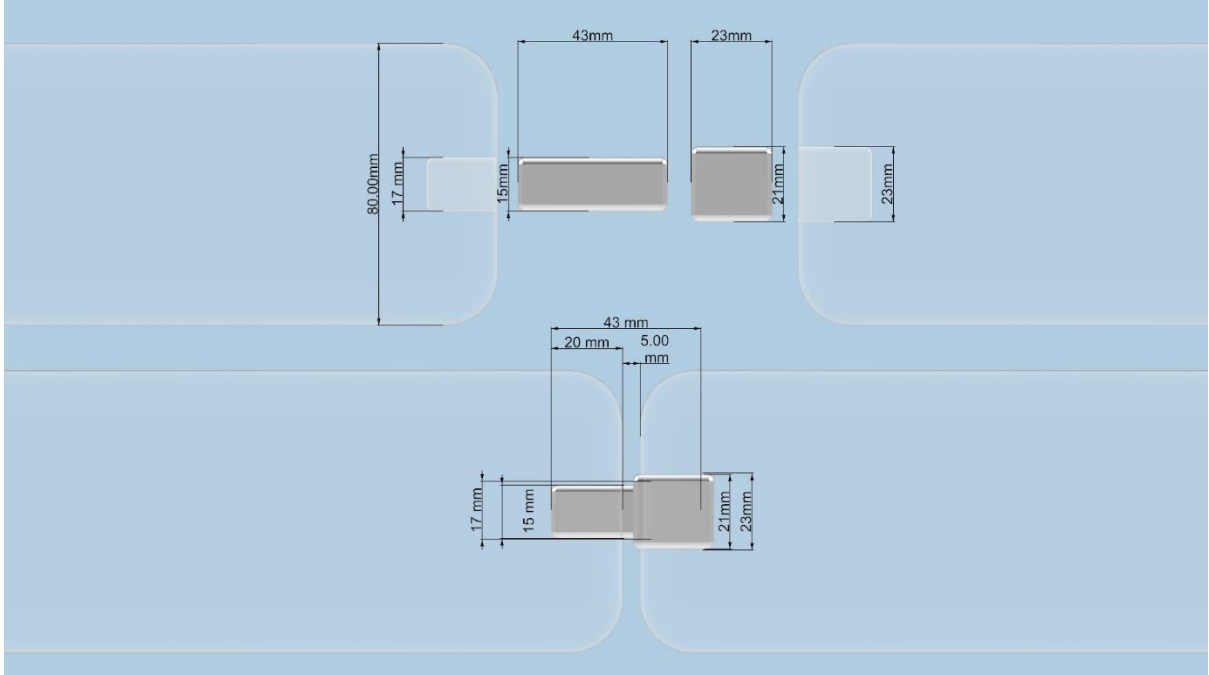
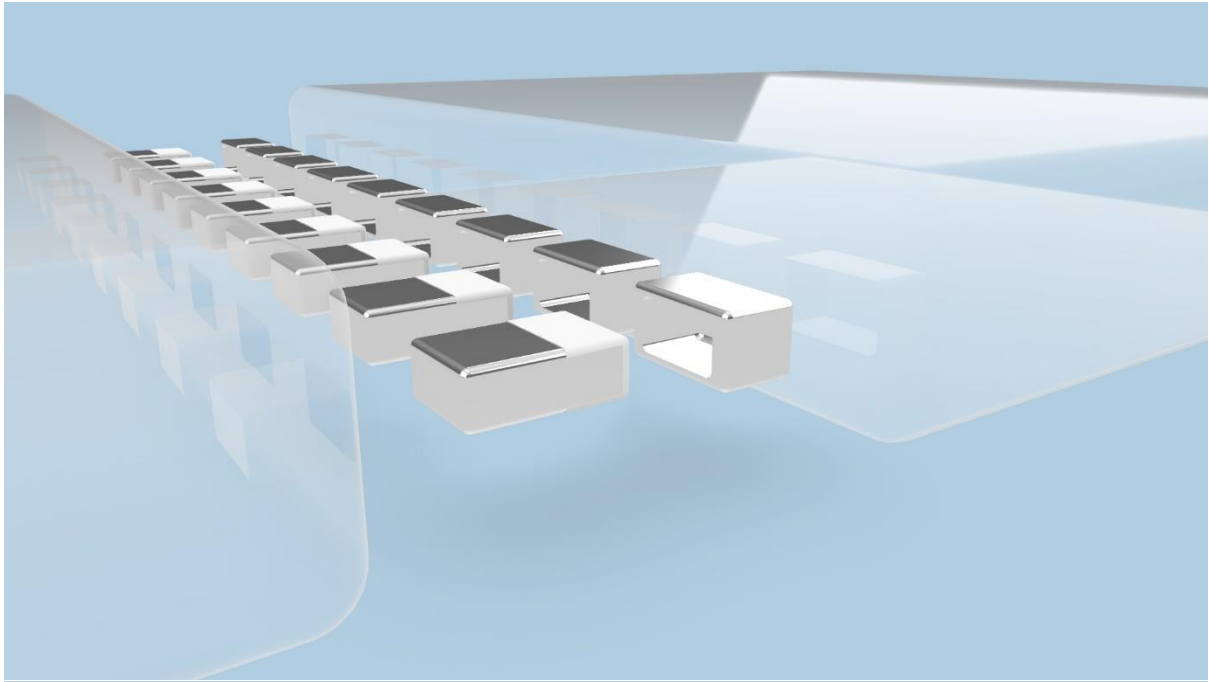


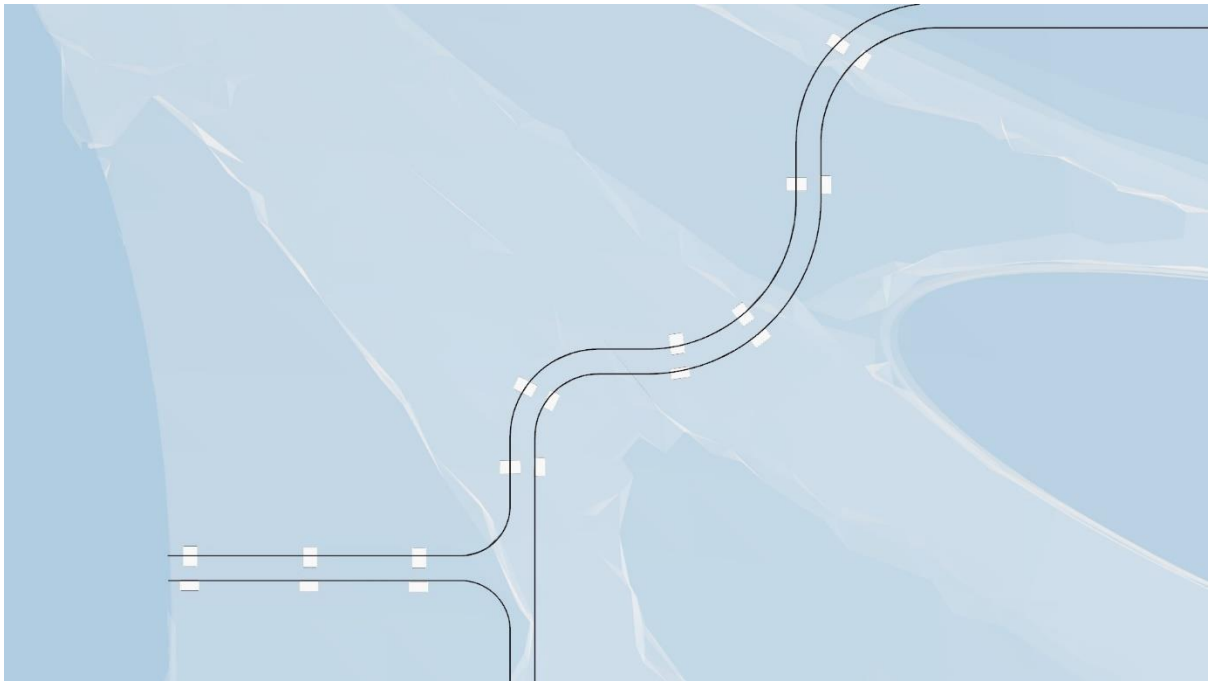
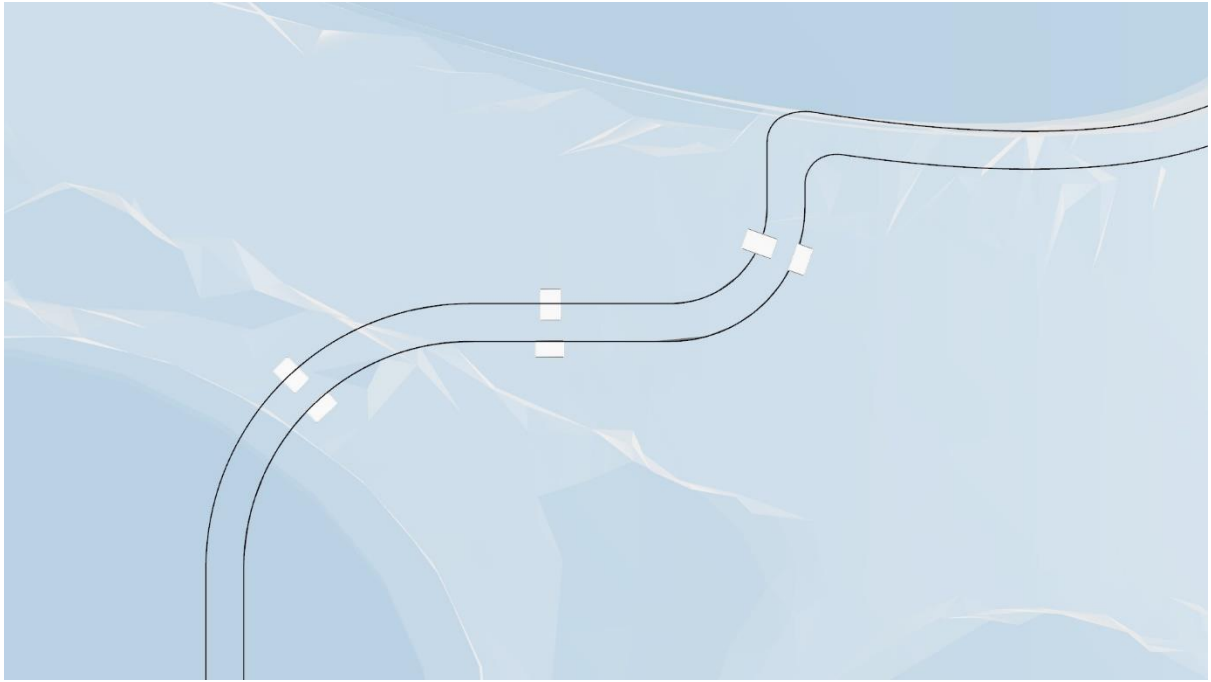
The slope in which glass changes in thickness has been shortened for the sake of fitting all in one drawing. In reality, the rate of thickness change will be more gradual. The split of the connection allows for easy assembly.

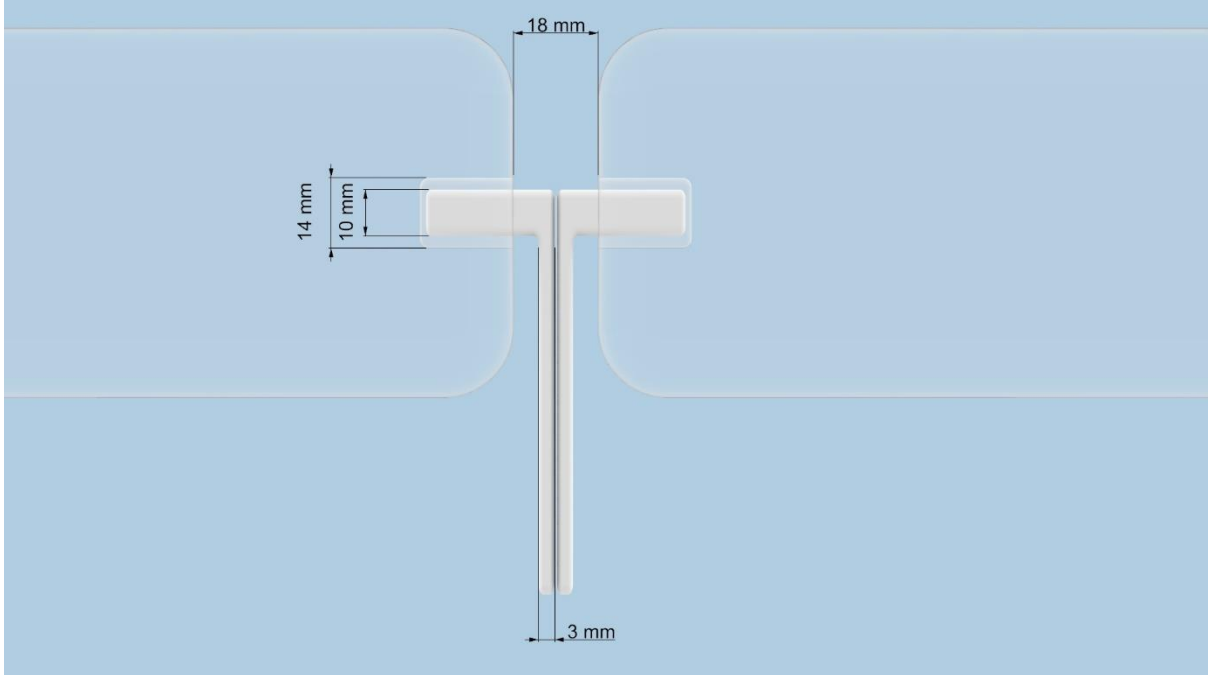
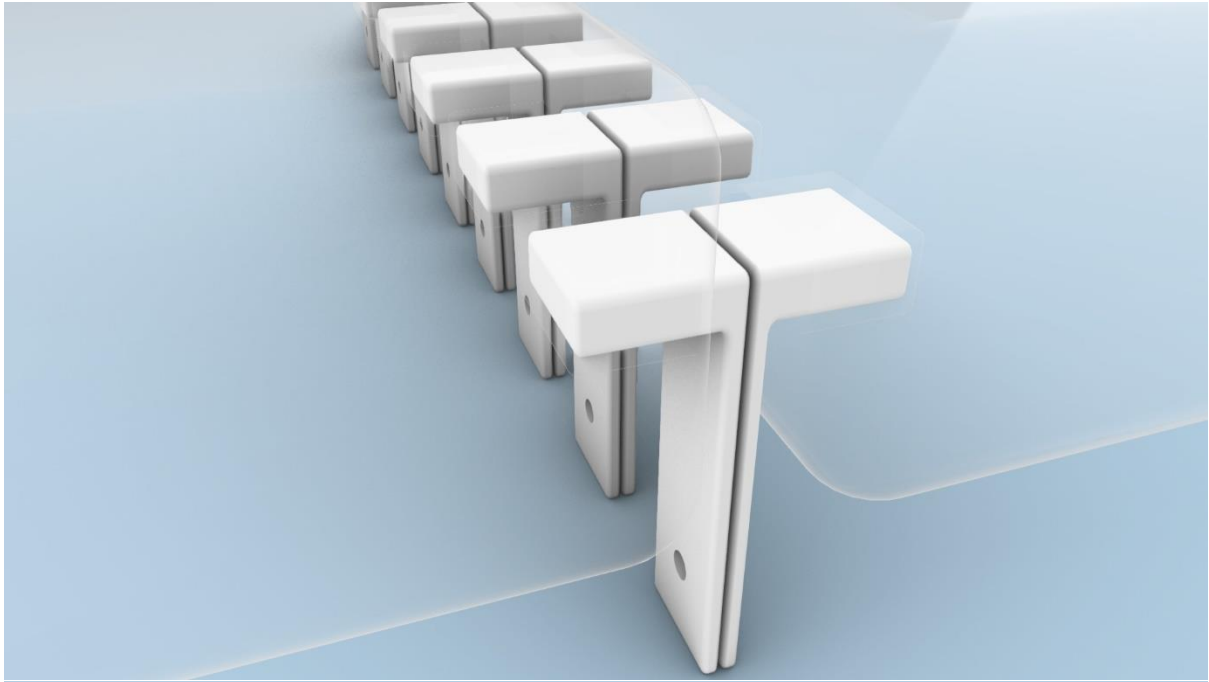


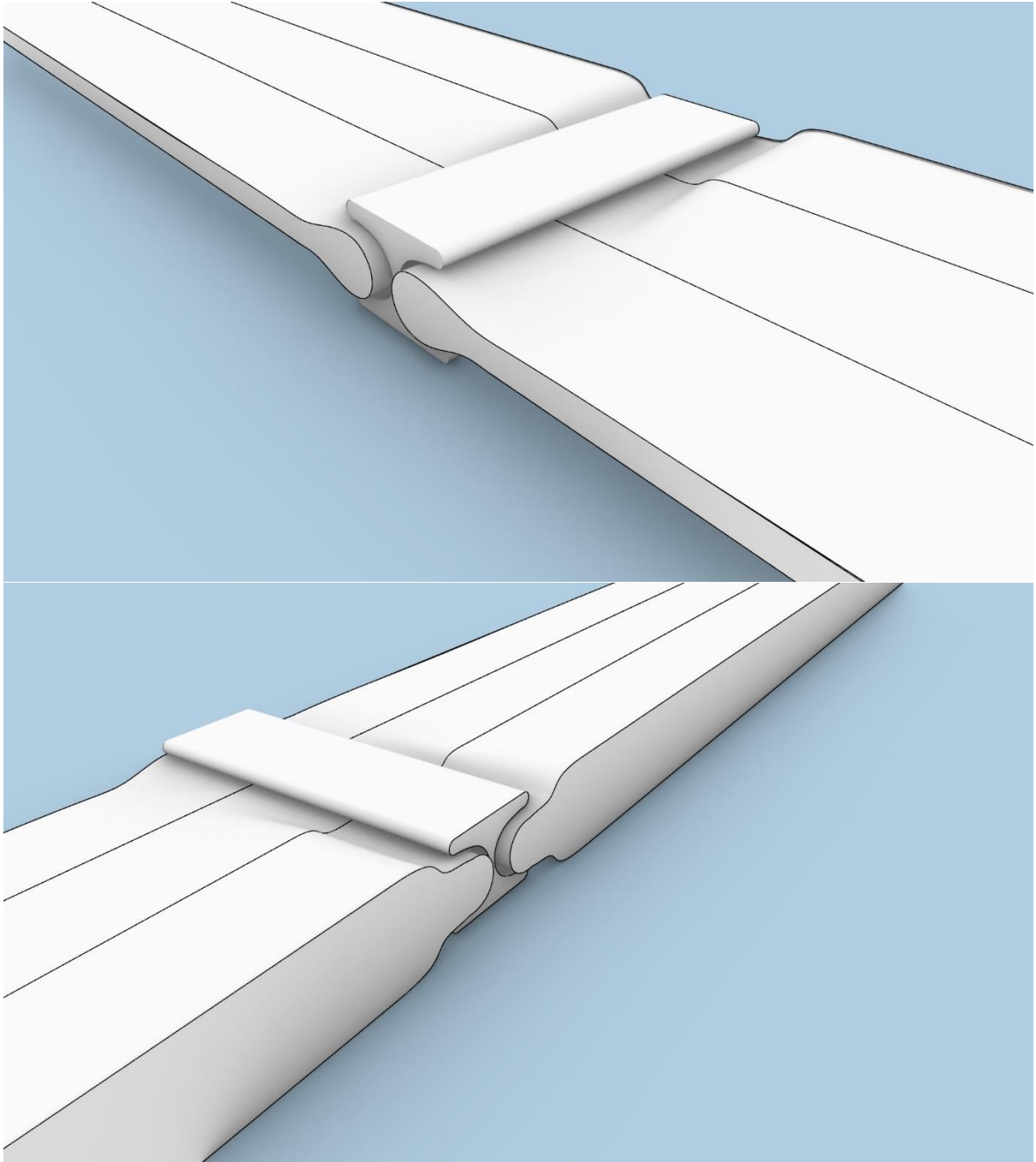


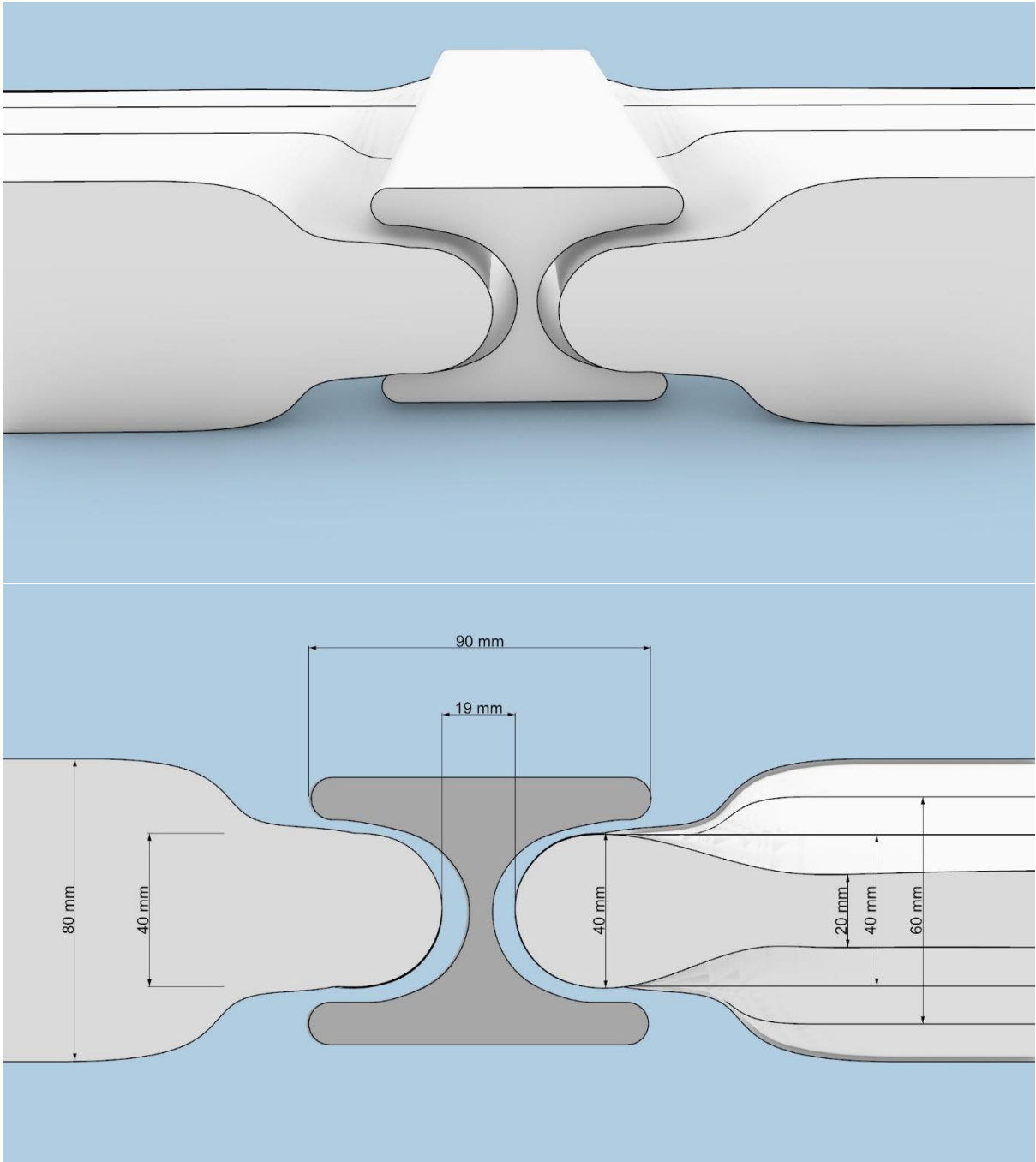


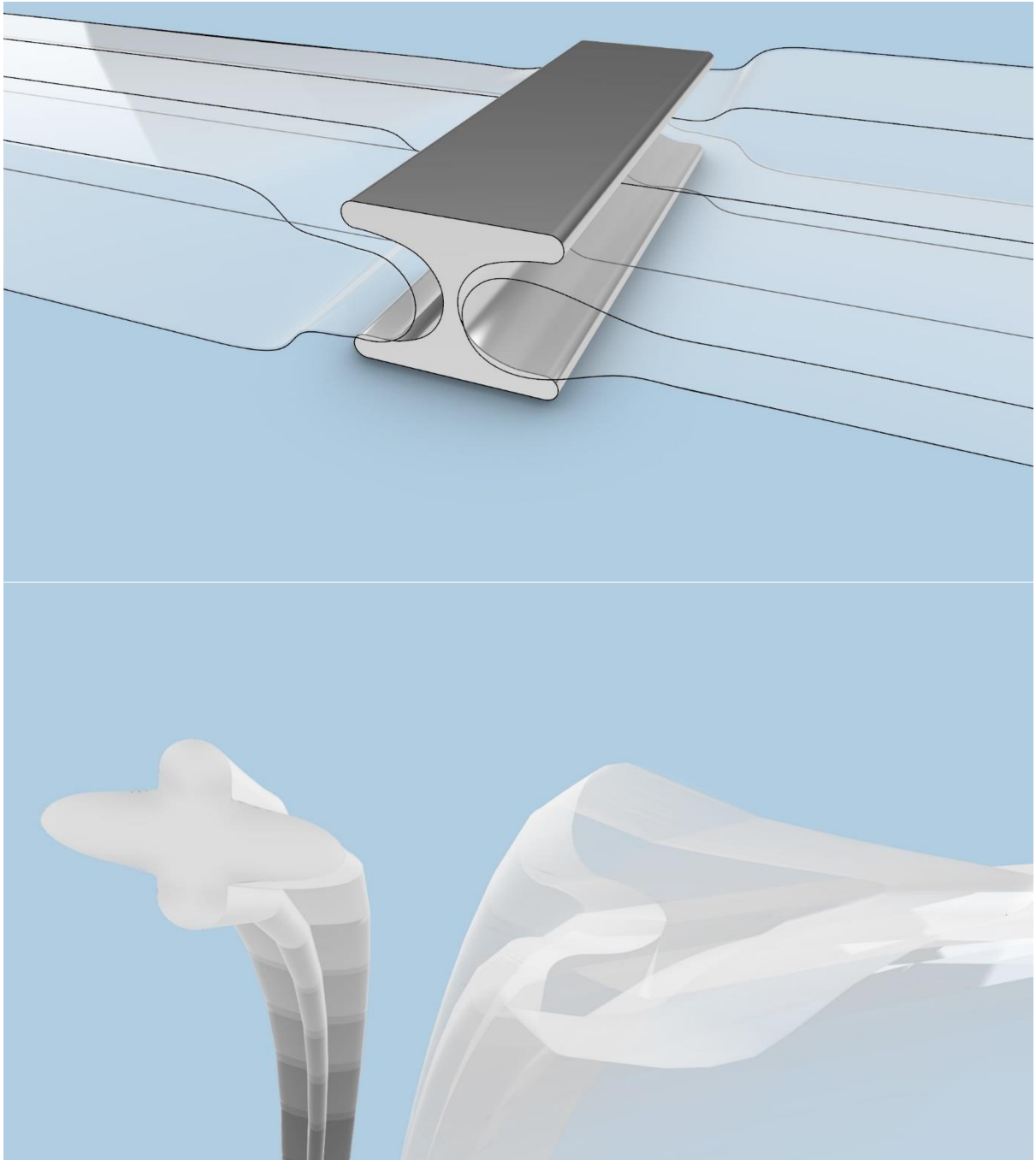


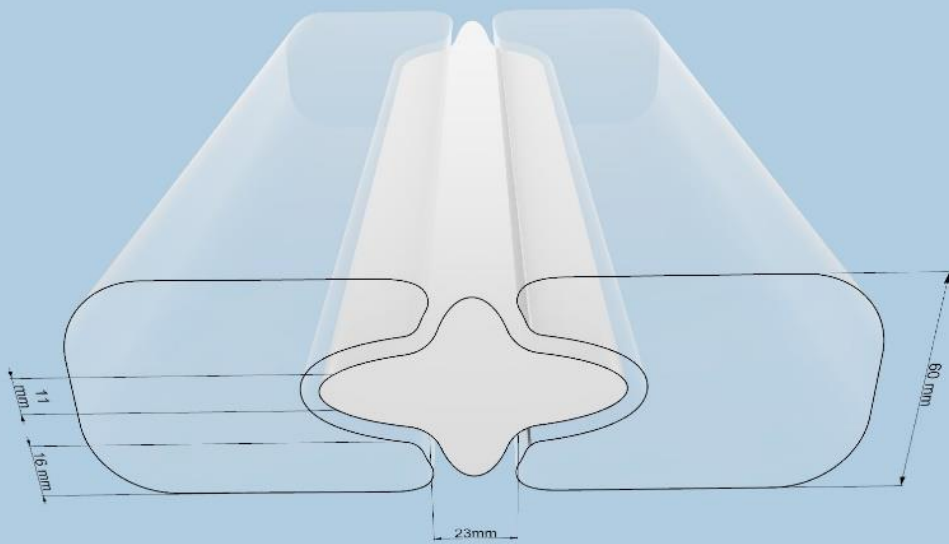
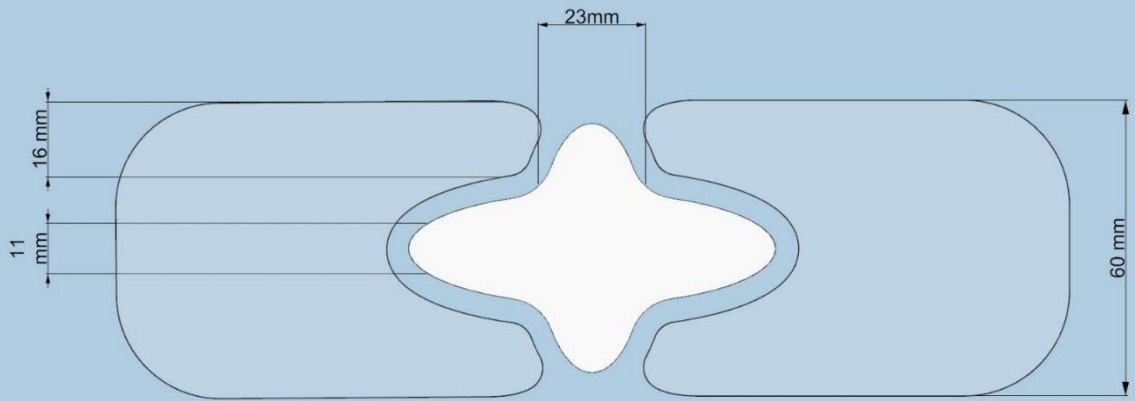


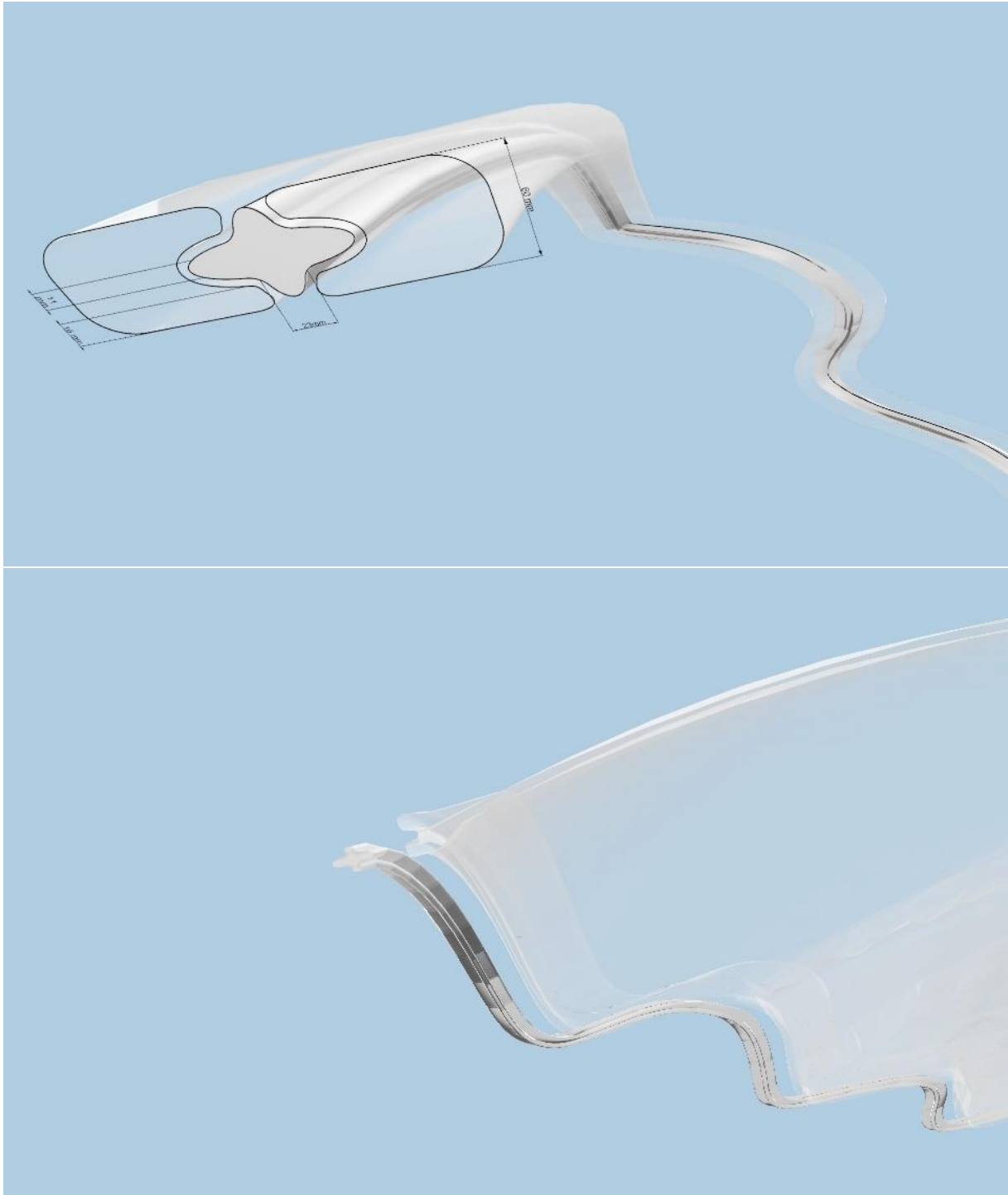


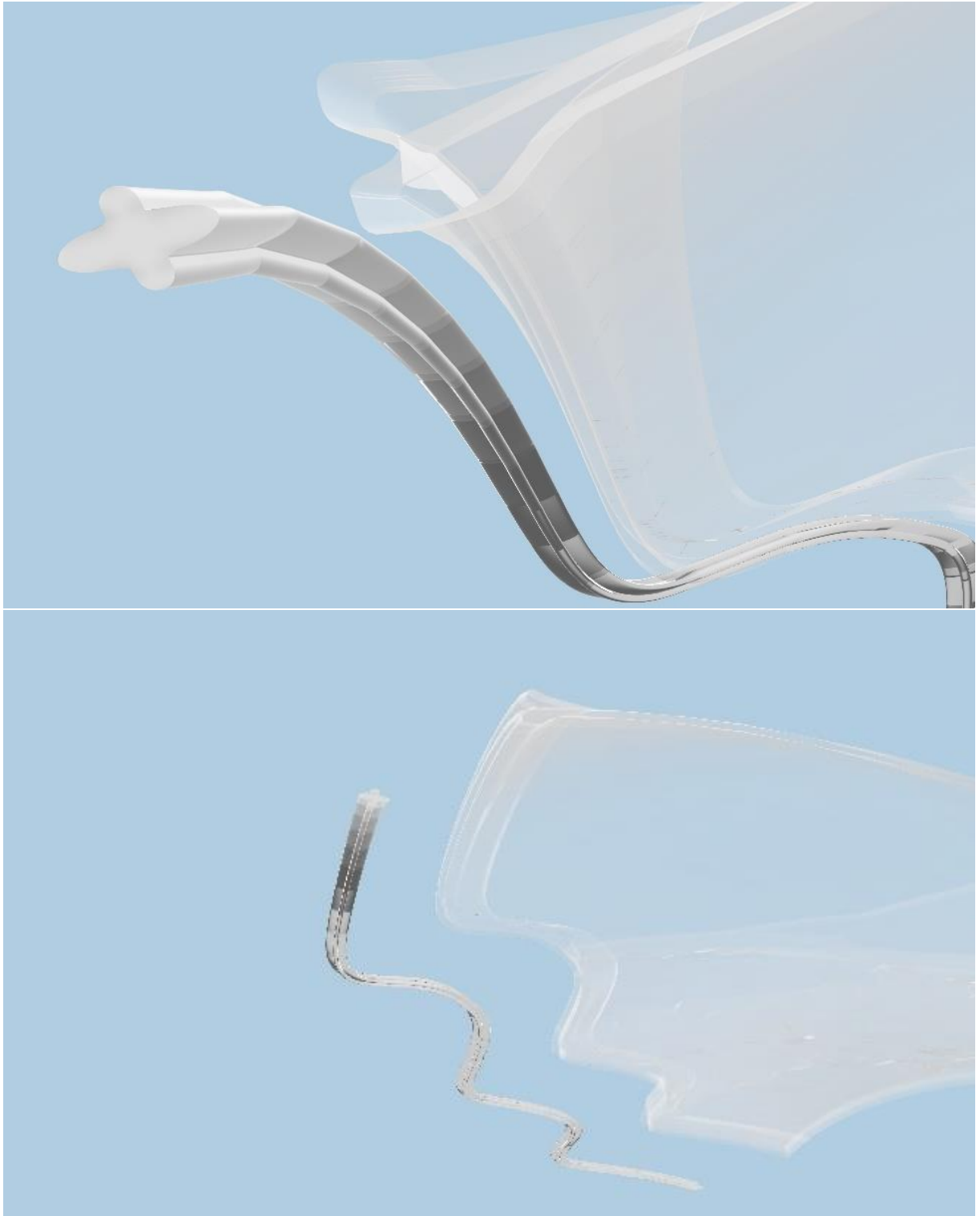


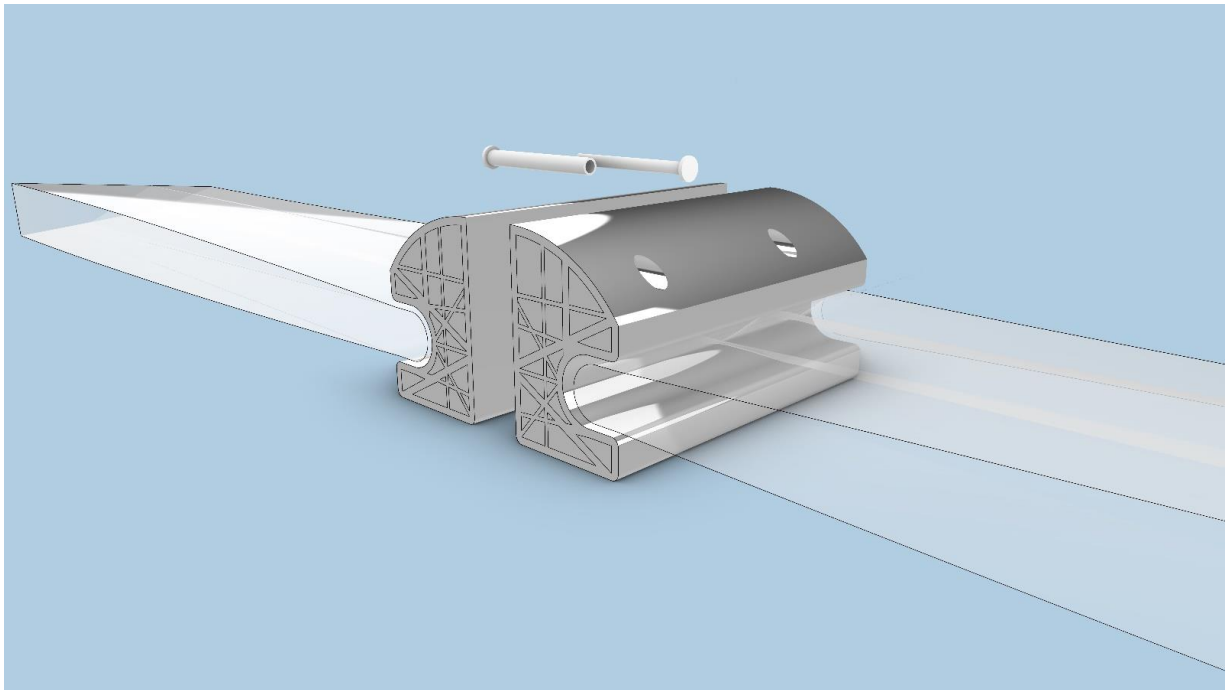
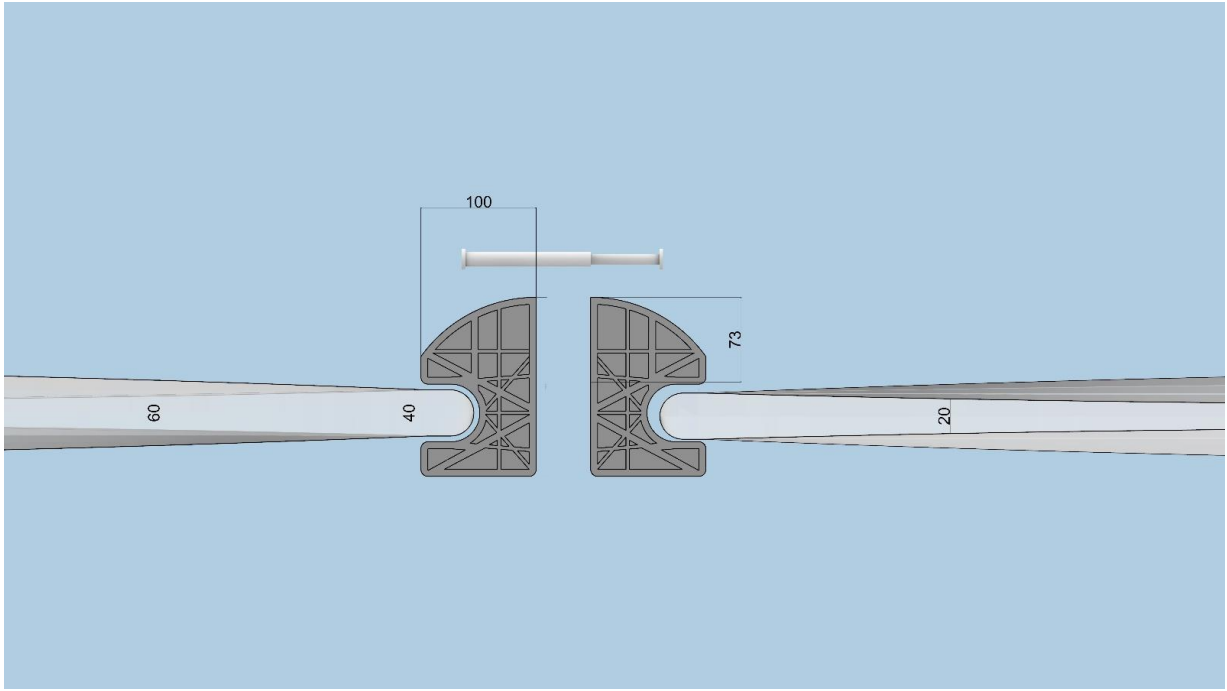


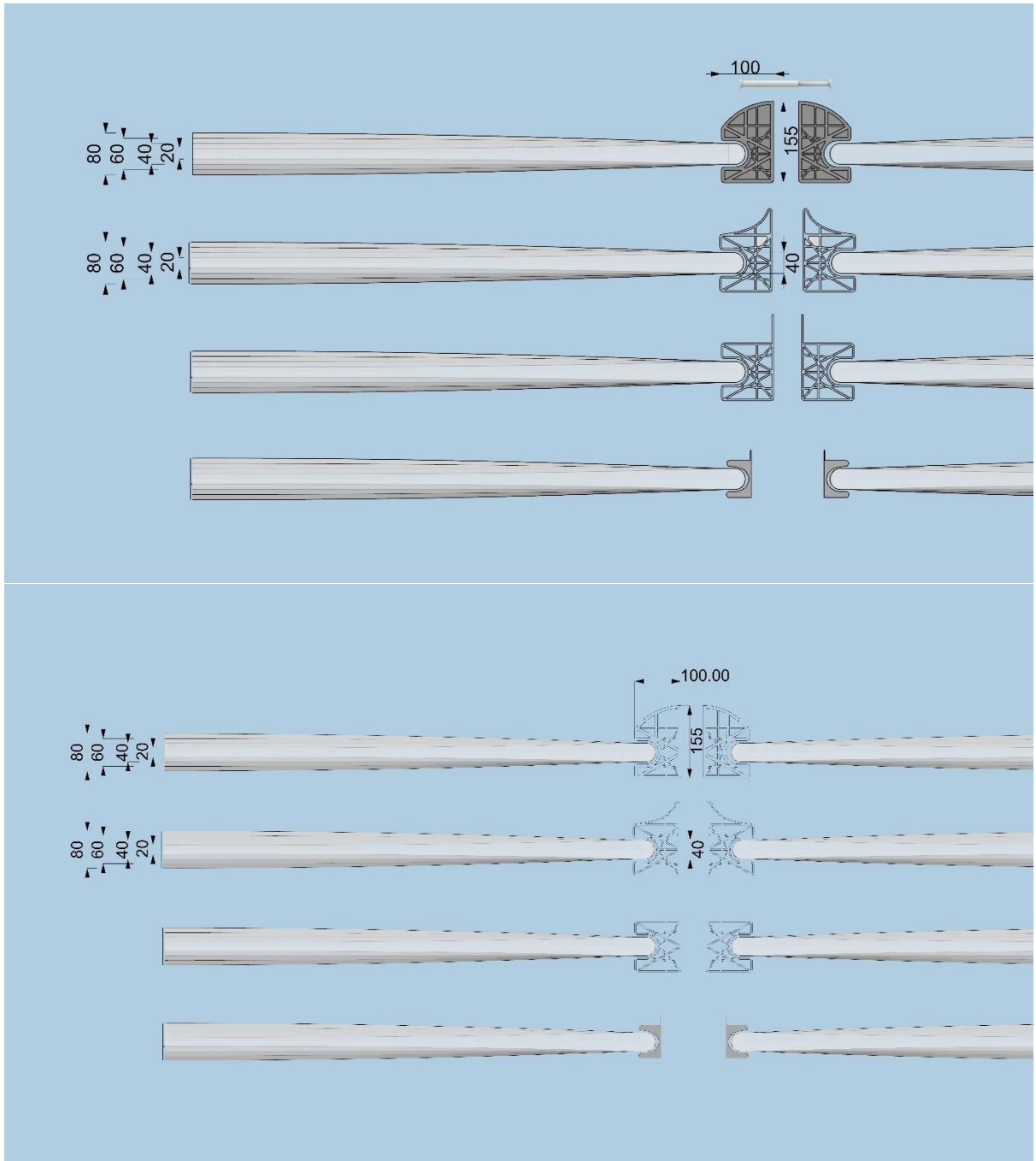












Bibliography

- ABT (2013). *Ambitions in Glass*. Retrieved on Jan 17 2020 from https://www.abt.eu/en/bestanden/Afbeeldingen/Organisatie/Kennisgebieden/4929-1/20130419_ABt_glass_brochure_def-eng.pdf
- Adriaenssens, S., Block, P., Veenendaal, D. and Williams, C. (2014). *Shell Structures for Architecture: Form Finding and Optimisation*. London: Taylor & Francis -Routledge.
- Adriaenssens, S., Block, P., Veenendaal, D., & Williams, C. J. K. (2014). *Shell Structures for Architecture: form finding and optimisation*. London: Taylor & Francis -Routledge.
- AGC. (2019). Linea Azzurra NEUTRAL FLOAT GLASS WITH A LIGHT AZURE TINT. Retrieved December 12, 2019, from <https://www.agc-yourglass.com/gb/en/products/planibel-clear/linea-azzurra>
- Akar. (n.d.). GLASS LAMINATION AUTOCLAVES. Retrieved April 16, 2020, from <http://www.akarmak.com.tr/en/autoclaves/glass-lamination-autoclaves>
- Alejano, L. R., & Bobet, A. (2012). Drucker–Prager Criterion. *Rock Mechanics and Rock Engineering*, 45(6), 995–999. doi: 10.1007/s00603-012-0278-2
- Andres, T. (2016, February 23). 10 incredible ways to see Iceland, land of fire and ice. Retrieved July 04, 2020, from <https://www.telegraph.co.uk/travel/tours/10-ways-to-see-iceland/>
- Apworks. (2020, April 01). Scalmalloy®. Retrieved May 22, 2020, from <https://apworks.de/en/scalmalloy/>
- ASC. (n.d.). ASC Process Systems is the manufacturer of the World's Largest Autoclave System. Retrieved April 16, 2020, from <http://www.aschome.com/index.php/en/asc-completes-worlds-largest-autoclave>
- Autodesk. (n.d.). What is Generative Design: Tools & Software. Retrieved December 19, 2019, from <https://www.autodesk.com/solutions/generative-design>.
- Bartels, N. A. J. & Houben, T. F. L. (2016). Retrieved from <https://research.tue.nl/en/studentTheses/structural-optimisation-for-3d-printing>
- Baldwin, E. (2018, October 17). The Immaculate Architectural Details of Apple Stores - Architizer Journal. Retrieved December 12, 2019, from <https://architizer.com/blog/inspiration/collections/apple-architecture/>.
- Bendsoe, M.P., Sigmund, O. (2004) *Topology Optimisation; Theory, Methods and Applications*. Springer- Verlag, Berlin/Heidelberg, Germany.
- Bendsoe, M., P. & Sigmund, O. (2004). *Topology Optimisation. Theory Methods and Application*, <https://doi.org/10.1007/978-3-662-05086-6>
- Beghini, L. L., Beghini, A., Katz, N., Baker, W. F., & Paulino, G. H. (2014). Connecting architecture and engineering through structural topology optimisation. *Engineering Structures*, 59, 716–726. doi:10.1016/j.engstruct.2013.10.032
- Bernhard, M., Kwon, H., Jipa, A., & Steiner, P. (2019, March 17). 3D Printed Slab. Retrieved January 6, 2020, from <http://dbt.arch.ethz.ch/project/topology-optimisation-3d-printed-slabs/>
- Bhatia, I. (2019). Shaping transparent sand in sand: Fabricating topologically optimised cast glass column using sand moulds. Delft University of Technology, Delft. Retrieved from <http://resolver.tudelft.nl/uuid:caabb4cd-1bf4-48bc-b04d-e5ff8a1d1580>
- Braaksma & Roos. (n.d.). BK City, Delft - Braaksma & Roos Architectenbureau Braaksma & Roos Architectenbureau. Retrieved July 04, 2020, from <http://www.braaksma-roos.nl/project/bk-city/>

- Bruggi, M., & Duysinx, P. (2012). Topology optimisation for minimum weight with compliance and stress constraints. *Structural and Multidisciplinary Optimisation*, 46(3), 369–384. doi: 10.1007/s00158-012-0759-7
- Bullseyeglass. (2019). Annealing Thick Slabs (*Celsius, rates in degrees per hour*). *Annealing Thick Slabs (Celsius, rates in degrees per hour)*. Retrieved from https://www.bullseyeglass.com/images/stories/bullseye/PDF/other_technical/2019b_annealing_thick_slabs_celsius.pdf
- Christensen, P.,W. & Klarbring,A. (2008). An Introduction to Structural Optimisation, 10.1007/978-1- 4020-8666-3
- Clark, N. S. (2009, October 27). 27 Heinz Isler Concrete Thin-Shells on Oct. 27th. Retrieved January 10, 2020, from <http://anengineersaspect.blogspot.com/2009/10/27-heinz-isler-concrete-thin-shells-on.html>.
- CONCR3DE. (2019). Hippo 3dPrinter. Retrieved April 20, 2020, from <https://concr3de.com/printers/hyppo-3dprinter/>
- Costanzi, C. B., Ahmed, Z., Schipper, H., Bos, F., Knaack, U., & Wolfs, R. (2018). 3D Printing Concrete on temporary surfaces: The design and fabrication of a concrete shell structure. *Automation in Construction*, 94, 395–404. doi: 10.1016/j.autcon.2018.06.013
- Cummings, K. (2001) *Techniques of kiln-formed glass*. (2nd ed.) London: A&C Black Publishers Limited
- Damen, W. (2019). Topologically Optimised Cast Glass Grid Shell Nodes. Delft University of Technology, Delft. Retrieved from <http://resolver.tudelft.nl/uuid:2afbfe96-c9bf-44d7-bfaa-d8a710fa1ce2>
- Devlin, K. (2019). The Amazing Evolution of Glass at Apple. Retrieved December 12, 2019, from <https://glassmagazine.com/glassblog/amazing-evolution-glass-apple-1513465>.
- Dongqi Group. (2016). QDX Series Double Girder Overhead Crane. Retrieved May 21, 2020, from <https://www.eurocranedq.com/qdx-double-girder-overhead-crane.html>
- Doyle, C. (2018, October 22). Five things to know before moving to the edge. Retrieved July 04, 2020, from <https://www.datacenterdynamics.com/en/opinions/five-things-know-moving-edge/>
- Dimas, M. (2020) In between, An interlayer material study for interlocking cast glass blocks. TU Delft
- Emami, N. (2013). Glass structures, from theory to practice. *Structures and Architecture*, 305–311. doi: 10.1201/b15267-41
- Eocengineers. (2020). Apple Jungfernteig. Retrieved May 21, 2020, from <https://www.eocengineers.com/en/projects/apple-jungfernteig-108>
- Eigenraam, P. (2018). Unit FF01 Form finding - Particle spring method. no. 20180301 Chair of Structural Mechanics, Faculty of Architecture and the Build Environment, Delft University of Technology. Retrieved on 20 Nov 2019 from <https://brightspace.tudelft.nl/d2l/le/clipboard/61259/22513/DownloadAttachment?fid=218923>
- Fernandes, P., Guedes, J.M., and Rodrigues H. (1999). Topology optimisation of three-dimensional linear elastic structures with a constraint on “perimeter”, *Computers and Structures* Volume 73, Issue 6 Pages 583-594 Retrieved on 17 Dec 2019 from [https://doi.org/10.1016/S0045-7949\(98\)00312-5](https://doi.org/10.1016/S0045-7949(98)00312-5)
- Frearson, A. (2017, September 04). Armadillo Vault is a pioneering stone structure without any glue. Retrieved May 26, 2020, from <https://www.dezeen.com/2016/05/31/armadillo-vault-block-research-group-eth-zurich-beyond-the-bending-limestone-structure-without-glue-venice-architecture-biennale-2016/>
- Goodno, B. J., & Gere, J. M. (2018). *Mechanics of Materials*. 20 Channel Center Street Boston, MA 02210 USA: Cengage Learning® Nelson Education Ltd. KNMI. (2010). Retrieved from <http://www.klimaatatlas.nl/klimaatatlas.php?wel=wind&ws=kaart&wom=Gemiddelde%20windsnelheid>

Grolms, M. (2016, June 2). Light Rider is the world's first 3D-printed motorcycle. Retrieved January 6, 2020, from <https://www.advancedsciencenews.com/light-rider-worlds-first-3d-printed-motorcycle/>.

Granta Design Limited. (2019). CEEduPack. Ver.19.2.0. Retrieved from <https://grantadesign.com/education/support/ces-edupack-support/>

Hassen, G., Bleyer J., & Buhan, P. (2017). *Elastic, Plastic and Yield Design of Reinforced Structures*. Elsevier. doi: ISBN: 9781785482052

Hein, B. (2014, December 12). Apple supreme design award for glass store in Turkey. Retrieved December 12, 2019, from <https://www.cultofmac.com/305967/apple-wins-supreme-engineering-award-glass-lantern-store-turkey/>.

Hiroshi Nakamura & NAP (2017, December 20). Optical Glass House / Hiroshi Nakamura & NAP. Retrieved December 12, 2019, from <https://www.archdaily.com/885674/optical-glass-house-hiroshi-nakamura-and-nap>.

Jewett, J. L., & Carstensen, J. V. (2019). Experimental investigation of strut-and-tie layouts in deep RC beams designed with hybrid bi-linear topology optimisation. *Engineering Structures*, 197, 109322. doi: 10.1016/j.engstruct.2019.109322

Jipa, A., Bernhard, M., Meibodi, M., & Dillenburger, B. (2016). 3D-Printed Stay-in-Place Formwork for Topologically Optimised Concrete Slabs. In *3D-Printed Stay-in-Place Formwork for Topologically Optimised Concrete Slabs*. Retrieved from <https://doi.org/10.3929/ethz-b-000237082>

Kaiser, N.D., Behr, R.A., Minor, J.E., Dharani, L.R., Ji, F., Kremer, P.A. (2000). Impact Resistance of Laminated Glass Using "Sacrificial Ply" Design Concept. *Journal of Architectural Engineering*, 6(1), 24-34. [https://doi.org/10.1061/\(ASCE\)1076-0431\(2000\)6:1\(24\)](https://doi.org/10.1061/(ASCE)1076-0431(2000)6:1(24))

Kimball Midwest (2018). *How To Work With Wire Rope and Wire Rope Clips*. Retrieved from <https://www.youtube.com/watch?v=Sc71eBlwh6c>

Klein, J., Stern, M., Franchin, G., Kayser, M., Inamura, C., Dave, S., ... Oxman, N. (2015). Additive Manufacturing of Optically Transparent Glass. *3D Printing and Additive Manufacturing*, 2(3), 92–105. doi: 10.1089/3dp.2015.0021

Knaack, U. (1998). *Konstruktiver Glasbau*. Köln: Rudolf Müller.

Louter, C. (Ed.), Bos, F., Belis, J., & Lebet, J-P. (2014). Why glass structures fail? - Learning from failures of glass structures. Challenging Glass 4 & COST Action TU0905 Final Conference: Conference on Architectural and Structural Applications of Glass. Ecole Polytechnique Fédérale de Lausanne (EPFL), Lausanne, Switzerland, 6-7 February 2014 (pp. 791-799). Boca Raton, FL: CRC Press/Balkema

Lundgren, J., & Palmqvist, C. (2012). Structural Form Optimisation Methods of numerical optimisation and applications on civil engineering structure/ Chalmers University of Technology, Göteborg, Sweden Retrieved from <http://publications.lib.chalmers.se/records/fulltext/162939.pdf>

MaterialDistrict. (2020). Manual MaterialDistrict 2020. Retrieved January 8, 2020, from <https://rotterdam.materialdistrict.com/exhibit/manual/>.

Minner, K. (2011, February 4). The Crown Fountain / Krueck & Sexton Architects. Retrieved December 13, 2019, from <https://www.archdaily.com/109201/the-crown-fountain-krueck-sexton-architects>.

Pedersen, O. E., Larsen, N. M., & Pigram, D. (2014). Post-tensioned Discrete Concrete Elements Developed for Free-form Construction. *Advances in Architectural Geometry 2014*, 15–28. doi: 10.1007/978-3-319-11418-7_2

Pilkington. (n.d.). The Float Process Step by step. Retrieved January 9, 2020, from <https://www.pilkington.com/en/global/about/education/the-float-process/the-float-process-step-by-step>.

- Pye, L. D., Joseph, Montenero, A., I. H., Karlsson, & K., Backman, R. (2005). *Properties of glass-forming melts*. Boca Raton, FL: St. Lucie.
- Rahman, A. M. E. R. A. R. B. A. (2016). Performance of physical shell foundation model under axial loading. Universiti Tun Hussein Onn Malaysia Retrieved from http://eprints.uthm.edu.my/id/eprint/9114/1/Amera_Ratia_Ab_Rahman.pdf
- Roeder, E. (1971). Extrusion of glass. *Journal of Non-Crystalline Solids*, 5(5), 377–388. doi: 10.1016/0022-3093(71)90039-1
- Saint Gobain. (2018, September 19). Mechanical properties. Retrieved January 10, 2020, from <https://www.saint-gobain-sekurit.com/content/mechanical-properties-0>.
- Snijder, A. H., L. P. L. Van Der Linden, Goulas, C., Louter, C., & Nijse, R. (2019). The glass swing: a vector active structure made of glass struts and 3D-printed steel nodes. *Glass Structures & Engineering*. doi: 10.1007/s40940-019-00110-9
- Stevens, P. (2019, June 27). MVRDV's transparent brick store in Amsterdam re-opens for Hermès. Retrieved December 12, 2019, from <https://www.designboom.com/architecture/mvrdv-hermes-store-amsterdam-crystal-houses-transparent-brick-facade-06-27-2019/>.
- Oikonomopoulou, F., Bristogianni, T., Veer, F. A., & Nijse, R. (2017). The construction of the Crystal Houses façade: challenges and innovations. *Glass Structures & Engineering*, 3(1), 87–108. doi: 10.1007/s40940-017-0039-4
- Oikonomopoulou, F., van den Broek, E., Bristogianni, T., Veer, F. A., & Nijse, R. (2017b). Design and experimental testing of the bundled glass column. *Glass Structures and Engineering*, 2(2), 183-200.
- Oikonomopoulou, F., Bristogianni, T., Barou, L., Veer, F., & Nijse, R. (2018). The potential of cast glass in structural applications. Lessons learned from large-scale castings and state-of-the art load-bearing cast glass in architecture. *Journal of Building Engineering*, 20, 213–234. doi: 10.1016/j.job.2018.07.014
- Oikonomopoulou, F., Bristogianni, T., Barou, L., Jacobs, E., Frigo, G., Veer, F., & Nijse, R. (2018a). Interlocking cast glass components, Exploring a demountable dry-assembly structural glass system. *Heron*, 63(1/2), 103-138.
- Oikonomopoulou, F. (2018b). Re3 glass blocks from waste glass can be dry-stacked. Retrieved April 17, 2020, from <https://materialdistrict.com/article/re3-glass-blocks-waste-glass/>
- Oikonomopoulou, F. (2019). Unveiling the third dimension of glass, A+BE | Architecture and the Built Environment, Delft University of Technology <http://resolver.tudelft.nl/uuid:16f1560f-1739-492c-bd95-3f47bf096182>
- O'Regan, C. (2014). *Structural Use of Glass in buildings* (2nd ed.). London, England: The Institution of Structural Engineers.
- Rozvany, G. (2001) Stress ratio and compliance-based methods in topology optimisation. *Structural and Multidisciplinary Optimisation* 21: 109. <https://doi.org/10.1007/s001580050175>
- Rozvany, G.I.N. (2009) A critical review of established methods of structural topology optimisation. *Structural Multidisciplinary Optimisation*, 37, 217-237.
- Schlaich, J. (2014). On architects and engineers. In *Shell Structures for Architecture: Form Finding and Optimisation*, pp. VIII–XI. London: Taylor & Francis -Routledge.
- Schittich, C., Staib, G., Balkow, D., Schuler, M., & Sobek, W. (2007). *Glass Construction Manual*. doi: 10.11129/detail.9783034615549

SCHOTT. (2007). Memorial Madrid in Spain with SCHOTT Borosilicate Glass. Retrieved December 12, 2019, from <https://www.us.schott.com/architecture/english/references/memorial-madrid.html>.

Schott. (2016). DURAN® Tubing, rods and capillaries made of borosilicate glass 3.3 [Brochure]. Elmsford, New York: Author. Retrieved June 05, 2020, from https://www.us.schott.com/d/tubing/9ae1bb17-dbe1-464e-ba27-99022b50a49b/20190523100021/schott_duran_brochure_us_final.pdf

Shand, E. B., & Armistead, W. H. (1958). *Glass engineering handbook*. New York: MacGraw-Hill.

Sigmund, O., & Maute, K. (2013). Topology optimisation approaches. *Structural and Multidisciplinary Optimisation*, 48(6), 1031-1055.

Simscale. (2019). What is von Mises Stress? Retrieved January 1, 2020, from <https://www.simscale.com/docs/content/simwiki/fea/what-is-von-mises-stress.html>.

Snijder, A., Nijse, R., & Louter, C. (2018). The glass truss bridge. *Heron*, 63(1/2), 139-157. [7].

Snijder, A. H., van der Linden, L. P. L., Goulas, C., Louter, C., & Nijse, R. (2019). The glass swing: a vector active structure made of glass struts and 3D-printed steel nodes. *Glass Structures and Engineering*. <https://doi.org/10.1007/s40940-019-00110-9>

Tepavčević, B., Stojaković, V., Mitov, D., Jovanović, M., & Bajšanski, I. (2016, May 4). Tessellated Shell Pavilion. Retrieved January 10, 2020, from <http://www.arhns.uns.ac.rs/cdd/967/>.

Ugural, A. C., & Fenster, S. K. (2012). *Advanced mechanics of materials and elasticity*. Upper Saddle River, NJ: Prentice Hall.

Unicranes (2020). Unic Cranes Products. Retrieved April 16, 2020, from <https://www.unicranes.com/spider-cranes/>

Van der Weijst, F. (2019). Delft. Retrieved from <http://resolver.tudelft.nl/uuid:37a693fc-4835-4d46-a4e1-086e96c2ef1a>

Voxeljet (2018). Servicebrochure. Retrieved on Dec 21 2019 from https://www.voxeljet.com/fileadmin/user_upload/PDFs/Servicebrochure_2018_web_01.pdf

Voxeljet (2018 b). *voxeljet 3D printer*. Retrieved from https://www.voxeljet.com/fileadmin/user_upload/PDFs/Technical_data_3D_printer_01.pdf

Wang, M.Y., Wang, X., Guo, D. (2003) A level set method for structural topology optimisation. *Computer methods in applied mechanics and engineering*, 192, 227-246
Wheatonarts. (n.d.). Visit. Retrieved December 19, 2019, from <https://www.wheatonarts.org/visit/>.

Williams, C. J. K. (2014). What is a shell? In *Shell Structures for Architecture: Form Finding and Optimisation*, pp. 21–31. London: Taylor & Francis -Routledge.